

ELG 6369

NONLINEAR MICROWAVE DEVICES AND EFFECTS

CHAPTER I

**INTRODUCTION TO MICROWAVE
COMPUTER-AIDED DESIGN**

Before starting a course on *Nonlinear Microwave Devices and Effects*, it is essential to review some basic concepts and properties of the electromagnetic (EM) spectrum and the meaning of linearity and nonlinearity in high-frequency components and circuits.

A - SPECIFICITY OF MICROWAVE FREQUENCIES

I – Electromagnetic spectrum

The microwave spectrum consists of several individual bands (Figures I-1 and I-2). Because of the link between the wavelength λ and the frequency f , each of these spectral ranges may be also called by its wavelength range. In practice, however, a wave is specified in terms of its wavelength when $\lambda < 1\text{mm}$ (millimeter range). Table I-1 shows the relation between frequency and wavelength, highlighting the microwave bands (formally from 300MHz to 300GHz)

Table I-1. Relation between frequency and wavelength.

Frequency		Wavelength	
30 MHz	→	10 m	
100 MHz	→	3 m	{ Metric Band
300 MHz	→	1m	
1 GHz	→	30 cm	{ Decimeter Band
3 GHz	→	10 cm	
10 GHz	→	3 cm	{ Centimeter Band
30 GHz	→	1 cm	
100 GHz	→	3 mm	{ Millimeter Band
300 GHz	→	1 mm	

↑ MICROWAVES ↓

The materials you receive for this course are protected by copyright and to be used for this course only. You do not have permission to upload the course materials, including any lecture recordings you may have, to any website. If you require clarification, please consult your professor.

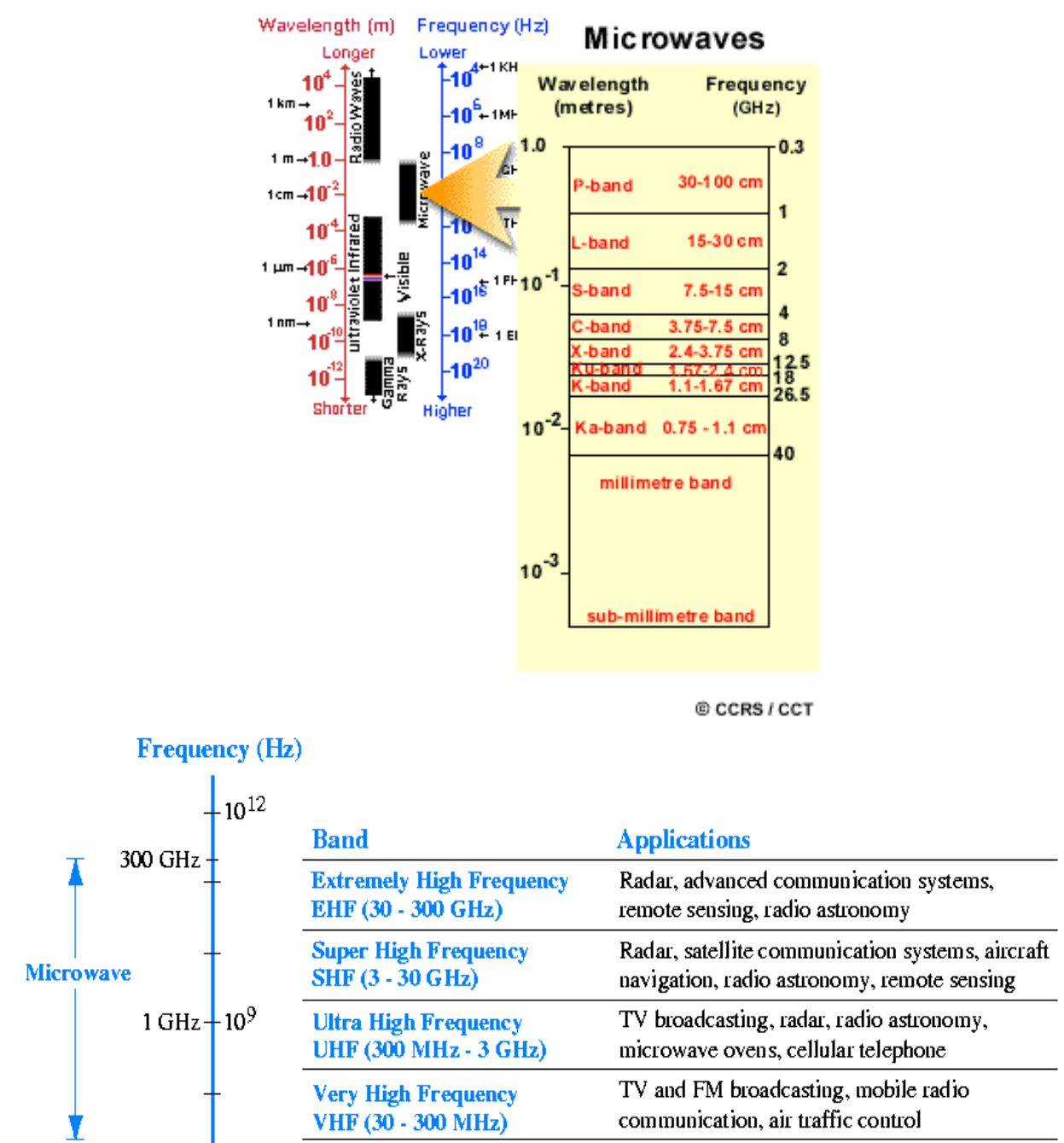


Figure I-1. (a) Individual bands of the RF/microwave spectrum (CCRS-Canada) and (b) their primary applications (F.T. Ulaby, *Fundamentals of Applied Electromagnetics*, Prentice Hall).

The materials you receive for this course are protected by copyright and to be used for this course only. You do not have permission to upload the course materials, including any lecture recordings you may have, to any website. If you require clarification, please consult your professor.

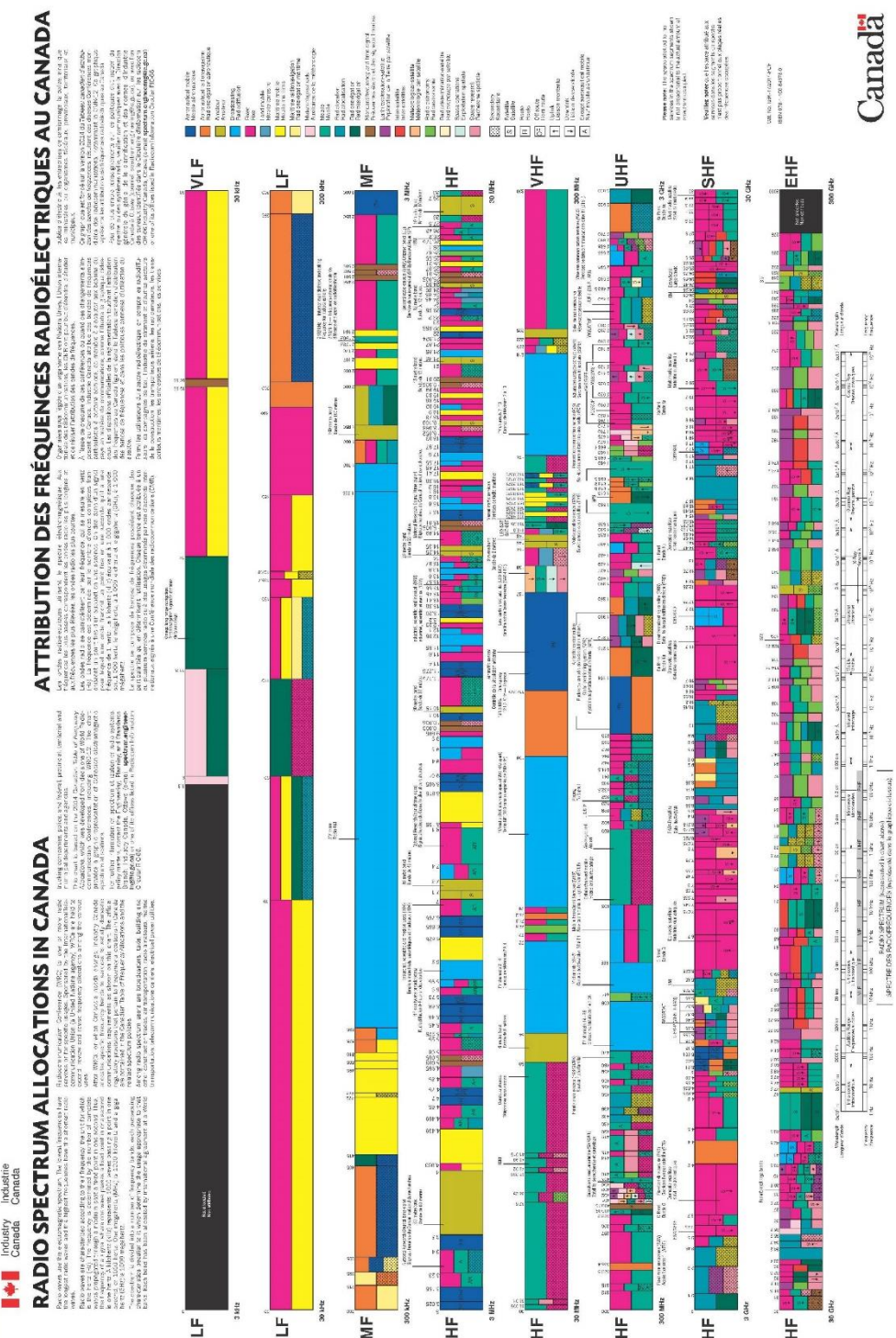


Figure I-2. Radio spectrum allocation in Canada (Industry Canada, 2014).

The materials you receive for this course are protected by copyright and to be used for this course only. You do not have permission to upload the course materials, including any lecture recordings you may have, to any website. If you require clarification, please consult your professor.

II – Relation between wavelength and physical length

In the space domain, the wavelength is equivalent to the period in the time domain. In low frequencies, it is common to use currents and voltages *with the assumption* that the operating wavelength λ is infinitely larger than the physical length d of a component $\{\lambda \gg d\}$ as shown in Figure I-3. Applied to a wire, this assumption means that (i) the current is invariant across the wire and (ii) that the difference in voltage between two different points of a wire is zero.

This assumption is no longer valid when the physical length d is in the same order as the wavelength λ ($\lambda \approx d$) (Figure I-4). The wire is then equivalent to a transmission line.

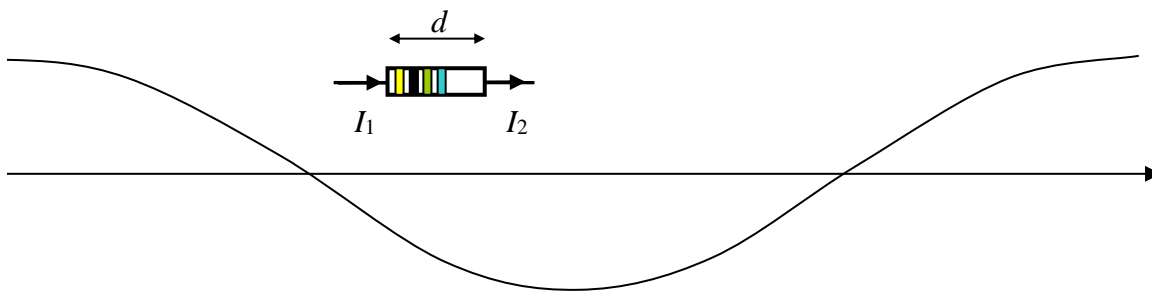


Figure I-3. Comparison between the physical length of a component and the operating wavelength. In low frequencies: $\{\lambda \gg d\} \rightarrow I_1 = I_2$.

The materials you receive for this course are protected by copyright and to be used for this course only. You do not have permission to upload the course materials, including any lecture recordings you may have, to any website. If you require clarification, please consult your professor.

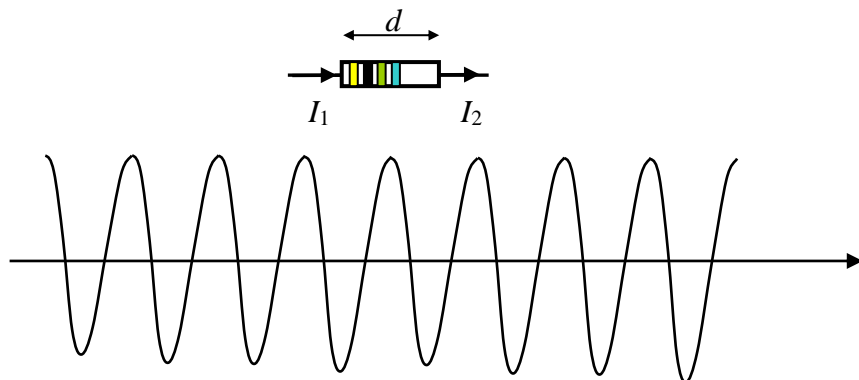


Figure I-4. Comparison between the physical length of a component and the operating wavelength. In high frequencies: $\{\lambda \approx d\} \rightarrow I_1 \neq I_2$.

III – RF/Microwave transmission lines

Rectangular/circular waveguides and planar lines (Table I-2) are the most widely used in the centimeter/millimeter bands.

B – MICROWAVE COMPUTER-AIDED DESIGN

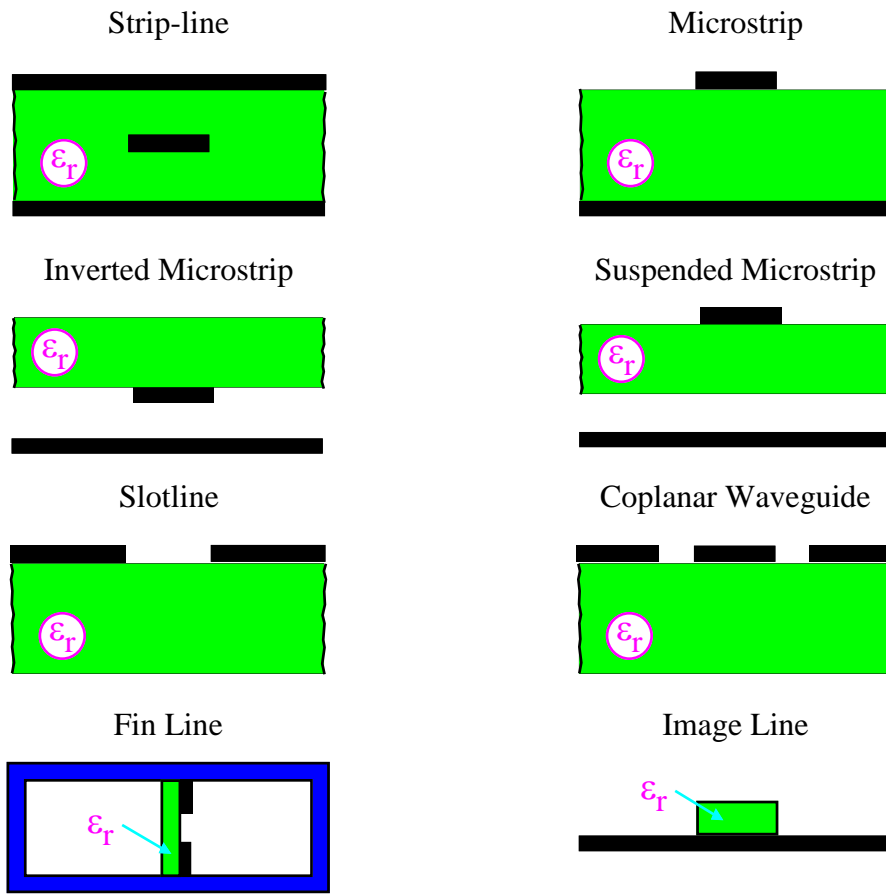
The drive in the electronics industry for manufacturability-driven design and time-to-market demands powerful and efficient Computer-Aided Design (CAD) techniques. As the signal speed and frequency increase, the dimensions of interconnects and active/passive components in multilayer circuits become a significant fraction of the signal wavelength.

Models with physical/geometrical information, including nonlinear and electromagnetic (EM) effects, become necessary.

The materials you receive for this course are protected by copyright and to be used for this course only. You do not have permission to upload the course materials, including any lecture recordings you may have, to any website. If you require clarification, please consult your professor.

Furthermore, the need for statistical analysis taking into account process variations and manufacturing tolerances in the components makes it extremely important that the component models are accurate and fast so the design solutions can be achieved feasibly and reliably. To highlight these aspects, let us consider a simple microwave communication network (Figure I-5).

Table I-2. Planar lines.



The materials you receive for this course are protected by copyright and to be used for this course only. You do not have permission to upload the course materials, including any lecture recordings you may have, to any website. If you require clarification, please consult your professor.

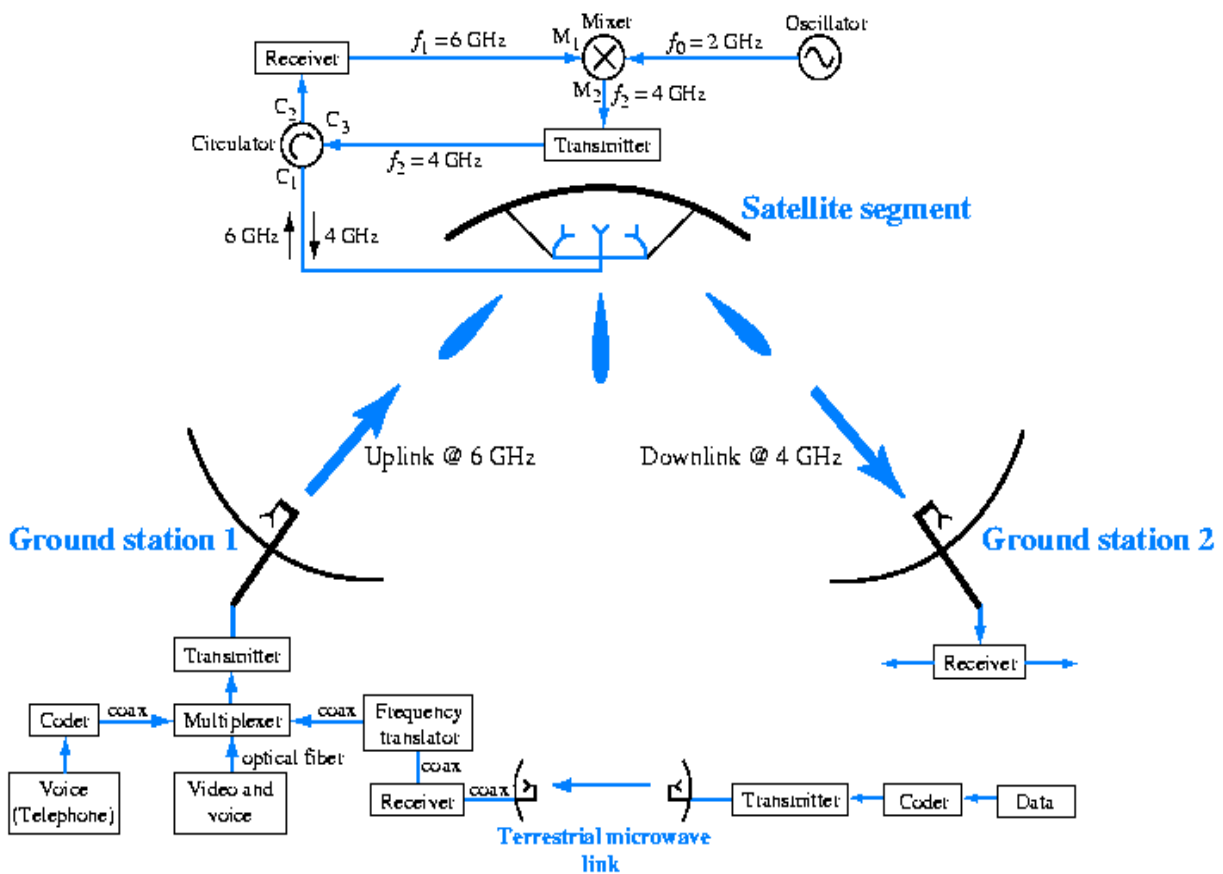


Figure I-5. Microwave communication network.

(F.T. Ulaby, *Fundamentals of Applied Electromagnetics*, Prentice Hall).

To achieve the complete design of this communication network, we have to consider several different aspects like those listed in Figure I-6. Just for the technical parts, we have to know that fields such as "microwave theory" or "signal propagation" do not refer to some very narrow expertise but involve much more extended aspects of electronics.

The materials you receive for this course are protected by copyright and to be used for this course only. You do not have permission to upload the course materials, including any lecture recordings you may have, to any website. If you require clarification, please consult your professor.

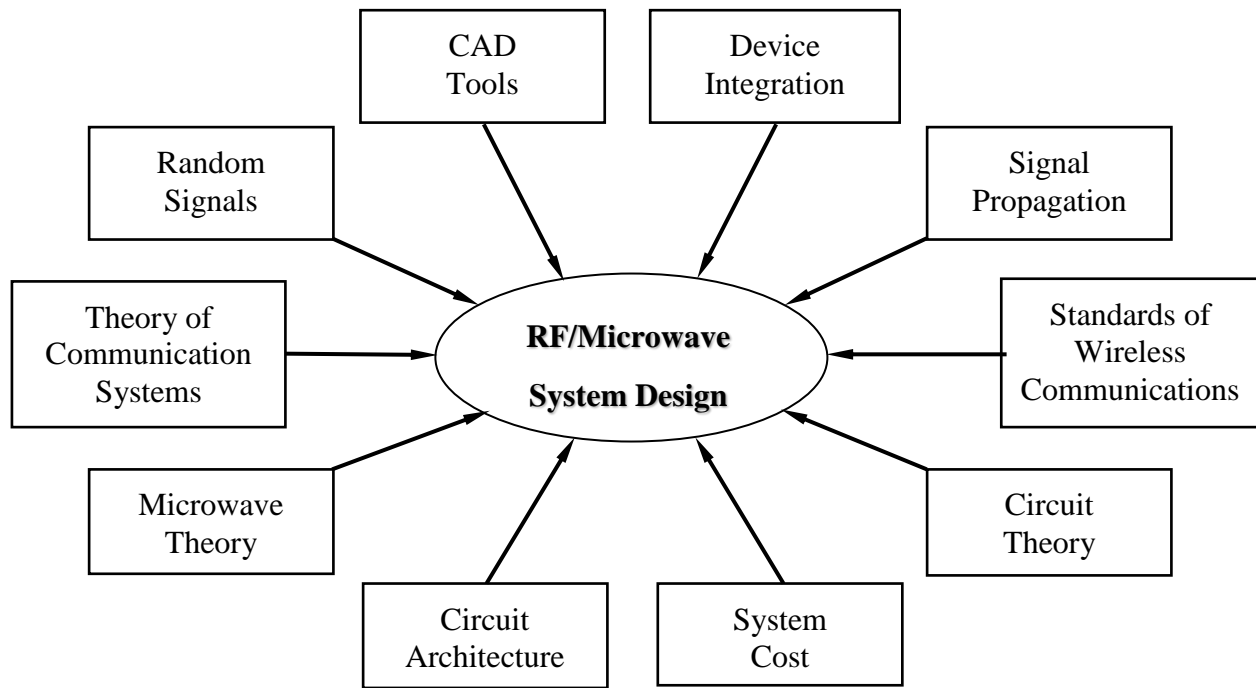


Figure I-6. Different aspects to be considered in designing a communication network.

Ever increasing demands for miniaturized microwave systems for use in wireless communications, aerospace and satellite applications led to renew intensity of interest in microwave planar systems. The availability of planar transmission line structures like microstrip lines or strip lines coupled with the rapid developments in microwave semiconductor devices and the techniques of thin film deposition and photolithography resulted in the technology of microwave integrated circuits.

Microwave Integrated Circuits (MICs) and Monolithic Microwave Integrated Circuits (MMICs) represent a quite important extension of hybrid integrated circuit technology to microwave frequencies. Microwave integrated circuits are responsible for both the extension of present markets and the opening of many new applications.

The materials you receive for this course are protected by copyright and to be used for this course only. You do not have permission to upload the course materials, including any lecture recordings you may have, to any website. If you require clarification, please consult your professor.

However, there are some difficulties associated with the use of MICs. For instance, microwave system designers had to incorporate tuners and adjustment screws in circuits like filters to optimize their performance after fabrication. Thus, device models have to be designed more accurately and CAD design, simulation and optimization techniques have therefore become a necessity.

On the other hand, the need for even more complex performance and functionalities has implied new and significant demand for “extreme” performance of RF/microwave systems. Designers have to perform systems working “at their limits” to assure maximum performance, save time-to-market and reduce costs. These new orientations in microwave CAD systems have highlighted the need for large-signal device/circuit models and techniques in order to model accurately their nonlinear behavior and to predict efficiently their nonlinear performance.

In a classical design procedure, one can start with the desired specifications and arrives at an initial system configuration. If the given specifications are not met, the system is tuned/optimized until the desired specifications are achieved. However, because of the ever-increasing complexity of modern systems, it is now crucial to utilize a Computer-aided design (CAD) approach. The CAD process consists then of three important segments, namely:

Modeling: This is the first step in any CAD process. Modeling involves characterization of various active/passive components to the extent of providing a numerical model that can be handled by the computer (or the simulator). Difficulties in modeling have limited the use of CAD techniques at microwave frequencies. Detailed simulation of active devices as well as numerical EM-based modeling of passive devices become quite involved and time consuming. Therefore, designers asked for simplified equivalent electrical circuit models and closed-form semi-empirical expressions that possess sufficient accuracy for system design. However, with the increasing complexity of microwave circuits, this approach is

The materials you receive for this course are protected by copyright and to be used for this course only. You do not have permission to upload the course materials, including any lecture recordings you may have, to any website. If you require clarification, please consult your professor.

now obsolete. Full electromagnetic (EM) effects as well as high-level nonlinear behaviors should be taken into account and included in any device model for efficient and accurate modeling process.

- Analysis:* The analysis provides the device/circuit responses to a given set of input data. Computer-aided analysis is the most developed and most widely used aspect of CAD. Mostly, microwave circuit/system analysis involves evaluation of scattering parameters (S-parameters) defined in appendix I. Another aspect related to the evaluation of system performance is the computation of system sensitivities. This involves calculation of the effect of variations in designable parameters on the system performance. The results are useful for two purposes: tolerance analysis and optimization using gradient methods.
- Optimization:* The process of iterative modifications of system parameters in order to achieve a given objective (i.e., to meet a set of given specifications) is termed as optimization. Optimization methods developed for microwave system design can be classed in two groups: gradient methods and direct search methods. In gradient methods, information about the derivatives of performance functions (with respect to designable parameters) is used to arrive at the modified set of parameters at each step in moving towards the optimum solution. These derivatives (or gradients) are obtained from the sensitivity analysis of the system at each step. Direct search methods, on the other hand, do not use gradient information and searching for the optimum solution in a systematic manner carries out the optimization. Because of the complexity involved in carrying out the sensitivity analysis for gradients methods, direct search methods are usually more popular in microwave device/circuit design.

The materials you receive for this course are protected by copyright and to be used for this course only. You do not have permission to upload the course materials, including any lecture recordings you may have, to any website. If you require clarification, please consult your professor.

After this review of computer-aided design procedures, some fundamental aspects of circuit theory must be redefined like the notions of linearity and nonlinearity, the concepts of frequency and time domain representations of a device/circuit.

C - ELEMENTS OF CIRCUIT THEORY

I - Fundamental concepts

In electronic engineering, a fundamental concept is that *all* electronic circuits/systems are nonlinear. However, a linear assumption can be used *as an approximation* for some circuits, which present very weakly nonlinear behaviors. Thus, a circuit designer has first to give answer to a basic question: *In my design, nonlinearities should be minimized or maximized?*

For example, in small-signal amplifiers, nonlinearities are responsible for phenomena that degrade the system performance (e.g., intermodulation distortions) and then should be minimized. On the other hand, mixing and frequency multiplication are possible *only if* the mixer or the frequency multiplier circuit exploits nonlinearities, and then, it is desirable to maximize nonlinearities and even to minimize some linear phenomena effects.

At this point, some terminology should be clarified. We are talking about small-signal, large-signal, linearity, nonlinearity, etc. Are these terms referring to similar concepts? Since the technical literature is often vague/confusing about these concepts, we should first define them precisely. Can we say that “nonlinear” and “large-signal” can be indifferently used to refer to the same concepts, causes and effects (and similarly between linear and small-signal)?

The materials you receive for this course are protected by copyright and to be used for this course only. You do not have permission to upload the course materials, including any lecture recordings you may have, to any website. If you require clarification, please consult your professor.

1 – Basic definitions and concepts

From a general point of view, we could say (referring to Wikipedia) that

- *Small-signal modeling* is a common analysis method used in electrical engineering to describe quasi-linear devices/behaviors in terms of linear equations. This linearization is done by first calculating (possibly by an iterative process if the circuit is complex) the DC bias point (that is, the voltage/current levels present when no signal is applied), and then forming linear approximations about this point.
- *Large-signal modeling* is a common analysis method used in electrical engineering to describe nonlinear devices/behaviors in terms of underlying nonlinear equations. Under "large signal conditions" nonlinear effects must be considered.

and from a circuit design point of view, we can say that

- *Small signal*: A small-signal circuit is a linear circuit in which the input or output signal strength does not affect the circuit's electrical properties. If we were to change the signal amplitude at the input to the amplifier, the output signal would change proportionally.
- *Large signal*: Opposite of small signal. For instance, a small-signal amplifier can be easily designed using S-parameters while power amplifiers cannot.

while from a signal point of view, we have

- *Small signal*: in small time-varying signals carried over a constant bias, the signal is small relative to the nonlinearity of the device.
- *Large signal*: in large time-varying signals carried over a constant bias, the signal is large enough so that the nonlinearity of the device cannot be ignored.

The materials you receive for this course are protected by copyright and to be used for this course only. You do not have permission to upload the course materials, including any lecture recordings you may have, to any website. If you require clarification, please consult your professor.

As for the concepts of linear and nonlinear, we can read that (again from Wikipedia)

- *Linear circuit*: electronic circuit whose output is a linear transform of its input. Superposition principle can be applied to satisfy the circuit behavior.
- *Nonlinear circuit*: a circuit which does not satisfy the superposition principle. Technically, a nonlinear system is any system where the variable(s) to be solved for cannot be written as a linear sum of independent elements.

Transposed to device modeling, we can say that small-signal or linear models are used to evaluate stability, linear gain, noise and bandwidth. As long as the signal is small relative to the nonlinearities of the device, the derivatives do not vary significantly, and can be treated as standard linear circuit elements. It can be solved directly.

Large-signal models are required for circuits that operate in large-signal regime such as power amplifiers and mixers.

Finally, from the simulation point of view

- Linear simulation means solving a linear circuit by LU decomposition and forward/backward substitution.
- Nonlinear simulation means solving a nonlinear circuit iteratively (e.g., by Newton iterations).

2 – Definition of linearity and nonlinearity in circuit theory

As illustration, let us consider the nonlinear characteristic of a two-port network shown in Figure I-7. If an input signal V_i imposes a small excursion around the DC operating point (Q point), the curve A₁B₁ is almost linear.

The materials you receive for this course are protected by copyright and to be used for this course only. You do not have permission to upload the course materials, including any lecture recordings you may have, to any website. If you require clarification, please consult your professor.

Therefore, the response V_o is linearly deduced from the input by

$$V_o = G V_i \quad (\text{I-1})$$

where G is called the small signal gain. This behavior defines the linearity concept where the excitation is assimilated to a “small signal” (“small signal approach”).

On the other hand, if the magnitude of the input signal V_i is high (Q point excursion over the arc A_2B_2), the network response cannot be deduced from equation (I-1) and the terms of higher orders of the signal V_i must be taken into account to accurately describe the output signal V_o .

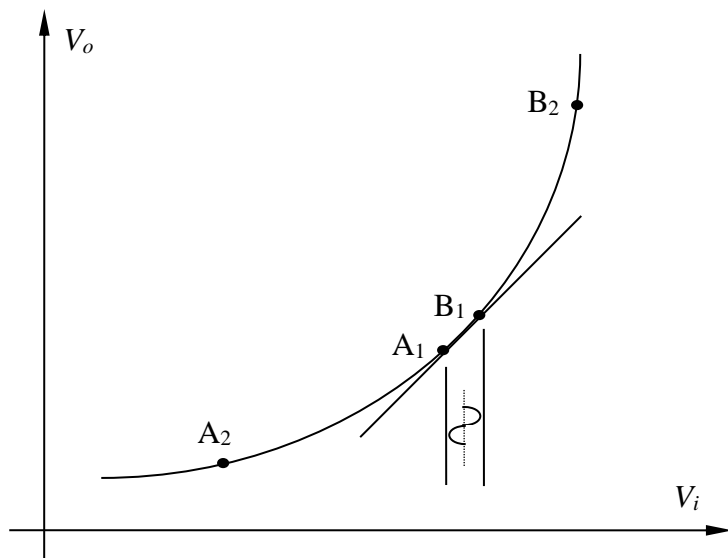


Figure I-7. Nonlinear transfer characteristic of a two-port network.

The materials you receive for this course are protected by copyright and to be used for this course only. You do not have permission to upload the course materials, including any lecture recordings you may have, to any website. If you require clarification, please consult your professor.

3 – Frequency generation

In the above Figure, the input-output relationship for the nonlinear case can be expressed as

$$V_o = AV_i + BV_i^2 + CV_i^3 + \dots \quad (\text{I-2})$$

The number of terms to consider is related to the magnitude of V_i . The use of trigonometric relations shows that each m^{th} term " $(V_i)^m$ " generates the harmonic mf_i of the fundamental input frequency f_i . This is the concept of "large signal" ("large signal approach").

A way of showing how new frequencies are generated in nonlinear circuits is to describe the input-output relationship via a power series and to assume a multi-tone excitation voltage. If we assume now that V_i is a two-tone excitation of the form:

$$V_i = v_i(t) = V_1 \cos(\omega_1 t) + V_2 \cos(\omega_2 t) \quad (\text{I-3})$$

Substituting this value in equation (I-2) gives, for the first term:

$$V_{oA} = v_{oA}(t) = A v_i(t) = AV_1 \cos(\omega_1 t) + AV_2 \cos(\omega_2 t) \quad (\text{I-4})$$

After performing the same for the second and third terms, we obtain

$$V_{oB} = v_{oB}(t) = B v_i^2(t) = \frac{1}{2} B \left\{ \begin{array}{l} V_1^2 + V_2^2 + V_1^2 \cos(2\omega_1 t) + V_2^2 \cos(2\omega_2 t) + \\ 2V_1 V_2 [\cos((\omega_1 + \omega_2)t) + \cos((\omega_1 - \omega_2)t)] \end{array} \right\} \quad (\text{I-5})$$

$$V_{oC} = v_{oC}(t) = C v_i^3(t) = \frac{1}{2} C \left\{ \begin{array}{l} V_1^3 \cos(3\omega_1 t) + V_2^3 \cos(3\omega_2 t) + \\ 3V_1^2 V_2 [\cos((2\omega_1 + \omega_2)t) + \cos((2\omega_1 - \omega_2)t)] + \\ 3V_2^2 V_1 [\cos((2\omega_2 + \omega_1)t) + \cos((2\omega_2 - \omega_1)t)] + \\ 3[V_1^3 + 2V_1 V_2^2 \cos(\omega_1 t)] + 3[V_2^3 + 2V_2 V_1^2 \cos(\omega_2 t)] \end{array} \right\} \quad (I-6)$$

We can see that a remarkable number of new frequencies have been generated. If a fourth- or fifth-degree of nonlinearity is included, the number of new frequencies will be even higher. The conceptual complexity of even simple nonlinearity is clearly highlighted.

4 – Commensurate and non-commensurate frequencies

A closer examination of the generated frequencies in equations (I-4) through (I-6) shows that all occur at a linear combination of the two excitation frequencies; in effect, at the frequencies:

$$\omega_{output} = \omega_{m,n} = m\omega_1 + n\omega_2 \quad (I-7)$$

where $m, n = \dots, -2, -1, 0, 1, 2, \dots$. $\omega_{m,n}$ is usually called the mixing frequency and the output voltage component at that frequency is called a mixing product. The sum of the absolute values of m and n is called the order of the mixing product. For the $\omega_{m,n}$ to be distinct, ω_1 and ω_2 must be non-commensurate: a pair of frequencies is commensurate if their ratio is a rational number, and the entire set is commensurate if all possible pairs are commensurate. It is usually assumed that the frequencies are non-commensurate when two or more arbitrary excitation frequencies exist.

5 – Properties and applications of nonlinear phenomena

The materials you receive for this course are protected by copyright and to be used for this course only. You do not have permission to upload the course materials, including any lecture recordings you may have, to any website. If you require clarification, please consult your professor.

a- Harmonic generation

One of the most obvious properties of a nonlinear system is its generation of harmonics of the excitation frequency. The m th harmonic of an excitation frequency is the m th-order mixing frequency. In some systems, like transmitters, harmonics and other spurious outputs may interfere with other communication systems and must be reduced.

b- Intermodulation

All the mixing frequencies in equations (I-4) through (I-6) that arise as linear combinations of two or more tones are called intermodulation (IM) products. IM products generated in an amplifier often present a serious problem because they represent spurious signals that interfere with, and can be mistaken for, desired signals.

Even-order IM products usually occur at frequencies well above or below the signals that generate them and then are often of little concern. The IM products of greatest concern are usually the third-order ones that occur at $2\omega_1 - \omega_2$ and $2\omega_2 - \omega_1$, because they are the strongest of all odd-order products, are close to the signals that generate them, and often cannot be rejected by filtering.

c- Saturation and desensitization

The excitation frequency output voltage in the above example is a function of power series terms other than the linear one. From equations (I-4) through (I-6), we find that the output voltage component at ω_1 is

$$v_{o1}(t) = \{AV_1 + 3CV_1^3\} \cos(\omega_1 t) \quad (\text{I-8})$$

If the coefficient C of the cubic term is negative, the response voltage saturates: it does not increase at a rate proportional to the increase in excitation input voltage. Saturation occurs in all circuits because the available output power is finite. If a circuit such as an amplifier is excited by a large and a small signal, and the large signal drives the circuit into saturation, gain is decreased for the weak signal as well. Saturation, therefore, causes a decrease in system sensitivity.

d- Cross modulation

Cross modulation is the transfer of modulation from one signal to another in a nonlinear circuit. To illustrate this concept, let us assume that the excitation signal is

$$v_i(t) = V_1 \cos(\omega_1 t) + \{1 + m(t)\} V_2 \cos(\omega_2 t) \quad (\text{I-9})$$

where $m(t)$ is a modulating waveform with $m(t) > -1$. The above equation describes a combination of an unmodulated carrier and an amplitude modulated signal. Substituting this excitation signal into the output signal in equation (I-2), gives an expression similar to the third-degree term at ω_1

$$V_{oC} = v_{oC}(t) = 3CV_1V_2^2 \{1 + 2m(t) + m^2(t)\} \cos(\omega_1 t) \quad (\text{I-10})$$

The materials you receive for this course are protected by copyright and to be used for this course only. You do not have permission to upload the course materials, including any lecture recordings you may have, to any website. If you require clarification, please consult your professor.

which shows that a distorted version of the modulation of the ω_2 signal has been transferred to the ω_1 carrier.

e- AM/PM conversion

AM/PM conversion is a phenomenon wherein changes in the amplitude of a signal applied to a nonlinear circuit cause a phase shift. This form of distortion can have serious consequences if it occurs in a system in which the signal's phase is important (e.g., phase-modulate communication systems). The output response at ω_1 frequency

$$v_{o1}(t) = \{AV_1 + 3CV_1^3\} \cos(\omega_1 t) \quad (\text{I-11})$$

shows that the first-and third-order output voltage components may be not in phase. This possibility is not predicted by equations (I-2) through (I-6) because these equations describe a memory-less nonlinearity. It is however possible for a phase difference to exist in a circuit having capacitive nonlinearities. The response is then the vector sum of two phasors

$$V_{o1}(\omega_1) = AV_1 + 3CV_1^3 \exp(j\theta) \quad (\text{I-12})$$

with θ the phase difference. Even if this phase difference remains constant with amplitude, the phase of the output voltage changes with variations in the excitation signal. Moreover, AM/PM conversion will be most serious as the circuit is driven into saturation.

f- Spurious responses

We saw that if the excitation signal is strong (or if the nonlinearity is significant), its harmonics are generated. In the two-tone case, the circuit has spurious responses at any frequency that satisfies the relation (I-7). Applied to mixers, this relation

$$\omega_{IF} = m\omega_{RF} + n\omega_{LO} \quad (\text{I-13})$$

shows that spurious responses are a form of two-tone intermodulation wherein one of the tones is the local oscillator.

II – Microwave circuits

I – Linear circuit

A linear circuit is defined as a circuit for which the superposition principle holds. Specifically, if excitations x_1 and x_2 are applied separately to a linear circuit having responses y_1 and y_2 , respectively, the response to the excitation $\{ ax_1 + bx_2 \}$ is $\{ ay_1 + by_2 \}$, where a and b are arbitrary real or complex constants or even time varying. This superposition concept can also be illustrated as follows: Let assume that the above two-port network (Figure I-3) has two solutions $[\mathbf{V}_1] = [V_{i1}, V_{o1}]^t$ and $[\mathbf{V}_2] = [V_{i2}, V_{o2}]^t$. In this case, the vector $\{ \lambda [\mathbf{V}_1] \}$ (λ is an arbitrary non-null complex variable) and the vector sum $\{ [\mathbf{V}_1] + [\mathbf{V}_2] \}$ are also solutions of the system. In fact, let us consider the impedance matrix $[\mathbf{Z}]$ of the two-port network and let $[\mathbf{I}]$ be the current vector across the input-output ports. We have

$$[\mathbf{V}] = [\mathbf{Z}(\mathbf{I})] [\mathbf{I}] \quad (\text{I-14})$$

The materials you receive for this course are protected by copyright and to be used for this course only. You do not have permission to upload the course materials, including any lecture recordings you may have, to any website. If you require clarification, please consult your professor.

Any couple $\{ [\mathbf{V}], [\mathbf{I}] \}$ is then solution. In fact, we can fix arbitrary the currents (vector $[\mathbf{I}]$) and deduce the voltages (vector $[\mathbf{V}]$). The impedance matrix $[\mathbf{Z}]$ is then homogeneous in $[\mathbf{I}]$ of zero degree and $\{ \lambda[\mathbf{I}], \lambda[\mathbf{V}] \}$ are also solutions. So

$$\lambda [\mathbf{V}] = [\mathbf{Z}(\lambda\mathbf{I})] \lambda [\mathbf{I}] \quad (\text{I-15})$$

Moreover, let $[\mathbf{0}]$ be the zero matrix. Then

$$\{ [\mathbf{Z}(\lambda\mathbf{I})] - [\mathbf{Z}(\mathbf{I})] \} [\mathbf{I}] = [\mathbf{0}] \quad (\text{I-16})$$

As the excitation is arbitrary, we have

$$[\mathbf{Z}(\lambda\mathbf{I})] = [\mathbf{Z}(\mathbf{I})] \quad \forall [\mathbf{I}] \quad (\text{I-17})$$

On the other hand, if $[\mathbf{I}_1]$ and $[\mathbf{I}_2]$ are two arbitrary solutions, we have

$$[\mathbf{V}_1] = [\mathbf{Z}(\mathbf{I}_1)] [\mathbf{I}_1] \quad \text{and} \quad [\mathbf{V}_2] = [\mathbf{Z}(\mathbf{I}_2)] [\mathbf{I}_2] \quad (\text{I-18})$$

This implies, $\forall [\mathbf{I}_1]$ and $[\mathbf{I}_2]$, that

$$\{ [\mathbf{V}_1] + [\mathbf{V}_2] \} = [\mathbf{Z}(\mathbf{I}_1)] [\mathbf{I}_1] + [\mathbf{Z}(\mathbf{I}_2)] [\mathbf{I}_2] = [\mathbf{Z}(\mathbf{I}_1 + \mathbf{I}_2)] \{ [\mathbf{I}_1] + [\mathbf{I}_2] \} \quad (\text{I-19})$$

The global response to N linear excitations is then equal to the sum of the N elementary responses. In other words, the response of a linear circuit includes only those frequencies present in the excitation waveforms (Figure I-8).

A linear circuit does not generate new frequencies.

The materials you receive for this course are protected by copyright and to be used for this course only. You do not have permission to upload the course materials, including any lecture recordings you may have, to any website. If you require clarification, please consult your professor.

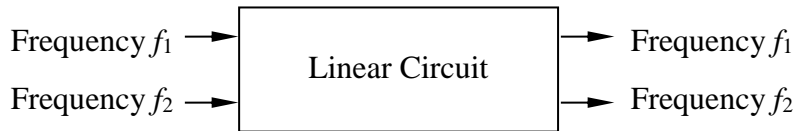


Figure I-8. Frequency response of a linear circuit

2 – Nonlinear circuit

A nonlinear circuit could be characterized as either strongly or weakly nonlinear circuit depending of the Q point excursion (arc A₂B₂ in Figure I-3). A weakly nonlinear circuit can be described with adequate accuracy by a few terms of a power series expansion of its characteristic.

Therefore, it is assumed that the nonlinearities in a weakly nonlinear circuit are weak enough that the DC operating point is not significantly perturbed (arc A₂B₂ slightly larger than A₁B₁).

Virtually, all active and passive components satisfy this definition if the excitation voltages are well within the components' *normal operating ranges* (slightly beyond the linear operation conditions). Then, another concept used for weak nonlinear circuits is the quasi-linearity. A quasi-linear circuit is one that can be treated for most purposes as a linear circuit, although it may include weak nonlinearities (e.g., intermodulation distortions in amplifiers).

The nonlinearities are weak enough that their effect on the linear part of the circuit's response is negligible. However, the circuit may generate distortion products that often are great enough to be of concern. A small signal transistor amplifier is an example of a quasi-linear circuit, as is a Class A power amplifier that is not driven into saturation. Thus, the response of a nonlinear circuit includes the excitation frequencies and all possible combination of them (Figure I-9).

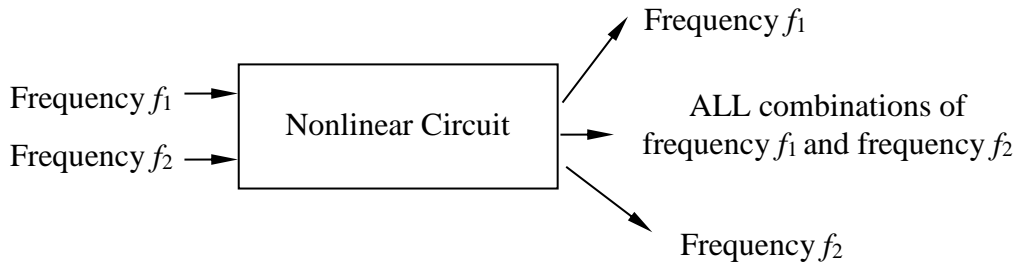


Figure I-9. Frequency response of a linear circuit

3 – Representation of a nonlinear circuit

Physical representation of a nonlinear system is in time domain. However, as the nonlinear behavior generate harmonics, it is common to represent a nonlinear network in the frequency domain. In this case, the nonlinear network is equivalent to a multifrequency multi-port network where each k th port is related to the k th harmonic of the excitation input frequency f . A current I_k and a voltage V_k present in this port are the Fourier coefficients respectively of $v(t)$ and $i(t)$ for the harmonic " kf ".

As illustration, a one-port network is represented in Figure I-10. A port "0" can be added for the zero frequency (DC coefficients).

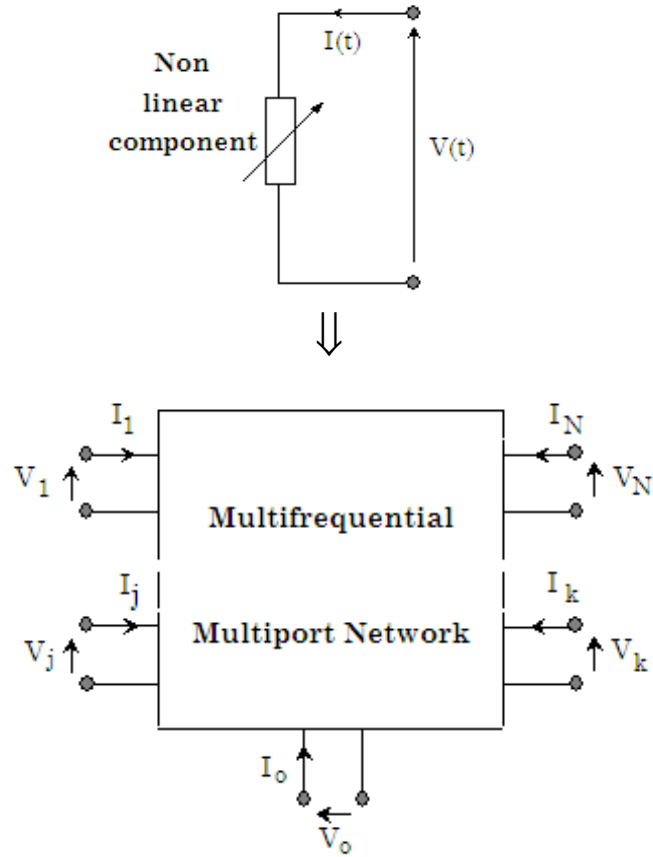


Figure I-10. Representation of a nonlinear dipole.

In this multifrequency multi-port, the sign ↑ refers to a nonlinear element.

APPENDIX I-1

LETTER DESIGNATIONS OF MICROWAVE BANDS

Name	FREQUENCY (GHz)			
	Radio Engin. (1)	US Navy (2)	RSGB (3)	
I		0.100 - 0.150		
G		0.150 - 0.225		
P	0.225 - 0.390	0.225 - 0.390		
L	0.390 - 1.550	0.390 - 1.550	1.000 - 2.000	
S	1.550 - 5.200	1.550 - 3.900	2.000 - 4.000	
C	3.900 - 6.200	3.900 - 6.200	4.000 - 8.000	
X	5.200 - 10.900	6.200 - 10.900	8.000 - 12.000	
K	K _u	10.900 - 15.350 - 17.250	10.900 - 15.250 - 17.250	18.000 - 12.000 - 18.000
	K _a	36.000	36.000 - 33.000 - 36.000	26.500 - 26.500 - 40.000
Q	36.000 - 46.000	36.000 - 46.000	30.000 - 50.000	
U			40.000 - 60.000	
V	46.000 - 56.000	46.000 - 56.000	50.000 - 75.000	
E			60.000 - 90.000	
W	56.000 - 100.000	56.000 - 100.000	75.000 - 110.000	
F			90.000 - 140.000	
D			110.000 - 170.000	

The materials you receive for this course are protected by copyright and to be used for this course only. You do not have permission to upload the course materials, including any lecture recordings you may have, to any website. If you require clarification, please consult your professor.

Different sources have used different frequency boundaries for letter designation of the microwave bands. Three of those are shown here:

- (1) *Reference Data for Radio Engineers*, 5th Ed., H.W. Sams & Co., Inc., Indianapolis, IN, 1970.
- (2) *US Navy Submarine Spectrum* <http://mintaka.spawar.navy.mil/ftp/pmw173/APX-C.pdf>.
- (3) *Radio Society of Great Britain* <http://www.rsgb.org.uk/society/uwinfo/uwfaq6.htm>

The materials you receive for this course are protected by copyright and to be used for this course only. You do not have permission to upload the course materials, including any lecture recordings you may have, to any website. If you require clarification, please consult your professor.

APPENDIX I-2

SCATTERING MATRIX

A – S MATRIX IN THE MICROWAVE FIELD

I - What are scattering parameters?

"Scattering" is an idea taken from billiards. One takes a cue ball and fires it up the table at a collection of other balls. After the impact, the energy and momentum in the cue ball is divided between all the balls involved in the impact. The cue ball "scatters" the stationary target balls and in turn is deflected or "scattered" by them.

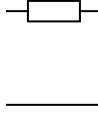
In a microwave circuit, the equivalent to the energy and momentum of the cue ball is the amplitude and phase of an incoming wave on a transmission line. This incoming wave is "scattered" by the circuit and its energy is partitioned between all the possible outgoing waves on all the other transmission lines connected to the circuit. The scattering parameters are fixed properties of the (linear) circuit, which describe how the energy couples between each pair of ports or transmission lines connected to the circuit. Formally, S-parameters can be defined for any collection of linear electronic components, whether or not the wave view of the power flow in the circuit is necessary. They are algebraically related to the impedance parameters (Z-parameters), to the admittance parameters (Y-parameters), and to notional characteristic impedance of the transmission lines.

The materials you receive for this course are protected by copyright and to be used for this course only. You do not have permission to upload the course materials, including any lecture recordings you may have, to any website. If you require clarification, please consult your professor.

II - Why scattering parameters?

I - Impedance and admittance matrices are not defined for all circuits

Serial impedance: Using Z-parameters, serial impedance is defined as

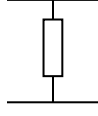
$$Z_{11} = \left. \frac{V_1}{I_1} \right|_{I_2=0}$$


But

$$I_2 = 0 \rightarrow I_1 = 0 \rightarrow Z_{11} = ????$$

In this case, it is not possible to define Z_{11} using the classical Z-parameters.

Parallel admittance: Using Y-parameters, parallel admittance is defined as

$$Y_{11} = \left. \frac{I_1}{V_1} \right|_{V_2=0}$$


But since

$$V_2 = 0 \rightarrow V_1 = 0 \rightarrow Y_{11} = ????$$

In this case, it is not possible to define Y_{11} using the classical Y-parameters.

⇒ The well-known Z- or Y-parameters are not universal.

2 - In HF, both voltages and currents cannot be measured in a direct manner

In high frequencies, the quantities that are directly measurable, by means of a small probe used to sample the relative field strength, are the standing wave ratio, the location of a field minimum, and the power. The two first lead directly to knowledge of the reflection coefficient. The measurement of power is needed only if the absolute value of the field in the device needs to be known. Another parameter that is directly measurable is the transmission coefficient.

3 - Short and open circuits cannot be assured accurately in high frequencies

So designers have to use parameters that are linked to power and reflection-transmission effects

III - Definitions

A N -port microwave network has N arms into which power can be fed and from which power can be taken. In general, power can get from any arm (as input) to any other arm (as output). There are thus N incoming waves and N outgoing waves. We also observe that power can be reflected by a port, so the input power to a single port can partition between all the ports of the network to form outgoing waves.

Associated with each port is the notion of a "reference plane" at which the wave amplitude and phase are defined. Usually the reference plane associated with a certain port is at the same place with respect to incoming and outgoing waves.

The N incoming wave complex amplitudes are usually designated by the N complex quantities a_N , and the N outgoing wave complex quantities are designated by the N complex quantities b_N .

The materials you receive for this course are protected by copyright and to be used for this course only. You do not have permission to upload the course materials, including any lecture recordings you may have, to any website. If you require clarification, please consult your professor.

The incoming wave quantities are assembled into an N -vector **[a]** and the outgoing wave quantities into an N -vector **[b]**.

The outgoing waves are expressed in terms of the incoming waves by the matrix equation

$$\begin{bmatrix} b_1 \\ \vdots \\ b_N \end{bmatrix} = \begin{bmatrix} S_{11} & \cdots & S_{1N} \\ \vdots & \ddots & \vdots \\ S_{N1} & \cdots & S_{NN} \end{bmatrix} \begin{bmatrix} a_1 \\ \vdots \\ a_N \end{bmatrix} \quad (\text{AI4-1})$$

where **[S]** is an $N \times N$ complex matrix called the "scattering matrix". It completely determines the behaviour of the network. In general, its elements, termed as "S-parameters", are all frequency-dependent. For example, the matrix equations for a 2-port network are

$$b_1 = S_{11} a_1 + S_{12} a_2 \quad (\text{AI4-2})$$

$$b_2 = S_{21} a_1 + S_{22} a_2 \quad (\text{AI4-3})$$

IV – How to obtain the S-matrix?

Let us consider a generator (a voltage source E with an internal impedance Z equal to the characteristic impedance Z_o). If this one-port circuit is loaded by an impedance Z_L (Figure AI4-1), the complex current and voltage can be defined as

$$I = \frac{E}{Z_o + Z_L} \quad V = \frac{EZ_L}{Z_o + Z_L} \quad (\text{AI4-4})$$

For maximum transfer power (matching), the impedance load is equal to the complex conjugate of the generator internal impedance. Therefore,

$$I = I_i = \frac{E}{Z_o + Z_o^*} \quad \text{and} \quad V = V_i = \frac{EZ_o^*}{Z_o + Z_o^*} \quad (\text{AI4-5})$$

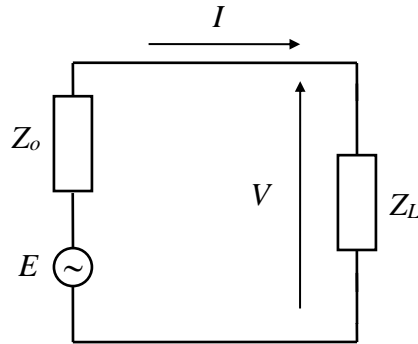


Figure AI4-1. One-port circuit.

Similarly, we can define the reflection parameters as

$$I_r = I_i - I \quad \text{and} \quad V_r = V - V_i \quad (\text{AI4-6})$$

or by using only the incident parameters

$$I_r = \frac{Z_L - Z_o^*}{Z_L + Z_o^*} \cdot I_i \quad \text{and} \quad V_r = \frac{Z_o Z_L - Z_o^*}{Z_o^* Z_L + Z_o} \cdot V_i \quad (\text{AI4-7})$$

These expressions allow defining the current reflection coefficient Γ_I and the voltage coefficient reflection Γ_V

$$\Gamma_I = \frac{I_r}{I_i} = \frac{Z_L - Z_o^*}{Z_L + Z_o} \quad \text{and} \quad \Gamma_V = \frac{V_r}{V_i} = \frac{Z_o Z_L - Z_o^*}{Z_o^* Z_L + Z_o} \quad (\text{AI4-8})$$

If the impedance Z_o is real and equal to R_o , then

$$\Gamma = \Gamma_I = \Gamma_V = \frac{Z_L - R_o}{Z_L + R_o} = \frac{z_L - 1}{z_L + 1} \quad (\text{AI4-9})$$

where z_L is the normalized impedance of Z_L . From the above equations we obtain

$$V_r = Z_o I_r \quad V_i = Z_o^* I_i \quad (\text{AI4-10})$$

This concept can be generalized to a N -port network:

$$[V_r] = [Z_o] [I_r] \quad [V_i] = [Z_o^*] [I_i] \quad (\text{AI4-11})$$

Thus, it is possible to define a vector **[a]** of input waves or « *incident waves* » as follows

$$[a] = \left(\frac{[Z_o] + [Z_o^*]}{2} \right)^{\frac{1}{2}} [I_i] \quad (\text{AI4-12})$$

$$\rightarrow \begin{bmatrix} a_1 \\ \vdots \\ a_N \end{bmatrix} = \begin{bmatrix} \sqrt{R_{o1}} & \cdots & 0 \\ \vdots & \ddots & \vdots \\ 0 & \cdots & \sqrt{R_{oN}} \end{bmatrix} \begin{bmatrix} I_{i1} \\ \vdots \\ I_{iN} \end{bmatrix} \quad (\text{AI4-13})$$

Similarly, we can define a vector **[b]** of output waves or « *reflected waves* » as

$$[\mathbf{b}] = \left(\frac{[\mathbf{Z}_o] + [\mathbf{Z}_o^*]}{2} \right)^{\frac{1}{2}} [\mathbf{I}_r] \quad (\text{AI4-14})$$

Finally, the scattering matrix **[S]** of the network should satisfy to the relation (AI4-1) with

$$[\mathbf{b}] = [\mathbf{S}] [\mathbf{a}] \quad (\text{AI4-15})$$

Note: If the network has internal independent generators, a wave vector **[c]** must be included in the above relation to show that the output waves **[b]** are the sum of the input waves **[a]** and those generated by the internal independent generators

$$[\mathbf{b}] = [\mathbf{S}] [\mathbf{a}] + [\mathbf{c}] \quad (\text{AI4-16})$$

B – PHYSICAL MEANING OF S-PARAMETERS

In the case of a microwave network having two ports only, an input and an output, the **S** matrix has four S-parameters. These four complex quantities actually contain eight separate numbers; the real and imaginary parts, or the modulus and the phase angle, of each of the four complex scattering parameters.

The materials you receive for this course are protected by copyright and to be used for this course only. You do not have permission to upload the course materials, including any lecture recordings you may have, to any website. If you require clarification, please consult your professor.

Let us consider the physical meaning of these S -parameters. If the output port 2 is terminated, that is, the transmission line is connected to a matched load impedance giving rise to no reflections, then there is no input wave on port 2. The input wave on port 1 (a_1) gives rise to a reflected wave at port 1 ($S_{11} \cdot a_1$) and a transmitted wave at port 2 that is absorbed in the termination on 2. The transmitted wave size is ($S_{21} \cdot a_1$). If the network has no loss and no gain, the output power must equal the input power and so in this case

$$|S_{11}|^2 + |S_{21}|^2 = 1 \quad (\text{AI4-17})$$

We see therefore that the sizes of S_{11} and S_{21} determine how the input power splits between the possible output paths. Let us consider a two-port network loaded by Z_1 and Z_2 respectively (Figure AI4-2) where the input and output port are matched by the characteristic impedances Z_{o1} and Z_{o2} respectively.

The incident and reflected waves at the input/output ports are related as

$$b_1 = S_{11}a_1 + S_{12}a_2 \quad (\text{AI4-18})$$

and

$$b_2 = S_{21}a_1 + S_{22}a_2 \quad (\text{AI4-19})$$

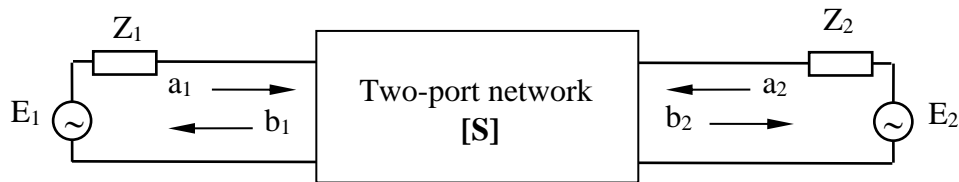


Figure AI4-2: Incident and reflected waves in a two-port network.

Using equations (AI4-18) and (AI4-19) each term of the S matrix can be defined as

$$S_{11} = \frac{b_1}{a_1} \Big|_{a_2=0} \quad S_{21} = \frac{b_2}{a_1} \Big|_{a_2=0}$$

$$S_{22} = \frac{b_2}{a_2} \Big|_{a_1=0} \quad S_{12} = \frac{b_1}{a_2} \Big|_{a_1=0}$$

- S_{11} is the input reflection coefficient when the output is matched ($Z_2 = Z_{o2}$).
- S_{22} is the output reflection coefficient when the input is matched ($Z_1 = Z_{o1}$).
- S_{21} is the direct transmission coefficient from input to output when the output is matched.
- S_{12} is the inverse transmission coefficient from output to input when the input is matched.

C - RELATION WITH POWER

We can relate between waves (incident and reflected) and power:

$|a_1|^2$: Incident power on port 1 = Available power from the source

The materials you receive for this course are protected by copyright and to be used for this course only. You do not have permission to upload the course materials, including any lecture recordings you may have, to any website. If you require clarification, please consult your professor.

$|a_2|^2$: Incident power on port 2 = Available power from the load

$|b_1|^2$: Reflected power from port 1 = Available power from the source minus input power

$|b_2|^2$: Reflected power from port 2 = Incident power to the load

$$\begin{aligned} \rightarrow |S_{11}|^2 & \frac{\text{Power reflected from the network input}}{\text{Incident power on the network input}} \\ \rightarrow |S_{22}|^2 & \frac{\text{Power reflected from the network output}}{\text{Incident power on the network output}} \\ \rightarrow |S_{12}|^2 & \frac{\text{Power delivered to the source}}{\text{Power available from the load}} = \text{Reverse Power Gain} \\ \rightarrow |S_{21}|^2 & \frac{\text{Power delivered to the load}}{\text{Power available from the source}} = \text{Direct Power Gain} \end{aligned}$$

The square of S_{21} magnitude is equal to *the power gain* when the output is matched:

$$|S_{21}|^2 = \frac{P_{L2}}{P_{S1}} = \frac{\frac{1}{2}|b_2|^2}{\frac{1}{2}|a_1|^2} \Bigg|_{a_2=0} \quad (\text{AI4-20})$$

Note: S_{21} relates power OUT of 2 to power IN to 1, and not the inverse. In general, the S-parameters tell us how much power "comes back" or "comes out" when we "throw power at" a network. They also contain phase shift information.

D – STABILITY

If a 1-port network has reflection gain, its S-parameter has size or modulus greater than unity. More power is reflected than is incident. The power usually comes from a dc power supply; Gunn diodes can be used as amplifiers in combination with circulators that separate the incoming and outgoing waves. Suppose the reflection gain from our 1-port is S_{11} , having modulus bigger than unity.

If the 1-port is connected to a transmission line with load impedance having reflection coefficient Γ_1 , then oscillations may well occur if $\Gamma_1 * S_{11}$ is bigger than unity. If an amplifier has either S_{11} or S_{22} greater than unity, then it is quite likely to oscillate or go unstable for some values of source or load impedance. If an amplifier (large S_{21}) has S_{12} that is not negligibly small, and if the output and input are mismatched, round trip gain may be greater than unity giving rise to oscillation. If the input line has a generator mismatch with reflection coefficient Γ_1 , and the load impedance on port 2 is mismatched with reflection coefficient Γ_2 , potential instability happens if $\Gamma_1 * S_{12} * \Gamma_2 * S_{21}$ is greater than unity.

E – NETWORK PROPERTIES

The S matrix is very useful for designers to highlight some network properties:

- Matched network:

$$S_{ii} = 0 \quad (\text{AI4-21})$$

The materials you receive for this course are protected by copyright and to be used for this course only. You do not have permission to upload the course materials, including any lecture recordings you may have, to any website. If you require clarification, please consult your professor.

- Reciprocal network:

$$S_{ij} = S_{ji} \quad \text{for} \quad i \neq j. \quad (\text{AI4-22})$$

- Lossless network.

$$\begin{aligned} \sum_i (|a_i|^2 - |b_i|^2) &= 0 \rightarrow [\mathbf{a}]^t * [\mathbf{a}] = [\mathbf{b}]^t * [\mathbf{b}] \\ \rightarrow [\mathbf{S}]^t * [\mathbf{S}] &= [\mathfrak{I}] \text{ with } [\mathfrak{I}] \text{ the identity matrix} \end{aligned} \quad (\text{AI4-23})$$

F – TRANSFER SCATTERING MATRIX

The transfer scattering matrix of a two-port, or $[\mathbf{T}]$ matrix, is defined by

$$\begin{bmatrix} b_1 \\ a_1 \end{bmatrix} = \begin{bmatrix} T_{11} & T_{12} \\ T_{21} & T_{22} \end{bmatrix} \begin{bmatrix} a_2 \\ b_2 \end{bmatrix} \quad (\text{AI4-24})$$

This matrix is efficient and useful for obtaining the overall scattering matrix of a cascade connection of two two-ports as it links between the waves at the input port and those at the output port

$$b_2 = T_{11}a_1 + T_{12}b_1 \quad (\text{AI4-25})$$

$$a_2 = T_{21}a_1 + T_{22}b_1 \quad (\text{AI4-26})$$

[S] and [T] matrices are related by the following relations:

$$[\mathbf{S}] = \begin{bmatrix} \frac{T_{12}}{T_{22}} & \frac{1}{T_{22}} \\ \frac{T_{11}T_{22} - T_{12}T_{21}}{T_{22}} & -\frac{T_{21}}{T_{22}} \end{bmatrix} \quad (\text{AI4-27})$$

and

$$[\mathbf{T}] = \begin{bmatrix} \frac{S_{12}S_{21} - S_{11}S_{22}}{S_{21}} & -\frac{S_{22}}{S_{21}} \\ \frac{S_{21}}{S_{21}} & \frac{1}{S_{21}} \\ \frac{S_{11}}{S_{21}} & \frac{1}{S_{21}} \end{bmatrix} \quad (\text{AI4-28})$$

G – RELATIONSHIPS BETWEEN [Z], [Y] AND [S] MATRICES

Relationships between scattering matrix and other representation matrices like impedance and admittance matrices are often used.

$$[\mathbf{S}] = \sqrt{[\mathbf{Y}_o]} \{ [\mathbf{Z}] - [\mathbf{Z}_o] \} \{ [\mathbf{Z}] + [\mathbf{Z}_o] \}^{-1} \sqrt{[\mathbf{Z}_o]} \quad (\text{AI4-29})$$

$$[\mathbf{S}] = \sqrt{[\mathbf{Z}_o]} \{ [\mathbf{Y}_o] - [\mathbf{Y}] \} \{ [\mathbf{Y}_o] + [\mathbf{Y}] \}^{-1} \sqrt{[\mathbf{Y}_o]} \quad (\text{AI4-30})$$

$$[\mathbf{Z}] = \sqrt{[\mathbf{Z}_o]} \{ [\mathbf{S}] + [\mathbf{S}] \} \{ [\mathbf{S}] - [\mathbf{S}] \}^{-1} \sqrt{[\mathbf{Z}_o]} \quad (\text{AI4-31})$$

$$[\mathbf{Y}] = \sqrt{[\mathbf{Y}_o]} \{ [\mathbf{S}] - [\mathbf{S}] \} \{ [\mathbf{S}] + [\mathbf{S}] \}^{-1} \sqrt{[\mathbf{Y}_o]} \quad (\text{AI4-32})$$

The materials you receive for this course are protected by copyright and to be used for this course only. You do not have permission to upload the course materials, including any lecture recordings you may have, to any website. If you require clarification, please consult your professor.

where $[Z_0]$ and $[Y_0]$ are diagonal matrices with diagonal elements given by the characteristic impedances Z_{ok} at various ports of the network. $[I]$ is the identity matrix.

I - Generalized relations

In the above relations, the characteristic impedances Z_{ok} are assumed to be real (which is almost the case in practical cases). But, in some more complex cases, where the characteristic impedances are complex, these relations can be generalized.

Then, for S_{ij} - Z_{ij} relationships:

$$S_{11} = \frac{(Z_{22} + Z_{o2})(Z_{11} - Z_{o1}^*) - Z_{12}Z_{21}}{\Delta Z} \quad (\text{AI4-33})$$

$$S_{12} = \frac{2Z_{12}\sqrt{R_{o1}R_{o2}}}{\Delta Z} \quad (\text{AI4-34})$$

and

$$S_{21} = \frac{2Z_{21}\sqrt{R_{o1}R_{o2}}}{\Delta Z} \quad (\text{AI4-35})$$

$$S_{22} = \frac{(Z_{11} + Z_{o1})(Z_{22} - Z_{o2}^*) - Z_{12}Z_{21}}{\Delta Z} \quad (\text{AI4-36})$$

with

$$\Delta Z = (Z_{11} + Z_{o1})(Z_{22} + Z_{o2}) - Z_{12}Z_{21} \quad (\text{AI4-37})$$

The materials you receive for this course are protected by copyright and to be used for this course only. You do not have permission to upload the course materials, including any lecture recordings you may have, to any website. If you require clarification, please consult your professor.

and similarly for S_{ij} - Z_{ij} relationships:

$$S_{11} = \frac{(1 - Y_{11}Z_{o1}^*)(1 + Y_{22}Z_{o2}) + Y_{12}Y_{21}Z_{o1}^*Z_{o2}}{\Delta Y} \quad (\text{AI4-38})$$

$$S_{12} = \frac{-2Y_{12}\sqrt{R_{o1}R_{o2}}}{\Delta Y} \quad (\text{AI4-39})$$

$$S_{21} = \frac{-2Y_{21}\sqrt{R_{o1}R_{o2}}}{\Delta Y} \quad (\text{AI4-40})$$

$$S_{22} = \frac{(1 + Y_{11}Z_{o1})(1 - Y_{22}Z_{o2}) + Y_{12}Y_{21}Z_{o1}Z_{o2}^*}{\Delta Y} \quad (\text{AI4-41})$$

$$\Delta Y = (1 + Y_{11}Z_{o1})(1 + Y_{22}Z_{o2}) - Y_{12}Y_{21}Z_{o1}Z_{o2} \quad (\text{AI4-42})$$

II – Simplified relations

In the case where all elements of $[Z_o]$ and $[Y_o]$ matrices are purely real and equal to Z_o and Y_o respectively, we can use simplified relationships between the S-parameters and the normalized impedance $[z]$ and admittance $[y]$ matrices:

$$[S] = \{[z] - [j]\} \{[z] + [j]\}^{-1} \quad (\text{AI4-43})$$

$$[S] = \{[j] - [y]\} \{[j] + [y]\}^{-1} \quad (\text{AI4-44})$$

$$[z] = \{[j] + [S]\} \{[j] - [S]\}^{-1} \quad (\text{AI4-45})$$

$$[y] = \{[j] - [S]\} \{[j] + [S]\}^{-1} \quad (\text{AI4-46})$$

The materials you receive for this course are protected by copyright and to be used for this course only. You do not have permission to upload the course materials, including any lecture recordings you may have, to any website. If you require clarification, please consult your professor.

where

$$y_{ij} = \frac{Y_{ij}}{Y_o} \quad \text{and} \quad z_{ij} = \frac{Z_{ij}}{Z_o}$$

H – TWO-PORT S-PARAMETERS CONVERSIONS

I – To S-parameters

Relations (AI4-43) and (AI4-46) allow us to obtain the useful relations from z- and y- to S-parameters for a two-port network.

1 - From z-parameters to S-parameters

$$S_{11} = \frac{(z_{22} + 1)(z_{11} - 1) - z_{12}z_{21}}{\Delta z} \quad (\text{AI4-47})$$

$$S_{12} = \frac{2z_{12}}{\Delta z} \quad (\text{AI4-48})$$

$$S_{21} = \frac{2z_{21}}{\Delta z} \quad (\text{AI4-49})$$

$$S_{22} = \frac{(z_{11} + 1)(z_{22} - 1) - z_{12}z_{21}}{\Delta z} \quad (\text{AI4-50})$$

$$\Delta z = (z_{11} + 1)(z_{22} + 1) - z_{12}z_{21} \quad (\text{AI4-51})$$

The materials you receive for this course are protected by copyright and to be used for this course only. You do not have permission to upload the course materials, including any lecture recordings you may have, to any website. If you require clarification, please consult your professor.

2 - From *y*-parameters to *S*-parameters

$$S_{11} = \frac{(1 - y_{11})(1 + y_{22}) + y_{12}y_{21}}{\Delta y} \quad (\text{AI4-52})$$

$$S_{12} = -\frac{2y_{12}}{\Delta y} \quad (\text{AI4-53})$$

$$S_{21} = -\frac{2y_{21}}{\Delta y} \quad (\text{AI4-54})$$

$$S_{22} = \frac{(1 + y_{11})(1 - y_{22}) + y_{12}y_{21}}{\Delta y} \quad (\text{AI4-55})$$

$$\Delta y = (1 + y_{11})(1 + y_{22}) - y_{12}y_{21} \quad (\text{AI4-56})$$

3 - From *S*-parameters to *z*-parameters

$$z_{11} = \frac{(1 + S_{11})(1 - S_{22}) + S_{12}S_{21}}{\Delta S_z} \quad (\text{AI4-57})$$

$$z_{12} = \frac{2S_{12}}{\Delta S_z} \quad (\text{AI4-58})$$

$$z_{21} = \frac{2S_{21}}{\Delta S_z} \quad (\text{AI4-59})$$

$$z_{22} = \frac{(1 - S_{11})(1 + S_{22}) + S_{12}S_{21}}{\Delta S_z} \quad (\text{AI4-60})$$

$$\Delta S_z = (1 - S_{11})(1 - S_{22}) - S_{12}S_{21} \quad (\text{AI4-61})$$

The materials you receive for this course are protected by copyright and to be used for this course only. You do not have permission to upload the course materials, including any lecture recordings you may have, to any website. If you require clarification, please consult your professor.

4 - From S-parameters to y-parameters

$$y_{11} = \frac{(1 - S_{11})(1 + S_{22}) + S_{12}S_{21}}{\Delta S_y} \quad (\text{AI4-62})$$

$$y_{12} = -\frac{2S_{12}}{\Delta S_y} \quad (\text{AI4-63})$$

$$y_{21} = -\frac{2S_{21}}{\Delta S_y} \quad (\text{AI4-64})$$

$$y_{22} = \frac{(1 + S_{11})(1 - S_{22}) + S_{12}S_{21}}{\Delta S_y} \quad (\text{AI4-65})$$

$$\Delta S_y = (1 + S_{11})(1 + S_{22}) - S_{12}S_{21} \quad (\text{AI4-64})$$

The materials you receive for this course are protected by copyright and to be used for this course only. You do not have permission to upload the course materials, including any lecture recordings you may have, to any website. If you require clarification, please consult your professor.

The following tables can be downloaded from

<http://anodegroup.univ-lille1.fr/publications/index.php?lg=en>

	S	Z	Y
S	$\begin{bmatrix} b_1 \\ b_2 \end{bmatrix} = \begin{bmatrix} S_{11} & S_{12} \\ S_{21} & S_{22} \end{bmatrix} \begin{bmatrix} a_1 \\ a_2 \end{bmatrix}$	$S_{11} = \frac{(Z_{11}-1)(Z_{22}+1)-Z_{12}Z_{21}}{(Z_{11}+1)(Z_{22}+1)-Z_{12}Z_{21}}$ $S_{12} = \frac{2Z_{12}}{(Z_{11}+1)(Z_{22}+1)-Z_{12}Z_{21}}$ $S_{21} = \frac{2Z_{21}}{(Z_{11}+1)(Z_{22}+1)-Z_{12}Z_{21}}$ $S_{22} = \frac{(Z_{11}+1)(Z_{22}-1)-Z_{12}Z_{21}}{(Z_{11}+1)(Z_{22}+1)-Z_{12}Z_{21}}$	$S_{11} = \frac{(1-Y_{11})(1+Y_{22})+Y_{12}Y_{21}}{(1+Y_{11})(1+Y_{22})-Y_{12}Y_{21}}$ $S_{12} = \frac{-2Y_{12}}{(1+Y_{11})(1+Y_{22})-Y_{12}Y_{21}}$ $S_{21} = \frac{-2y_{21}}{(1+Y_{11})(1+Y_{22})-Y_{12}Y_{21}}$ $S_{22} = \frac{(1+Y_{11})(1-Y_{22})+Y_{12}Y_{21}}{(1+Y_{11})(1+Y_{22})-Y_{12}Y_{21}}$
Z	$Z_{11} = \frac{(1+S_{11})(1-S_{22})+S_{12}S_{21}}{(1-S_{11})(1-S_{22})-S_{12}S_{21}}$ $Z_{12} = \frac{2S_{12}}{(1-S_{11})(1-S_{22})-S_{12}S_{21}}$ $Z_{21} = \frac{2S_{21}}{(1-S_{11})(1-S_{22})-S_{12}S_{21}}$ $Z_{22} = \frac{(1-S_{11})(1+S_{22})+S_{12}S_{21}}{(1-S_{11})(1-S_{22})-S_{12}S_{21}}$	$\begin{bmatrix} V_1 \\ V_2 \end{bmatrix} = \begin{bmatrix} Z_{11} & Z_{12} \\ Z_{21} & Z_{22} \end{bmatrix} \begin{bmatrix} I_1 \\ I_2 \end{bmatrix}$	$\frac{Y_{22}}{\Delta Y} \quad \frac{-Y_{12}}{\Delta Y}$ $\frac{-Y_{21}}{\Delta Y} \quad \frac{Y_{11}}{\Delta Y}$

The materials you receive for this course are protected by copyright and to be used for this course only. You do not have permission to upload the course materials, including any lecture recordings you may have, to any website. If you require clarification, please consult your professor.

$Y_{11} = \frac{(1-S_{11})(1+S_{22}) + S_{12}.S_{21}}{(1+S_{11})(1+S_{22}) - S_{12}.S_{21}}$ $Y_{12} = \frac{-2.S_{12}}{(1+S_{11})(1+S_{22}) - S_{12}.S_{21}}$ $Y_{21} = \frac{-2.S_{21}}{(1+S_{11})(1+S_{22}) - S_{12}.S_{21}}$ $Y_{22} = \frac{(1+S_{11})(1-S_{22}) + S_{12}.S_{21}}{(1+S_{11})(1+S_{22}) - S_{12}.S_{21}}$	$\begin{matrix} Z_{22} & -Z_{12} \\ \frac{\Delta Z}{\Delta Z} & \frac{Z_{11}}{\Delta Z} \\ -Z_{21} & \frac{Z_{11}}{\Delta Z} \end{matrix}$	$\begin{bmatrix} I_1 \\ I_2 \end{bmatrix} = \begin{bmatrix} Y_{11} & Y_{12} \\ Y_{21} & Y_{22} \end{bmatrix} \begin{bmatrix} V_1 \\ V_2 \end{bmatrix}$
---	--	--

	S	H	A
S $\begin{bmatrix} b_1 \\ b_2 \end{bmatrix} = \begin{bmatrix} S_{11} & S_{12} \\ S_{21} & S_{22} \end{bmatrix} \begin{bmatrix} a_1 \\ a_2 \end{bmatrix}$	$S_{11} = \frac{(h_{11}-1)(h_{22}+1) - h_{12}.h_{21}}{(h_{11}+1)(h_{22}+1) - h_{12}.h_{21}}$ $S_{12} = \frac{2.h_{12}}{(h_{11}+1)(h_{22}+1) - h_{12}.h_{21}}$ $S_{21} = \frac{-2.h_{21}}{(h_{11}+1)(h_{22}+1) - h_{12}.h_{21}}$ $S_{22} = \frac{(h_{11}+1)(h_{22}-1) + h_{12}.h_{21}}{(h_{11}+1)(h_{22}+1) - h_{12}.h_{21}}$	$S_{11} = \frac{A+B-C-D}{A+B+C+D}$ $S_{12} = \frac{2.(AD-BC)}{A+B+C+D}$ $S_{21} = \frac{2}{A+B+C+D}$ $S_{22} = \frac{-A+B-C+D}{A+B+C+D}$	
Z $Z_{11} = \frac{(1+S_{11})(1-S_{22}) + S_{12}.S_{21}}{(1-S_{11})(1-S_{22}) - S_{12}.S_{21}}$ $Z_{12} = \frac{2.S_{12}}{(1-S_{11})(1-S_{22}) - S_{12}.S_{21}}$ $Z_{21} = \frac{2.S_{21}}{(1-S_{11})(1-S_{22}) - S_{12}.S_{21}}$ $Z_{22} = \frac{(1-S_{11})(1+S_{22}) + S_{12}.S_{21}}{(1-S_{11})(1-S_{22}) - S_{12}.S_{21}}$	$\begin{matrix} \Delta h & h_{12} \\ \frac{h_{22}}{h_{22}} & \frac{h_{12}}{h_{22}} \\ -\frac{h_{12}}{h_{22}} & \frac{1}{h_{22}} \\ \frac{h_{22}}{h_{22}} & \frac{h_{12}}{h_{22}} \end{matrix}$	$\begin{matrix} A & \Delta A \\ \frac{C}{C} & \frac{C}{C} \\ 1 & D \\ \frac{C}{C} & C \end{matrix}$	

The materials you receive for this course are protected by copyright and to be used for this course only. You do not have permission to upload the course materials, including any lecture recordings you may have, to any website. If you require clarification, please consult your professor.

Y	$Y_{11} = \frac{(1-S_{11})(1+S_{22}) + S_{12}.S_{21}}{(1+S_{11})(1+S_{22}) - S_{12}.S_{21}}$ $Y_{12} = \frac{-2.S_{12}}{(1+S_{11})(1+S_{22}) - S_{12}.S_{21}}$ $Y_{21} = \frac{-2.S_{21}}{(1+S_{11})(1+S_{22}) - S_{12}.S_{21}}$ $Y_{22} = \frac{(1+S_{11})(1-S_{22}) + S_{12}.S_{21}}{(1+S_{11})(1+S_{22}) - S_{12}.S_{21}}$	$\frac{1}{h_{11}} \quad \frac{h_{12}}{h_{11}}$ $\frac{h_{21}}{h_{11}} \quad \frac{\Delta h}{h_{11}}$	$\frac{D}{B} \quad \frac{-\Delta A}{B}$ $\frac{-1}{B} \quad \frac{A}{B}$
----------	---	--	--

	S	Z	Y
H	$h_{11} = \frac{(1+S_{11})(1+S_{22}) - S_{12}.S_{21}}{(1-S_{11})(1+S_{22}) + S_{12}.S_{21}}$ $h_{12} = \frac{2.S_{12}}{(1-S_{11})(1+S_{22}) + S_{12}.S_{21}}$ $h_{21} = \frac{-2.S_{21}}{(1-S_{11})(1+S_{22}) + S_{12}.S_{21}}$ $h_{22} = \frac{(1-S_{11})(1-S_{22}) - S_{12}.S_{21}}{(1-S_{11})(1+S_{22}) + S_{12}.S_{21}}$	$\frac{\Delta Z}{Z_{22}} \quad \frac{Z_{12}}{Z_{22}}$ $\frac{-Z_{21}}{Z_{22}} \quad \frac{1}{Z_{22}}$	$\frac{Y_{22}}{\Delta Y} \quad \frac{-Y_{12}}{\Delta Y}$ $\frac{-Y_{21}}{\Delta Y} \quad \frac{Y_{11}}{\Delta Y}$
A	$A = \frac{(1+S_{11})(1-S_{22}) + S_{12}.S_{21}}{2.S_{21}}$ $B = \frac{(1+S_{11})(1+S_{22}) - S_{12}.S_{21}}{2.S_{21}}$ $C = \frac{(1-S_{11})(1-S_{22}) - S_{12}.S_{21}}{2.S_{21}}$ $D = \frac{(1-S_{11})(1+S_{22}) + S_{12}.S_{21}}{2.S_{21}}$	$\frac{Z_{11}}{Z_{21}} \quad \frac{\Delta Z}{Z_{21}}$ $\frac{1}{Z_{21}} \quad \frac{Z_{22}}{Z_{21}}$	$\frac{-Y_{22}}{Y_{21}} \quad \frac{-1}{Y_{21}}$ $\frac{-\Delta Y}{Y_{21}} \quad \frac{-Y_{11}}{Y_{21}}$

The materials you receive for this course are protected by copyright and to be used for this course only. You do not have permission to upload the course materials, including any lecture recordings you may have, to any website. If you require clarification, please consult your professor.

	S	H	A
H	$h_{11} = \frac{(1+S_{11})(1+S_{22}) - S_{12}.S_{21}}{(1-S_{11})(1+S_{22}) + S_{12}.S_{21}}$ $h_{12} = \frac{2.S_{12}}{(1-S_{11})(1+S_{22}) + S_{12}.S_{21}}$ $h_{21} = \frac{-2.S_{21}}{(1-S_{11})(1+S_{22}) + S_{12}.S_{21}}$ $h_{22} = \frac{(1-S_{11})(1-S_{22}) - S_{12}.S_{21}}{(1-S_{11})(1+S_{22}) + S_{12}.S_{21}}$	$\begin{bmatrix} V_1 \\ I_2 \end{bmatrix} = \begin{bmatrix} h_{11} & h_{12} \\ h_{21} & h_{22} \end{bmatrix} \begin{bmatrix} I_1 \\ V_2 \end{bmatrix}$	$\frac{B}{D} \quad \frac{\Delta A}{D}$ $\frac{-1}{D} \quad \frac{C}{D}$
A	$A = \frac{(1+S_{11})(1-S_{22}) + S_{12}.S_{21}}{2.S_{21}}$ $B = \frac{(1+S_{11})(1+S_{22}) - S_{12}.S_{21}}{2.S_{21}}$ $C = \frac{(1-S_{11})(1-S_{22}) - S_{12}.S_{21}}{2.S_{21}}$ $D = \frac{(1-S_{11})(1+S_{22}) + S_{12}.S_{21}}{2.S_{21}}$	$\frac{-\Delta h}{h_{21}} \quad \frac{-h_{11}}{h_{21}}$ $\frac{-h_{22}}{h_{21}} \quad \frac{-1}{h_{21}}$	$\begin{bmatrix} V_1 \\ I_1 \end{bmatrix} = \begin{bmatrix} A & B \\ C & D \end{bmatrix} \begin{bmatrix} V_2 \\ -I_2 \end{bmatrix}$

The materials you receive for this course are protected by copyright and to be used for this course only. You do not have permission to upload the course materials, including any lecture recordings you may have, to any website. If you require clarification, please consult your professor.

From To	Z	Y	CH
Z	$\begin{bmatrix} Z_{11} & Z_{12} \\ Z_{21} & Z_{22} \end{bmatrix}$	$\frac{1}{ Y } \begin{bmatrix} Y_{22} & -Y_{12} \\ -Y_{21} & Y_{11} \end{bmatrix}$	$\frac{1}{CH_{21}} \begin{bmatrix} CH_{11} & CH \\ 1 & CH_{22} \end{bmatrix}$
Y	$\frac{1}{ Z } \begin{bmatrix} Z_{22} & -Z_{12} \\ -Z_{21} & Z_{11} \end{bmatrix}$	$\begin{bmatrix} Y_{11} & Y_{12} \\ Y_{21} & Y_{22} \end{bmatrix}$	$\frac{1}{CH_{21}} \begin{bmatrix} CH_{22} & - CH \\ -1 & CH_{11} \end{bmatrix}$
CH	$\frac{1}{Z_{21}} \begin{bmatrix} Z_{11} & Z \\ 1 & Z_{22} \end{bmatrix}$	$\frac{1}{Y_{21}} \begin{bmatrix} -Y_{22} & -1 \\ - Y & -Y_{11} \end{bmatrix}$	$\begin{bmatrix} CH_{11} & CH_{12} \\ CH_{21} & CH_{22} \end{bmatrix}$

		From C		
		Admittance C_Y	Impedance C_Z	Chain C_A
	Admittance C_Y	$\begin{bmatrix} 1 & 0 \\ 0 & 1 \end{bmatrix}$	$\begin{bmatrix} Y_{11} & Y_{12} \\ Y_{21} & Y_{22} \end{bmatrix}$	$\begin{bmatrix} -Y_{11} & 1 \\ -Y_{21} & 0 \end{bmatrix}$
	Impedance C_Z	$\begin{bmatrix} Z_{11} & Z_{12} \\ Z_{21} & Z_{22} \end{bmatrix}$	$\begin{bmatrix} 1 & 0 \\ 0 & 1 \end{bmatrix}$	$\begin{bmatrix} 1 & -Z_{11} \\ 0 & -Z_{21} \end{bmatrix}$
	Chain C_A	$\begin{bmatrix} 0 & CH_{12} \\ 1 & CH_{22} \end{bmatrix}$	$\begin{bmatrix} 1 & -CH_{11} \\ 0 & -CH_{21} \end{bmatrix}$	$\begin{bmatrix} 1 & 0 \\ 0 & 1 \end{bmatrix}$
To C'				

The materials you receive for this course are protected by copyright and to be used for this course only. You do not have permission to upload the course materials, including any lecture recordings you may have, to any website. If you require clarification, please consult your professor.

I – SYMMETRIC TWO-PORT S-PARAMETERS CALCULATION

I - Method of 3 points

For this method, we need a short-circuit, an open-circuit and a matched load.

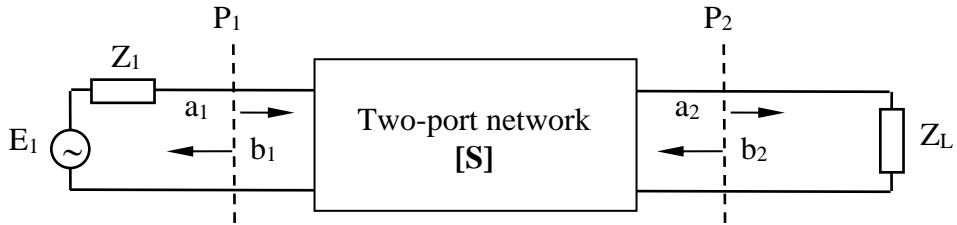


Figure AI4-3: Incident and reflected waves in a two-port network.

$$\text{At } P_1 : \Gamma_1 = \frac{b_1}{a_1} \quad \text{At } P_2 : \Gamma_2 = \frac{b_2}{a_2}$$

We measure

$$\Gamma_1 = S_{11} + \frac{S_{21} S_{12} \Gamma_2}{1 - S_{22} \Gamma_2} = S_{11} + \frac{S_{21}^2 \Gamma_2}{1 - S_{22} \Gamma_2}$$

$$1^{st} \text{ point: } Z_L = 0 \quad \Gamma_{2sc} = -1 \quad \Gamma_{1sc} = S_{11} + \frac{S_{21}^2 \Gamma_{2sc}}{1 - S_{22} \Gamma_{2sc}} = S_{11} - \frac{S_{21}^2}{1 + S_{22}}$$

$$2^{nd} \text{ point: } Z_L = \infty \quad \Gamma_{2oc} = +1 \quad \Gamma_{1oc} = S_{11} + \frac{S_{21}^2 \Gamma_{2oc}}{1 - S_{22} \Gamma_{2oc}} = S_{11} + \frac{S_{21}^2}{1 - S_{22}}$$

$$3^{rd} \text{ point: } Z_L = Z_o \quad \Gamma_{2m} = 0 \quad \Gamma_{1m} = S_{11} + \frac{S_{21}^2 \Gamma_{2m}}{1 - S_{22} \Gamma_{2m}} = S_{11}$$

$$S_{11} = \Gamma_{1m} \quad S_{22} = \frac{2\Gamma_{1m} - (\Gamma_{1sc} + \Gamma_{loc})}{\Gamma_{1sc} - \Gamma_{loc}} \quad S_{21} = \left[\frac{2(\Gamma_{1m} - \Gamma_{1sc})(\Gamma_{1m} - \Gamma_{loc})}{\Gamma_{1sc} - \Gamma_{loc}} \right]^{\frac{1}{2}}$$

II - Method of 4 points

For this method, we need only a movable short-circuit or tuning piston.

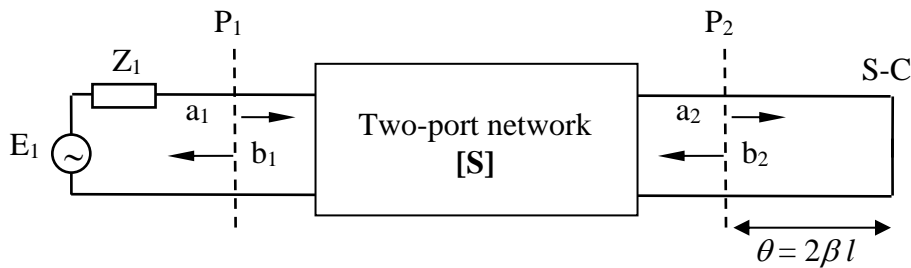


Figure AI4-3: Incident and reflected waves in a two-port network.

$$\text{At } P_1 : \Gamma_1 = \frac{b_1}{a_1} \quad \text{At } P_2 : \Gamma_2 = \frac{b_2}{a_2} = \Gamma_{sc} e^{-2j\beta l} = -e^{-2j\beta l}$$

We measure

$$\Gamma_1 = S_{11} + \frac{S_{21} S_{12} \Gamma_2}{1 - S_{22} \Gamma_2} = S_{11} + \frac{S_{21}^2 \Gamma_2}{1 - S_{22} \Gamma_2}$$

for 4 different positions of the short-circuit

$$1^{st} \text{ point:} \quad l = l_1 \quad \Gamma_2^{(1)} = -e^{-2j\beta l_1} = -e^{-j\theta} \quad \Gamma_1 = \Gamma_1^{(1)}$$

$$2^{nd} \text{ point:} \quad l = l_1 + \lambda/8 \quad \Gamma_2^{(2)} = -e^{-2j\beta l_1 + \pi/2} = j e^{-j\theta} \quad \Gamma_1 = \Gamma_1^{(2)}$$

$$3^{rd} \text{ point: } l = l_1 + 2\lambda/8 \quad \Gamma_2^{(3)} = -e^{-2j\beta l_1 + \pi} = e^{-j\theta} \quad \Gamma_1 = \Gamma_1^{(3)}$$

$$4^{th} \text{ point: } l = l_1 + 3\lambda/8 \quad \Gamma_2^{(4)} = -e^{-2j\beta l_1 + 3\pi/2} = -je^{-j\theta} \quad \Gamma_1 = \Gamma_1^{(4)}$$

$$F_1 = \frac{1}{4} \left[(\Gamma_1^{(1)} - \Gamma_1^{(3)}) + j(\Gamma_1^{(2)} - \Gamma_1^{(4)}) \right] \quad F_2 = \frac{1}{4} \left[(\Gamma_1^{(1)} - \Gamma_1^{(3)}) - j(\Gamma_1^{(2)} - \Gamma_1^{(4)}) \right]$$

$$F_3 = \frac{1}{4} \left[(\Gamma_1^{(1)} + \Gamma_1^{(3)}) - (\Gamma_1^{(2)} + \Gamma_1^{(4)}) \right] \quad F_4 = \frac{1}{4} \left[(\Gamma_1^{(1)} + \Gamma_1^{(3)}) + (\Gamma_1^{(2)} + \Gamma_1^{(4)}) \right]$$

$$S_{11} = F_4 - \frac{F_2 F_3}{F_1} \quad S_{22} = -\frac{F_2}{F_1} e^{j\theta} \quad S_{21} = \left[-F_1 e^{j\theta} \left(1 - \left(\frac{F_2}{F_1} \right)^2 \right) \right]^{\frac{1}{2}}$$

The materials you receive for this course are protected by copyright and to be used for this course only. You do not have permission to upload the course materials, including any lecture recordings you may have, to any website. If you require clarification, please consult your professor.

APPENDIX I-3

GENERALIZED SCATTERING MATRIX

A – INCIDENT AND REFLECTED WAVES

Using equations (AI4-12) and (AI4-14), the incident and reflected waves of an N -port network can be redefined as

$$[\mathbf{a}] = [\mathbf{R}] \{ [\mathbf{V}] + [\mathbf{Z}_o] [\mathbf{I}] \} \quad (\text{AI5-1})$$

$$[\mathbf{b}] = [\mathbf{R}] \{ [\mathbf{V}] - [\mathbf{Z}_o]^+ [\mathbf{I}] \} \quad (\text{AI5-2})$$

$$[\mathbf{Z}_o] = \begin{bmatrix} Z_{o1} & \cdots & 0 \\ \vdots & \ddots & \vdots \\ 0 & \cdots & Z_{oN} \end{bmatrix} \quad [\mathbf{Z}_o]^+ = ([\mathbf{Z}_o]^t)^* \quad (\text{AI5-3})$$

$$[\mathbf{R}] = \frac{1}{\sqrt{2}} \begin{bmatrix} \sqrt{\frac{1}{\text{Re}(Z_{o1})}} & \cdots & 0 \\ \vdots & \ddots & \vdots \\ 0 & \cdots & \sqrt{\frac{1}{\text{Re}(Z_{oN})}} \end{bmatrix} = \frac{1}{\sqrt{2}} \begin{bmatrix} \sqrt{\frac{1}{R_{o1}}} & \cdots & 0 \\ \vdots & \ddots & \vdots \\ 0 & \cdots & \sqrt{\frac{1}{R_{oN}}} \end{bmatrix} \quad (\text{AI5-4})$$

The materials you receive for this course are protected by copyright and to be used for this course only. You do not have permission to upload the course materials, including any lecture recordings you may have, to any website. If you require clarification, please consult your professor.

Let $[\mathbf{Z}_N]$ be the impedance matrix of the N -port

$$[\mathbf{V}] = [\mathbf{Z}_N][\mathbf{I}] \quad (\text{AI5-5})$$

Using (AI4-29) and the above relations, the scattering matrix can be expressed as

$$[\mathbf{S}] = [\mathbf{R}] \left\{ [\mathbf{Z}_N] - [\mathbf{Z}_o]^+ \right\} \left\{ [\mathbf{Z}_N] + [\mathbf{Z}_o] \right\}^{-1} [\mathbf{R}]^{-1} \quad (\text{AI5-6})$$

$$\rightarrow [\mathbf{Z}_N] = [\mathbf{R}]^{-1} \left\{ [\mathfrak{I}] - [\mathbf{S}] \right\}^{-1} \left\{ [\mathbf{S}] [\mathbf{Z}_o] + [\mathbf{Z}_o]^+ \right\} [\mathbf{R}] \quad (\text{AI5-7})$$

$[\mathfrak{I}]$ is the identity matrix. If we change the characteristic impedances, the new $[\mathbf{S}]$ matrix can be written as

$$[\mathbf{S}'] = [\mathbf{R}] \left\{ [\mathbf{Z}_N] - [\mathbf{Z}_o']^+ \right\} \left\{ [\mathbf{Z}_N] + [\mathbf{Z}_o'] \right\}^{-1} [\mathbf{R}']^{-1} \quad (\text{AI5-8})$$

Thus, using (AI5-7), the relation between $[\mathbf{S}]$ and $[\mathbf{S}']$ can be stated as

$$[\mathbf{S}'] = [\mathbf{R}] \left\{ \left\{ [\mathbf{R}]^{-1} \left\{ [\mathfrak{I}] - [\mathbf{S}] \right\}^{-1} \left\{ [\mathbf{S}] [\mathbf{Z}_o] + [\mathbf{Z}_o]^+ \right\} [\mathbf{R}] \right\} - [\mathbf{Z}_o']^+ \right\} \\ \left\{ \left\{ [\mathbf{R}]^{-1} \left\{ [\mathfrak{I}] - [\mathbf{S}] \right\}^{-1} \left\{ [\mathbf{S}] [\mathbf{Z}_o] + [\mathbf{Z}_o]^+ \right\} [\mathbf{R}] \right\} + [\mathbf{Z}_o'] \right\}^{-1} [\mathbf{R}']^{-1} \quad (\text{AI5-9})$$

By defining a reflection coefficient matrix as

$$[\Gamma] = \begin{bmatrix} \Gamma_1 & \cdots & 0 \\ \vdots & \ddots & \vdots \\ 0 & \cdots & \Gamma_N \end{bmatrix} \quad \text{with} \quad \Gamma_k = \frac{Z_{ok}' - Z_{ok}}{Z_{ok}' + Z_{ok}^*} \quad (\text{AI5-10})$$

The materials you receive for this course are protected by copyright and to be used for this course only. You do not have permission to upload the course materials, including any lecture recordings you may have, to any website. If you require clarification, please consult your professor.

and using matrix properties such as $[\mathbf{A}] [\mathbf{B}] [\mathbf{C}] = [\mathbf{C}] [\mathbf{B}] [\mathbf{A}]$, which allow us to write

$$\{[\mathfrak{J}] - [\mathbf{S}]\}^{-1} \{[\mathbf{S}] - [\Gamma]^+\} \{[\mathfrak{J}] - [\Gamma]^+\}^{-1} = \{[\mathfrak{J}] - [\Gamma]^+\}^{-1} \{[\mathbf{S}] - [\Gamma]^+\} \{[\mathfrak{J}] - [\mathbf{S}]\}^{-1}$$

we obtain

$$[\mathbf{S}'] = [\mathbf{A}]^{-1} \{[\mathbf{S}] - [\Gamma]^+\} \{[\mathfrak{J}] - [\Gamma][\mathbf{S}]\}^{-1} [\mathbf{A}]^+ \quad (\text{AI5-11})$$

where $[\mathbf{A}]$ is a diagonal matrix defined as

$$[\mathbf{A}] = [\mathbf{R}']^{-1} [\mathbf{R}] \{[\mathfrak{J}] - [\Gamma]^+\} \quad \text{with} \quad A_{ii} = |1 - \Gamma_i|^{-1} (1 - \Gamma_i^*) (1 - |\Gamma_i|^2)^{1/2} \quad (\text{AI5-12})$$

The form of equation (AI5-11) is very useful as we will see in the following example. In fact, let us consider the circuit shown on Figure AI5-1. A component of scattering matrix $[\mathbf{S}]$ is excited by a voltage source of magnitude E and internal impedance Z_S and loaded by Z_L . The reflection coefficients of these impedances are noted Γ_S and Γ_L respectively.

In this case,

$$\begin{aligned} [\Gamma] &= \begin{bmatrix} \Gamma_S & 0 \\ 0 & \Gamma_L \end{bmatrix} \quad \text{with} \quad \Gamma_S = \frac{Z_S - Z_o}{Z_S + Z_o^*} \quad \text{and} \quad \Gamma_L = \frac{Z_L - Z_o}{Z_L + Z_o^*} \\ \rightarrow [\mathbf{A}] &= \begin{bmatrix} A_S & 0 \\ 0 & A_L \end{bmatrix} = \begin{bmatrix} \sqrt{\frac{\text{Re}(Z_S)}{Z_o}} (1 - \Gamma_S^*) & 0 \\ 0 & \sqrt{\frac{\text{Re}(Z_L)}{Z_o}} (1 - \Gamma_L^*) \end{bmatrix} \end{aligned}$$

The materials you receive for this course are protected by copyright and to be used for this course only. You do not have permission to upload the course materials, including any lecture recordings you may have, to any website. If you require clarification, please consult your professor.

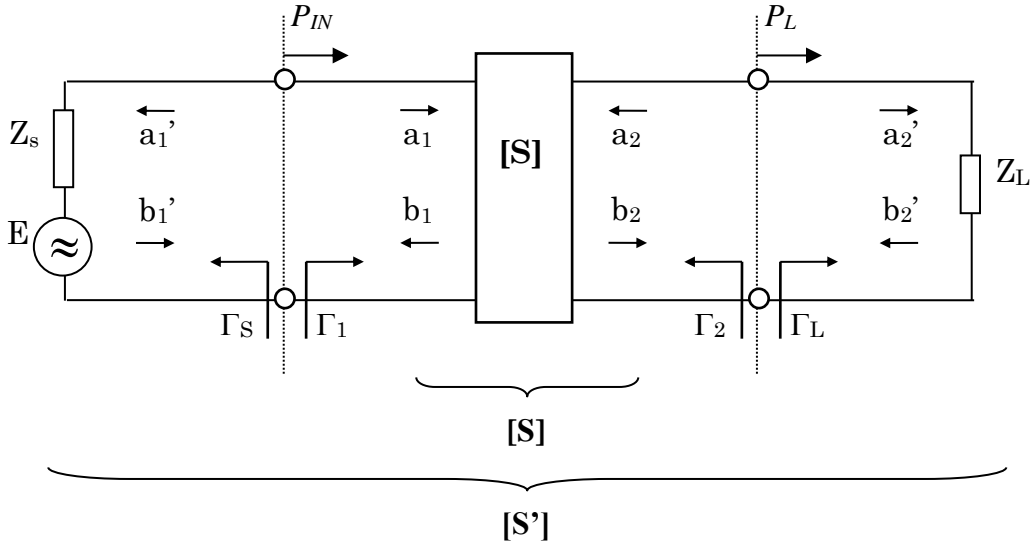


Fig. AI5-1. Two-port transistor representation in terms of scattering parameters.

Thus, using (AI5-11), we can easily deduce the overall scattering matrix $[S']$ of the whole circuit directly from the scattering matrix $[S]$ of the component, e.g.,

$$S_{21}' = \frac{A_S}{A_L} S_{21} \frac{1 - |\Gamma_L|^2}{(1 - \Gamma_S S_{11})(1 - \Gamma_L S_{22}) - \Gamma_S \Gamma_L S_{12} S_{21}} \quad (\text{AI5-13})$$

from which we can express for instance the transducer power gain of an amplifier

$$G_T = |S_{21}'|^2 = |S_{21}|^2 \frac{(1 - |\Gamma_S|^2)(1 - |\Gamma_L|^2)}{|(1 - \Gamma_S S_{11})(1 - \Gamma_L S_{22}) - \Gamma_S \Gamma_L S_{12} S_{21}|^2} \quad (\text{AI5-14})$$

APPENDIX I-4

X MATRIX

A – X MATRIX IN THE MICROWAVE FIELD

In the last few years, a new set of parameters has been introduced to the microwave community by Agilent. As stated by this company, such parameters, called X-parameters, can characterize nonlinear component/circuit/system behaviors more accurately than the conventional S-parameters. According to the paper “X-parameters: Commercial implementations of the latest technology enable mainstream applications,” by David Root, published in 2009 in Microwave Journal (<http://mwexpert.typepad.com/home/2009/09/index.html>):

“X-parameters unify S-parameters, load-pull, and modern wave-form measurements for more complete nonlinear characterization and predictive nonlinear design of RF and microwave components and systems. Benefits never thought possible are being realized today by practicing engineers.”

In summary, X-parameters can act as “nonlinear/large signal” S-parameters. Taking the problem of *Integrating Power Amplifiers into Cell Phones*, the author showed that X-parameters can solve a typical nonlinear problem which cannot be solved through conventional small-signal S-parameters, i.e., the generation by the PA of distortion products in-band and also at harmonics that can interfere with the proper functioning of the cell phone, in order for the PA to be easily integrated into a handset and ensure, at the design stage, that it will still meet the overall system specifications

The materials you receive for this course are protected by copyright and to be used for this course only. You do not have permission to upload the course materials, including any lecture recordings you may have, to any website. If you require clarification, please consult your professor.

when it interacts with other components, such as additional amplifiers or the antenna, in the phone. More details can be found in:

J. Horn, J. Verspecht, D. Gunyan , L. Betts, D. E. Root, and Joakim Eriksson,
“X-Parameter Measurement and Simulation of a GSM Handset Amplifier,”
European Microwave Conf., Amsterdam, Oct. 2008.

The materials you receive for this course are protected by copyright and to be used for this course only. You do not have permission to upload the course materials, including any lecture recordings you may have, to any website. If you require clarification, please consult your professor.

APPENDIX I-5

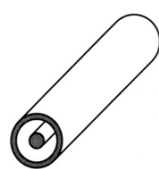
PROPERTIES OF SOME RF/MICROWAVE TRANSMISSION LINES

From csm00.csu.edu.tw/0244/971/MicrowaveCourse/Chapter3.ppt

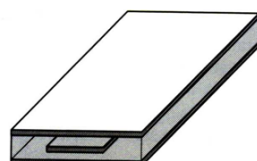
Conventional Transmission Lines and Waveguides



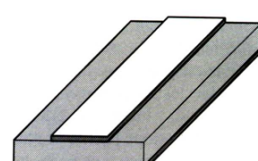
(a) Open two-wire line



(b) Coaxial line



(e) Stripline



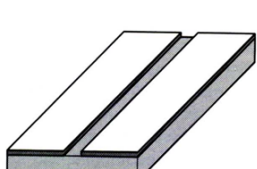
(f) Microstrip



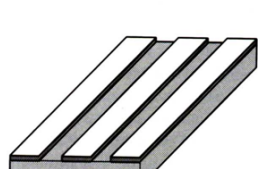
(c) Rectangular waveguide



(d) Circular waveguide



(g) Slotline



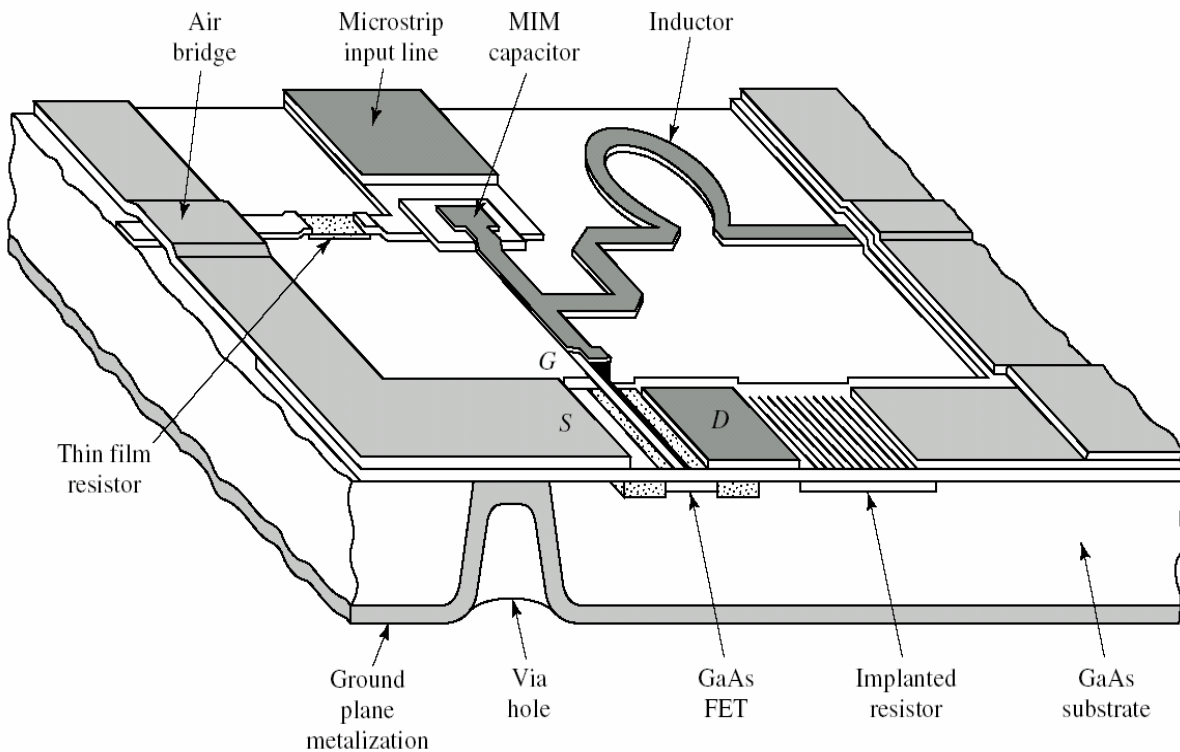
(h) Coplanar waveguide

Good for Long Distance
Communication

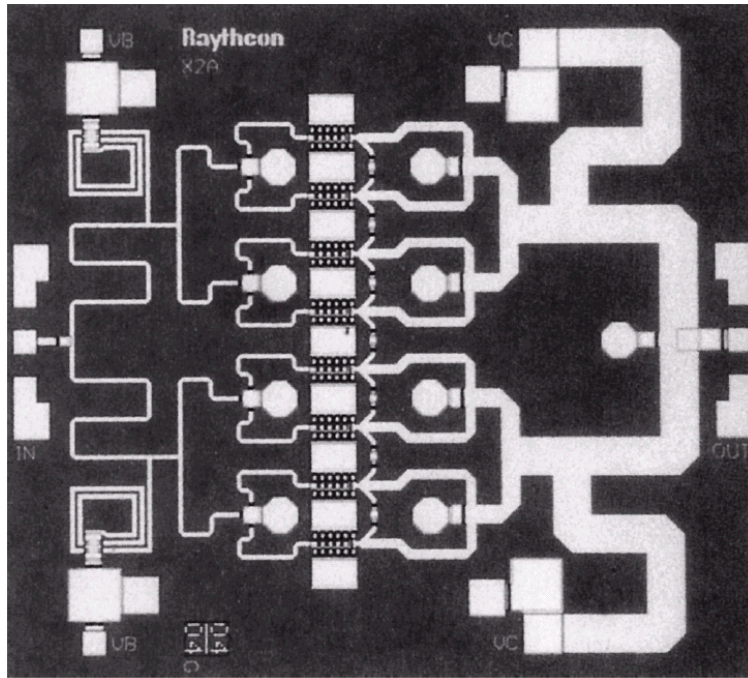
Good for Microwave Integrated Circuit
(MIC) Applications

The materials you receive for this course are protected by copyright and to be used for this course only. You do not have permission to upload the course materials, including any lecture recordings you may have, to any website. If you require clarification, please consult your professor.

Case of monolithic circuits



The materials you receive for this course are protected by copyright and to be used for this course only. You do not have permission to upload the course materials, including any lecture recordings you may have, to any website. If you require clarification, please consult your professor.

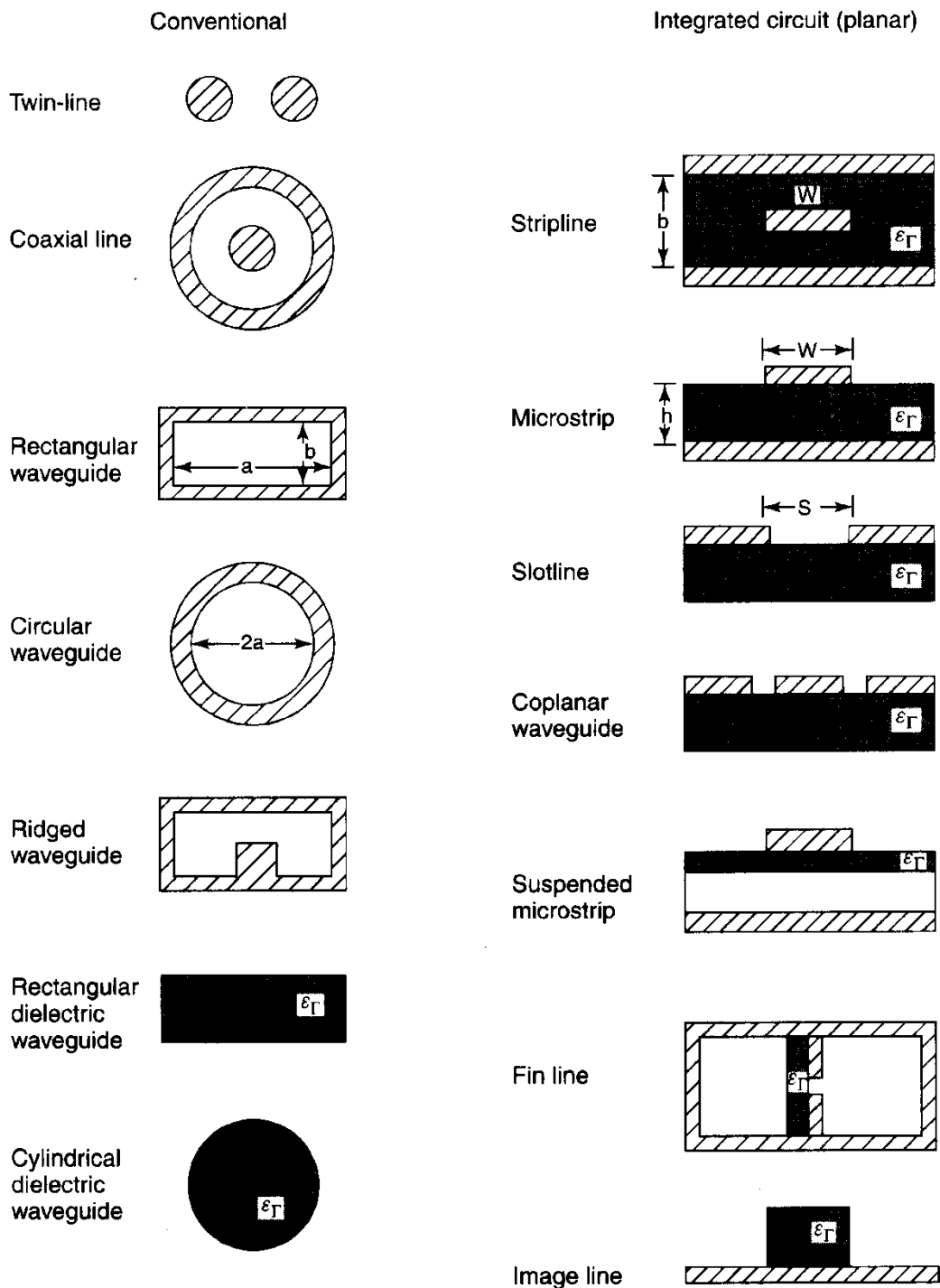


The materials you receive for this course are protected by copyright and to be used for this course only. You do not have permission to upload the course materials, including any lecture recordings you may have, to any website. If you require clarification, please consult your professor.

TABLE 3.7. Comparison Between Monolithic and Hybrid MICs

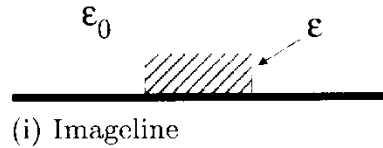
Feature	Monolithic	Hybrid
Substrate	Semi-insulator	insulator
Interconnections	Deposited	Wire-bonded/deposited
Distributed elements	Microstrip or coplanar waveguide	Microstrip and/or coplanar lines
Lumped elements	Deposited	Discrete/deposited
Solid-state devices	Deposited	Discrete
Controlled parasitics	Yes	No
Labor intensive	No	Yes
Repairability	No	Yes
Equipment costs	High	Low
Mass production	Yes	No
Debugging	Difficult	Easy
Integration with digital and electrooptic ICs	Possible	Impossible
NRE Cost	Very high	Low
Production Cost in high volume	Low	High
Size and weight	Small	Large
Design flexibility	Very good	Good
Circuit tweaking	Impractical	Practical
Broadband performance	Relatively good	Limited
Reproducibility	Excellent	Fair to good
Reliability	Excellent	Fair to good

The materials you receive for this course are protected by copyright and to be used for this course only. You do not have permission to upload the course materials, including any lecture recordings you may have, to any website. If you require clarification, please consult your professor.



The materials you receive for this course are protected by copyright and to be used for this course only. You do not have permission to upload the course materials, including any lecture recordings you may have, to any website. If you require clarification, please consult your professor.

(a) Completely
non-TEM



(i) Imageline

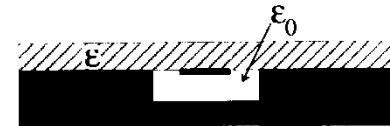
(b) Quasi-TEM



(ii) Microstrip



(iv) Inverted microstrip

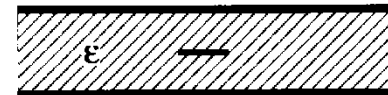


(vi) Trapped Inverted
Microstrip (TIM)



(v) Slotline

(c) TEM

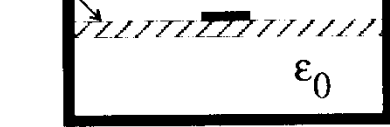


(x) Stripline



(xi) Embedded differential
line

(vii) Suspended stripline



(viii) Coplanar waveguide
(CPW)

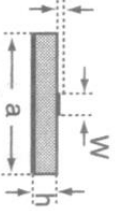
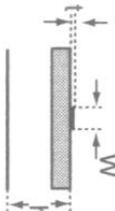
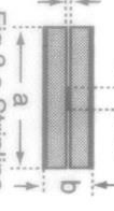
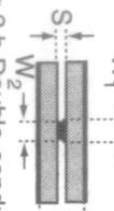
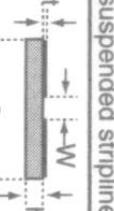
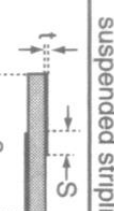
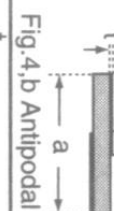
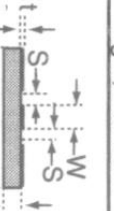
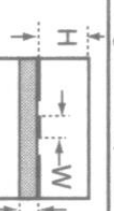
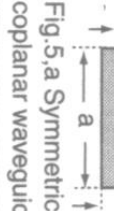
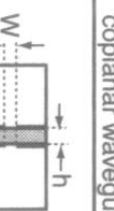
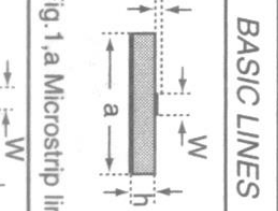
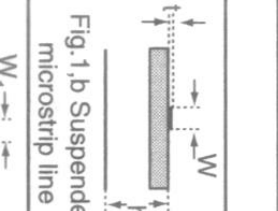
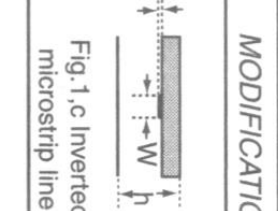
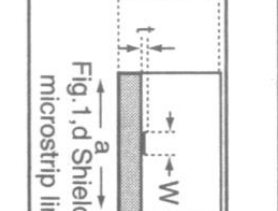
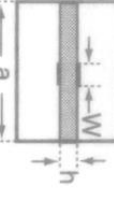
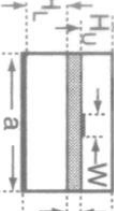
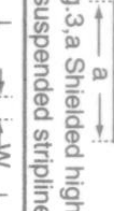
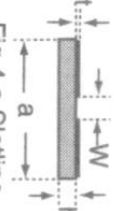
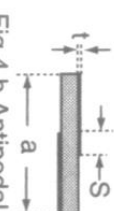
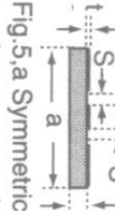
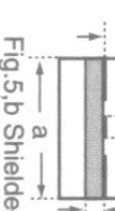


(ix) Differential line or
coplanar strips (CPS)

The materials you receive for this course are protected by copyright and to be used for this course only. You do not have permission to upload the course materials, including any lecture recordings you may have, to any website. If you require clarification, please consult your professor.

Transmission Line	Useful Frequency range (GHz)	Impedance Range (Ω)	Cross-Sectional Dimensions	<i>Q</i> -Factor	Power Rating	Active Device Mounting	Mounting	Potential for Low-Cost Production
Rectangular waveguide	<300	100–500	Moderate to large	High	High	Easy	Easy	Poor
Coaxial line	<50	10–100	Moderate	Moderate	Low	Fair	Fair	Poor
Stripline	<10	10–100	Moderate	Small	Low	Easy	Fair	Good
Microstrip line	≤100	10–100	Small	Moderate	Low	Easy	Fair	Good
Suspended stripline	≤150	20–150	Small	Moderate	Low	Easy	Fair	Fair
Finline	≤150	20–400	Moderate	Moderate	Low	Easy	Fair	Fair
Slotline	≤60	60–200	Small	Low	Low	Fair	Fair	Good
Coplanar waveguide	≤60	40–150	Small	Low	Low	Fair	Fair	Good
Image guide	<300	30–30	Moderate	High	Low	Poor	Poor	Good
Dielectric line	<300	20–50	Moderate	High	Low	Poor	Fair	Fair

The materials you receive for this course are protected by copyright and to be used for this course only. You do not have permission to upload the course materials, including any lecture recordings you may have, to any website. If you require clarification, please consult your professor.

BASIC LINES		MODIFICATIONS	
			
microstrip line			
			
stripline			
suspended stripline			
slotline			
coplanar waveguide			
finline			
			
			
			
			
			
			
			
			

The materials you receive for this course are protected by copyright and to be used for this course only. You do not have permission to upload the course materials, including any lecture recordings you may have, to any website. If you require clarification, please consult your professor.

Image Line

- Behavior likes a dielectric slab waveguide (thick strip) for use into hundreds GHz.
- Several thousand unloaded Q -factor. But $f_{op} \downarrow \Rightarrow Q \downarrow$.
- Poor compatibility with active devices, mutual coupling, and radiation from discontinuities and bends.

Microstrip

- The most popular MIC TL with a very simple geometric planar structure.
- Advantage: Zero cutoff frequency, light weight, small size, low cost, easy fabrication and integration, low dispersion, and broadband operation (frequency range from a few GHZ, or even lower, up to at least many tens of GHz).
- At millimetre-wave range, problems such as loss, higher-order modes, and fabrication tolerances become exceedingly difficult to meet using HMICs.

Finline

- Advantage:
 - 1) Low loss (typically a factor about three better than microstrip).
 - 2) Simpler fabrication in comparison with inverted and trapped-inverted microstrip.
 - 3) Operation frequency up to 100GHz.
- Disadvantage in biasing problem.
- Application in compatibility with solid-state device is fairly good, especially in the case of beam-lead devices, 10% bandwidth of band pass filters, quadrature hybrids, waveguide transitions, and balanced mixer circuits.

Inverted microstrip

- Advantages in comparison with microstrip :
 - 1) Wider line width for the same Z_0 , and this both reduces conductor dissipation and relaxes fabrication tolerances.

The materials you receive for this course are protected by copyright and to be used for this course only. You do not have permission to upload the course materials, including any lecture recordings you may have, to any website. If you require clarification, please consult your professor.

- 2) Structure utilizing air between the strip and ground plane gives higher Q , wavelength, operation frequency, and avoids interference.

Slotline

- Guide mode of architecture makes it particularly suitable for applications where substrate is ferrite (components such as circulators and isolators).
- Disadvantages :
 - 1) Impedances below 60Ω are difficult to realize.
 - 2) Q factor is significantly lower than other structures considered here.
 - 3) Circuit structures often involve difficult registration problems (especially with metallization on the opposite side to the slot).

Trapped Inverted Microstrip (TIM)

- Advantages is similar to that of IM; moreover, a ‘slot’ or ‘channel’-shaped ground plane provides inherent suppression of some higher-order modes
- Manufacturing difficulties are particularly significant with HMICs.

Coplanar waveguide

- Advantages in comparison with microstrip :
 - 1) Easier grounding of surface-mounted (or BGA mounted) component.
 - 2) Lower fabrication costs.
 - 3) Reduced dispersion and radiation losses.
 - 4) Photolithographically defined structures with relatively low dependence on substrate thickness.

Coplanar strip (CPS) and Differential Line

- CPS: one of the conductors is grounded; differential line: none of the conductors is grounded.
- Advantage of differential line:

The materials you receive for this course are protected by copyright and to be used for this course only. You do not have permission to upload the course materials, including any lecture recordings you may have, to any website. If you require clarification, please consult your professor.

- 1) It is suitable for RFICs and high-speed digital ICs (but not for HMIC due to radiation losses and most passive components are single-ended).
 - 2) This line is popular for use in long bus lines and clock distribution nets on chip as the signal return path.
- The differential line has a virtual ground itself (a real metallic ground is not necessary).

Stripline

- Completely filled microstrip, i.e. a symmetrical structure results in TEM transmission
- Advantages :
 - 1) lower loss.
 - 2) Fairly high Q -factor.
 - 3) Waveguide modes can easily be exited at higher frequencies.
- Disadvantages:
 - 1) Insufficient space for the incorporation of semiconductor devices.
 - 2) Mode suppression gives rise to design problem.
 - 3) Not compatible with shunt-mounted devices.
- Z_0 and Q -factor are criterion for circuit applications.

Structure	Z_0 (Ω)
Microstrip	11–110
Inverted microstrip	11–130
Trapped inverted microstrip (TIM)	14–140
Suspended stripline	40–150
Coplanar waveguide (CPW)	40–110
Differential line, Coplanar strips (CPS)	40–110
Slotline	35–250
Finline	10–400
Imageline	≈ 26

The materials you receive for this course are protected by copyright and to be used for this course only. You do not have permission to upload the course materials, including any lecture recordings you may have, to any website. If you require clarification, please consult your professor.

Structure	Unloaded Q , Q_u
Microstrip	250
Inverted microstrip	400
Trapped inverted microstrip (TIM)	450
Suspended stripline	600
Coplanar waveguide (CPW)	200
Differential line, Coplanar strips (CPS)	200
Slotline	200
Finline	550
Imageline	2500

The materials you receive for this course are protected by copyright and to be used for this course only. You do not have permission to upload the course materials, including any lecture recordings you may have, to any website. If you require clarification, please consult your professor.

Transmission Line	Q-Factor	Radiation	Dispersive	Impedance Range (Ohm)	Chip Mounting
Microstrip line	250 (dielectric substrate) 100–150 (Si, GaAs substrate)	Low (for high ϵ) High (for low ϵ)	Low	20–120	Difficult for shunt; easy for series
Stripline	400	Low	None	35–250	Poor
Suspended stripline	500	Low	None	40–150	Fair
Slotline	100	Medium	High	60–200	Easy for shunt; difficult for series
Coplanar waveguide	150	Medium	Low	20–250	Easy for series and shunt
Finline	500	None	Low	10–400	Fair

The materials you receive for this course are protected by copyright and to be used for this course only. You do not have permission to upload the course materials, including any lecture recordings you may have, to any website. If you require clarification, please consult your professor.

Substrates:

- Many factors, mechanical, thermal, electronics, and economic, leading to the correct choice of substrate deeply influence MIC design.
- The kinds of questions include:
 - 1) Cost
 - 2) Thin-film or thick-film technology
 - 3) Frequency range
 - 4) Surface roughness (this will influence conductor losses and metal-film adhesion)
 - 5) Mechanical strength, flexibility, and thermal conductivity
 - 6) Sufficient surface area

Organic PCBs (Printed Circuit Boards)

- FR4
 - 1) Low cost, rigid structure, and multi-layer capability.
 - 2) Applications for operation frequency below a few GHz. $f_{op} \downarrow \Rightarrow$ Loss ↓
- RT/Duroid
 - 1) Low loss and good for RF applications.
 - 2) Board has a wide selected range for permittivity. e.g. RT/Duroid 5870 with $\epsilon_r = 2.33$, RT/Duroid 5880 with $\epsilon_r = 2.2$, and RT/Duroid 6010 with $\epsilon_r = 10.2$.
 - 3) Board is soft leading to less precise dimensional control.

Softboard

- 1) Plastic substrate with good flexibility.
- 2) This board is suitable for experimental circuits operating below a few GHz and array antennas operating up to and beyond 20 GHz.

Ceramic Substrate (Alumina)

- 1) Good for operation frequency up to 40 GHz.
-

The materials you receive for this course are protected by copyright and to be used for this course only. You do not have permission to upload the course materials, including any lecture recordings you may have, to any website. If you require clarification, please consult your professor.

- 2) Metallic patterns can be implemented on ceramic substrate using thin-film or thick-film technology.
- 3) Passive components of extremely small volume can be implemented because the ceramic substrate can be stacked in many tens of layers or more, e.g. low temperature co-fired ceramic (LTCC).
- 4) Good thermal conductivity.
- 5) Alumina purity below 85% should result in high conductor and dielectric losses and poor reproducibility.

Quartz

- 1) Production circuits for millimetric wave applications from tens of GHz up to perhaps 300 GHz, and suitable for use in finline and image line MIC structures.
- 2) Lower permittivity of property allows larger distributed circuit elements to be incorporated.

Sapphire

- The most expensive substrate with following advantages:
 - 1) Transparent feature is useful for accurately registering chip devices.
 - 2) Fairly high permittivity ($\epsilon_r = 10.1 \sim 10.3$), reproducible (all pieces are essentially identical in dielectric properties), and thermal conductivity (about 30% higher than the best alumina).
 - 3) Low power loss.
- Disadvantages:
 - 1) Relatively high cost.
 - 2) Substrate area is limited (usually little more than 25 mm square).
 - 3) Dielectric anisotropy poses some additional circuit design problems.

The materials you receive for this course are protected by copyright and to be used for this course only. You do not have permission to upload the course materials, including any lecture recordings you may have, to any website. If you require clarification, please consult your professor.

Material	Surface roughness (μm)	$10^4 \tan \delta$ (at 10 GHz)	ϵ_r	Thermal conductivity ($\text{W/cm}^2/\text{°C}$)	K	Dielectric strength (kV/cm)
Air (dry)	N/A	≈ 0	1	0.00024	30	
Alumina:						
99.5%	0.05–0.25	1–2	10.1	0.37	4×10^3	
96%	5–20	6	9.6	0.28	4×10^3	
85%	30–50	15	8.5	0.2	4×10^3	
Sapphire ¹	0.005–0.025	0.4–0.7	9.4, 11.6	0.4	4×10^3	
Glass, typical	0.025	20	5	0.01	–	
Polyimide	–	50	3.2	0.002	4.3	
Irradiated polyolefin	1		2.3	0.001	≈ 300	
Quartz (fused) i.e. SiO_2	0.006–0.025	1	3.8	0.01	10×10^3	
Beryllia (BeO) ²	0.05–1.25	1	6.6	2.5	–	
Rutile	0.25–2.5	4	100	–	–	
Ferrite/garnet	0.25	2	13–16	0.03	4×10^3	
FR4 circuit board	≈ 6	100	4.3–4.5	0.005	–	
RT-duroid [®] 5880	0.75–1 ³ 4.25–8.75 ⁴	5–15	2.16–2.24	0.0026	–	
RT-duroid [®] 6010	0.75–1 ³ 4.25–8.75 ⁴	10–60	10.2–10.7	0.0041	–	
AT-1000 [®]	–	20	10.0–13.0	0.0037	–	
Cu-flon	–	4.5	2.1	–	–	

The materials you receive for this course are protected by copyright and to be used for this course only. You do not have permission to upload the course materials, including any lecture recordings you may have, to any website. If you require clarification, please consult your professor.

Material	Surface roughness (μm)	$10^4 \tan \delta$ (at 10 GHz)	ϵ_r	Thermal conductivity ($\text{W/cm}^2/\text{°C}$)	con- K	Dielectric strength (kV/cm)
Si (high resistivity)	0.025	10–100	11.9	0.9	—	300
GaAs	0.025	6	12.85	0.3	—	350
InP	0.025	10	12.4	0.4	—	350
SiO ₂ (on-chip)	—	—	4.0–4.2	—	—	—
polyarylether (SILK TM)	CMP ⁵	—	2.65	0.19 @ 25°C	—	—
silicon oxycarbide (SiCOH)	CMP ⁵	—	2.7	0.23 @ 125°C	—	—
LTCC (typical, green tape TM951)	0.22	15	7.8	3	—	400

The materials you receive for this course are protected by copyright and to be used for this course only. You do not have permission to upload the course materials, including any lecture recordings you may have, to any website. If you require clarification, please consult your professor.

REFERENCES

General references

- [1] S.A. Maas, *Nonlinear microwave circuits*, Norwood MA: Artech House, 1988.
- [2] F.T. Ulaby, *Fundamentals of applied electromagnetics*, Upper Saddle River NJ: Prentice Hall, 2007.
- [3] S.M. Wentworth, *Fundamentals of electromagnetics with engineering applications*, John Wiley and Sons, 2005.
- [4] Small signal: http://en.wikipedia.org/wiki/Small_signal_model
- [5] Large signal: http://en.wikipedia.org/wiki/Large_signal
- [6] http://www.qsl.net/va3iul/Homebrew_RF_Circuit_Design_Ideas/Homebrew_RF_Circuit_Design_Ideas.htm
- [7] <http://www.microwaves101.com/index.cfm>
- [8] <http://www.slideshare.net/AviatNetworks/the-evolution-of-microwave-communication>
- [9] <http://en.wikipedia.org/wiki/Microwave>

S Matrix

- [1] H.J. Carlin, "The scattering matrix in network theory," *IRE Trans. Circuit Theory*, Vol. 3, 88-97, June 1956.
 - [2] K. Kurokawa, "Power waves and the scattering matrix," *IEEE Trans. Microwave Theory Tech.*, Vol 13, 194-202, Mar. 1965.
 - [3] Hewlett-Packard, *S-Parameters, circuit analysis and design*, Application note N° 95, 1968.
 - [4] K.C. Gupta, R. Garg, R. Chadha, *Computer aided design of microwave circuits*, Dedham MA : Artech House, 1981.
 - [5] G.D. Vendelin, A.M. Pavio, U. L. Rohde, *Microwave circuit design using linear and nonlinear techniques*, New York : Wiley & Sons, 1990.
 - [6] <http://anodegroup.univ-lille1.fr/publications/>
-

The materials you receive for this course are protected by copyright and to be used for this course only. You do not have permission to upload the course materials, including any lecture recordings you may have, to any website. If you require clarification, please consult your professor.

Linear-Nonlinear Analysis

- [1] R.W. Newcomb, *Linear multiport synthesis*, New York: Mc Graw-Hill, 1956.
 - [2] L.O. Chua, C.A. Desoer, E.S. Kuh, *Linear and nonlinear circuits*, NY: McGraw-Hill, 1987.
 - [3] G.L. Heiter, "Characterization of nonlinearities in microwave devices and systems," *IEEE Trans. Microwave Theory Tech.*, Vol 21, 797-805, Dec. 1973.
 - [4] V. Rizzoli, A. Neri, "State of the art and present trends in nonlinear microwave CAD techniques," *IEEE Trans. Microwave Theory Tech.*, Vol 36, 343-365, Feb. 1988.
 - [5] M.B. Steer, "Simulation of nonlinear microwave circuits - an historical perspective and comparisons," in *IEEE Int. Microwave Symp. Dig.*, Boston, 599-602, 1991.
 - [6] V. Volterra, *Theory of functionals and of integral and integro-differential equations*, New-York: Dover, 1959.
 - [7] V. Rizzoli, A. Lipparini, E. Marazzi, "A general purpose program for nonlinear microwave circuit design," *IEEE Trans. Microwave Theory Tech.*, Vol 31, 762-770, Sept. 1983.
 - [8] K.S. Kundert, A. Sangiovanni-Vincentelli, "Simulation of nonlinear circuits in the frequency domain," *IEEE Trans. Computer-Aided Design*, Vol 5, 521-535, Oct. 1986.
 - [9] M.B. Steer, C.R. Chang, G.W. Rhyne, "Computer aided analysis of nonlinear microwave circuits using frequency domain spectral balance techniques: the state of the art," *Int. J. on Microwave and Millimeter CAE*, Vol 1, Apr. 1991.
 - [10] R.J. Gilmore, M.B. Steer, "Nonlinear circuit analysis using the method of harmonic balance - a review of the art: Part I, Introductory concepts; Part II, Advanced concepts," *Int. J. on Microwave and Millimeter CAE*, Vol 1, Jan. / Apr. 1991.
 - [11] R.R. Tummala, M. Swaminathan, M.M. Tentzeris, J. Laskar, G.-K. Chang, S. Sitaraman, D. Keezer, D. Guidotti, Z. Huang, K. Lim, L. Wan, S.K. Bhattacharya, V. Sundaram, F. Liu, and P. M. Raj, "The SOP for miniaturized, mixed-signal computing, communication, and consumer systems of the next decade," *IEEE Trans. Advanced Packaging*, vol. 27, 2004, pp. 250-267.
-

The materials you receive for this course are protected by copyright and to be used for this course only. You do not have permission to upload the course materials, including any lecture recordings you may have, to any website. If you require clarification, please consult your professor.

- [12] B. Razavi, “Design considerations for future RF circuits,” *IEEE Int. CAS-Symp.*, New Orleans, LA, USA, May 27-30, 2007, 741-744.
- [13] R. Chau, “Challenges and opportunities of emerging nanotechnology for VLSI nanoelectronics,” *Int. Semiconductor Device Research Symp.*, Maryland, MD, USA, Dec. 12-14, 2007.
- [14] Y. Sun and L.F. Eastman, “Trade-offs and challenges of short channel design on millimetre-wave power performance of GaN HFETs,” *Electronics Letters*, vol. 41, 2005, 854-855.

The materials you receive for this course are protected by copyright and to be used for this course only. You do not have permission to upload the course materials, including any lecture recordings you may have, to any website. If you require clarification, please consult your professor.



Experiment No. 4

Linear and Non-Linear Systems

By: Prof. Gabriel M. Rebeiz
The University of Michigan
EECS Dept.
Ann Arbor, Michigan

Any system (amplifier, filter, circuit, etc.) which has a transfer function:

$$V_O = A V_I \text{ where } A \equiv H(\omega)$$

is a *linear* system. The transfer function, A, can have a different value and phase for different frequencies as we have measured in the lab (20 Hz - 20 kHz audio amplifier, low-Q and high-Q filters, etc.). Linear systems have several basic properties which make them desirable for use in electric circuits. Some of these properties are:

1. Linearity: If the input is a signal a_1 and the output signal is $b_1(t)$, then if the input is $na_1(t)$, the output will be exactly $nb_1(t)$ ($n = \text{constant}$). (At any frequency, V_O/V_I is a straight line!).
2. Superposition: If the input is a signal a_1 and the output signal is b_1 , and if the input signal is a_2 and the output signal is b_2 , then if the input is $a_1 + a_2$, the output will be *exactly* $b_1 + b_2$.

Talking in frequency domain, the input signal contains a frequency f , then the output will have the same *exact* frequency f , and the only difference between the input and output is an amplitude and phase change. If the input signal contains several frequencies (f_1, f_2, f_3), then the output signal will have *exactly* the same frequencies (f_1, f_2, f_3) each changed differently in its amplitude and phase, depending on the transfer function. However, *no* new frequencies are generated in linear systems.

A *non-linear* transfer function is represented by:

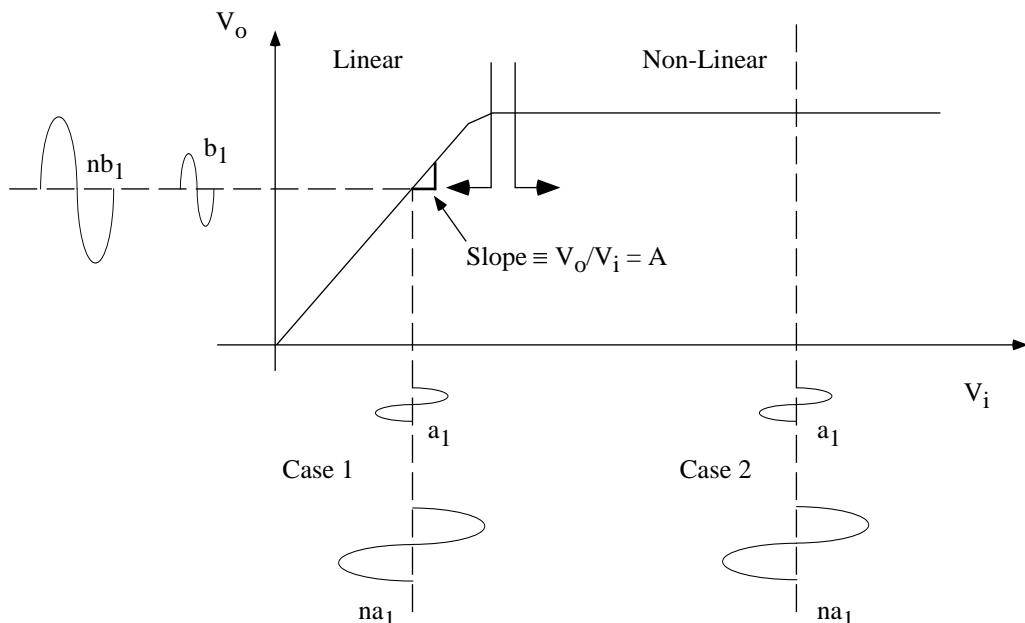
$$V_O = A V_I + B V_I^2 + C V_I^3 + \dots \quad \text{where } A, B, C \text{ are dependent on frequency} \\ (A \equiv H(\omega), B \equiv B(\omega), C \equiv C(\omega) \dots)$$

The above mentioned properties of linearity and superposition do not apply in non-linear systems. In non-linear systems, if the input signal is $a_1(t)$, and the output signal is $b_1(t)$, then if the input is $na_1(t)$, the output is not necessarily $nb_1(t)$! Figure 1 shows an amplifier operating in the linear and non-linear regime. In the non-linear region, the output is constant *independent* of the input! As is evident, in a non-linear system, the output does not have the same form as the input in time domain. This means that if the input signal contains a frequency f , then the output signal will not only contain f but also $2f, 3f, \dots$, each at a different amplitude depending on $B(\omega), C(\omega)$, etc. The $2f, 3f, \dots$ components are called *harmonics* of the signal. They are generally non-desirable components in amplifiers, filters, etc. (systems which should act linearly). Remember in EECS 210 how an amplifier generates a lot of harmonics when driven into clipping (non-linear behavior)!

Real-Life Amplifiers:

In real life, linear amplifiers have some very small non-linear components (that is, the straight line is not perfectly straight). In audio amplifiers, it is important to keep the non-linear components (the harmonics) below -40 dB of the fundamental component. This translates to a total harmonic distortion of:

$$THD \leq \frac{\sqrt{\sum P_{\text{harmonics}}}}{\sqrt{P_{\text{signal}}}} \leq \frac{\sqrt{0.0001}}{\sqrt{1}} \leq 1\%.$$



Since most amplifiers clip asymmetrically, they generate only V_i^3 , V_i^5 , etc. components. The transfer function is therefore $V_o = AV_i + BV_i^3 + CV_i^5 + \dots$. If the V_i^3 is the largest component, then for a THD of 1%, $B = 0.01 \equiv -40$ dB (for $A = 1$, or $B/A = 0.01$ for $A \neq 1$). Some people can hear this distortion level and hi-fi audio amplifiers are designed to give a THD of 0.1% and even 0.01%. For a THD of 0.01%, $B = 0.0001 \equiv -80$ dB (for $A = 1$, or $B/A = 0.0001$ for $A \neq 1$), which is a -80 dB third harmonic component compared to the fundamental! In communication systems, especially those radiating KWs of power such as radio stations, TV stations, radars, etc., it is important to keep the system very linear and to generate very low (-60 to -80 dB is very common) harmonic levels so as not to interfere with other stations at the harmonic frequencies. This means if a TV station is radiating 50 KW at 200 MHz with a -60 dB harmonic content, it will not radiate more than 50 mW(!) at 400 MHz, 600 MHz, etc. For low power applications (0.2-1W) such as hand-held analog telephones at 50 MHz and digital phones at 800-900 MHz, the harmonic content is about -30 dB.

Operation of Diodes in Small-Signal (Linear) Regime:

A diode is a very non-linear device. The I-V curve is *exponential* and is given by $I = I_s(e^{V_n V_T} - 1)$. However, as discussed in class, if a small-signal, V_S , is applied across the diode around a DC bias condition of (I_D , V_D), then the diode equation can be written as:

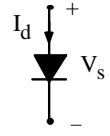


$$I_d = I_D \left(\frac{V_s}{nV_T} + \frac{1}{2!} \left(\frac{V_s}{nV_T} \right)^2 + \frac{1}{3!} \left(\frac{V_s}{nV_T} \right)^3 + \dots \right).$$

The small signal (linear component) is $i_d = I_D \frac{V_s}{nV_T}$, which is, of course, at the same frequency as V_s . The other components, V_s^2 , V_s^3 , ... are non-linear components and generate higher order harmonics. In class, we said that $V_{spk} < 5$ mV for "small-signal" or "linear" operation. Let us now calculate the harmonic content for different values of V_{spk} .

$$V_s = A \cos(\omega t) \quad (V_{spk} = A)$$

$$I_d = I_D \left(\frac{A \cos(\omega t)}{nV_T} + \frac{1}{2} \frac{A^2 \cos^2(\omega t)}{n^2 V_T^2} + \frac{1}{6} \frac{A^3 \cos^3(\omega t)}{n^3 V_T^3} + \dots \right)$$



Fundamental Component:

$$I_{d(f)} \approx \frac{I_D A}{nV_T} \cos(\omega t) + \frac{1}{8} \frac{I_D A^3}{n^3 V_T^3} \cos(\omega t)$$

negligible for $A \ll nV_T$

Second Harmonic (and DC!) Components:

$$I_{d(2f)} \approx \frac{I_D A^2}{4n^2 V_T^2} \cos(2\omega t)$$

$$I_{d(DC)} = \frac{1}{4} \frac{I_D^2 A}{n^2 V_T^2}$$

Look: a DC component!

Third Harmonic Component:

$$I_{d(3f)} \approx \frac{I_D A^3}{24n^3 V_T^3} \cos(3\omega t)$$

Dividing, we have:

$$\frac{|I_{(2f)}|}{|I_{(f)}|} \approx \frac{1}{4} \left(\frac{A}{nV_T} \right) \quad \text{and} \quad \frac{|I_{(3f)}|}{|I_{(f)}|} \approx \frac{1}{24} \left(\frac{A}{nV_T} \right)^2$$

and



$nV_T = 30\text{mV}$			
$V_{spk} = A$ (mV)	$\frac{I_{2f}}{I_f}$ (dB)	$\frac{I_{3f}}{I_f}$ (dB)	THD
1	-42	-87	< 1%
5	-28	-59	~ 4%
10	-22	-47	~ 8%

with V_{spk} being the voltage across the *diode junction*.

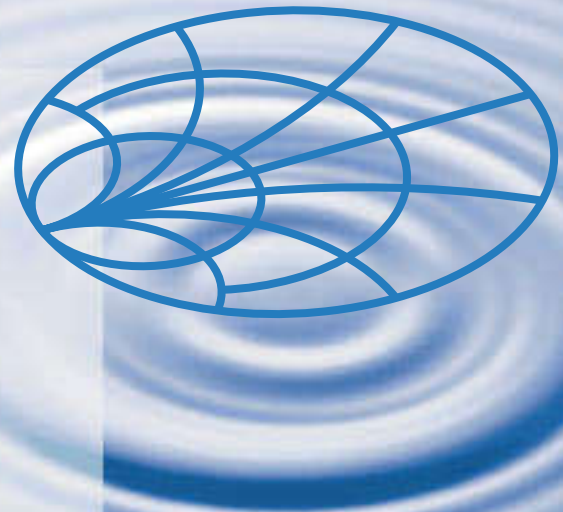
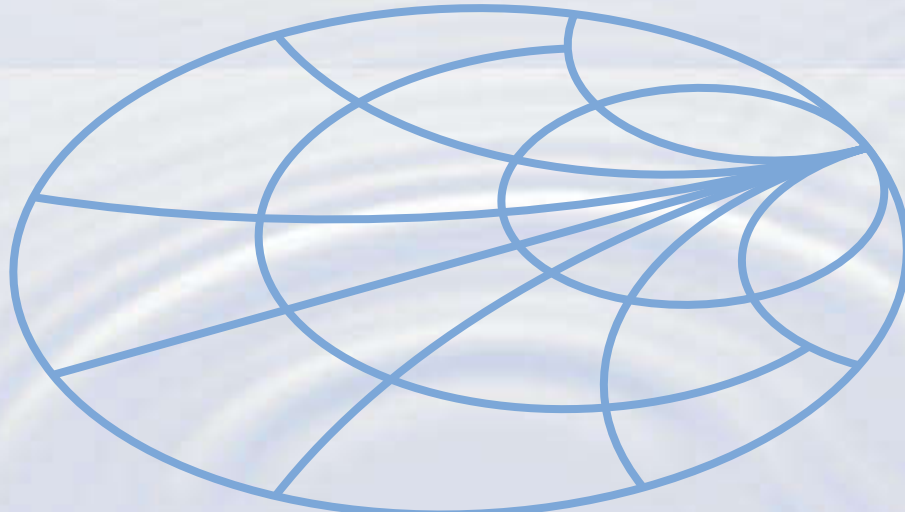
It is seen that the second and third harmonic levels are strongly dependent on the peak input voltage (A). So, by limiting V_{spk} ($= A$) ≤ 5 mV, we ensure that all harmonic are less than -28 dB and that the THD is less than 4%. This may simply not be enough in many applications, and we may limit $V_{spk} \leq 1$ mV if we want the harmonics to be less than -40 dB.

Non-Linear Systems Put To Good Use:

Do not think that non-linear systems are all bad! In many industrial problems, the process is non-linear and it is best to use a non-linear system to control it. Also, most biological sensors are non-linear (your eye, ear, pain sensors immediately go non-linear and saturate if too much light, sound, or pain is applied). Finally, in communication systems, many non-linear devices are expressly used to translate frequencies from 800-900 MHz to 10-20 MHz (and vice versa). These components are called "mixers" and "multipliers" and are used in every communication system today. You will study them in detail in EECS 411 and 522.

Test & Measurement

Application Note 95-1



S-Parameter Techniques

for Faster, More Accurate Network Design

<http://www.hp.com/go/tmappnotes>

Contents

- [1. Foreword and Introduction](#)
- [2. Two-Port Network Theory](#)
- [3. Using S-Parameters](#)
- [4. Network Calculations with Scattering Parameters](#)
- [5. Amplifier Design using Scattering Parameters](#)
- [6. Measurement of S-Parameters](#)
- [7. Narrow-Band Amplifier Design](#)
- [8. Broadband Amplifier Design](#)
- [9. Stability Considerations and the Design of
Reflection Amplifiers and Oscillators](#)

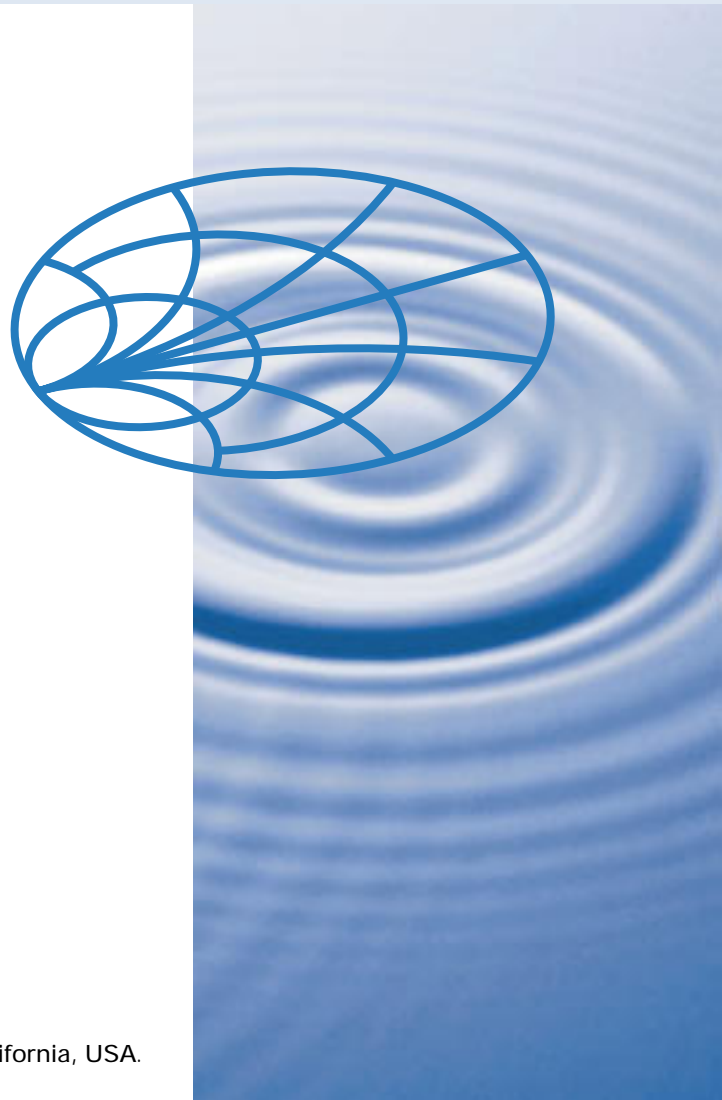
Appendix A. [Additional Reading on S-Parameters](#)

Appendix B. [Scattering Parameter Relationships](#)

Appendix C. [The Software Revolution](#)

[Relevant Products, Education and Information](#)

[Contacting Hewlett-Packard](#)



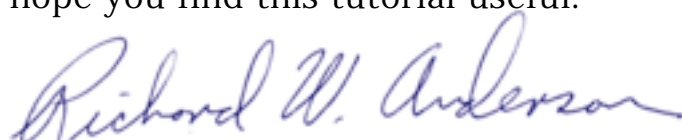
Foreword

This application note is based on an article written for the February 1967 issue of the *Hewlett-Packard Journal*, yet its content remains important today. S-parameters are an essential part of high-frequency design, though much else has changed during the past 30 years. During that time, HP has continuously forged ahead to help create today's leading test and measurement environment.

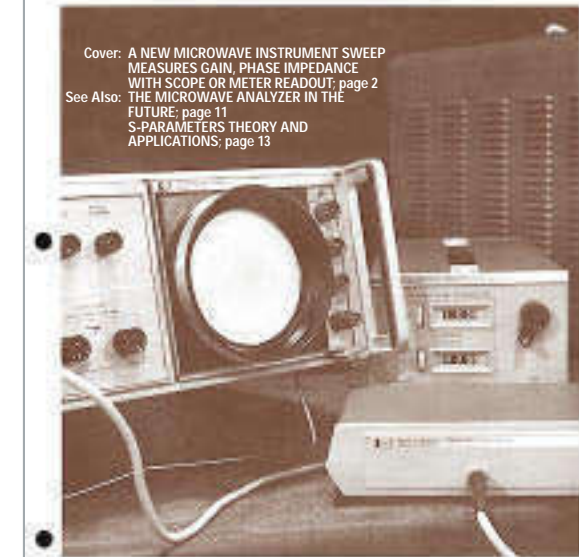
We continuously apply our capabilities in measurement, communication, and computation to produce innovations that help you to improve your business results. In wireless communications, for example, we estimate that 85 percent of the world's GSM (Groupe Speciale Mobile) telephones are tested with HP instruments. Our accomplishments 30 years hence may exceed our boldest conjectures.

This interactive application note revises and updates the 1967 article for online electronic media. It reflects the changes in our industry, while reminding us of the underlying scientific basis for the technology, and takes advantage of a potent new information dissemination capability, the World Wide Web. We hope you find this tutorial useful.

Richard Anderson,
HP Vice President and General Manager,
Microwave and Communications Group



HEWLETT-PACKARD JOURNAL



FEBRUARY 1967

February 1967 HP Journal
Cover of issue in which the original "S-Parameters Theory and Application," written during Christmas holiday 1966, first appeared. HP Journal is now online at: www.hp.com/go/journal

1 Introduction

Linear networks, or nonlinear networks operating with signals sufficiently small to cause the networks to respond in a linear manner, can be completely characterized by parameters measured at the network terminals (ports) without regard to the contents of the networks. Once the parameters of a network have been determined, its behavior in any external environment can be predicted, again without regard to the contents of the network.

S-parameters are important in microwave design because they are easier to measure and work with at high frequencies than other kinds of parameters. They are conceptually simple, analytically convenient, and capable of providing a great insight into a measurement or design problem.

To show how s-parameters ease microwave design, and how you can best take advantage of their abilities, this application note describes s-parameters and flow graphs, and relates them to more familiar concepts such as transducer power gain and voltage gain. Data obtained with a network analyzer is used to illustrate amplifier design.

Test & Measurement
Application Note 95-1
S-Parameter Techniques

Maxwell's equations

All electromagnetic behaviors can ultimately be explained by Maxwell's four basic equations:

$$\nabla \cdot \mathbf{D} = \rho \quad \nabla \times \mathbf{E} = -\frac{\partial \mathbf{B}}{\partial t}$$

$$\nabla \cdot \mathbf{B} = 0 \quad \nabla \times \mathbf{H} = \mathbf{j} + \frac{\partial \mathbf{D}}{\partial t}$$

However, it isn't always possible or convenient to use these equations directly. Solving them can be quite difficult. Efficient design requires the use of approximations such as lumped and distributed models.

2

Two-Port Network Theory

Although a network may have any number of ports, network parameters can be explained most easily by considering a network with only two ports, an input port and an output port, like the network shown in Figure 1. To characterize the performance of such a network, any of several parameter sets can be used, each of which has certain advantages. Each parameter set is related to a set of four variables associated with the two-port model. Two of these variables represent the excitation of the network (independent variables), and the remaining two represent the response of the network to the excitation (dependent variables). If the network of Fig. 1 is excited by voltage sources V_1 and V_2 , the network currents I_1 and I_2 will be related by the following equations (assuming the network behaves linearly):

$$I_1 = y_{11} V_1 + y_{12} V_2 \quad (1)$$

$$I_2 = y_{21} V_1 + y_{22} V_2 \quad (2)$$

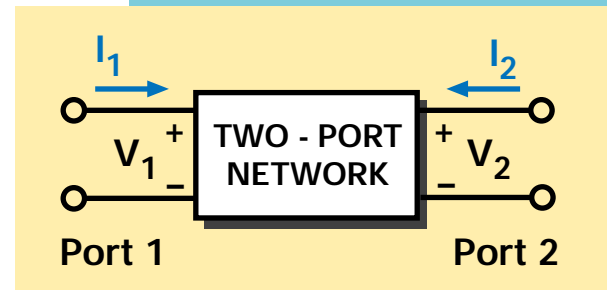


Figure 1
 General two-port network.

Why are models needed?
 Models help us predict the behavior of components, circuits, and systems. Lumped models are useful at lower frequencies, where some physical effects can be ignored because they are so small. Distributed models are needed at RF frequencies and higher to account for the increased behavioral impact of those physical effects.

2

Two-Port Network Theory

In this case, with port voltages selected as independent variables and port currents taken as dependent variables, the relating parameters are called short-circuit admittance parameters, or y -parameters. In the absence of additional information, four measurements are required to determine the four parameters y_{11} , y_{12} , y_{21} , y_{22} . Each measurement is made with one port of the network excited by a voltage source while the other port is short circuited. For example, y_{21} , the forward transadmittance, is the ratio of the current at port 2 to the voltage at port 1 with port 2 short circuited, as shown in equation 3.



$$y_{21} = \frac{I_2}{V_1} \Big|_{V_2=0} \text{ (output short circuited)} \quad (3)$$

Two-port models

Two-port, three-port, and n -port models simplify the input / output response of active and passive devices and circuits into "black boxes" described by a set of four linear parameters. Lumped models use representations such as Y (conductances), Z (resistances), and h (a mixture of conductances and resistances). Distributed models use s -parameters (transmission and reflection coefficients).

2

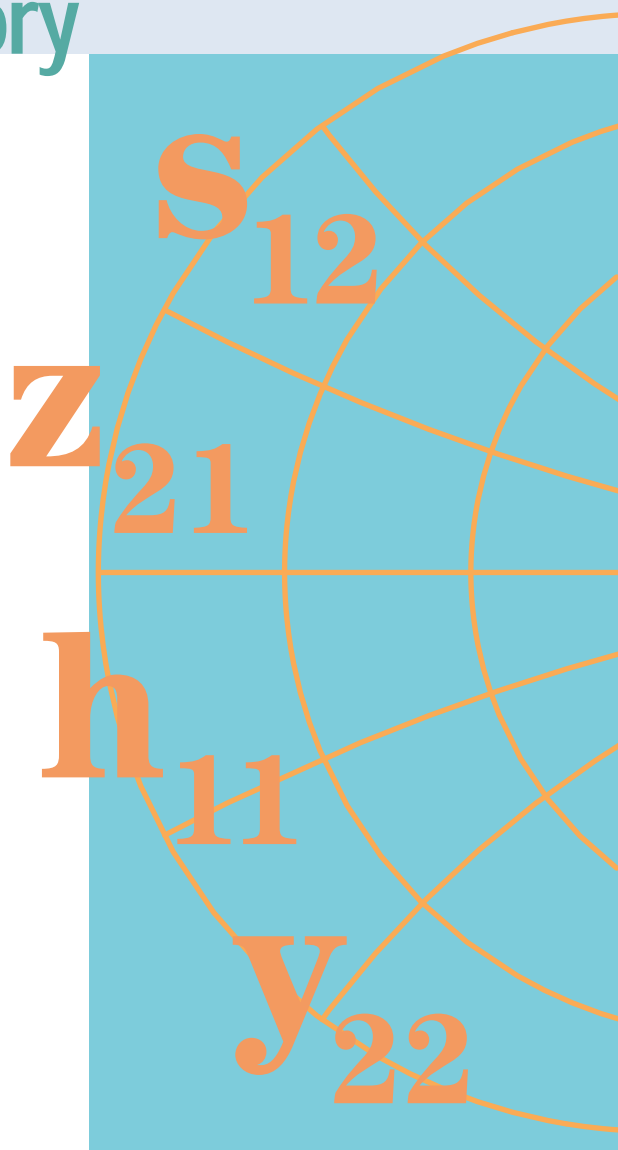
Two-Port Network Theory

If other independent and dependent variables had been chosen, the network would have been described, as before, by two linear equations similar to equations 1 and 2, except that the variables and the parameters describing their relationships would be different.

However, all parameter sets contain the same information about a network, and it is always possible to calculate any set in terms of any other set.

“Scattering parameters,” which are commonly referred to as s-parameters, are a parameter set that relates to the traveling waves that are scattered or reflected when an n-port network is inserted into a transmission line.

Appendix B “Scattering Parameter Relationships” contains tables converting scattering parameters to and from conductance parameters (y), resistance parameters (z), and a mixture of conductances and resistances parameters (h).



3 Using S-Parameters

The ease with which scattering parameters can be measured makes them especially well suited for describing transistors and other active devices. Measuring most other parameters calls for the input and output of the device to be successively opened and short circuited. This can be hard to do, especially at RF frequencies where lead inductance and capacitance make short and open circuits difficult to obtain. At higher frequencies these measurements typically require tuning stubs, separately adjusted at each measurement frequency, to reflect short or open circuit conditions to the device terminals. Not only is this inconvenient and tedious, but a tuning stub shunting the input or output may cause a transistor to oscillate, making the measurement invalid.

S-parameters, on the other hand, are usually measured with the device imbedded between a $50\ \Omega$ load and source, and there is very little chance for oscillations to occur.



50 Ω
load and source

3 Using S-Parameters

Another important advantage of s-parameters stems from the fact that traveling waves, unlike terminal voltages and currents, do not vary in magnitude at points along a lossless transmission line. This means that scattering parameters can be measured on a device located at some distance from the measurement transducers, provided that the measuring device and the transducers are connected by low-loss transmission lines.

Derivation

Generalized scattering parameters have been defined by [K. Kurokawa \[Appendix A\]](#). These parameters describe the interrelationships of a new set of variables (a_i , b_i). The variables a_i and b_i are normalized complex voltage waves incident on and reflected from the i^{th} port of the network. They are defined in terms of the terminal voltage V_i , the terminal current I_i , and an arbitrary reference impedance Z_i , where the asterisk denotes the complex conjugate:

$$a_i = \frac{V_i + Z_i I_i}{2\sqrt{|\operatorname{Re} Z_i|}} \quad (4)$$

$$b_i = \frac{V_i - Z_i^* I_i}{2\sqrt{|\operatorname{Re} Z_i|}} \quad (5)$$



Transmission and Reflection

When light interacts with a lens, as in this photograph, part of the light incident on the woman's eyeglasses is reflected while the rest is transmitted. The amounts reflected and transmitted are characterized by optical reflection and transmission coefficients. Similarly, scattering parameters are measures of reflection and transmission of voltage waves through a two-port electrical network.

3 Using S-Parameters

For most measurements and calculations it is convenient to assume that the reference impedance Z_i is positive and real. For the remainder of this article, then, all variables and parameters will be referenced to a single positive real impedance, Z_0 .

The wave functions used to define s-parameters for a two-port network are shown in Fig. 2.

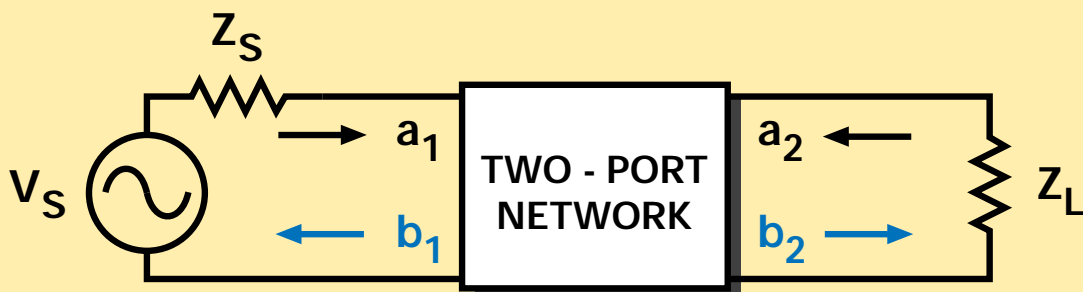


Figure 2

Two-port network showing incident waves (a_1, a_2) and reflected waves (b_1, b_2) used in s-parameter definitions. The flow graph for this network appears in [Figure 3](#).

Scattering parameters relationship to optics
 Impedance mismatches between successive elements in an RF circuit relate closely to optics, where there are successive differences in the index of refraction. A material's characteristic impedance, Z_0 , is inversely related to the index of refraction, N:

$$Z_0 \sqrt{\frac{e}{377}} = \frac{1}{N}$$

The s-parameters s_{11} and s_{22} are the same as optical reflection coefficients; s_{12} and s_{21} are the same as optical transmission coefficients.

3 Using S-Parameters

The independent variables a_1 and a_2 are normalized incident voltages, as follows:

$$a_1 = \frac{V_1 + I_1 Z_0}{2\sqrt{Z_0}} = \frac{\text{voltage wave incident on port 1}}{\sqrt{Z_0}} = \frac{V_{i1}}{\sqrt{Z_0}}$$

$$a_2 = \frac{V_2 + I_2 Z_0}{2\sqrt{Z_0}} = \frac{\text{voltage wave incident on port 2}}{\sqrt{Z_0}} = \frac{V_{i2}}{\sqrt{Z_0}}$$

Dependent variables b_1 , and b_2 , are normalized reflected voltages:

$$b_1 = \frac{V_1 - I_1 Z_0}{2\sqrt{Z_0}} = \frac{\text{voltage wave reflected from port 1}}{\sqrt{Z_0}} = \frac{V_{r1}}{\sqrt{Z_0}}$$

$$b_2 = \frac{V_2 - I_2 Z_0}{2\sqrt{Z_0}} = \frac{\text{voltage wave reflected from port 2}}{\sqrt{Z_0}} = \frac{V_{r2}}{\sqrt{Z_0}}$$

(6)

(7)

(8)

(9)



3 Using S-Parameters

The linear equations describing the two-port network are then:

$$b_1 = s_{11} a_1 + s_{12} a_2 \quad (10)$$

$$b_2 = s_{21} a_1 + s_{22} a_2 \quad (11)$$

The s-parameters s_{11} , s_{22} , s_{21} , and s_{12} are:

$$s_{11} = \left. \frac{b_1}{a_1} \right|_{a_2=0} = \text{Input reflection coefficient with the output port terminated by a matched load } (Z_L = Z_0 \text{ sets } a_2=0) \quad (12)$$

$$s_{22} = \left. \frac{b_2}{a_2} \right|_{a_1=0} = \text{Output reflection coefficient with the input terminated by a matched load } (Z_S = Z_0 \text{ sets } V_s=0) \quad (13)$$

$$s_{21} = \left. \frac{b_2}{a_1} \right|_{a_2=0} = \text{Forward transmission (insertion) gain with the output port terminated in a matched load.} \quad (14)$$

$$s_{12} = \left. \frac{b_1}{a_2} \right|_{a_1=0} = \text{Reverse transmission (insertion) gain with the input port terminated in a matched load.} \quad (15)$$

Limitations of lumped models

At low frequencies most circuits behave in a predictable manner and can be described by a group of replaceable, lumped-equivalent black boxes. At microwave frequencies, as circuit element size approaches the wavelengths of the operating frequencies, such a simplified type of model becomes inaccurate. The physical arrangements of the circuit components can no longer be treated as black boxes. We have to use a distributed circuit element model and s-parameters.

3 Using S-Parameters

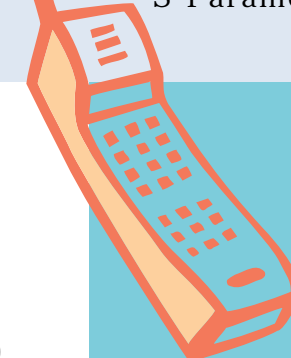
Notice that

$$s_{11} = \frac{b_1}{a_1} = \frac{\frac{V_1}{I_1} - Z_0}{\frac{V_1}{I_1} + Z_0} = \frac{Z_1 - Z_0}{Z_1 + Z_0} \quad (16)$$

and $Z_1 = Z_0 \frac{(1 + s_{11})}{(1 - s_{11})}$ (17)

where $Z_1 = \frac{V_1}{I_1}$ is the input impedance at port 1.

This relationship between reflection coefficient and impedance is the basis of the Smith Chart transmission-line calculator. Consequently, the reflection coefficients s_{11} and s_{22} can be plotted on Smith charts, converted directly to impedance, and easily manipulated to determine matching networks for optimizing a circuit design.



S-parameters

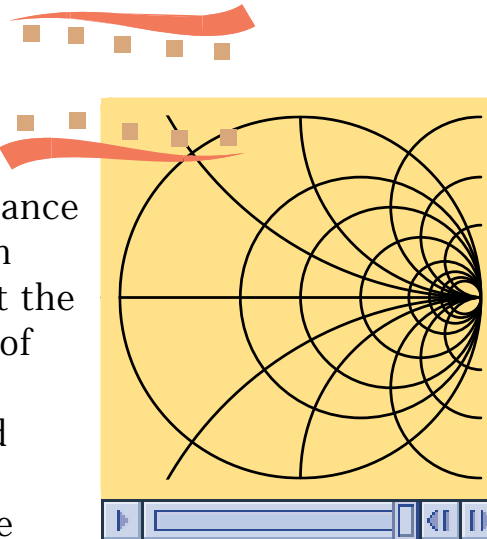
S-parameters and distributed models provide a means of measuring, describing, and characterizing circuit elements when traditional lumped-equivalent circuit models cannot predict circuit behavior to the desired level of accuracy. They are used for the design of many products, such as cellular telephones.

3 Using S-Parameters

Smith Chart Transformation

The movie at the right animates the mapping between the complex impedance plane and the Smith Chart. The Smith Chart is used to plot reflectances, but the circular grid lines allow easy reading of the corresponding impedance. As the animation shows, the rectangular grid lines of the impedance plane are transformed to circles and arcs on the Smith Chart.

Vertical lines of constant resistance on the impedance plane are transformed into circles on the Smith Chart. Horizontal lines of constant reactance on the impedance plane are transformed into arcs on the Smith Chart. The transformation between the impedance plane and the Smith Chart is nonlinear, causing normalized resistance and reactance values greater than unity to become compressed towards the right side of the Smith Chart.



Animation 1

Transformation between the impedance plane and the Smith Chart. Click over image to animate.

Showing transformations graphically

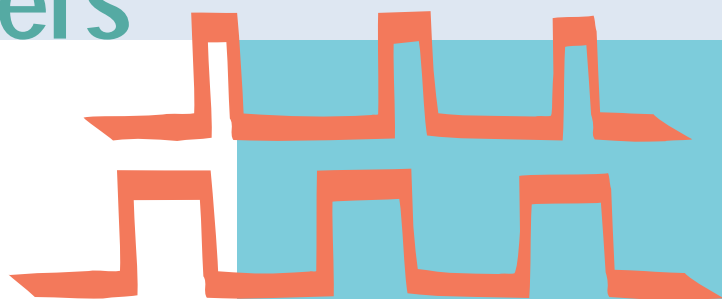
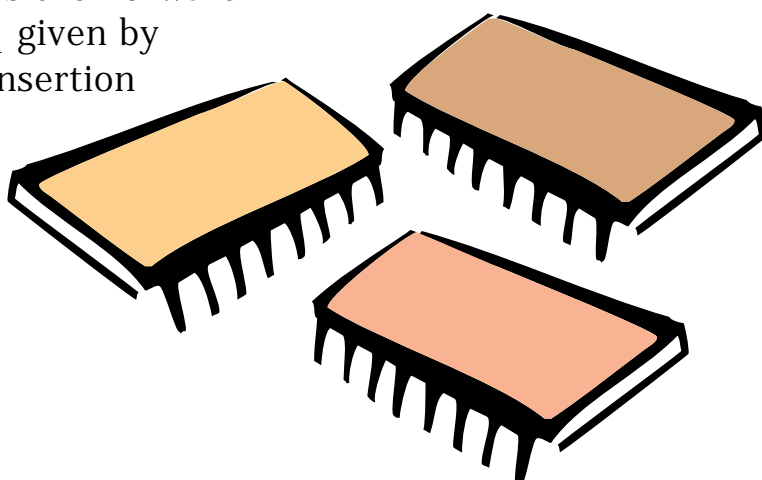
To ease his RF design work, Bell Lab's Phillip H. Smith developed increasingly accurate and powerful graphical design aids. One version, a polar coordinate form, worked for all values of impedance components, but Smith suspected that a grid with orthogonal circles might be more practical. In 1937 he constructed the basic Smith Chart still used today, using a transformation developed by co-workers E.B. Ferrell and J.W. McRae that accommodates all data values from zero to infinity.

3 Using S-Parameters

Advantages of S-Parameters

The previous equations show one of the important advantages of s-parameters, namely that they are simply gains and reflection coefficients, both familiar quantities to engineers.

By comparison, some of the y-parameters described earlier in this article are not so familiar. For example, the y-parameter corresponding to insertion gain s_{21} is the 'forward trans-admittance' y_{21} given by equation 3. Clearly, insertion gain gives by far the greater insight into the operation of the network.



Digital pulses

Digital pulses are comprised of high-order harmonic frequencies that determine the shape of the pulse. A short pulse with steep edges has a signal spectrum with relatively high power levels at very high frequencies. As a result, some elements in modern high-speed digital circuits require characterization with distributed models and s-parameters for accurate performance prediction.

3 Using S-Parameters

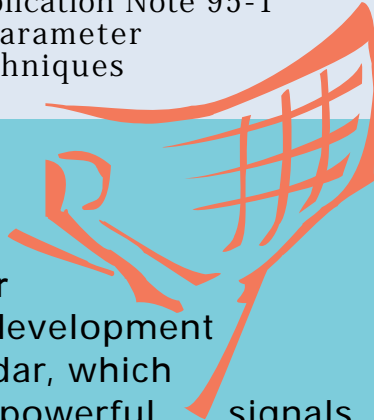
Another advantage of s-parameters springs from the simple relationship between the variables a_1 , a_2 , b_1 , and b_2 , and various power waves:

$|a_1|^2$ = Power incident on the input of the network.
= Power available from a source impedance Z_0 .

$|a_2|^2$ = Power incident on the output of the network.
= Power reflected from the load.

$|b_1|^2$ = Power reflected from the input port of the network.
= Power available from a Z_0 source minus the power delivered to the input of the network.

$|b_2|^2$ = Power reflected from the output port of the network.
= Power incident on the load.
= Power that would be delivered to a Z_0 load.



Radar

The development of radar, which uses powerful signals at short wavelengths to detect small objects at long distances, provided a powerful incentive for improved high frequency design methods during World War II. The design methods employed at that time combined distributed measurements and lumped circuit design. There was an urgent need for an efficient tool that could integrate measurement and design. The Smith Chart met that need.

3 Using S-Parameters

The previous four equations show that s-parameters are simply related to power gain and mismatch loss, quantities which are often of more interest than the corresponding voltage functions:

$$|s_{11}|^2 = \frac{\text{Power reflected from the network input}}{\text{Power incident on the network input}}$$

$$|s_{22}|^2 = \frac{\text{Power reflected from the network output}}{\text{Power incident on the network output}}$$

$$|s_{21}|^2 = \frac{\text{Power delivered to a } Z_0 \text{ load}}{\text{Power available from } Z_0 \text{ source}}$$

= Transducer power gain with Z_0 load and source

$$|s_{12}|^2 = \text{Reverse transducer power gain with } Z_0 \text{ load and source}$$

4 Network Calculations with Scattering Parameters

Signal Flow Graphs

Scattering parameters turn out to be particularly convenient in many network calculations. This is especially true for power and power gain calculations. The transfer parameters s_{12} and s_{21} are a measure of the complex insertion gain, and the driving point parameters s_{11} and s_{22} are a measure of the input and output mismatch loss. As dimensionless expressions of gain and reflection, the s-parameters not only give a clear and meaningful physical interpretation of the network performance, but also form a natural set of parameters for use with signal flow graphs [See references here and also in [Appendix A](#)].

Of course, it is not necessary to use signal flow graphs in order to use s-parameters, but flow graphs make s-parameter calculations extremely simple. Therefore, they are strongly recommended. Flow graphs will be used in the examples that follow.

References

J. K. Hunton, 'Analysis of Microwave Measurement Techniques by Means of Signal Flow Graphs,' IRE Transactions on Microwave Theory and Techniques, Vol. MTT-8, No. 2, March, 1960.

N. Kuhn, 'Simplified Signal Flow Graph Analysis,' Microwave Journal, Vol. 6, No. 11, November, 1963.

4 Network Calculations with Scattering Parameters

In a signal flow graph, each port is represented by two nodes. Node a_n represents the wave coming into the device from another device at port n, and node b_n represents the wave leaving the device at port n. The complex scattering coefficients are then represented as multipliers on branches connecting the nodes within the network and in adjacent networks. Fig. 3, right, is the flow graph representation of the system of Fig. 2.

Figure 3 shows that if the load reflection coefficient Γ_L is zero ($Z_L = Z_0$) there is only one path connecting b_1 to a_1 (flow graph rules prohibit signal flow against the forward direction of a branch arrow). This confirms the definition of s_{11} :

$$s_{11} = \left. \frac{b_1}{a_1} \right|_{a_2 = \Gamma_L b_2 = 0}$$

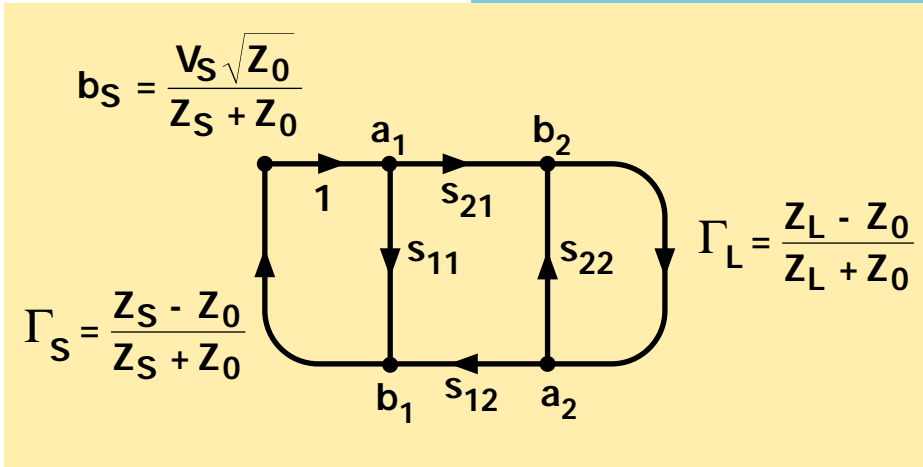


Figure 3
 Flow graph for
 two-port network
 appearing in [Figure 2](#).

4 Network Calculations with Scattering Parameters

The simplification of network analysis by flow graphs results from the application of the “non-touching loop rule.” This rule applies a generalized formula to determine the transfer function between any two nodes within a complex system. The non-touching loop rule is explained below.

The Nontouching Loop Rule

The nontouching loop rule provides a simple method for writing the solution of any flow graph by inspection. The solution T (the ratio of the output variable to the input variable) is defined, where:

T_k = path gain of the k^{th} forward path

$$\begin{aligned}\Delta &= 1 - \sum (\text{all individual loop gains}) \\ &\quad + \sum (\text{loop gain products of all possible combinations of 2 nontouching loops}) \\ &\quad - \sum (\text{loop gain products of all possible combinations of 3 nontouching loops}) \\ &\quad + \dots\end{aligned}$$

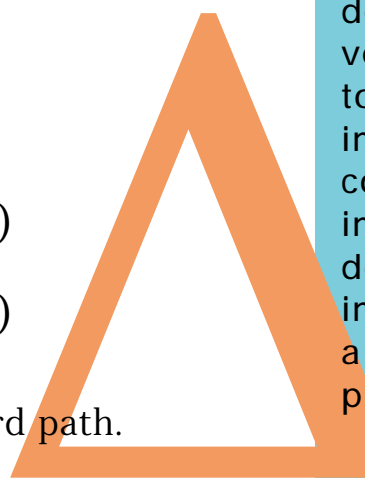
Δ_k = The value of Δ not touching the k^{th} forward path.

$$T = \frac{\sum T_k \Delta_k}{\Delta}$$

Test & Measurement
Application Note 95-1
S-Parameter Techniques

Better Smith Charts

On the copyrighted Smith Chart, curves of constant standing wave ratio, constant attenuation, and constant reflection coefficient are all circles coaxial with the center of the diagram. Refinements to the original form have enhanced its usefulness. In an article published in 1944, for example, Smith described an improved version and showed how to use it with either impedance or admittance coordinates. More recent improvements include double Smith Charts for impedance matching and a scale for calculating phase distance.



4 Network Calculations with Scattering Parameters

A path is a continuous succession of branches, and a forward path is a path connecting the input node to the output node, where no node is encountered more than once. Path gain is the product of all the branch multipliers along the path. A loop is a path that originates and terminates on the same node, no node being encountered more than once. Loop gain is the product of the branch multipliers around the loop.

For example, in [Figure 3](#) there is only one forward path from b_s to b_2 , and its gain is s_{21} . There are two paths from b_s to b_1 ; their path gains are $s_{21}s_{12}G_L$ and s_{11} respectively. There are three individual loops, only one combination of two nontouching loops, and no combinations of three or more nontouching loops. Therefore, the value of D for this network is

$$D = 1 - (s_{11}G_S + s_{21}s_{12}G_LG_S + s_{22}G_L) + s_{11}s_{22}G_LG_S$$

The transfer function from b_s to b_2 is therefore

$$\frac{b_2}{b_s} = \frac{s_{21}}{D}$$

Test & Measurement
Application Note 95-1
S-Parameter Techniques

S_{11} S_{12}
 S_{21} S_{22}

S-parameters & Smith Charts

Invented in the 1960's, S-parameters are a way to combine distributed design and distributed measurement. s_{11} and s_{22} , the two s-parameters typically represented using Smith Charts, are similar to lumped models in many respects because they are related to the input impedance and output impedance, respectively. The Smith Chart performs a highly useful translation between the distributed and lumped models and is used to predict circuit and system behavior.

4 Network Calculations with Scattering Parameters

Test & Measurement
Application Note 95-1
S-Parameter Techniques

Transducer Power Gain

Using scattering parameter flow-graphs and the non-touching loop rule, it is easy to calculate the transducer power gain with an arbitrary load and source. In the following equations, the load and source are described by their reflection coefficients G_L and G_S , respectively, referenced to the real characteristic impedance Z_0 .

Transducer power gain:

$$G_T = \frac{\text{Power delivered to the load}}{\text{Power available from the source}} = \frac{P_L}{P_{avS}}$$

$$P_L = P(\text{incident on load}) - P(\text{reflected from load})$$

$$= |b_2|^2 (1 - |G_L|^2)$$

$$P_{avS} = \frac{|b_S|^2}{(1 - |G_S|^2)}$$

$$G_T = \left| \frac{b_2}{b_S} \right|^2 (1 - |G_S|^2) (1 - |G_L|^2)$$

G
T

4 Network Calculations with Scattering Parameters

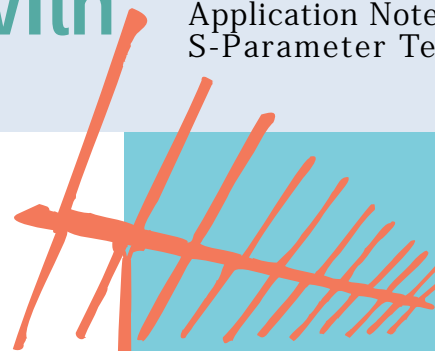
Using the non-touching loop rule,

$$\begin{aligned}\frac{b_2}{b_S} &= \frac{s_{21}}{1 - s_{11}\Gamma_S - s_{22}\Gamma_L - s_{21}s_{12}\Gamma_L\Gamma_S + s_{11}\Gamma_S s_{22}\Gamma_L} \\ &= \frac{s_{21}}{(1 - s_{11}\Gamma_S)(1 - s_{22}\Gamma_L) - s_{21}s_{12}\Gamma_L\Gamma_S} \\ G_T &= \frac{|s_{21}|^2 (1 - |\Gamma_S|^2) (1 - |\Gamma_L|^2)}{|(1 - s_{11}\Gamma_S)(1 - s_{22}\Gamma_L) - s_{21}s_{12}\Gamma_L\Gamma_S|^2}\end{aligned}\tag{18}$$

Two other parameters of interest are:

- 1) Input reflection coefficient with the output termination arbitrary and $Z_S = Z_0$.

$$\begin{aligned}s'_{11} &= \frac{b_1}{a_1} = \frac{s_{11}(1 - s_{22}\Gamma_L) + s_{21}s_{12}\Gamma_L}{1 - s_{22}\Gamma_L} \\ &= s_{11} + \frac{s_{21}s_{12}\Gamma_L}{1 - s_{22}\Gamma_L}\end{aligned}\tag{19}$$



Obtaining maximum performance
S-parameters are used to characterize RF and microwave components that must operate together, including amplifiers, transmission lines, and antennas (and free space). Because s-parameters allow the interactions between such components to be simply predicted and calculated, they make it possible to maximize performance in areas such as power transfer, directivity, and frequency response.

4 Network Calculations with Scattering Parameters

2) Voltage gain with arbitrary source and load impedances

$$A_V = \frac{V_2}{V_1} \quad V_1 = (a_1 + b_1)\sqrt{Z_0} = V_{i1} + V_{r1}$$

$$V_2 = (a_2 + b_2)\sqrt{Z_0} = V_{i2} + V_{r2}$$

$$a_2 = \Gamma_L b_2$$

$$b_1 = s'_{11} a_1$$

$$A_V = \frac{b_2(1 + \Gamma_L)}{a_1(1 + s'_{11})} = \frac{s_{21}(1 + \Gamma_L)}{(1 - s_{22}\Gamma_L)(1 + s'_{11})} \quad (20)$$

[Appendix B](#) contains formulas for calculating many often-used network functions (power gains, driving point characteristics, etc.) in terms of scattering parameters. Also included are conversion formulas between [s-parameters and h-, y-, and z-parameters](#), which are other parameter sets used very often for specifying transistors at lower frequencies.



Waveguides

A radar system delivers a large amount of energy from a microwave (μW) source to the transmitting antenna. The high field strengths cause short circuits in standard wires, cabling, and coax, so waveguides are used. These hollow metal tube constructions conduct μW energy much like a plumbing system. In the design of waveguides, we can test for signal reflections and transmission quality with s-parameters.

5 Amplifier Design

Using Scattering Parameters

The remainder of this application note will show with several examples how s-parameters are used in the design of transistor amplifiers and oscillators. To keep the discussion from becoming bogged down in extraneous details, the emphasis in these

examples will be on s-parameter design *methods*, and mathematical manipulations will be omitted wherever possible.

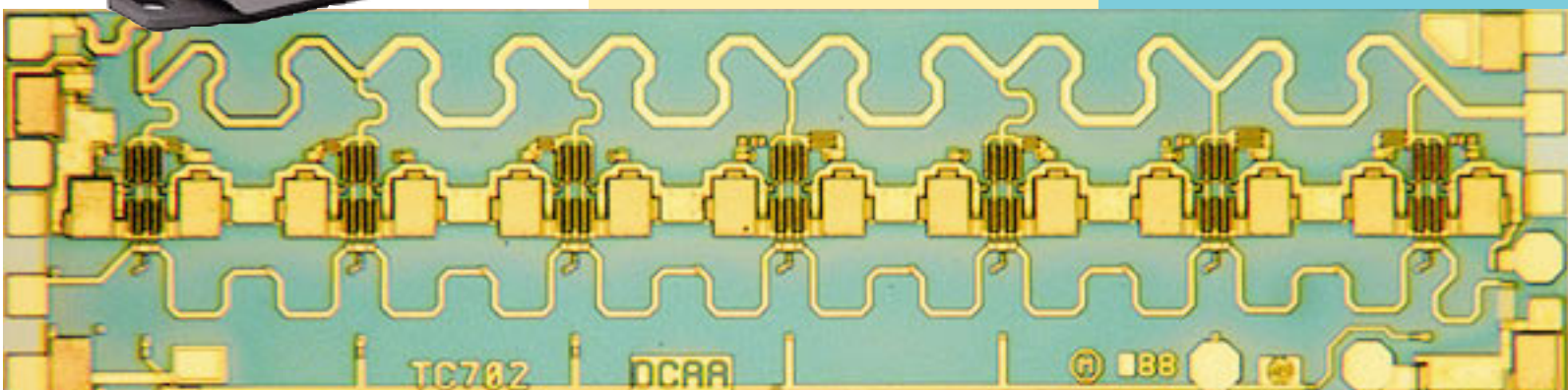


The HP 83017A microwave system amplifier achieves 0.5–26.5 GHz bandwidth by incorporating the HP TC702 GaAs MESFET TWA IC.

Test & Measurement
Application Note 95-1
S-Parameter Techniques

Traveling wave amplifier

S-parameters are extensively used for designing RF/ μ W circuits such as the HP TC702 distributed traveling wave amplifier (TWA) enlarged in the photograph below. The frequency-dependent impedances (or dispersion) in this integrated circuit can not be modeled by lumped-equivalent circuit elements, but s-parameters can accurately characterize the amplifier's response.



6 Measurement of S-Parameters

Most design problems will begin with a tentative selection of a device and the measurement of its s-parameters.

Figures 4a – 4e, which appear to the right and on the next two pages, are a set of oscilloscograms showing complete s-parameter data between 100 MHz and 1.7 GHz for a 2N3478 transistor in the common-emitter configuration.

These graphs are the results of swept-frequency measurements made with the classic HP 8410A microwave network analyzer. They were originally published as part of the 1967 *HP Journal* article. Measurements made with a modern network analyzer are presented at the end of this section. While the measurement tools have changed over the past 30 years, the basic measurement techniques have not.

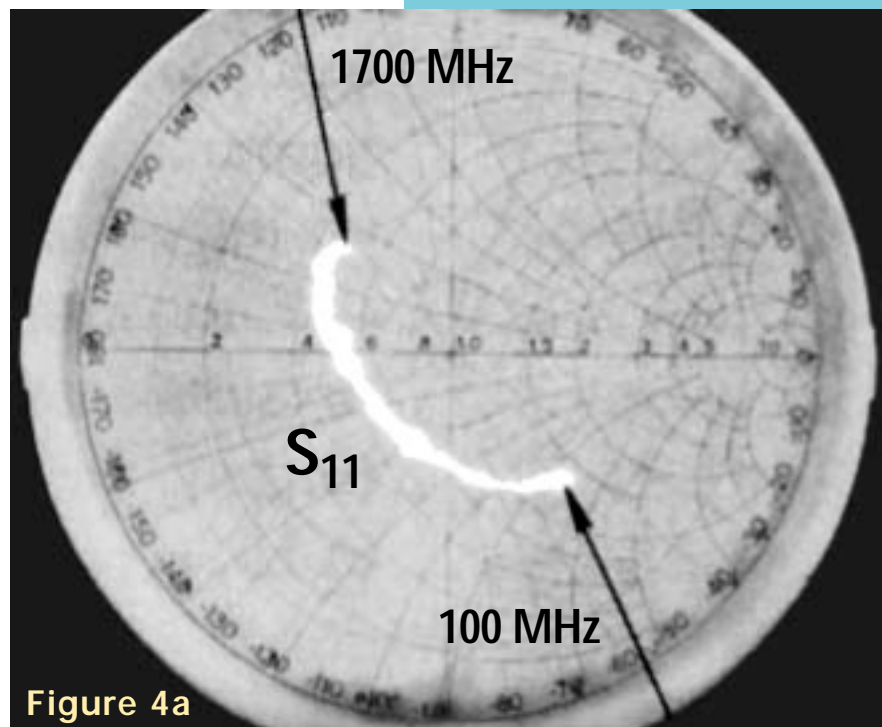


Figure 4a

S_{11} of a 2N3478 transistor measured with the classic HP 8410A network analyzer. Outermost circle on Smith Chart overlay corresponds to $|S_{11}| = 1$. The movement of S_{11} with frequency is approximately along circles of constant resistance, indicative of series capacitance and inductance.

6 Measurement of S-Parameters

Test & Measurement
Application Note 95-1
S-Parameter Techniques

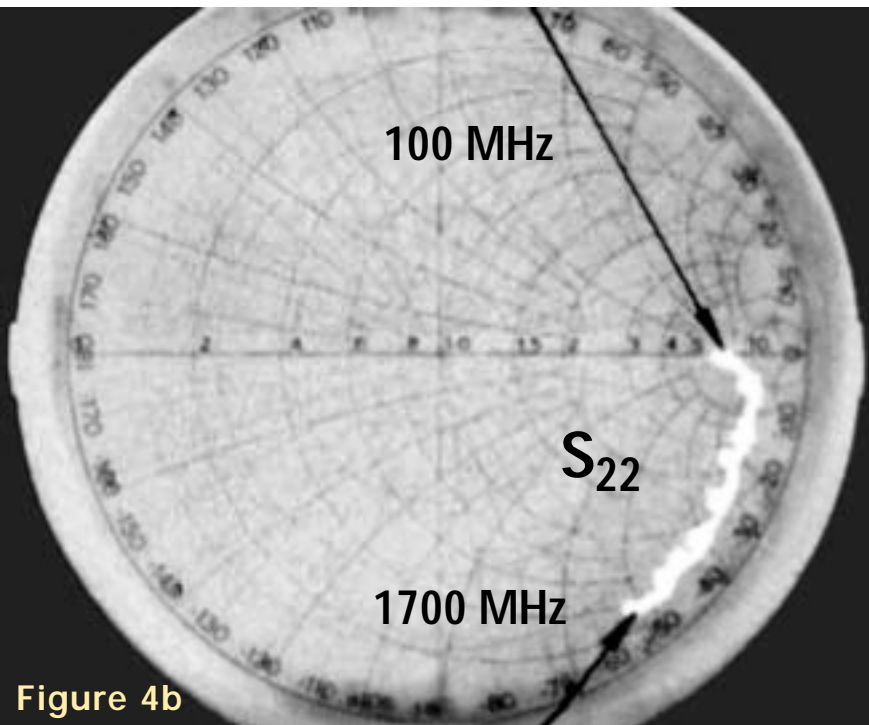


Figure 4b

Displayed on the same scale as Figure 4a, s_{22} moves between the indicated frequencies roughly along circles of constant conductance, characteristic of a shunt RC equivalent circuit.

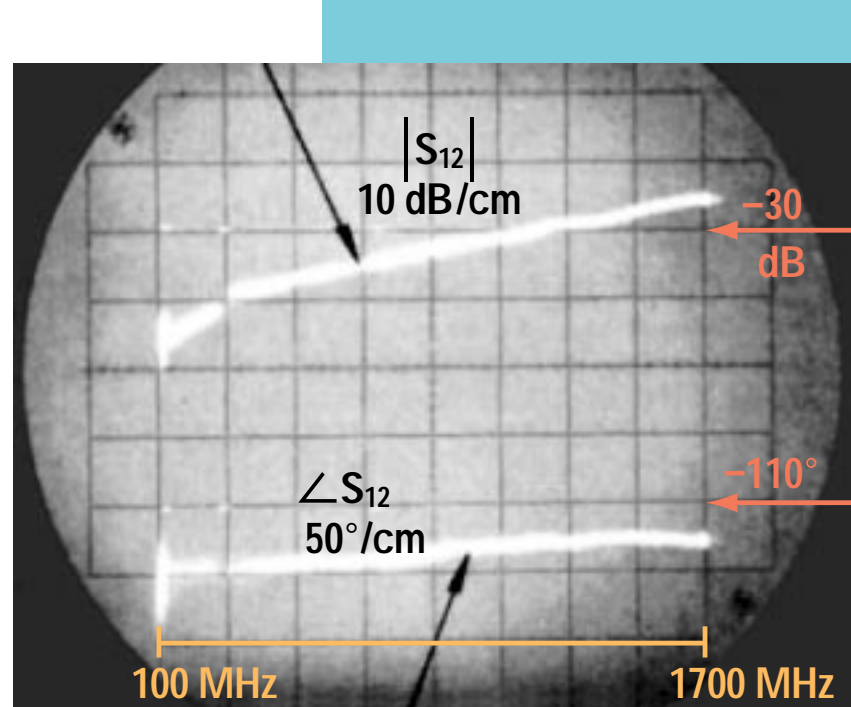


Figure 4c

Magnitude and phase of s_{12} . While the phase of s_{12} is relatively insensitive to the frequency, the magnitude of s_{12} increases about 6dB/octave.

6 Measurement of S-Parameters

Test & Measurement
Application Note 95-1
S-Parameter Techniques

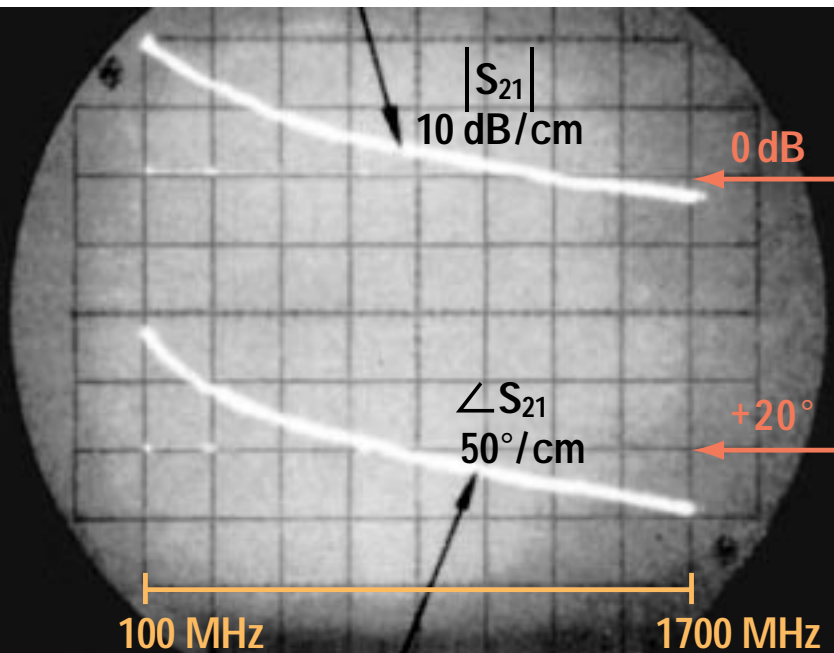


Figure 4d – Magnitude and phase of s_{21} .
The magnitude of s_{21} decays with a slope of about 6 dB/octave , while the phase decreases linearly above 500 MHz .

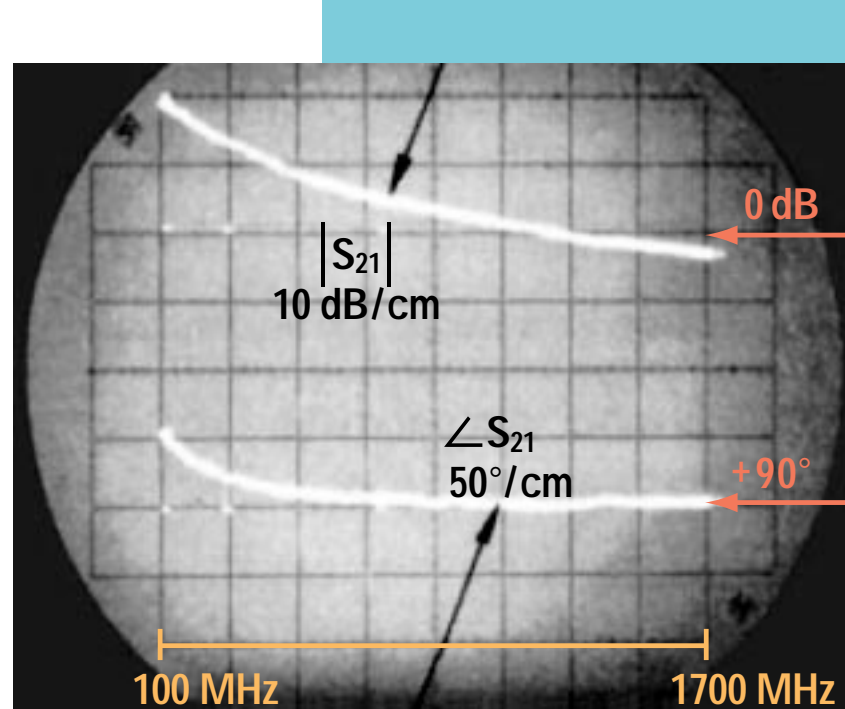


Figure 4e – Removing Linear Phase Shift.
Magnitude and phase of s_{21} measured with a line stretcher adjusted to remove the linear phase shift above 500 MHz .

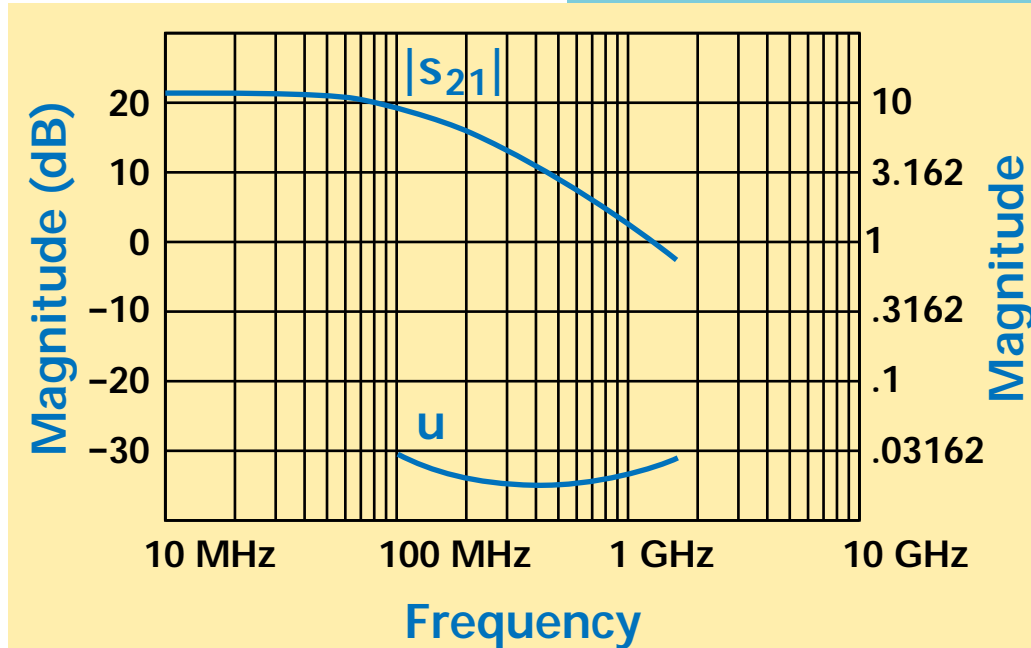
6 Measurement of S-Parameters

In Fig. 4f, the magnitude of s_{21} from Fig. 4d is replotted on a logarithmic frequency scale, along with additional data on s_{21} below 100 MHz, measured with a vector voltmeter. The magnitude of s_{21} is essentially constant to 125 MHz, and then it rolls off at a slope of 6 dB/octave.

The phase of s_{21} , as seen in Fig. 4d, varies linearly with frequency above about 500 MHz. By adjusting a calibrated line stretcher in the network analyzer, a compensating linear phase shift was introduced, and the phase curve of Fig. 4e resulted. To go from the phase curve of Fig. 4d to that of Fig. 4e required 3.35 cm of line, that is equivalent to a pure time delay of 112 picoseconds.

Figure 4f

Top curve: $|s_{21}|$ from Fig. 4 is replotted on a logarithmic frequency scale. Data below 100 MHz was measured with an HP 8405A vector voltmeter. The bottom curve [u, the unilateral figure of merit,](#) calculated from s-parameters.



6 Measurement of S-Parameters

After removal of the constant-delay, or linear-phase, component, the phase angle of s_{21} for this transistor (Fig. 4e) varies from 180° at dc to $+90^\circ$ at high frequencies, passing through $+135^\circ$ at 125 MHz, the -3 dB point of the magnitude curve. In other words, s_{21} behaves like a single pole in the frequency domain, and it is possible to write a closed expression for it. This expression is

$$s_{21} = \frac{-s_{210} e^{-j\omega T_0}}{1 + j \frac{\omega}{\omega_0}} \quad (21)$$

where

$$T_0 = 112 \text{ ps}$$

$$\omega = 2 \text{ pF}$$

$$\omega_0 = 2 \pi \times 125 \text{ MHz}$$

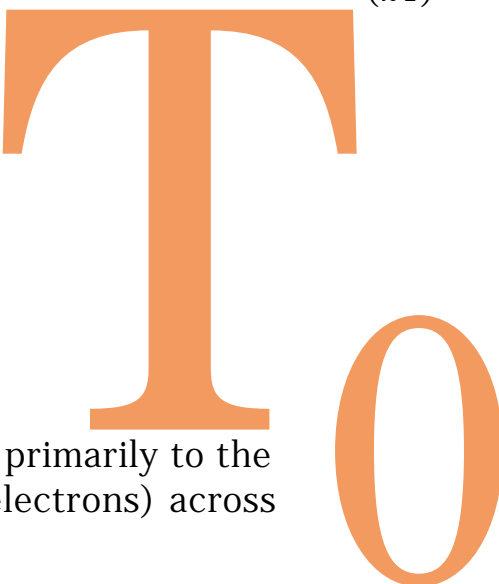
$$s_{210} = 11.2 = 21 \text{ dB}$$

The time delay $T_0 = 112 \text{ ps}$ is due primarily to the transit time of minority carriers (electrons) across the base of this npn transistor.

Test & Measurement
Application Note 95-1
S-Parameter Techniques

Importance of simple approximations

Using first-order approximations such as equation 21 is an important step in circuit design. The intuitive sense that designers gain from developing an understanding of these approximations can eliminate much frustration. The acquired insight can save hours of time that otherwise might be wasted generating designs that cannot possibly be realized in the lab, while also decreasing development costs.

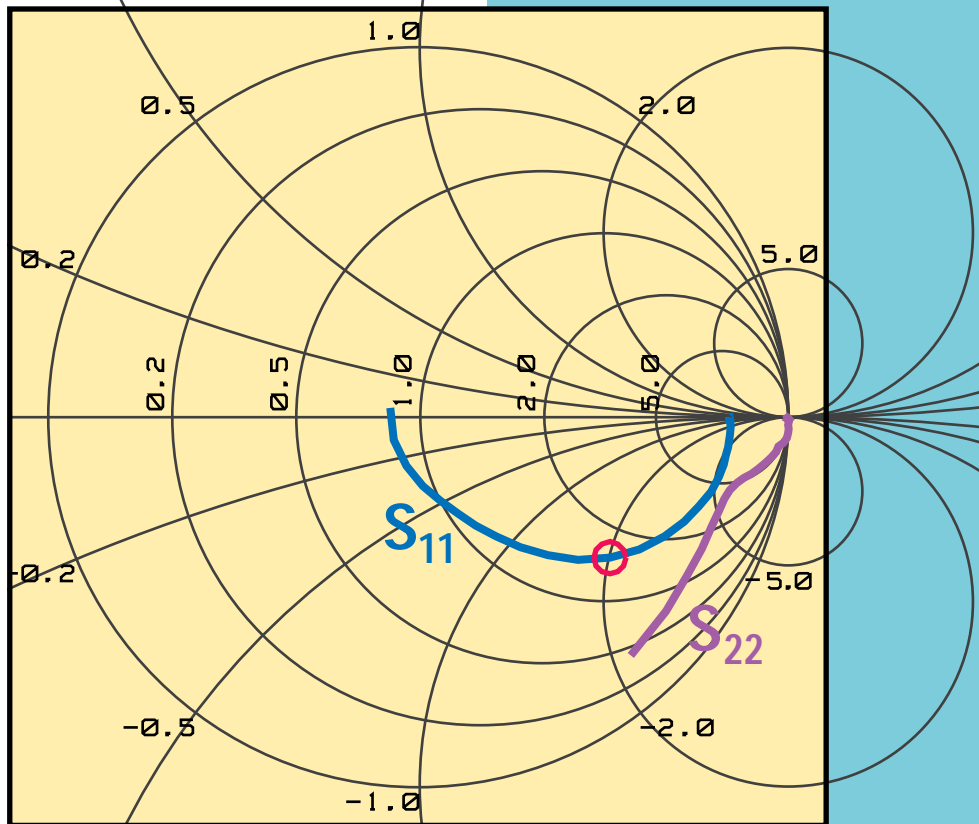


6 Measurement of S-Parameters

The s-parameters of an 2N3478 transistor shown in Figures 4a through 4f were measured with the classic HP 8410A network analyzer. In Figures 5a through 5e, the s-parameters of an 2N3478 transistor are shown re-measured with a modern HP 8753 network analyzer. Figures 5a through 5e represent the actual s-parameters of this transistor between 0.300 MHz and 1.00 GHz.

Figure 5a

S-parameters of 2N3478 transistor in common-emitter configuration, measured by an HP 8753 network analyzer. This plot shows s_{11} and s_{22} on a Smith Chart. The **marker** set at 47 MHz represents the -3 dB gain roll off point of s_{21} . The frequency index of this point is referenced in the other plots.



6 Measurement of S-Parameters

Test & Measurement
Application Note 95-1
S-Parameter Techniques

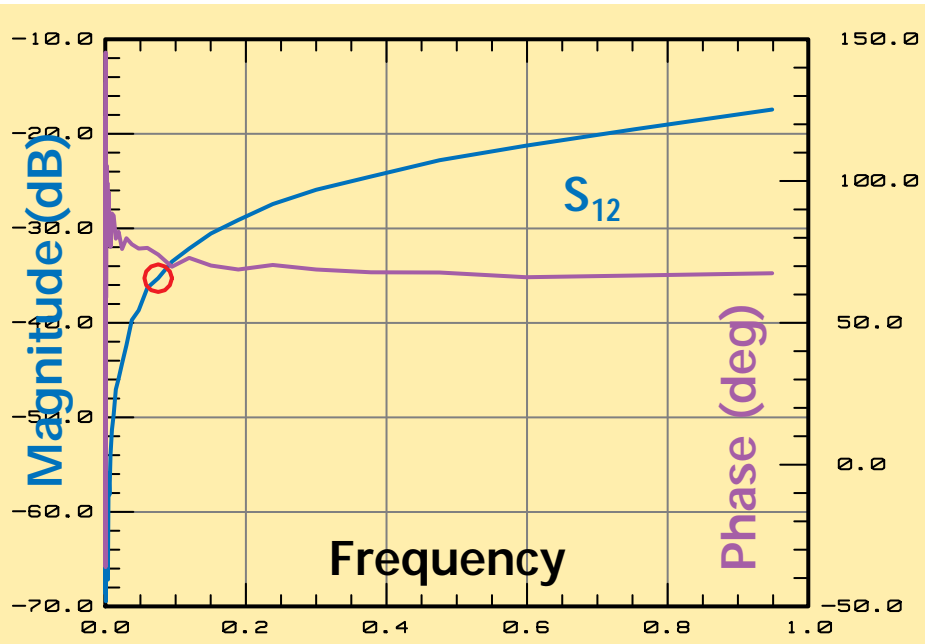


Figure 5b

A plot of the magnitude and phase of s_{12} . While the **phase** of s_{12} depends only weakly on the frequency, the **magnitude** increases rapidly at low frequencies.

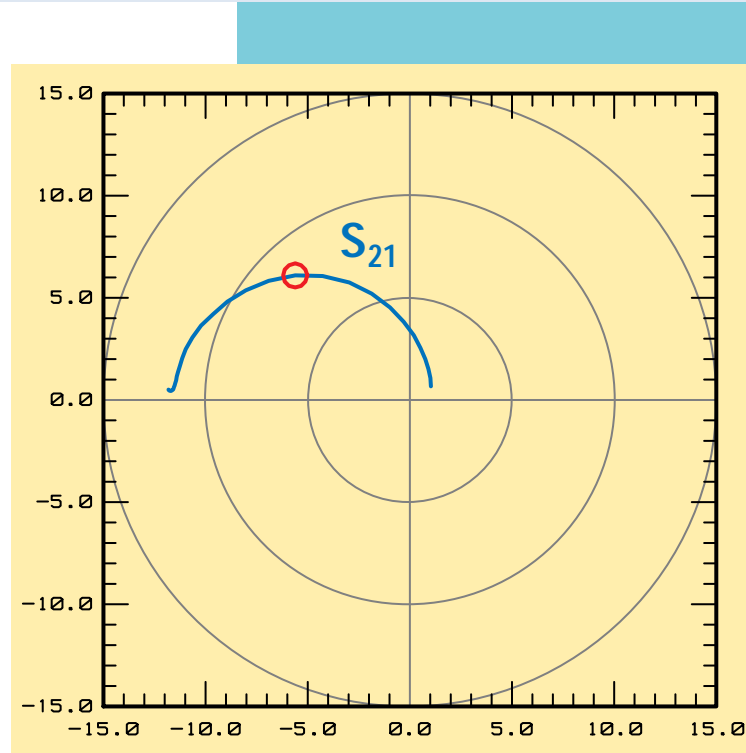


Figure 5c

A polar plot of s_{21} . The **frequency marker** shown is at the -3 dB point. Both the phase angle and magnitude decrease dramatically as the frequency is increased.

6 Measurement of S-Parameters

Test & Measurement
Application Note 95-1
S-Parameter Techniques

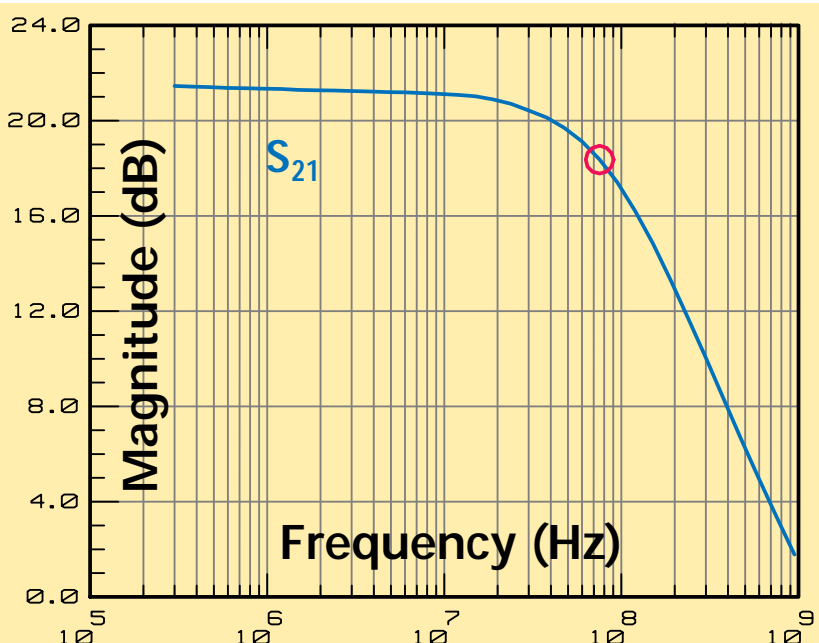


Figure 5d

The **magnitude** of s_{21} plotted on a log scale showing the 6 dB/octave roll-off above 75 MHz.

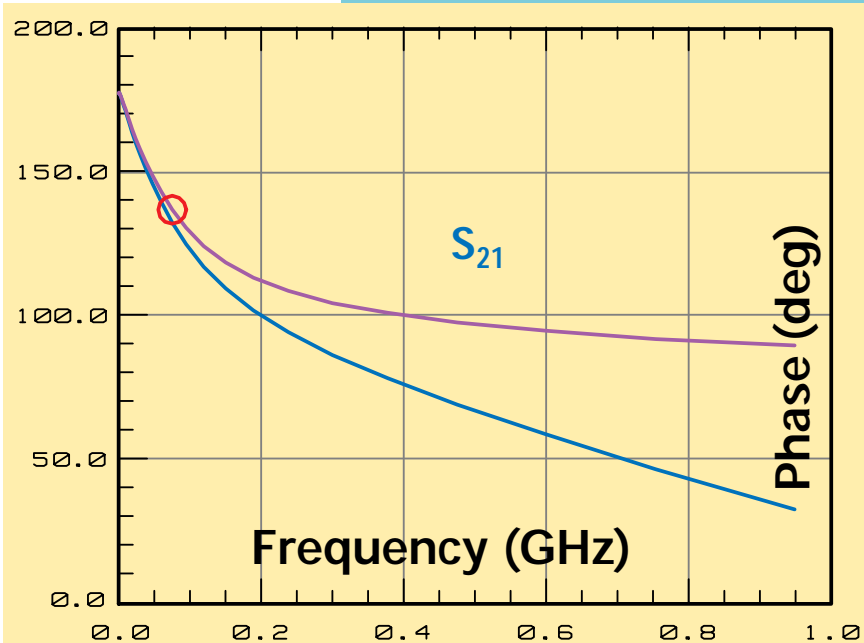


Figure 5e

The phase angle, in degrees, of s_{21} . A time delay of 167 ps was de-embedded from the **measured data** using the analyzer's electrical-delay feature to get a **response** with a single-pole transfer characteristic. Removing this time delay allows the phase distortion to be viewed with much greater resolution.

6 Measurement of S-Parameters

In Fig. 5d, the magnitude of s_{21} from Fig. 5c is replotted on a logarithmic frequency scale. The magnitude of s_{21} is essentially constant to 75 MHz, and then rolls off at a slope of 6 dB/octave. The phase angle of s_{21} as seen in Fig. 5e varies linearly with frequency above 500 MHz. To better characterize phase distortion, a compensating linear phase shift was introduced electronically in the network analyzer. This established an accurate calibration for measuring the device, resulting in the **second phase curve** of [Figure 5e](#).

To go from the **first phase curve** of Fig. 5e to the **second phase curve** required removing a pure time delay of 167 picoseconds. Thirty years ago this operation was accomplished by de-embedding 5.0 cm of line using a calibrated line stretcher. Today it's performed by software in the network analyzer.

After removal of the constant-delay, or linear-phase, component, the phase angle of s_{21} for this transistor (Fig. 5e) varies from 180° at dc to $+90^\circ$ at high frequencies, passing through $+135^\circ$ at 75 MHz, the -3 dB point of the magnitude curve. In other words, s_{21} behaves like a single pole in the frequency domain.

Test & Measurement
Application Note 95-1
S-Parameter Techniques

Vector Network Analyzers

Most modern design projects, RF through lightwave, use sophisticated simulation software to model system performance from components through subsystems. These programs require complete s-parameter data on each component. Measurements are made with a VNA, [Vector Network Analyzer](#), an instrument that accurately measures the s-parameters, transfer function, or impedance characteristic of linear networks across a broad range of frequencies.

6 Measurement of S-Parameters

Since s_{21} behaves like a single pole in the frequency domain, it is possible to write a closed expression for it. This expression is the same as equation 21, repeated here.

$$s_{21} = \frac{-s_{210} e^{-j\omega T_0}}{1 + j \frac{\omega}{\omega_0}}$$

where

$$T_0 = 167 \text{ ps}$$

$$\omega = 2\pi f$$

$$\omega_0 = 2\pi \cdot 75 \text{ MHz}$$

$$s_{210} = 8.4 = 18.5 \text{ dB}$$

The time delay $T_0 = 167 \text{ ps}$ is due primarily to the transit time of minority carriers (electrons) across the base of this npn transistor. Removing this time delay using the electrical-delay feature of the vector network analyzer allows the phase distortion to be viewed with much greater resolution.

Using the first-order, single-pole approximation for s_{21} is an important step in circuit design. Today, however, we have design technology undreamed of in 1967. Subsequently, through the process of [electronic design automation \(EDA\)](#), computer-aided engineering (CAE) tools now can be used iteratively to simulate and refine the design. These tools combine accurate models with performance-optimization and yield-analysis capabilities.

Test & Measurement
Application Note 95-1
S-Parameter Techniques

Complete network characterization

Vector Network Analyzers (VNA) are ideal for applications requiring complete network characterization. They use narrow-band detection to achieve wide dynamic range and provide noise-free data. VNAs are often combined with powerful computer-based [electronic design automation \(EDA\)](#) systems to both measure data, and simulate and optimize the performance of the complete system implementation being developed.

6 Measurement of S-Parameters

Test & Measurement
Application Note 95-1
S-Parameter Techniques

Explanation of Measurement Discrepancies

You may have noticed a difference between the measured and calculated data from the 1967 *HP Journal* article and the data obtained for this updated application note. Both sets of data are fundamentally correct. Two major sources account for these differences:

Measurement techniques – Early network analyzers did not have onboard computers, an HP-IB standard, or high-resolution graphics to perform calibration, extract precision numerical data, or display electronic markers. Calibration techniques used in 1967 were procedurally and mathematically simpler than those used today. Modern network analyzers contain sophisticated automated techniques that enhance measurement processing capabilities and reduce operator errors.

Device differences – Semiconductor manufacturing processes evolve over time. Device engineers attempt to produce identical transistors with different processes. Nevertheless, successive generations of parts like the 2N3478 can exhibit unintentional, and sometimes unavoidable, performance differences, especially in characteristics not guaranteed on the datasheet.

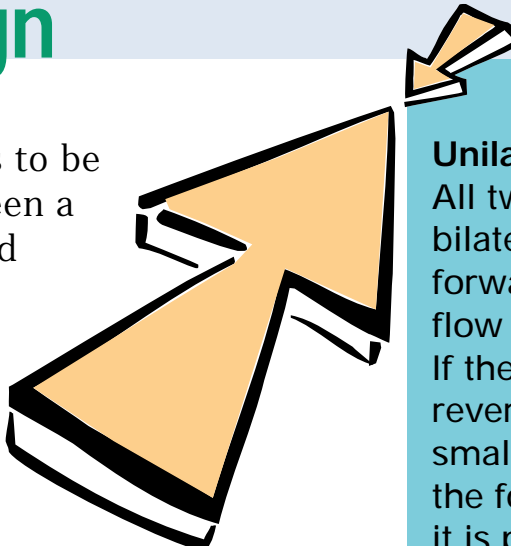


7 Narrow-Band Amplifier Design

Suppose now that this 2N3478 transistor is to be used in a simple amplifier, operating between a 50Ω source and a 50Ω load, and optimized for power gain at 300 MHz by means of lossless input and output matching networks. Since reverse gain s_{12} for this transistor is quite small—50 dB smaller than forward gain s_{21} , according to Fig. 4—there is a possibility that it can be neglected. If this is so, the design problem will be much simpler, because setting s_{12} equal to zero will make the design equations much less complicated.

In determining how much error will be introduced by assuming $s_{12} = 0$, the first step is to calculate the unilateral figure of merit u , using the formula given in Appendix B. That is,

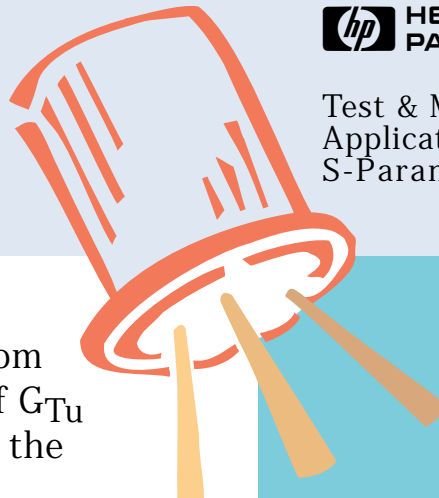
$$u = \frac{|s_{11}s_{12}s_{21}s_{22}|}{\left(1 - |s_{11}|^2\right)\left(1 - |s_{22}|^2\right)} \quad (22)$$



Test & Measurement
Application Note 95-1
S-Parameter Techniques

Unilateral figure of merit
All two-port models are bilateral, so both the forward and reverse signal flow must be considered. If the signal flow in the reverse direction is much smaller than the flow in the forward direction, it is possible to make the simplification that the reverse flow is zero.

The unilateral figure of merit is a quick calculation that can be used to determine where this simplification can be made without significantly affecting the accuracy of the model.



7 Narrow-Band Amplifier Design

A plot of u as a function of frequency, calculated from the measured parameters, appears in Fig. 4f. Now if G_{Tu} is the transducer power gain with $s_{12} = 0$ and G_T is the actual transducer power gain, the maximum error introduced by using G_{Tu} instead of G_T is given by the following relationship:

$$\frac{1}{(1+u)^2} < \frac{G_T}{G_{Tu}} < \frac{1}{(1-u)^2} \quad (23)$$

From Fig. 4f, the maximum value of u is about 0.03, so the maximum error in this case turns out to be about ± 0.25 dB at 100 MHz. This is small enough to justify the assumption that $s_{12} = 0$.

Incidentally, a small reverse gain, or feedback factor, s_{12} , is an important and desirable property for a transistor to have, for reasons other than it simplifies amplifier design. A small feedback factor means that the input characteristics of the completed amplifier will be independent of the load, and the output will be independent of the source impedance. In most amplifiers, isolation of source and load is an important consideration.

High-frequency transistors
 Discrete transistors were the mainstay of high-frequency system design in 1967 when Dick Anderson wrote the article on which this application note is based. Thirty years later, discrete devices are still available, manufactured and selected for specific, often exceptional, performance characteristics. Discrete transistors remain the best choice for many applications, such as sensitive first-stage amplifiers in satellite TV receivers.

7 Narrow-Band Amplifier Design

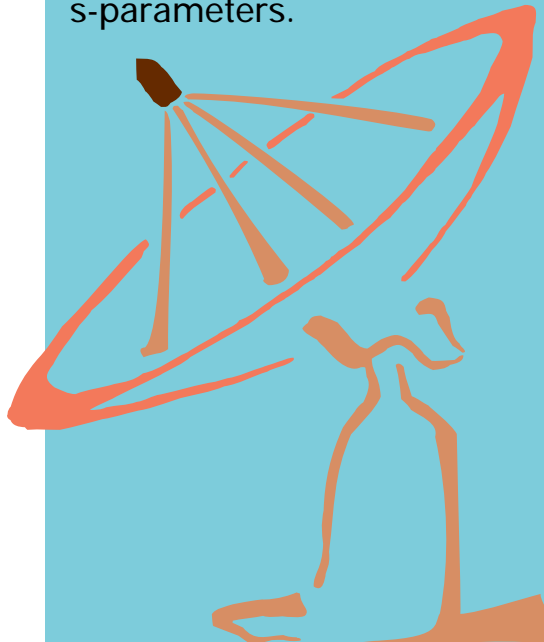
Returning now to the 300-MHz amplifier design, the unilateral expression for transducer power gain, obtained either by setting $s_{12} = 0$ in equation 18 or looking in [Appendix B](#), is

$$G_{Tu} = \frac{|s_{21}|^2 (1 - |\Gamma_S|^2) (1 - |\Gamma_L|^2)}{|1 - s_{11}\Gamma_S|^2 |1 - s_{22}\Gamma_L|^2} \quad (24)$$

When $|s_{11}|$ and $|s_{22}|$ are both less than one, as they are in this case, maximum G_{Tu} occurs for $\Gamma_S = s^{*}_{11}$ and $\Gamma_L = s^{*}_{22}$ ([Appendix B](#)).

The next step in the design is to synthesize matching networks that will transform the $50\ \Omega$ load and source impedances to the impedances corresponding to reflection coefficients of s^{*}_{11} and s^{*}_{22} , respectively. Since this is to be a single-frequency amplifier, the matching networks need not be complicated. Simple series-capacitor, shunt-inductor networks will not only do the job, but will also provide a handy means of biasing the transistor—via the inductor—and of isolating the dc bias from the load and the source.

Satellite Broadcast Signals
 Satellites provide broad geographical signal coverage over a wide band of frequencies by using high power vacuum tubes, called Traveling Wave Tubes (TWTs), which are best characterized by s-parameters.



7 Narrow-Band Amplifier Design

Values of L and C to be used in the matching networks for the 300-MHz amplifier are determined using the Smith Chart of Fig. 6, which is shown on the next page. First, points corresponding to s_{11} , s^*_{11} , s_{22} , and s^*_{22} at 300 MHz are plotted. Each point represents the tip of a vector leading away from the center of the chart, its length equal to the magnitude of the reflection coefficient being plotted, and its angle equal to the phase of the coefficient.

Next, a combination of constant-resistance and constant-conductance circles is found, leading from the center of the chart, representing 50Ω , to s^*_{11} and s^*_{22} . The circles on the Smith Chart are constant-resistance circles; increasing series capacitive reactance moves an impedance point counter-clockwise along these circles.

You will find an interactive Impedance Matching Model at the HP Test & Measurement website listed below. Challenge yourself to impedance matching games based on principles and examples discussed in this application note! Click on the URL below or type the address in your browser.

<http://www.hp.com/go/tminteractive>

Matching networks

Matching networks are extra circuit elements added to a device or circuit to cancel out or compensate for undesired characteristics or performance variations at specified frequencies.

To eliminate reflections in an amplifier, one matching network is carefully designed to transform the 50Ω load impedance to s^*_{11} . Another matching network transforms the 50Ω source impedance to s^*_{22} .

7 Narrow-Band Amplifier Design

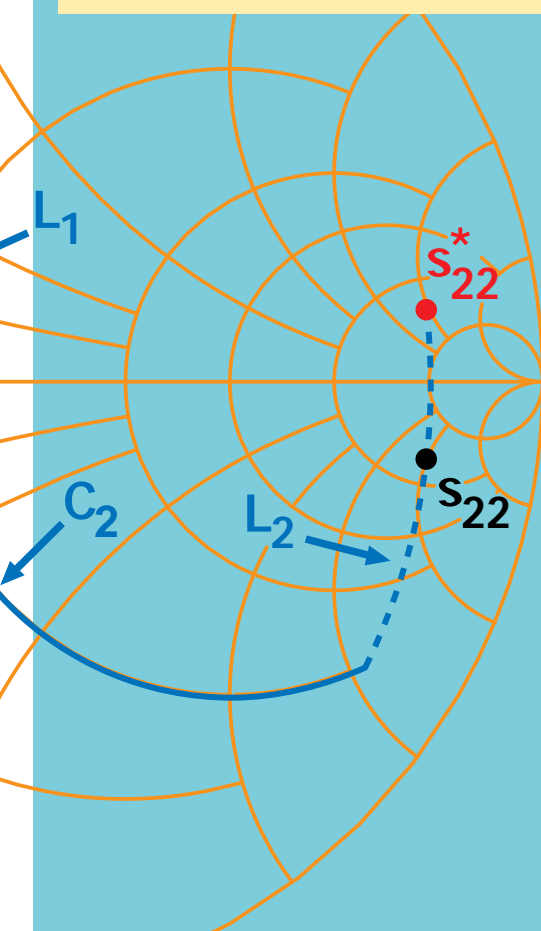
Test & Measurement
Application Note 95-1
S-Parameter Techniques

In this case, the circle to be used for finding series C is the one passing through the center of the chart, as shown by the solid line in Fig. 6.

Increasing shunt inductive susceptance moves impedance points clockwise along constant-conductance circles. These circles are like the constant-resistance circles, but they are on another Smith Chart, one that is just the reverse of the chart shown in Fig. 6.

The constant-conductance circles for shunt L all pass through the leftmost point of the chart rather than the rightmost point. The circles to be used are those passing through s^{*11} and s^{*22} , as shown by the dashed lines in Fig. 6.

Figure 6
Smith Chart for 300-MHz amplifier design example.



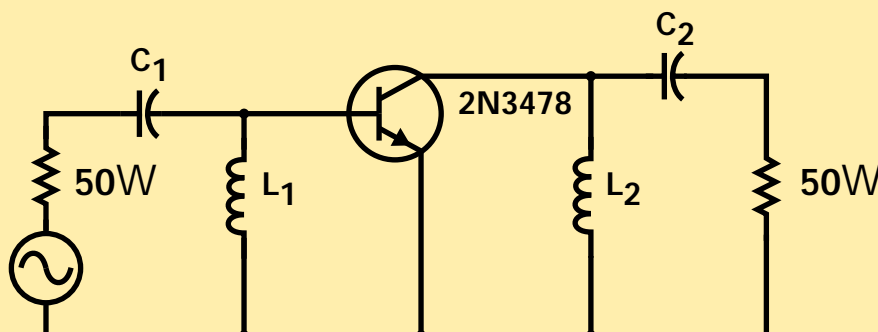
7 Narrow-Band Amplifier Design

Once these circles have been located, the normalized values of L and C needed for the matching networks are calculated from readings taken from the reactance and susceptance scales of the Smith Charts.

Each element's reactance or susceptance is the difference between the scale readings at the two end points of a circular arc. Which arc corresponds to which element is indicated in Fig. 6.

The final network and the element values, normalized and unnormalized, are shown in Fig. 7.

Figure 7
 A 300-MHz amplifier with matching networks for maximum power gain.



Calculations:

$$X_{L_2} = \frac{50}{0.32} = 156 \text{ W}$$

$$L_2 = \frac{156}{2 \pi (0.3 \times 10^9)} = 83 \text{ nH}$$

$$C_2 = \frac{1}{2 \pi (0.3 \times 10^9)(3.5)(50)} = 3 \text{ pF}$$

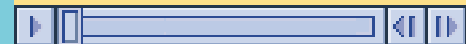
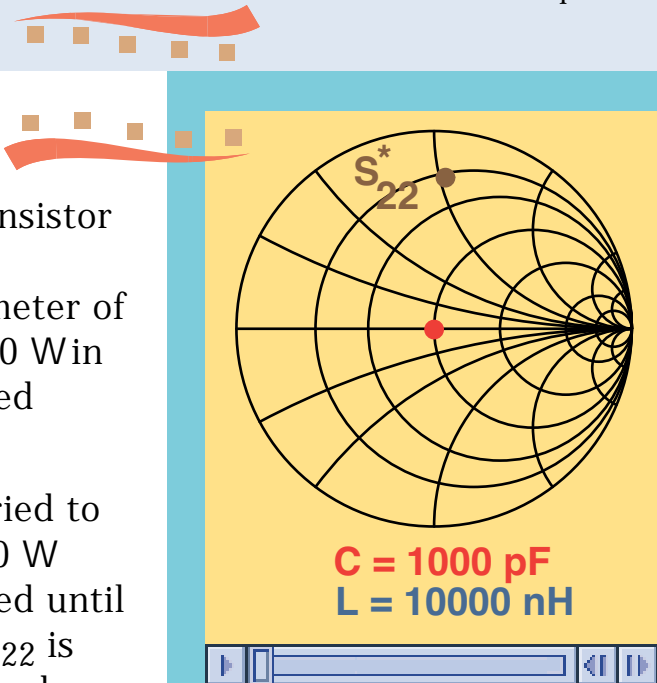
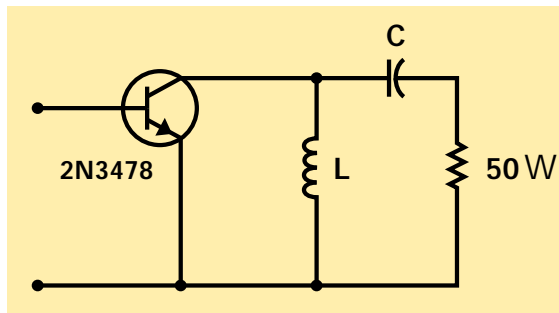
$$C_1 = \frac{1}{2 \pi (0.3 \times 10^9)(0.42)(50)} = 25 \text{ pF}$$

$$L_1 = \frac{50}{2 \pi (0.3 \times 10^9)(1.01)} = 26 \text{ nH}$$

7 Narrow-Band Amplifier Design

The animation to the right demonstrates how to use a Smith Chart to design a matching network between a transistor output and a resistive load. As previously described, to maximize the power delivered to the load, the s^*_{22} parameter of the transistor must be matched to the load impedance, 50 W in this 300-MHz amplifier example. This matching is achieved using the LC circuit shown at the right.

Starting from the 50 W load, the series capacitance is varied to move the impedance point along the circle of constant 50 W resistance on the Smith Chart. The capacitance is adjusted until it intersects the constant conductance circle on which s^*_{22} is sitting. Varying the shunt inductance then moves the impedance point along this constant conductance circle as indicated by the admittance Smith Chart. To reach s^*_{22} , the shunt inductance is adjusted until the impedance point reaches s^*_{22} .



Animation 2
 Impedance matching using the Smith Chart for the matching network shown at the left. Click over the chart to start animation.

8 Broadband Amplifier Design

Designing a broadband amplifier, that is, one which has nearly constant gain over a prescribed frequency range, is a matter of surrounding a transistor with external elements in order to compensate for the variation of forward gain, $|s_{21}|$ with frequency.

This can be done in either of two ways—first, negative feedback, or second, selective mismatching of the input and output circuitry. We will use the second method. When feedback is used, it is usually convenient to convert to y- or z-parameters (for shunt or series feedback, respectively) using the conversion equations given in [Appendix B](#) and a digital computer.

[Equation 24](#) for the unilateral transducer power gain can be factored into three parts, as shown to the right:

Test & Measurement
Application Note 95-1
S-Parameter Techniques

$$G_{Tu} = G_0 G_1 G_2$$

$$G_0 = |s_{21}|^2$$

$$G_1 = \frac{1 - |\Gamma_s|^2}{|1 - s_{11} \Gamma_s|^2}$$

$$G_2 = \frac{1 - |\Gamma_L|^2}{|1 - s_{22} \Gamma_L|^2}$$

8 Broadband Amplifier Design

Test & Measurement
Application Note 95-1
S-Parameter Techniques

When a broadband amplifier is designed by selective mismatching, the gain contributions of G_1 and G_2 are varied to compensate for the variations of $G_0 = |s_{21}|^2$ with frequency.

Suppose that the 2N3478 transistor whose s-parameters are given in Fig. 4 is to be used in a broadband amplifier that will operate from 300 MHz to 700 MHz. The amplifier is to be driven from a 50Ω source and is to drive a 50Ω load.

According to Figure 4f,

$$\begin{aligned} |s_{21}|^2 &= 13 \text{ dB at } 300 \text{ MHz} \\ &= 10 \text{ dB at } 450 \text{ MHz} \\ &= 6 \text{ dB at } 700 \text{ MHz} \end{aligned}$$

To realize an amplifier with a constant gain of 10 dB, source and load matching networks must be found that will decrease the gain by 3 dB at 300 MHz, leave the gain the same at 450 MHz, and increase the gain by 4 dB at 700 MHz.

dB

8 Broadband Amplifier Design

Although in the general case both a source matching network and a load matching network would be designed, $G_{1\max}$ (i.e., G_1 for $\Gamma_s = s^{*}_{11}$) for this transistor is less than 1 dB over the frequencies of interest, which means there is little to be gained by matching the source.

Consequently, for this example, only a load-matching network will be designed. Procedures for designing source-matching networks are identical to those used for designing load-matching networks.

The first step in the design of the load-matching network is to plot s^{*}_{22} over the required frequency range on the Smith Chart, Fig. 8a.

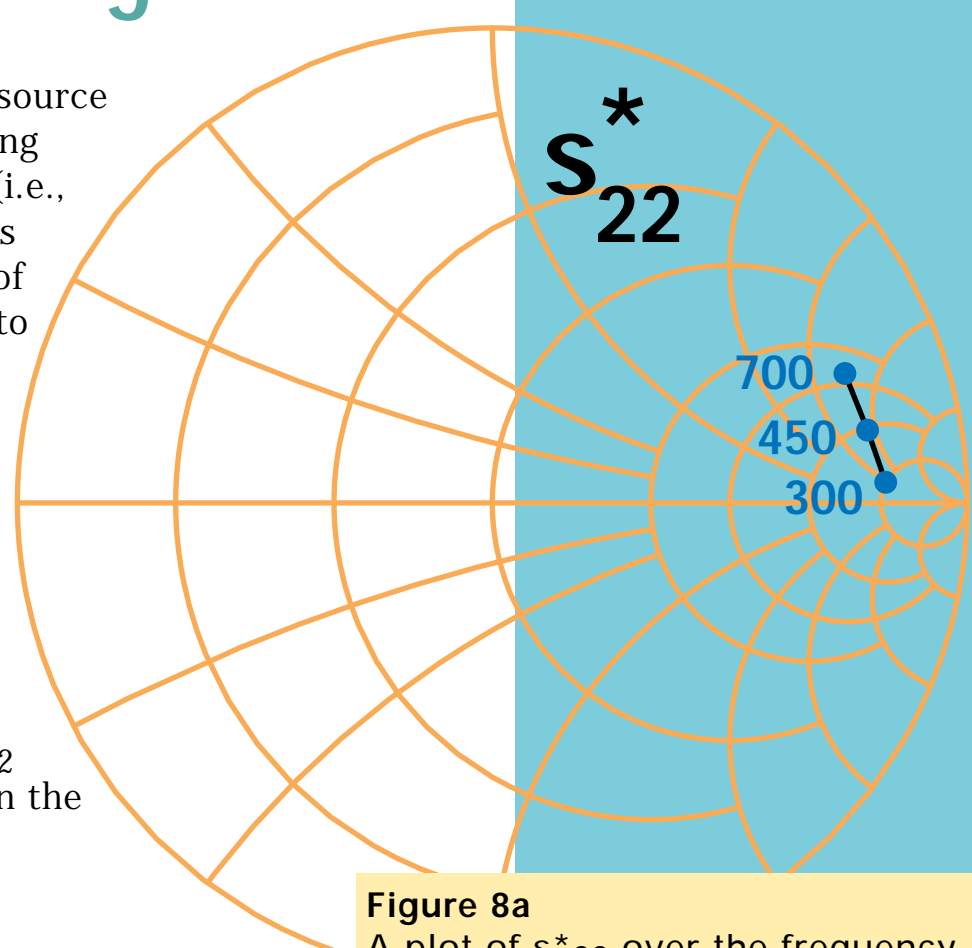


Figure 8a
A plot of s^{*}_{22} over the frequency range from 300 MHz to 700 MHz.

8 Broadband Amplifier Design

Test & Measurement
Application Note 95-1
S-Parameter Techniques

Next, a set of constant-gain circles is drawn. As shown in Fig. 8b, each circle is drawn for a single frequency; its center is on a line between the center of the Smith Chart and the point representing s^{*}_{22} at that frequency. The distance from the center of the Smith Chart to the center of the constant gain circle is given by the following equations, which also appear in [Appendix B](#):

$$r_2 = \frac{1 - g_2 |s_{22}|}{1 - |s_{22}|^2 (1 - g_2)}$$

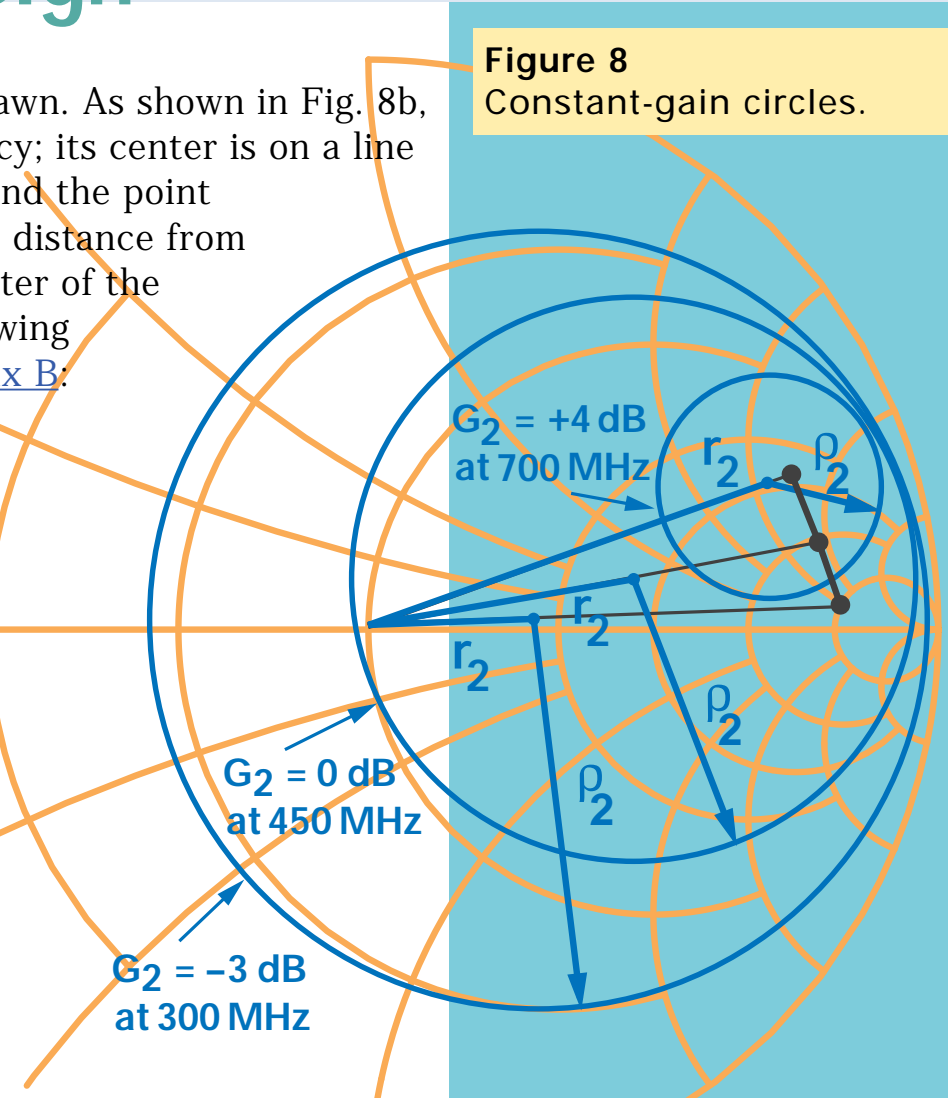
where

$$g_2 = \frac{G_2}{G_{2\max}} = G_2 (1 - |s_{22}|^2)$$

The radius of the constant-gain circle is:

$$\rho_2 = \frac{\sqrt{1 - g_2} (1 - |s_{22}|^2)}{1 - |s_{22}|^2 (1 - g_2)}$$

Figure 8
Constant-gain circles.



8 Broadband Amplifier Design

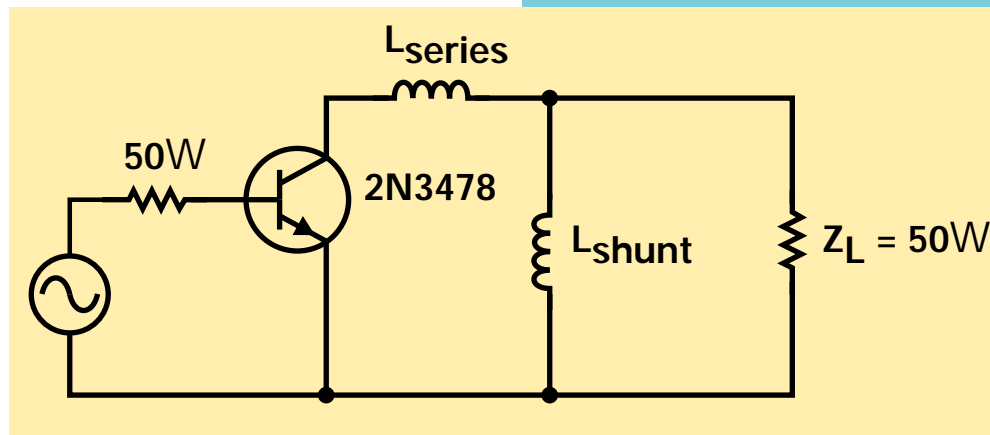
For this example, three circles will be drawn, one for $G_2 = -3$ dB at 300 MHz, one for $G_2 = 0$ dB at 450 MHz, and one for $G_2 = +4$ dB at 700 MHz. Since $|s_{22}|$ for this transistor is constant at 0.85 over the frequency range [see Figure 4(b)], $G_{2\max}$ for all three circles is $(0.278)^{-1}$, or 5.6 dB. The three constant-gain circles are indicated in Fig. 8b.

The required matching network must transform the center of the Smith Chart, representing 50 W, to some point on the -3 dB circle at 300 MHz, to some point on the 0 dB circle at 450 MHz, and to some point on the +4 dB circle at 700 MHz. There are undoubtedly many networks that

will do this. One satisfactory solution is a combination of two inductors, one in shunt and one in series, as shown in Fig. 9.

Test & Measurement
Application Note 95-1
S-Parameter Techniques

Figure 9
A combination of shunt and series inductances is a suitable matching network for the broadband amplifier.

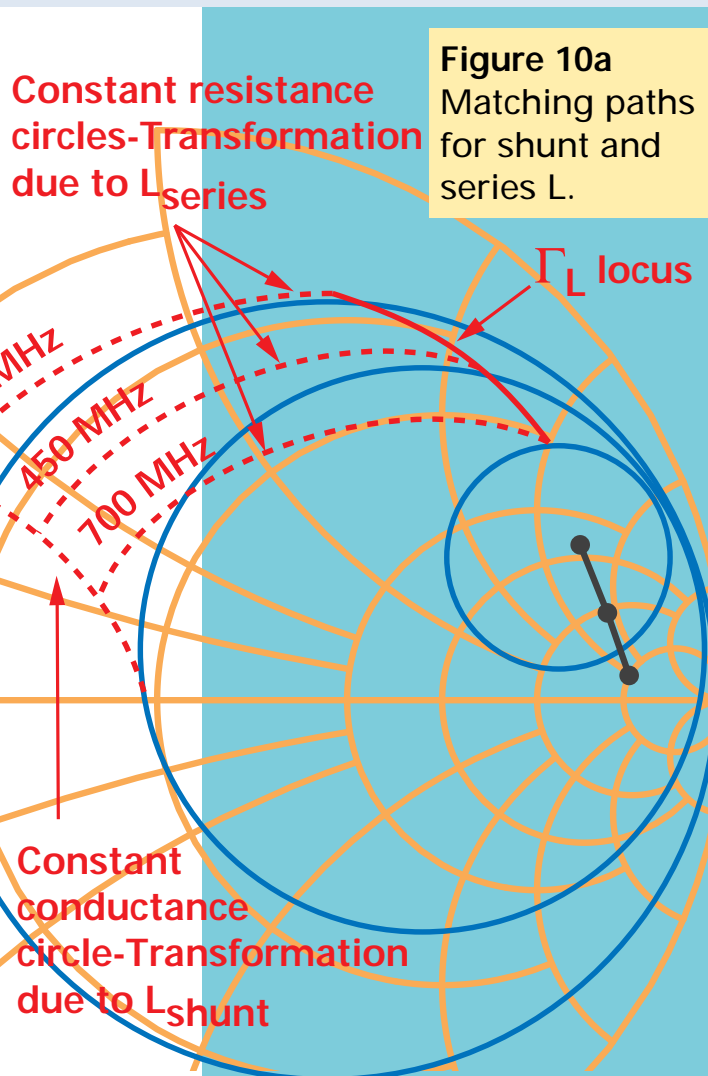


8 Broadband Amplifier Design

Shunt and series elements move impedance points on the Smith Chart along constant-conductance and constant-resistance circles, as explained in the narrow-band design example. As shown in Fig. 10a, the shunt inductance transforms the 50Ω load along a circle of constant conductance and varying (with frequency) inductive susceptance. The series inductor transforms the combination of the 50Ω load and the shunt inductance along circles of constant resistance and varying inductive reactance.

Optimizing the values of shunt and series L is an iterative process with two goals:

- the transformed load reflection terminates on the right gain circle at each frequency, and
- the susceptance component decreases with frequency and the reactance component increases with frequency. (This rule applies to inductors; capacitors would behave in the opposite way.)



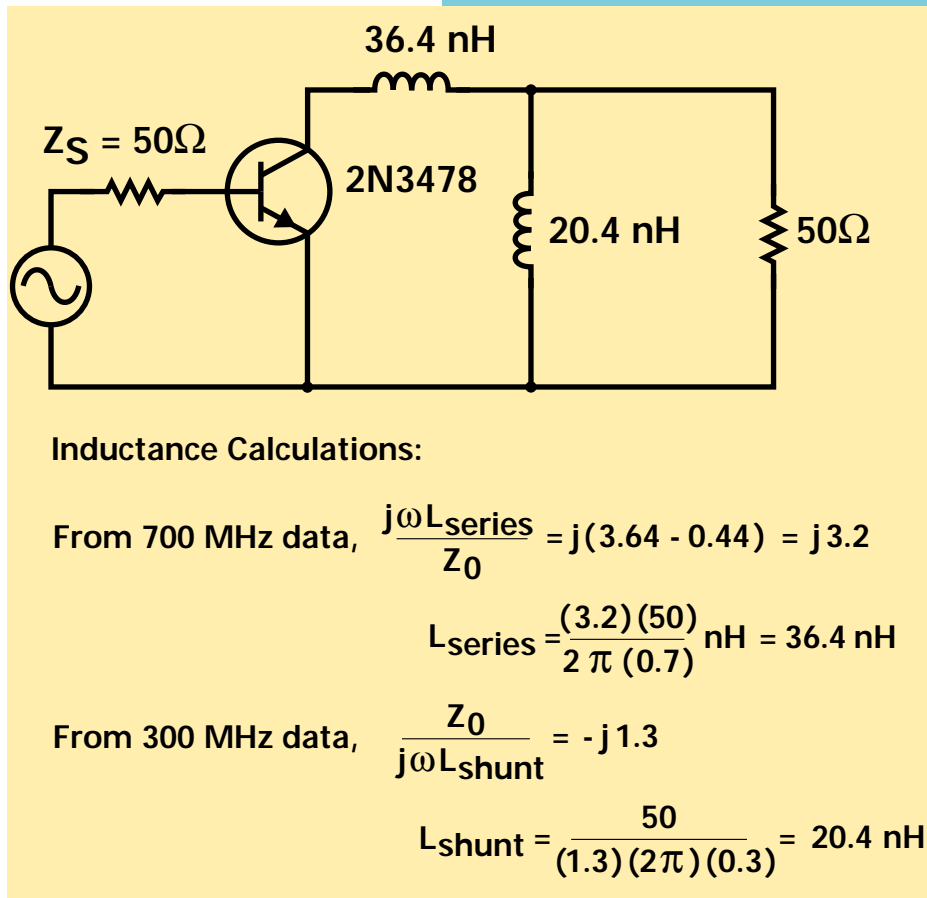
8 Broadband Amplifier Design

Once appropriate constant-conductance and constant-resistance circles have been found, the reactances and susceptances of the elements can be read directly from the Smith Chart. Then the element values are calculated, the same as they were for the narrow-band design.

Figure 10b is a schematic diagram of the completed broadband amplifier, with unnormalized element values.

Figure 10b

Broadband amplifier with constant gain of 10 dB from 300 MHz to 700 MHz.



9 Stability Considerations

Design of Reflection Amplifiers and Oscillators

When the real part of the input impedance of a network is negative, the corresponding input reflection coefficient ([Equation 17](#)) is greater than one, and the network can be used as the basis for two important types of circuits, reflection amplifiers and oscillators. A reflection amplifier (Fig. 11) can be realized with a circulator—a nonreciprocal three-port device—and a negative-resistance device.

The circulator is used to separate the incident (input) wave from the larger wave reflected by the negative-resistance device. Theoretically, if the circulator is perfect and has a positive real characteristic impedance Z_0 , an amplifier with infinite gain can be built by selecting a negative-resistance device whose input impedance has a real part equal to $-Z_0$ and an imaginary part equal to zero (the imaginary part can be set equal to zero by tuning if necessary).

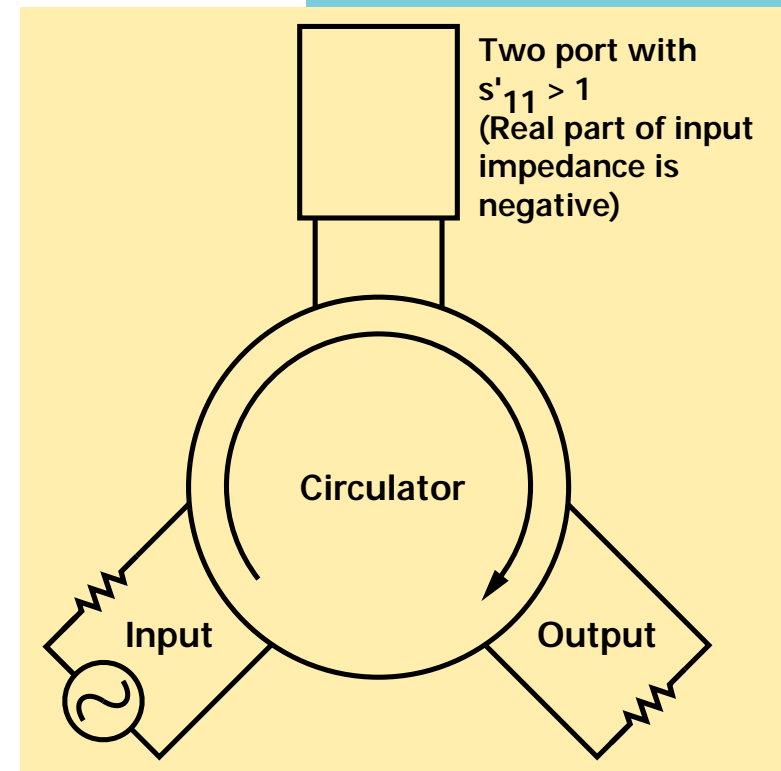


Figure 11
Reflection amplifier consists of circulator and transistor with negative input resistance.

9

Stability Considerations

Amplifiers, of course, are not supposed to oscillate, whether they are reflection amplifiers or some other kind. There is a convenient criterion based upon scattering parameters for determining whether a device is stable or potentially unstable with given source and load impedances. Referring again to the flow graph of [Figure 3](#), the ratio of the reflected voltage wave b_1 to the input voltage wave b_s is

$$\frac{b_1}{b_s} = \frac{s\$\$1}{1 - G_s s\$\$1}$$

where $s\$\1 is the input reflection coefficient with $G_s = 0$ ($Z_2 = Z_0$) and an arbitrary load impedance Z_L , as defined in [Equation 19](#).

If at some frequency

$$G_s s\$\$1 = 1 \quad (25)$$

the circuit is unstable and it will oscillate at that frequency.

On the other hand, if

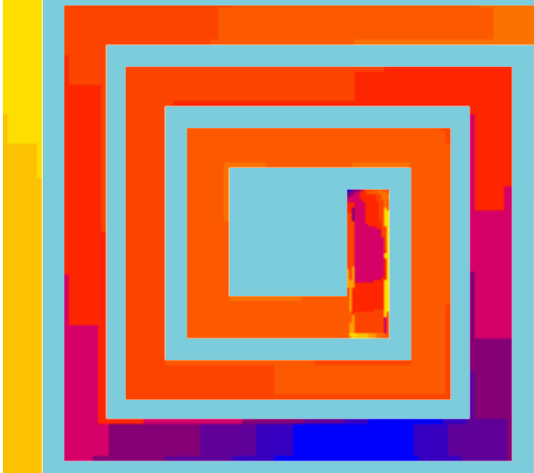
$$|s\$\$1| < \left| \frac{1}{G_s} \right|$$

the device is unconditionally stable and will not oscillate, whatever the phase angle of G_s might be.

Test & Measurement
Application Note 95-1
S-Parameter Techniques

Computer Aided Engineering tools (CAE)

CAE software tools are used in the design process to simulate actual device and circuit behavior so designs can be evaluated before they're built. The CAE approach is faster, produces accurate results, and is easier to follow than manual methods using graphical design aids. CAE tools are part of the total engineering solution.



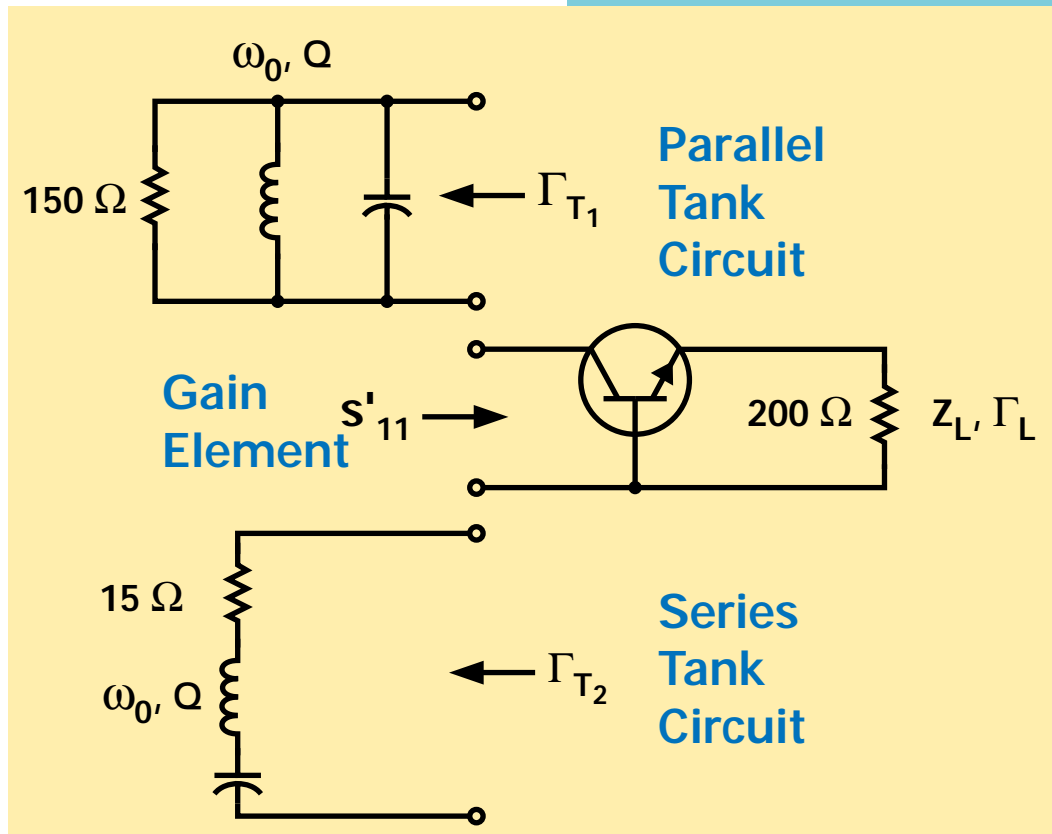
9

Stability Considerations

To see how these principles of stability are applied in design problems, consider the transistor oscillator design illustrated in Fig. 12. In this case the input reflection coefficient s'_{11} is the reflection coefficient looking into the collector circuit, and the 'source' reflection coefficient Γ_s is one of the two tank-circuit reflection coefficients, Γ_{T1} or Γ_{T2} . From equation 19,

$$s'_{11} = s_{11} + \frac{s_{12}s_{21}\Gamma_L}{1 - s_{22}\Gamma_L}$$

Figure 12 The transistor oscillator is designed by choosing a tank circuit such that $\Gamma_s s'_{11} = 1$



9

Stability Considerations

To make the transistor oscillate, $s\$\1 and G_s must be adjusted so that they satisfy equation 25. There are four steps in the design procedure:

- Measure the four scattering parameters of the transistor as functions of frequency.
- Choose a load reflection coefficient G_L that makes $s\$\1 greater than unity. In general, it may also take an external feedback element that increases $s_{12} s_{21}$ to make $s\$\1 greater than one.
- Plot $1/s\$\1 on a Smith Chart. (If the network analyzer is being used to measured the s-parameters of the transistor, $1/s\$\1 can be measured directly by reversing the reference and test channel connections between the reflection test unit and the harmonic frequency converter. The polar display with a Smith Chart overlay then gives the desired plot immediately.)
- Connect either the series or the parallel tank circuit to the collector circuit and tune it so that G_{T1} or G_{T2} is large enough to satisfy equation 25. (The tank circuit reflection coefficient plays the role of G_s in this equation.)

9

Stability Considerations

Figure 13 shows a Smith Chart plot of $1/sG_1$ for a high frequency transistor in the common-base configuration. Load impedance Z_L is 200 W, which means that G_L referred to 50 W is 0.6. Reflection coefficients G_{T1} and G_{T2} are also plotted as functions of the resonant frequencies of the two tank circuits. Oscillations occur when the locus of G_{T1} or G_{T2} passes through the shaded region. Thus, this transistor would oscillate from 1.5 to 2.5 GHz with a series tuned circuit, and from 2.0 to 2.7 GHz with a parallel tuned circuit.

— Dick Anderson, 1967 and 1997

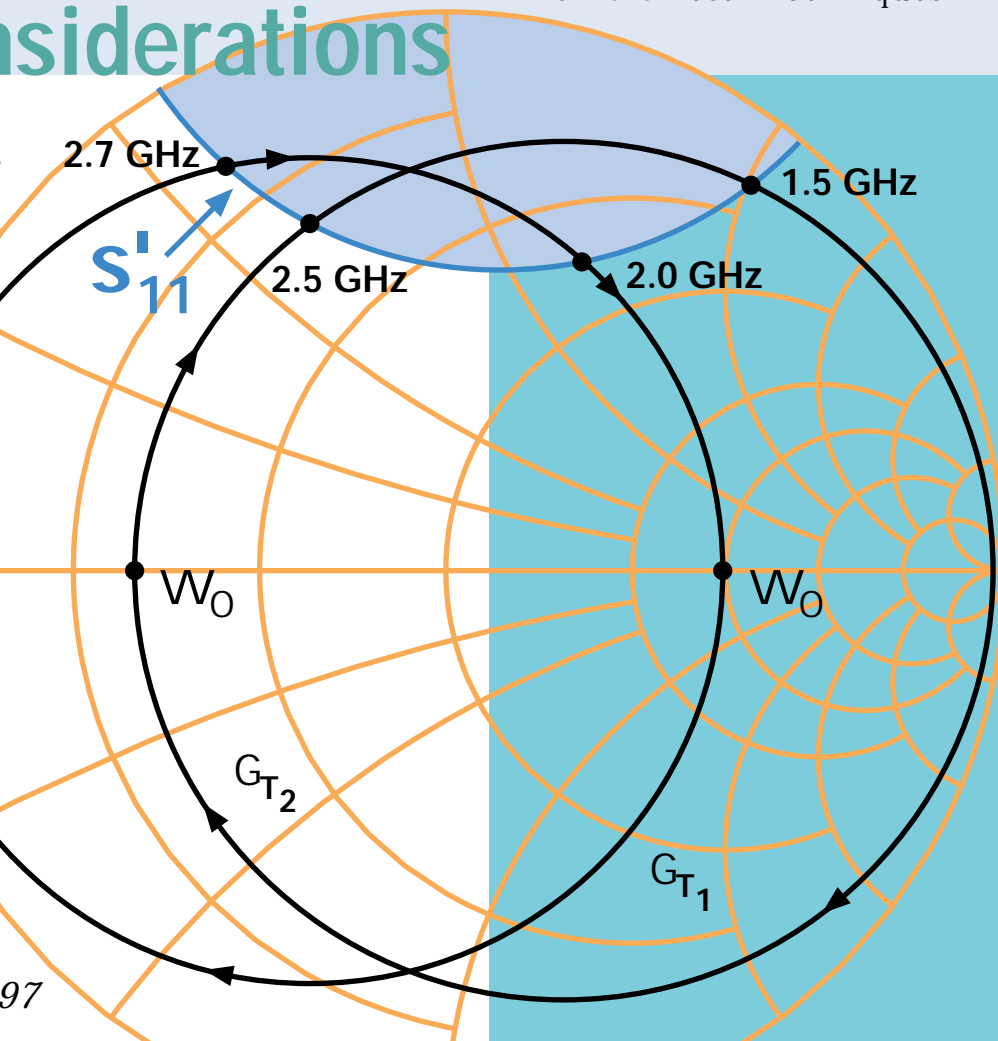
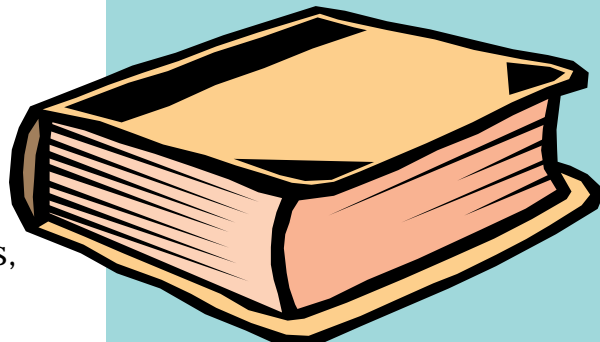


Figure 13 The transistor will oscillate in the shaded area between 1.5 and 2.5 GHz with a series-tuned circuit and between 2.0 and 2.7 GHz with a parallel-tuned circuit.

A Additional Reading on S-Parameters

In addition to previous references listed earlier and repeated again here, the following papers and books were listed in the 1967 *HP Journal* article as sources for information on s-parameter design procedures and flow graphs. Current references are also mentioned.

- J. K. Hunton, ‘Analysis of Microwave Measurement Techniques by Means of Signal Flow Graphs,’ IRE Transactions on Microwave Theory and Techniques, Vol. MTT- 8, No. 2, March, 1960.
- D.C Youla, ‘On Scattering Matrices Normalized to Complex Port Numbers,’ Proc. IRE, Vol. 49, No. 7, July, 1961.
- J.G. Linvill and J.F. Gibbons, ‘Transistors and Active Circuits,’ McGraw-Hill, 1961. (No s-parameters, but good treatment of Smith Chart design methods.)
- N. Kuhn, ‘Simplified Signal Flow Graph Analysis,’ Microwave Journal, Vol. 6, No, 11, November, 1963.
- K. Kurokawa, ‘Power Waves and the Scattering Matrix,’ IEEE Transactions on Microwave Theory and Techniques, Vol. MTT-13, No. 2, March, 1965.



A Additional Reading on S-Parameters

- F. Weinert, 'Scattering Parameters Speed Design of High-Frequency Transistor Circuits,' Electronics, Vol. 39, No. 18, Sept. 5, 1966.
- G. Fredricks, 'How to Use S-Parameters for Transistor Circuit Design,' EEE Vol. 14, No. 12, Dec., 1966.

Among many modern reference sources on the subject, the following book, first published in 1969, is definitely a classic:

- Smith, Phillip H., 'Electronic Applications of the Smith Chart in Waveguide, Circuit and Component Analysis,' Noble Publishing Classic Series, Tucker, Georgia, 1995, ISBN-1-884932-39-8, 237 pp.

We also mention a useful textbook containing 5 chapters, 2 appendices, and problem sets. This text presents a unified treatment of the analysis and design of microwave transistor amplifiers using scattering parameters techniques:

- G. Gonzalez, 'Microwave Transistor Amplifiers: Analysis and Design,' Prentice Hall, 1984, ISBN 0-13-581646-7, 240 pp.

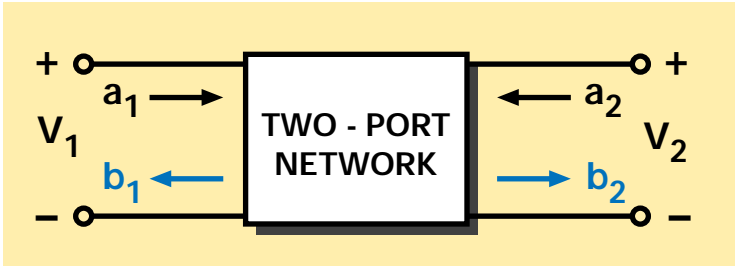
Test & Measurement
Application Note 95-1
S-Parameter Techniques

Keep up to date

This book by P. H. Smith referenced here must be considered the ultimate source on Smith Charts. Many excellent articles on the use of Smith charts have appeared in trade publications such as the *Microwave Journal*, and educational Smith Chart software is sold over the internet.



B Scattering Parameter Relationships



Input reflection coefficient with arbitrary Z_L

$$s'_{11} = s_{11} + \frac{s_{12} s_{21} \Gamma_L}{1 - s_{22} \Gamma_L}$$

Output reflection coefficient with arbitrary Z_S

$$s'_{22} = s_{22} + \frac{s_{12} s_{21} \Gamma_S}{1 - s_{11} \Gamma_S}$$

Voltage gain with arbitrary Z_L and Z_S

$$A_V = \frac{V_2}{V_1} = \frac{s_{21}(1 + \Gamma_L)}{(1 - s_{22} \Gamma_L)(1 + s'_{11})}$$

$$\begin{aligned} b_1 &= s_{11} a_1 + s_{12} a_2 \\ b_2 &= s_{21} a_1 + s_{22} a_2 \end{aligned}$$

B Scattering Parameter Relationships

Power Gain

$$G = \frac{\text{Power delivered to load}}{\text{Power input to network}} = \frac{|s_{21}|^2 \frac{\alpha}{\epsilon} - |G_L|^2 \frac{\alpha}{\epsilon}}{\frac{\alpha}{\epsilon} - |s_{11}|^2 \frac{\alpha}{\epsilon} + |G_L|^2 \frac{\alpha}{\epsilon} |s_{22}|^2 - |D|^2 \frac{\alpha}{\epsilon} - 2\text{Re}(G_L N)}$$

Available Power Gain

$$G_A = \frac{\text{Power available from network}}{\text{Power available from source}} = \frac{|s_{21}|^2 \frac{\alpha}{\epsilon} - |G_S|^2 \frac{\alpha}{\epsilon}}{\frac{\alpha}{\epsilon} - |s_{22}|^2 \frac{\alpha}{\epsilon} + |G_S|^2 \frac{\alpha}{\epsilon} |s_{11}|^2 - |D|^2 \frac{\alpha}{\epsilon} - 2\text{Re}(G_S M)}$$

Transducer Power Gain

$$G_T = \frac{\text{Power delivered to load}}{\text{Power available from source}} = \frac{|s_{21}|^2 \frac{\alpha}{\epsilon} - |G_S|^2 \frac{\alpha}{\epsilon} |s_{11}|^2 - |G_L|^2 \frac{\alpha}{\epsilon}}{|(1 - s_{11} G_S)(1 - s_{22} G_L) - s_{12} s_{21} G_L G_S|^2}$$

B Scattering Parameter Relationships

Unilateral Transducer Power Gain ($s_{12} = 0$)

$$G_{Tu} = \frac{|s_{21}|^2 (1 - |\Gamma_S|^2) (1 - |\Gamma_L|^2)}{|1 - s_{11}\Gamma_S|^2 |1 - s_{22}\Gamma_L|^2} = G_0 G_1 G_2$$

Maximum Unilateral Transducer Power Gain when $|s_{11}| < 1$

and $|s_{22}| < 1$. Maximum obtained for $\Gamma_S = s_{11}^*$ and $\Gamma_L = s_{22}^*$

$$G_u = \frac{|s_{21}|^2}{\left(1 - |s_{11}|^2\right)\left(1 - |s_{22}|^2\right)} = G_0 G_1 \max G_2 \max$$

$$G_0 = |s_{21}|^2$$

$$G_1 = \frac{1 - |\Gamma_S|^2}{|1 - s_{11}\Gamma_S|^2}$$

$$G_2 = \frac{1 - |\Gamma_L|^2}{|1 - s_{22}\Gamma_L|^2}$$

$$G_{i \max} = \frac{1}{1 - |s_{ii}|^2}$$

$i = 1, 2$

B Scattering Parameter Relationships

Constant Gain Circles (Unilateral case: $s_{12} = 0$)

- center of constant gain circle is on line between center of Smith Chart and point representing s^*_{ii}
- distance of center of circle from center of Smith Chart:

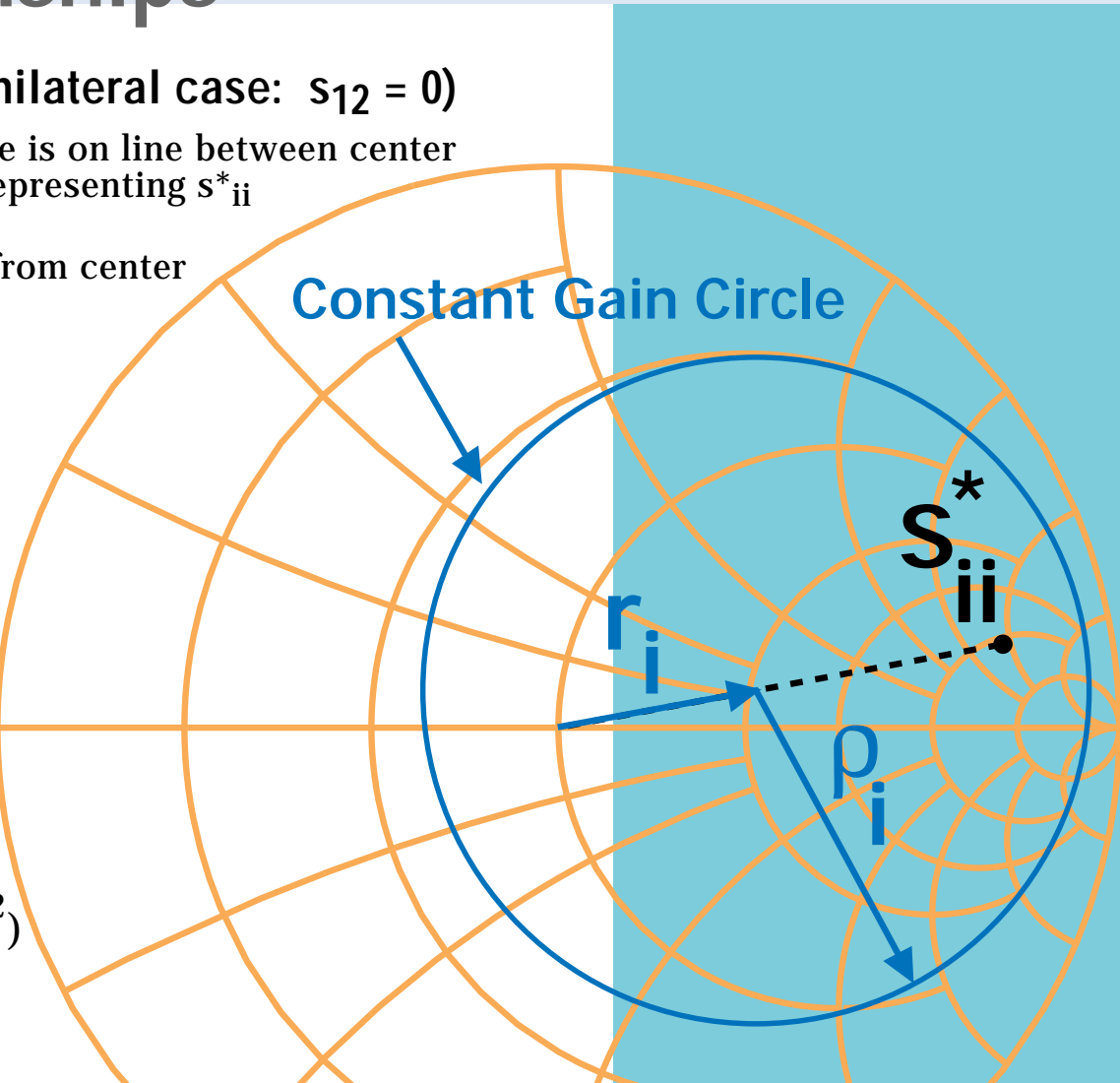
$$r_i = \frac{g_i |s_{ii}|}{1 - |s_{ii}|^2 (1 - g_i)}$$

- radius of circle:

$$\rho_i = \frac{\sqrt{1 - g_i} (1 - |s_{ii}|^2)}{1 - |s_{ii}|^2 (1 - g_i)}$$

where $i = 1, 2$, and

$$g_i = \frac{G_i}{G_i \text{ max}} = G_i (1 - |s_{ii}|^2)$$



B Scattering Parameter Relationships

Test & Measurement
Application Note 95-1
S-Parameter Techniques

Unilateral Figure of Merit

$$u = \frac{|s_{11}s_{22}s_{12}s_{21}|}{\left(1 - |s_{11}|^2\right)\left(1 - |s_{22}|^2\right)}$$

Error Limits on Unilateral Gain Calculations

$$\frac{1}{(1+u^2)} < \frac{G_T}{G_{Tu}} < \frac{1}{(1-u^2)}$$



Unilateral figure of merit
All two-port models are bilateral, so both the forward and reverse signal flow must be considered. If the signal flow in the reverse direction is much smaller than the flow in the forward direction, it's possible to make the simplification that the reverse flow is zero.

The unilateral figure of merit is a quick calculation that can be used to determine where this simplification can be made without significantly affecting the accuracy of the model.

B Scattering Parameter Relationships

Conditions for Absolute Stability :

No passive source or load will cause a network to oscillate, if conditions a, b, and c are all satisfied.

Condition that a two - port network can be simultaneously matched with a real source and load:

$K > 1$ or $C < 1$ where C = Linvill C Factor and

$$C = K^{-1}$$

$$K = \frac{1 + |D|^2 - |S_{11}|^2 - |S_{22}|^2}{2|S_{12}S_{21}|}$$

a. $|S_{11}| < 1, |S_{22}| < 1$

b. $\left| \frac{|S_{12}S_{21}| - |M^*|}{|S_{11}|^2 - |D|^2} \right| > 1$

c. $\left| \frac{|S_{12}S_{21}| - |N^*|}{|S_{22}|^2 - |D|^2} \right| > 1$

$$D = S_{11}S_{22} - S_{12}S_{21}$$

$$M = S_{11} - D S_{22}^*$$

$$N = S_{22} - D S_{11}^*$$

B Scattering Parameter Relationships

Source and load for Simultaneous Match

$$\Gamma_{mS} = M^* \left[\frac{B_1 \pm \sqrt{B_1^2 - 4|M|^2}}{2|M|^2} \right]$$

$$\Gamma_{mL} = N^* \left[\frac{B_2 \pm \sqrt{B_2^2 - 4|N|^2}}{2|N|^2} \right]$$

(Use minus sign
 when B_1 is positive,
 plus sign when
 B_1 is negative.)

$$B_1 = 1 + |s_{11}|^2 - |s_{22}|^2 - |D|^2$$

$$B_2 = 1 + |s_{22}|^2 - |s_{11}|^2 - |D|^2$$

Maximum Available Power Gain

$$\text{If } K > 1, G_A \text{ max} = \left| \frac{s_{21}}{s_{12}} \left(K \pm \sqrt{K^2 - 1} \right) \right|$$

where $K = C^{-1}$

B Scattering Parameter Relationships

s-parameters in terms of z-parameters	z-parameters in terms of s-parameters
$s_{11} = \frac{(z_{11} - 1)(z_{22} + 1) - z_{12}z_{21}}{(z_{11} + 1)(z_{22} + 1) - z_{12}z_{21}}$ $s_{12} = \frac{2z_{12}}{(z_{11} + 1)(z_{22} + 1) - z_{12}z_{21}}$ $s_{21} = \frac{2z_{21}}{(z_{11} + 1)(z_{22} + 1) - z_{12}z_{21}}$ $s_{22} = \frac{(z_{11} + 1)(z_{22} - 1) - z_{12}z_{21}}{(z_{11} + 1)(z_{22} + 1) - z_{12}z_{21}}$	$z_{11} = \frac{(1 + s_{11})(1 - s_{22}) + s_{12}s_{21}}{(1 - s_{11})(1 - s_{22}) - s_{12}s_{21}}$ $z_{12} = \frac{2s_{12}}{(1 - s_{11})(1 - s_{22}) - s_{12}s_{21}}$ $z_{21} = \frac{2s_{21}}{(1 - s_{11})(1 - s_{22}) - s_{12}s_{21}}$ $z_{22} = \frac{(1 + s_{22})(1 - s_{11}) + s_{12}s_{21}}{(1 - s_{11})(1 - s_{22}) - s_{12}s_{21}}$

S

Z

B Scattering Parameter Relationships

s-parameters in terms of y-parameters	y-parameters in terms of s-parameters
$s_{11} = \frac{(1 - y_{11})(1 + y_{22}) + y_{12}y_{21}}{(1 + y_{11})(1 + y_{22}) - y_{12}y_{21}}$ $s_{12} = \frac{-2y_{12}}{(1 + y_{11})(1 + y_{22}) - y_{12}y_{21}}$ $s_{21} = \frac{-2y_{21}}{(1 + y_{11})(1 + y_{22}) - y_{12}y_{21}}$ $s_{22} = \frac{(1 + y_{11})(1 - y_{22}) + y_{12}y_{21}}{(1 + y_{11})(1 + y_{22}) - y_{12}y_{21}}$	$y_{11} = \frac{(1 + s_{22})(1 - s_{11}) + s_{12}s_{21}}{(1 + s_{11})(1 + s_{22}) - s_{12}s_{21}}$ $y_{12} = \frac{-2s_{12}}{(1 + s_{11})(1 + s_{22}) - s_{12}s_{21}}$ $y_{21} = \frac{-2s_{21}}{(1 + s_{11})(1 + s_{22}) - s_{12}s_{21}}$ $y_{22} = \frac{(1 + s_{11})(1 - s_{22}) + s_{12}s_{21}}{(1 + s_{11})(1 + s_{22}) - s_{12}s_{21}}$

S Y

B Scattering Parameter Relationships

s-parameters in terms of h-parameters	h-parameters in terms of s-parameters
$s_{11} = \frac{(h_{11} - 1)(h_{22} + 1) - h_{12}h_{21}}{(h_{11} + 1)(h_{22} + 1) - h_{12}h_{21}}$ $s_{12} = \frac{2h_{12}}{(h_{11} + 1)(h_{22} + 1) - h_{12}h_{21}}$ $s_{21} = \frac{-2h_{21}}{(h_{11} + 1)(h_{22} + 1) - h_{12}h_{21}}$ $s_{22} = \frac{(1 + h_{11})(1 - h_{22}) + h_{12}h_{21}}{(h_{11} + 1)(h_{22} + 1) - h_{12}h_{21}}$	$h_{11} = \frac{(1 + s_{11})(1 + s_{22}) - s_{12}s_{21}}{(1 - s_{11})(1 + s_{22}) + s_{12}s_{21}}$ $h_{12} = \frac{2s_{12}}{(1 - s_{11})(1 + s_{22}) + s_{12}s_{21}}$ $h_{21} = \frac{-2s_{21}}{(1 - s_{11})(1 + s_{22}) + s_{12}s_{21}}$ $h_{22} = \frac{(1 - s_{22})(1 - s_{11}) - s_{12}s_{21}}{(1 - s_{11})(1 + s_{22}) + s_{12}s_{21}}$

S

h

B Scattering Parameter Relationships

The h-, y-, and z-parameters listed in previous tables are all normalized to Z_0 . If h' , y' , z' are the actual parameters, then:

$$z'_{11} = z_{11}Z_0$$

$$y'_{11} = y_{11} / Z_0$$

$$h'_{11} = h_{11}Z_0$$

$$z'_{12} = z_{12}Z_0$$

$$y'_{12} = y_{12} / Z_0$$

$$h'_{12} = h_{12}$$

$$z'_{21} = z_{21}Z_0$$

$$y'_{21} = y_{21} / Z_0$$

$$h'_{21} = h_{21}$$

$$z'_{22} = z_{22}Z_0$$

$$y'_{22} = y_{22} / Z_0$$

$$h'_{22} = h_{22} / Z_0$$

Test & Measurement
Application Note 95-1
S-Parameter Techniques

Parameter Normalization

The various scattering parameters are all normalized by the reference impedance, Z_0 . This impedance is usually the characteristic impedance of the transmission line in which the network of interest is embedded. Normalizing the scattering parameters makes the Smith Chart readily applicable to transmission lines of any impedance. In addition, impedance and admittance values can be plotted on the same chart.

Z
0

C CAE tools for High-Frequency Design

Electronic Design Automation (EDA) The Software Revolution

In the 30 years that have elapsed since the publication of Dick Anderson's article, computer aided engineering (CAE) tools have been developed for the high-frequency design methods that were traditionally implemented using pencil and paper. These computer software programs run on UNIX workstations and PCs, and do much more than merely assist in computation-intensive design tasks.

Modern CAE tools for high-frequency design eliminate the need for simplifying assumptions (such as, $s_{12} = 0$) and can accurately simulate actual device, circuit, or system behavior. They enable broadband solutions, offer optimization and yield-analysis capabilities, and provide answers to "What if?" questions. CAE tools also speed the analysis of a wide range of RF and microwave devices, circuits, and systems, for a shorter time to market, while lowering costs.

Test & Measurement
Application Note 95-1
S-Parameter Techniques



C CAE tools for High-Frequency Design

The CAE tools of interest to RF and microwave designers include those summarized below:

Small-signal (s-parameter) simulation —

Small-signal analysis CAE tools simulate response over a range of frequencies, so actual implementations perform more closely to design parameters. Matching circuits are easily determined, and can be readily optimized, saving time. A yield-analysis feature allows the selection of components in matching networks for the best production yield, saving costs.

Large-signal simulation — This powerful analysis tool includes the harmonic balance implementation, useful for oscillator design and many other problems.

Circuit Envelope simulation — Efficiently analyzes circuits and feedback loops in the presence of modulated or transient high-frequency signals.

Circuit Envelope Simulation

The waveform above typifies the modulated and transient signals that can be efficiently analyzed using circuit envelope simulator software. Circuit envelope simulation is orders of magnitude faster than traditional SPICE simulation software if the envelope bandwidth of the RF carrier frequency is much smaller than the carrier frequency itself. This is the case in many communications, and radar circuits and subsystems.

C CAE tools for High-Frequency Design

Time-domain analysis — A CAE tool that is especially useful for simulating the response of digital systems at high clock rates.

Planar electromagnetic analysis — This simulator accurately computes the s-, y-, or z-parameters of arbitrarily shaped, multilayer planar structures such as striplines.

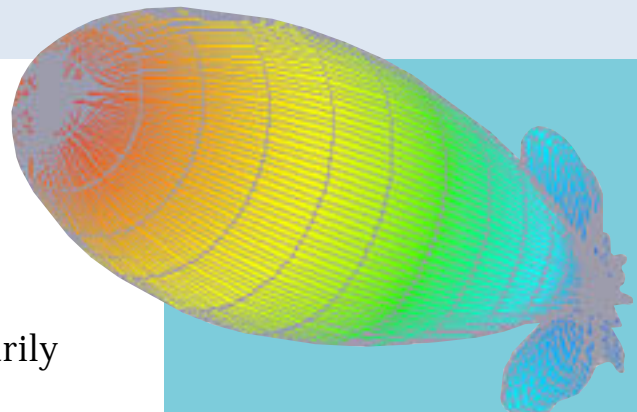
3D electromagnetic analysis — This CAE tool accurately computes the s-parameters for passive, three-dimensional, multiport structures.

System analysis — System and board-level simulators offer discrete-time and frequency-domain capabilities; can analyze and optimize complicated system topologies; handle complex waveforms; and perform physical layout design.

Modeling systems — Hardware and software are combined to extract parameters needed for accurate active device modeling.

Visit the HP EEsop website for the latest in CAE news, products, software, and solutions.

Test & Measurement
Application Note 95-1
S-Parameter Techniques



High Flying Software
The pattern of a horn antenna, displayed using HP High-Frequency Structure Simulator 3D electromagnetic visualization software, shows beam shapes in both azimuth and elevation in a single plot.

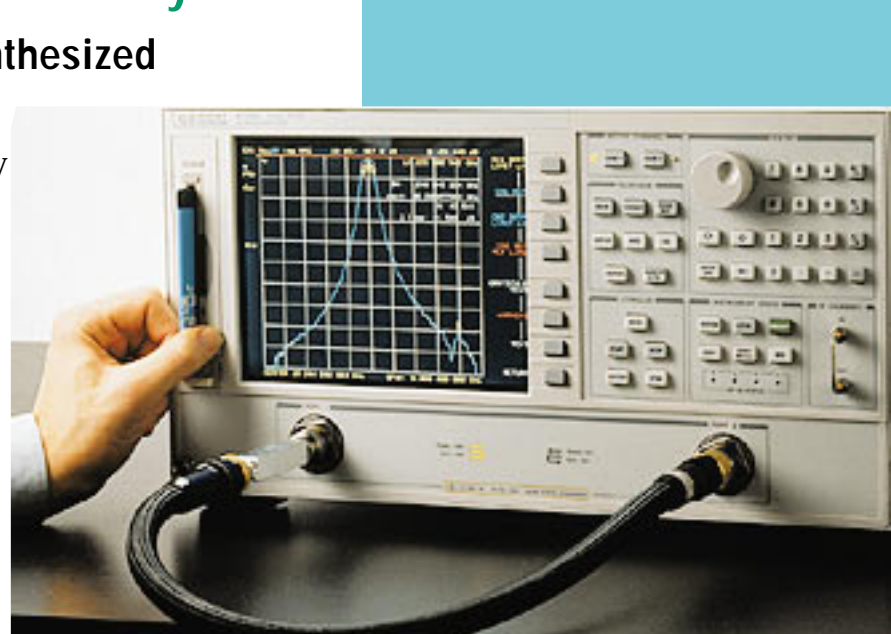
Relevant Products

HP 8720D Series Vector Network Analyzers

Vector network analyzers with built-in synthesized sources cover 50 MHz to up to 40 GHz

The HP 8720D vector network analyzer family characterizes RF and microwave components from 50 MHz up to 40 GHz. They combine a fast synthesized source, tuned receiver, and S-parameter test set in a single instrument. The devices have the performance and flexibility to solve difficult measurement problems and cut test times, all at an attractive cost. Use them to quickly and accurately measure magnitude and phase of all four s-parameters, as well as group delay, plus the absolute output power of microwave components.

Productivity is enhanced with pass/fail testing, direct printer/plotter output of results, advanced marker functions, save/recall of test configurations to internal memory or a built-in floppy disk drive, and test sequencing for automation. Options allow high-power tests, frequency offset mixer testing, and high-accuracy noncoaxial and on-wafer measurements.



Features of HP 8720D VNA's

- Built-in synthesized source with 1 Hz resolution
- Allows measuring all four s-parameters with a single connection
- Continuous updates for two-port error correction

<http://www.hp.com/go/tmdatasheets>

Test & Measurement
Application Note 95-1
S-Parameter Techniques

Relevant Products

HP 8510C Microwave Network Analyzers

Microwave network analyzers with coverage up to 110 GHz

The HP 8510C microwave vector network analyzer family provide complete solutions for characterizing the linear behavior of either active or passive networks over the 45 MHz to 110 GHz range. A complete system consists of the HP 8510C network analyzer, an s-parameter test set, and a compatible RF source. Also available are fully integrated systems, tested and verified prior to shipment.

The HP 8510C displays measurement results in log/linear magnitude, phase, or group delay format on a large, color CRT with two independent, yet identical, channels. The impact of systematic errors is removed by virtually "real-time" error correction, so a test device can be adjusted while it's being measured. Effective directivity and source match can be improved to as much as 60 dB. The HP 85161B software leads the operator one step at a time, from setup and calibration to hardcopy results.

Visit the HP Test & Measurement website and find more than 1,000 up to date product datasheets. (Adobe Acrobat users with the Weblink plug-in may click directly on the URL below.)

Test & Measurement
Application Note 95-1
S-Parameter Techniques



Features of the HP 8510C

- 45 MHz to 110 GHz frequency range
- Real-time error-corrected measurements
- 60 dB effective directivity and source match
- Up to 100 dB dynamic range
- 0.001 dB, 0.01 degree, 0.01 ns resolution
- Optional time domain and pulsed RF measurement capability

<http://www.hp.com/go/tmdatasheets>

Relevant Products

HP 8753D RF Network Analyzer

RF network analyzer with integrated s-parameter test set performs characterizations from 30 kHz to 6 GHz

The HP 8753D RF vector network analyzer will simplify and speed your device, component, or network measurements in the 30 kHz to 6 GHz range. A 1-Hz resolution swept synthesized source, s-parameter test set, and sensitive receiver are integrated into this compact instrument, which is simple to set up and use in the lab or on the production line. The HP 8753D provides magnitude and phase information, offers up to 110 dB dynamic range, makes group delay and time domain measurements, and uses vector accuracy enhancement to minimize measurement uncertainty.

To increase your throughput in production, the HP 8753D offers features such as the test sequence function, which allows you to make a measurement once from the front panel and automatically save the keystrokes without an external computer. The analyzer's fast CPU clock rate, LIF and DOS formats for output to the built-in disk drive or an external disk drive, and a 512 KB nonvolatile memory also help improve your productivity.



Features of the HP 8753D

- Built-in s-parameter test set, synthesized source
- Optional time-domain and swept-harmonic measurements
- Up to 110 dB dynamic range
- Superb accuracy, with comprehensive calibration
- Save/recall to built-in disk drive

<http://www.hp.com/go/tmdatasheets>

Relevant Products

CAE solutions for RF and microwave design

Time to market is critical to product success in today's competitive environment. CAE tools from Hewlett-Packard's EEsof Division give companies a competitive edge by simplifying and expediting the development of RF and microwave circuits and systems. For cost savings and manufacturing yield improvements, designs can be accurately modeled, simulated, and optimized before they are actually produced.

A comprehensive set of CAE tools from HP EEsof includes high-frequency circuit, electro-magnetic, and system simulators, layout tools, device modeling systems and libraries, and links to instrumentation and third-party design software. Visit the HP EEsof website for a continuously updated list of news, products, software, and solutions.

Test & Measurement
Application Note 95-1
S-Parameter Techniques

SOLUTIONS FROM HP EEsof



<http://www.hp.com/go/hpeesof>

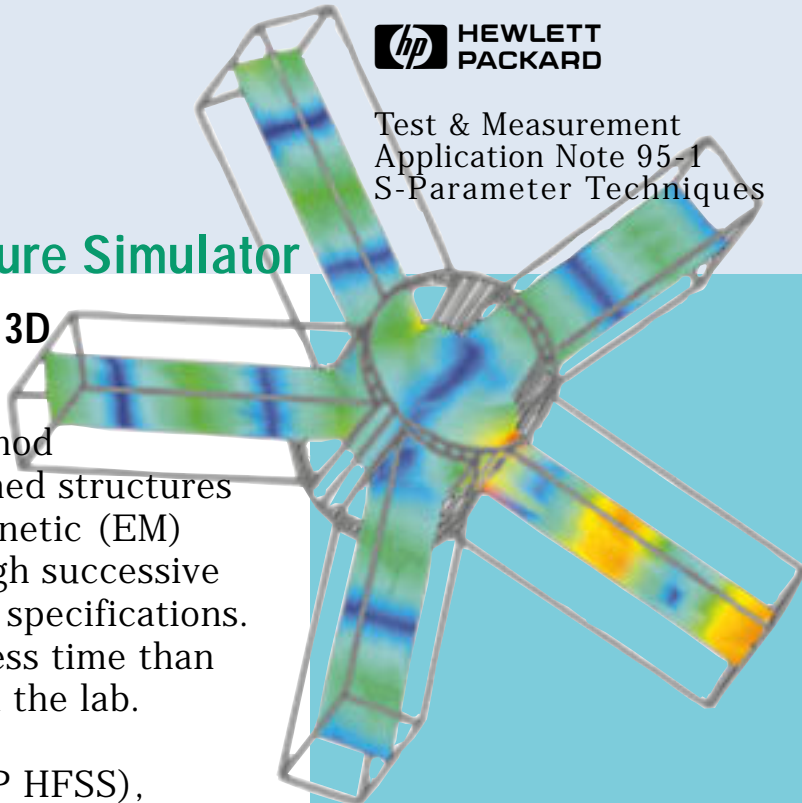
Relevant Products

HP 85180A High Frequency Structure Simulator

Fast, accurate electromagnetic simulation of 3D high-frequency structures saves design time

With today's computer technology, the best method for designing high frequency circuits and machined structures is to compute their behavior with 3D electromagnetic (EM) simulator software, making improvements through successive simulations, then building designs to the refined specifications. This approach is more cost effective and takes less time than building and testing prototype after prototype in the lab.

The HP High Frequency Structure Simulator (HP HFSS), Release 5.0, models arbitrarily-shaped, passive 3D structures such as antennas, machined components, and RF and digital circuits. Using accuracy-driven adaptive solution refinement, the software produces accurate results ten times faster, using half the memory of previous releases. Its drawing environment and parts library simplify specifying complex structures. For comprehensive evaluations, animated EM fields, surface currents, vector plots, antenna polar patterns and tabular, generalized s-parameters and Smith charts can be viewed.



Features of the HP 85180A

- Reduces "cut and try" prototyping, for lower development costs and a quicker time to market
- Yields accurate results ten times faster, using half the memory of previous releases
- Requires minimal user knowledge of EM field theory
- For PC and UNIX platforms

<http://www.hp.com/go/hpeesof>

Relevant Services

RF and microwave education and training

HP offers an extensive curriculum of education services at locations worldwide. To help high-frequency design engineers learn how to use CAE tools quickly, we provide training courses taught by the experts from HP's EEsof Division. Advanced RF/microwave CAE courses are also conducted to help extend the capabilities and hone the skills of experienced CAE users.



HP education classes are scheduled regularly. The curriculum can be tailored to a company's special needs, and training sessions can be conducted at its site.

Visit HP's World Wide Website for the complete and continuously updated list of Test & Measurement class schedules and locations around the world. Click on the URL below or type the address in your browser. Register directly online!



Test & Measurement
Application Note 95-1
S-Parameter Techniques



<http://www.hp.com/go/tmeducation>

Worldwide Contacts

Hewlett-Packard Test & Measurement offices

Asia-Pacific

Hewlett-Packard Asia Pacific Ltd.
Hewlett-Packard Hong Kong Ltd.
17-21/F Shell Tower, Times Square
1 Matheson Street, Causeway Bay
Hong Kong
85 2 599 7777

For Japan: **0120-421-345**

Australia/New Zealand

Hewlett-Packard Australia Ltd.
31-41 Joseph Street
Blackburn, Victoria 3130
Australia
1 800 627 485

Canada

Hewlett-Packard Ltd.
5150 Spectrum Way
Mississauga, Ontario L4W 5G1
905 206 4725

Europe/Middle East/Africa

Hewlett-Packard S.A.
150, Route du Nant-d'Avril
1217 Meyrin 1
Geneva, Switzerland

For Europe:

41 22 780 81 11

For Middle East/Africa:

41 22 780 41 11

Visit HP's World Wide Website for the complete and up to date listing of Test & Measurement sales office addresses and call center phone numbers. Click on the URL below or type the address in your browser.

<http://www.hp.com/go/tmdir>

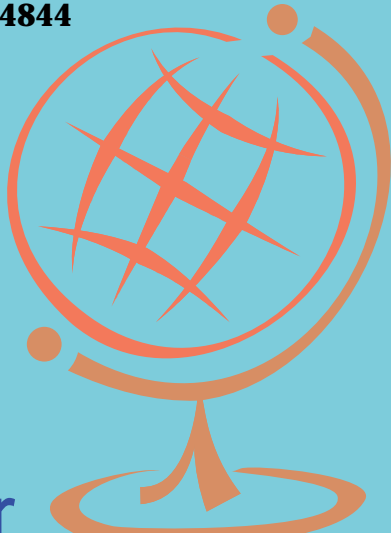
Test & Measurement
Application Note 95-1
S-Parameter Techniques

Latin America

Latin American Region
Headquarters
Hewlett-Packard Company
Waterford Building, Suite 950
5200 Blue Lagoon
Miami, FL 33126
305-267-4245

United States of America

Hewlett-Packard Company
800-452-4844



Copyrights and Credits

Authors, contributors and producers

Authors

Dick Anderson – original author of this application note.

Lee Smith – S-parameter guru, mathematical programming, technical illustrations, updated & revised content, and animations.

Jeff Gruszynski – expert domain consultant, content perspectives, side-bars text, and source images.

Contributors

Walt Patstone – technical content and side-bar editing.

Chuck McGuire, Mike

C'debaca – new s-parameter measurements & device output.

Graphic & Interaction Design

Ev Shafrir – original concept, art direction, interaction design, digital publishing & production, content supervision, overall direction, & project management.

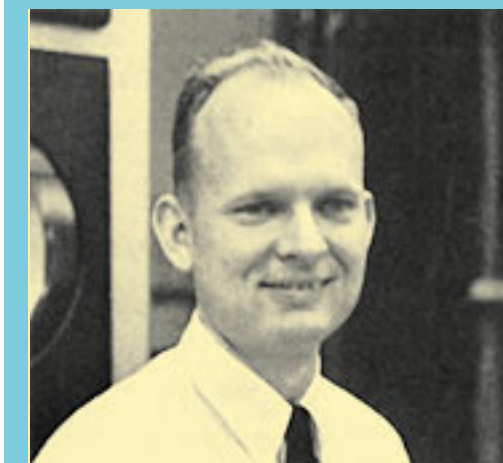
Christina Bangle – free-style illustrations and graphic reviews.

Kathy Cunningham – page layout design and Quark guru.

Leann Scully – source images.

Business Manager

Nyna Casey – funding, support, excitement, and encouragement.



Richard W. Anderson

Holds a 1959 BSEE degree from Utah State University and a 1963 MSEE degree from Stanford University. During his 37 years with HP Dick has contributed to the development of numerous microwave and other T&M instruments. Currently, he is HP Vice President, and General Manager of the T&M Microwave and Communications Group.

Conversions Between S , Z , Y , h , $ABCD$, and T Parameters which are Valid for Complex Source and Load Impedances

Dean A. Frickey, *Member, IEEE*

Abstract—This paper provides tables which contain the conversion between the various common two-port parameters, Z , Y , h , $ABCD$, S , and T . The conversion are valid for complex normalizing impedances. An example is provided which verifies the conversions to and from S parameters.

I. INTRODUCTION

MOST microwave textbooks these days seem to provide a table of the conversion between the various 2-port parameters. These 2-port parameters often include Z (impedance), Y (admittance), h (hybrid), $ABCD$ (chain), S (scattering), and T (chain scattering or chain transfer). While the scattering parameters have been shown [1] to be valid for complex normalizing impedances (with positive real parts), the tables in [2]–[15] are not valid for complex source and load impedances. Often, the tables only provide conversions for the cases where port 1 and port 2 normalizing impedances are equal, i.e., $Z_{01} = Z_{02} = Z_0$. Some have results in which Z_{01} and Z_{02} are normalized to 1. Others provide equations for port 1 and port 2 impedances Z_{01} and Z_{02} to be unique. However, in all of these cases, the results are not valid when the impedances, Z_{01} and Z_{02} , or just Z_0 , are complex.

Of the two-port parameters mentioned, only the S and T parameters are dependent upon the source and load impedances. In this paper, the derivations of the conversions from the S and T parameters to the other 2-port parameters includes complex source and load impedances. The equations developed in this work are valid with port 1 and port 2 normalizing impedances complex and unique. When the normalizing impedances are real, the results simplify to those shown in other references. To make the list complete, the conversions between the Z , Y , h , and $ABCD$ parameters as well as between S and T parameters are included.

II. DERIVATION

Two-port parameters are defined for a general 2-port network as shown in Fig. 1. Using the voltages and currents defined in this figure, the various 2-port parameters are written as

Manuscript received December 2, 1992; revised April 13, 1993.
The author is with EG&G Idaho, Idaho Falls, ID 83415.
IEEE Log Number 9214525.

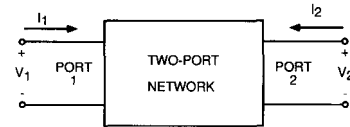


Fig. 1. A general two-port network with voltages and currents defined.

Z parameters

$$V_1 = Z_{11} \cdot I_1 + Z_{12} \cdot I_2 \quad (1a)$$

$$V_2 = Z_{21} \cdot I_1 + Z_{22} \cdot I_2, \quad (1b)$$

Y parameters

$$I_1 = Y_{11} \cdot V_1 + Y_{12} \cdot V_2 \quad (2a)$$

$$I_2 = Y_{21} \cdot V_1 + Y_{22} \cdot V_2, \quad (2b)$$

h parameters

$$V_1 = h_{11} \cdot I_1 + h_{12} \cdot V_2 \quad (3a)$$

$$I_2 = h_{21} \cdot I_1 + h_{22} \cdot V_2, \quad (3b)$$

$ABCD$ parameters

$$V_1 = A \cdot V_2 - B \cdot I_2 \quad (4a)$$

$$I_1 = C \cdot V_2 - D \cdot I_2, \quad (4b)$$

S parameters

$$b_1 = S_{11} \cdot a_1 + S_{12} \cdot a_2 \quad (5a)$$

$$b_2 = S_{21} \cdot a_1 + S_{22} \cdot a_2, \quad (5b)$$

TABLE I
EQUATIONS FOR THE CONVERSION BETWEEN S PARAMETERS AND Z , Y , h , AND $ABCD$ PARAMETERS WITH A SOURCE IMPEDANCE Z_{01} AND LOAD IMPEDANCE Z_{02}

$S_{11} = \frac{(Z_{11}-Z_{01}^*)(Z_{22}+Z_{02})-Z_{12}Z_{21}}{(Z_{11}+Z_{01})(Z_{22}+Z_{02})-Z_{12}Z_{21}}$	$Z_{11} = \frac{(Z_{01}^*+S_{11}Z_{01})(1-S_{22})+S_{12}S_{21}Z_{01}}{(1-S_{11})(1-S_{22})-S_{12}S_{21}}$
$S_{12} = \frac{2Z_{12}(R_{01}R_{02})^{1/2}}{(Z_{11}+Z_{01})(Z_{22}+Z_{02})-Z_{12}Z_{21}}$	$Z_{12} = \frac{2S_{12}(R_{01}R_{02})^{1/2}}{(1-S_{11})(1-S_{22})-S_{12}S_{21}}$
$S_{21} = \frac{2Z_{21}(R_{01}R_{02})^{1/2}}{(Z_{11}+Z_{01})(Z_{22}+Z_{02})-Z_{12}Z_{21}}$	$Z_{21} = \frac{2S_{21}(R_{01}R_{02})^{1/2}}{(1-S_{11})(1-S_{22})-S_{12}S_{21}}$
$S_{22} = \frac{(1-Y_{11}Z_{01}^*)(1+Y_{22}Z_{02})+Y_{12}Y_{21}Z_{01}Z_{02}}{(1+Y_{11}Z_{01})(1+Y_{22}Z_{02})-Y_{12}Y_{21}Z_{01}Z_{02}}$	$Z_{22} = \frac{(1-S_{11})(Z_{02}^*+S_{22}Z_{02})+S_{12}S_{21}Z_{02}}{(1-S_{11})(1-S_{22})-S_{12}S_{21}}$
$S_{11} = \frac{-2Y_{12}(R_{01}R_{02})^{1/2}}{(1+Y_{11}Z_{01})(1+Y_{22}Z_{02})-Y_{12}Y_{21}Z_{01}Z_{02}}$	$Y_{11} = \frac{(1-S_{11})(Z_{02}^*+S_{22}Z_{02})+S_{12}S_{21}Z_{02}}{(Z_{01}^*+S_{11}Z_{01})(Z_{02}^*+S_{22}Z_{02})-S_{12}S_{21}Z_{01}Z_{02}}$
$S_{12} = \frac{-2Y_{21}(R_{01}R_{02})^{1/2}}{(1+Y_{11}Z_{01})(1+Y_{22}Z_{02})-Y_{12}Y_{21}Z_{01}Z_{02}}$	$Y_{12} = \frac{-2S_{12}(R_{01}R_{02})^{1/2}}{(Z_{01}^*+S_{11}Z_{01})(Z_{02}^*+S_{22}Z_{02})-S_{12}S_{21}Z_{01}Z_{02}}$
$S_{21} = \frac{-2Y_{12}(R_{01}R_{02})^{1/2}}{(1+Y_{11}Z_{01})(1+Y_{22}Z_{02})-Y_{12}Y_{21}Z_{01}Z_{02}}$	$Y_{21} = \frac{-2S_{21}(R_{01}R_{02})^{1/2}}{(Z_{01}^*+S_{11}Z_{01})(Z_{02}^*+S_{22}Z_{02})-S_{12}S_{21}Z_{01}Z_{02}}$
$S_{22} = \frac{(1+Y_{11}Z_{01})(1-Y_{22}Z_{02})+Y_{12}Y_{21}Z_{01}Z_{02}}{(1+Y_{11}Z_{01})(1+Y_{22}Z_{02})-Y_{12}Y_{21}Z_{01}Z_{02}}$	$Y_{22} = \frac{(Z_{01}^*+S_{11}Z_{01})(1-S_{22})+S_{12}S_{21}Z_{01}}{(Z_{01}^*+S_{11}Z_{01})(Z_{02}^*+S_{22}Z_{02})-S_{12}S_{21}Z_{01}Z_{02}}$
$S_{11} = \frac{(h_{11}-Z_{01}^*)(1+h_{22}Z_{02})-h_{12}h_{21}Z_{02}}{(Z_{01}+h_{11})(1+h_{22}Z_{02})-h_{12}h_{21}Z_{02}}$	$h_{11} = \frac{(Z_{01}^*+S_{11}Z_{01})(Z_{02}^*+S_{22}Z_{02})-S_{12}S_{21}Z_{01}Z_{02}}{(1-S_{11})(Z_{02}^*+S_{22}Z_{02})+S_{12}S_{21}Z_{02}}$
$S_{12} = \frac{2h_{12}(R_{01}R_{02})^{1/2}}{(Z_{01}+h_{11})(1+h_{22}Z_{02})-h_{12}h_{21}Z_{02}}$	$h_{12} = \frac{2S_{12}(R_{01}R_{02})^{1/2}}{(1-S_{11})(Z_{02}^*+S_{22}Z_{02})+S_{12}S_{21}Z_{02}}$
$S_{21} = \frac{-2h_{21}(R_{01}R_{02})^{1/2}}{(Z_{01}+h_{11})(1+h_{22}Z_{02})-h_{12}h_{21}Z_{02}}$	$h_{21} = \frac{-2S_{21}(R_{01}R_{02})^{1/2}}{(1-S_{11})(Z_{02}^*+S_{22}Z_{02})+S_{12}S_{21}Z_{02}}$
$S_{22} = \frac{(Z_{01}+h_{11})(1-h_{22}Z_{02}^*)+h_{12}h_{21}Z_{02}}{(Z_{01}+h_{11})(1+h_{22}Z_{02})-h_{12}h_{21}Z_{02}}$	$h_{22} = \frac{(1-S_{11})(1-S_{22})-S_{12}S_{21}}{(1-S_{11})(Z_{02}^*+S_{22}Z_{02})+S_{12}S_{21}Z_{02}}$
$S_{11} = \frac{AZ_{02}+B-CZ_{01}^*Z_{02}-DZ_{01}^*}{AZ_{02}+B+CZ_{01}Z_{02}+DZ_{01}}$	$A = \frac{(Z_{01}^*+S_{11}Z_{01})(1-S_{22})+S_{12}S_{21}Z_{01}}{2S_{21}(R_{01}R_{02})^{1/2}}$
$S_{12} = \frac{2(AD-BC)(R_{01}R_{02})^{1/2}}{AZ_{02}+B+CZ_{01}Z_{02}+DZ_{01}}$	$B = \frac{(Z_{01}^*+S_{11}Z_{01})(Z_{02}^*+S_{22}Z_{02})-S_{12}S_{21}Z_{01}Z_{02}}{2S_{21}(R_{01}R_{02})^{1/2}}$
$S_{21} = \frac{2(R_{01}R_{02})^{1/2}}{AZ_{02}+B+CZ_{01}Z_{02}+DZ_{01}}$	$C = \frac{(1-S_{11})(1-S_{22})-S_{12}S_{21}}{2S_{21}(R_{01}R_{02})^{1/2}}$
$S_{22} = \frac{-AZ_{02}^*+B-CZ_{01}Z_{02}+DZ_{01}}{AZ_{02}+B+CZ_{01}Z_{02}+DZ_{01}}$	$D = \frac{(1-S_{11})(Z_{02}^*+S_{22}Z_{02})+S_{12}S_{21}Z_{02}}{2S_{21}(R_{01}R_{02})^{1/2}}$



Fig. 2. A general two port network with a 's and b 's defined.

T parameters¹

$$a_1 = T_{11} \cdot b_2 + T_{12} \cdot a_2 \quad (6a)$$

$$b_1 = T_{21} \cdot b_2 + T_{22} \cdot a_2 \quad (6b)$$

where the a 's and b 's are shown in Fig. 2 and defined below.

$$a_j = \left[\frac{Z_{0j} + Z_{0j}^*}{2} \right]^{1/2} \cdot I_{ji} \quad (7a)$$

$$b_j = \left[\frac{Z_{0j} + Z_{0j}^*}{2} \right]^{1/2} \cdot I_{jr} \quad (7b)$$

¹Some authors, (e.g. Rizzi [16]) define the T parameters as $b_1 = T_{11} \cdot a_2 + T_{12} \cdot b_2$, and $a_1 = T_{21} \cdot a_2 + T_{22}b_2$. In this case, the parameters can just be switched from what is derived in this paper. T_{11} and T_{22} are switched, T_{12} and T_{21} are switched.

where * indicates complex conjugate and Z_{0j} is the normalizing impedance for the j th port. For two-port networks, Z_{01} and Z_{02} are the source and load impedances of the system in which the S parameters of the two-port are measured or calculated. I_{ji} and I_{jr} are the incident and reflected currents for the j th port. Knowing that,

$$I_j = I_{ji} - I_{jr} \quad (8)$$

we can solve (7a) and (7b) for I_{ji} and I_{jr} and substitute them into (8) to get,

$$I_j = \left[\frac{2}{Z_{0j} + Z_{0j}^*} \right]^{1/2} \cdot (a_j - b_j). \quad (9)$$

Knowing also that,

$$V_j = V_{ji} + V_{jr} \quad (10)$$

where V_{ji} and V_{jr} are the incident and reflected voltage at the j th port, we can substitute the expressions for I_{ji} and I_{jr} along with

$$V_{ji} = I_{ji} \cdot Z_{0j}^* \quad V_{jr} = I_{jr} \cdot Z_{0j}$$

into (10) to get,

$$V_j = \left[\frac{2}{Z_{0j} + Z_{0j}^*} \right]^{1/2} \cdot (a_j \cdot Z_{0j}^* + b_j \cdot Z_{0j}). \quad (11)$$

TABLE II
EQUATIONS FOR THE CONVERSION BETWEEN T PARAMETERS AND Z , Y , h , AND $ABCD$ PARAMETERS WITH A SOURCE IMPEDANCE Z_{01} AND LOAD IMPEDANCE Z_{02}

$T_{11} = \frac{(Z_{11} + Z_{01})(Z_{22} + Z_{02}) - Z_{12}Z_{21}}{2Z_{21}(R_{01}R_{02})^{1/2}}$	$Z_{11} = \frac{Z_{01}^*(T_{11} + T_{12}) + Z_{01}(T_{21} + T_{22})}{T_{11} + T_{12} - T_{21} - T_{22}}$
$T_{12} = \frac{(Z_{11} + Z_{01})(Z_{02}^* - Z_{22}) + Z_{12}Z_{21}}{2Z_{21}(R_{01}R_{02})^{1/2}}$	$Z_{12} = \frac{2(R_{01}R_{02})^{1/2}(T_{11}T_{22} - T_{12}T_{21})}{T_{11} + T_{12} - T_{21} - T_{22}}$
$T_{21} = \frac{(Z_{11} - Z_{01})(Z_{22} + Z_{02}) - Z_{12}Z_{21}}{2Z_{21}(R_{01}R_{02})^{1/2}}$	$Z_{21} = \frac{2(R_{01}R_{02})^{1/2}}{T_{11} + T_{12} - T_{21} - T_{22}}$
$T_{22} = \frac{(Z_{01}^* - Z_{11})(Z_{22} - Z_{02}^*) + Z_{12}Z_{21}}{2Z_{21}(R_{01}R_{02})^{1/2}}$	$Z_{22} = \frac{Z_{02}^*(T_{11} - T_{21}) - Z_{02}(T_{12} - T_{22})}{T_{11} + T_{12} - T_{21} - T_{22}}$
$T_{11} = \frac{(-1 - Y_{11}Z_{01})(1 + Y_{22}Z_{02}) + Y_{12}Y_{21}Z_{01}Z_{02}}{2Y_{21}(R_{01}R_{02})^{1/2}}$	$Y_{11} = \frac{Z_{02}^*(T_{11} - T_{21}) - Z_{02}(T_{12} - T_{22})}{T_{11}Z_{01}^*Z_{02}^* - T_{12}Z_{01}^*Z_{02} + T_{21}Z_{01}Z_{02}^* - T_{22}Z_{01}Z_{02}}$
$T_{12} = \frac{(1 + Y_{11}Z_{01})(1 - Y_{22}Z_{02}^*) + Y_{12}Y_{21}Z_{01}Z_{02}^*}{2Y_{21}(R_{01}R_{02})^{1/2}}$	$Y_{12} = \frac{-2(R_{01}R_{02})^{1/2}(T_{11}T_{22} - T_{12}T_{21})}{T_{11}Z_{01}^*Z_{02}^* - T_{12}Z_{01}^*Z_{02} + T_{21}Z_{01}Z_{02}^* - T_{22}Z_{01}Z_{02}}$
$T_{21} = \frac{(Y_{11}Z_{01}^* - 1)(1 + Y_{22}Z_{02}) - Y_{12}Y_{21}Z_{01}^*Z_{02}}{2Y_{21}(R_{01}R_{02})^{1/2}}$	$Y_{21} = \frac{-2(R_{01}R_{02})^{1/2}}{T_{11}Z_{01}^*Z_{02}^* - T_{12}Z_{01}^*Z_{02} + T_{21}Z_{01}Z_{02}^* - T_{22}Z_{01}Z_{02}}$
$T_{22} = \frac{(1 - Y_{11}Z_{01}^*)(1 - Y_{22}Z_{02}^*) - Y_{12}Y_{21}Z_{01}^*Z_{02}^*}{2Y_{21}(R_{01}R_{02})^{1/2}}$	$Y_{22} = \frac{Z_{01}^*(T_{11} + T_{12}) + Z_{01}(T_{21} + T_{22})}{T_{11}Z_{01}^*Z_{02}^* - T_{12}Z_{01}^*Z_{02} + T_{21}Z_{01}Z_{02}^* - T_{22}Z_{01}Z_{02}}$
$T_{11} = \frac{(-h_{11} - Z_{01})(1 + h_{22}Z_{02}) + h_{12}h_{21}Z_{02}}{2h_{21}(R_{01}R_{02})^{1/2}}$	$h_{11} = \frac{Z_{02}^*(T_{11}Z_{01}^* + T_{21}Z_{01}) - Z_{02}(T_{12}Z_{01}^* + T_{22}Z_{01})}{Z_{02}^*(T_{11} - T_{21}) - Z_{02}(T_{12} + T_{22})}$
$T_{12} = \frac{(h_{11} + Z_{01})(1 - h_{22}Z_{02}^*) + h_{12}h_{21}Z_{02}^*}{2h_{21}(R_{01}R_{02})^{1/2}}$	$h_{12} = \frac{2(R_{01}R_{02})^{1/2}(T_{11}T_{22} - T_{12}T_{21})}{Z_{02}^*(T_{11} - T_{21}) - Z_{02}(T_{12} + T_{22})}$
$T_{21} = \frac{(Z_{01}^* - h_{11})(1 + h_{22}Z_{02}) + h_{12}h_{21}Z_{02}}{2h_{21}(R_{01}R_{02})^{1/2}}$	$h_{21} = \frac{-2(R_{01}R_{02})^{1/2}}{Z_{02}^*(T_{11} - T_{21}) - Z_{02}(T_{12} + T_{22})}$
$T_{22} = \frac{(h_{11} - Z_{01}^*)(1 - h_{22}Z_{02}^*) + h_{12}h_{21}Z_{02}^*}{2h_{21}(R_{01}R_{02})^{1/2}}$	$h_{22} = \frac{T_{11} + T_{12} - T_{21} - T_{22}}{Z_{02}^*(T_{11} - T_{21}) - Z_{02}(T_{12} + T_{22})}$
$T_{11} = \frac{AZ_{02} + B + CZ_{01}Z_{02} + DZ_{01}}{2(R_{01}R_{02})^{1/2}}$	$A = \frac{Z_{01}^*(T_{11} + T_{12}) + Z_{01}(T_{21} + T_{22})}{2(R_{01}R_{02})^{1/2}}$
$T_{12} = \frac{AZ_{02}^* - B + CZ_{01}Z_{02}^* - DZ_{01}}{2(R_{01}R_{02})^{1/2}}$	$B = \frac{Z_{02}^*(T_{11}Z_{01}^* + T_{21}Z_{01}) - Z_{02}(T_{12}Z_{01}^* + T_{22}Z_{01})}{2(R_{01}R_{02})^{1/2}}$
$T_{21} = \frac{AZ_{02} + B - CZ_{01}Z_{02} - DZ_{01}}{2(R_{01}R_{02})^{1/2}}$	$C = \frac{T_{11} + T_{12} - T_{21} - T_{22}}{2(R_{01}R_{02})^{1/2}}$
$T_{22} = \frac{AZ_{02}^* - B - CZ_{01}Z_{02}^* + DZ_{01}^*}{2(R_{01}R_{02})^{1/2}}$	$D = \frac{Z_{02}^*(T_{11} - T_{21}) - Z_{02}(T_{12} - T_{22})}{2(R_{01}R_{02})^{1/2}}$

Solving (9) and (11) for a_j and b_j gives

$$a_j = \frac{V_j + Z_{0j}I_j}{[2(Z_{0j} + Z_{0j}^*)]^{1/2}} \quad (12)$$

$$b_j = \frac{V_j - Z_{0j}^*I_j}{[2(Z_{0j} + Z_{0j}^*)]^{1/2}}. \quad (13)$$

Equations (12) and (13) are (3) and (4) in [1] and served as the starting point.

The notation, $S \leftrightarrow Z$, indicates the conversion from S parameters to Z parameters and Z parameters to S parameters. Since S and T parameters are defined in terms of a 's and b 's, they will contain the source and load normalizing impedances Z_{01} and Z_{02} . The other 2-port parameters are defined independent of the source and load impedances.

To derive the conversions, $S \leftrightarrow Z$, $S \leftrightarrow Y$, $S \leftrightarrow h$, $S \leftrightarrow ABCD$, $T \leftrightarrow Z$, $T \leftrightarrow Y$, $T \leftrightarrow h$, and $T \leftrightarrow ABCD$, it is necessary to use (9), (11)–(13). For example, to derive the expressions for S parameters in terms of the Z parameters, first substitute (9) and (11) into (1a) and (1b) and solve for b_1

and b_2 to get in the form of (5a) and (5b). Likewise, to get the expressions for the Z parameters in terms of the S parameters, substitute (12) and (13) into (5a) and (5b) and solve for V_1 and V_2 to get in the form of (1a) and (1b).

Since Z , Y , h , and $ABCD$ parameters do not require normalizing impedances, the conversions, $Z \leftrightarrow Y$, $Z \leftrightarrow h$, $Z \leftrightarrow ABCD$, $Y \leftrightarrow h$, $Y \leftrightarrow ABCD$, and $h \leftrightarrow ABCD$, as well as $S \leftrightarrow T$, are straight forward. These conversions are accomplished by rearranging one set of equations into the form of the other. These conversions appear in many of the references cited and are included here for completeness.

III. RESULTS

The results are given in the following tables. In these tables, Z_{01} and Z_{02} are the source and load impedances of the system to which the S and T parameters pertain. Complex conjugate is indicated by $*$, and R_{01} and R_{02} are the real parts of Z_{01} and Z_{02} .

Table I gives the conversions between S parameters and Z , Y , h , and $ABCD$ parameters. Table II gives the conversions

TABLE III
EQUATIONS FOR THE CONVERSION BETWEEN S PARAMETERS AND NORMALIZED Z , Y , h ,
AND $ABCD$ PARAMETERS WITH A SOURCE IMPEDANCE Z_{01} AND LOAD IMPEDANCE Z_{02}

$S_{11} = \frac{[Z_{11n} - Z_{01}^*] (Z_{22n} + 1) - Z_{12n} Z_{21n}}{(Z_{11n} + 1)(Z_{22n} + 1) - Z_{12n} Z_{21n}}$	$Z_{11n} = \frac{[Z_{01}^* + S_{11}] (1 - S_{22}) + S_{12} S_{21}}{(1 - S_{11})(1 - S_{22}) - S_{12} S_{21}}$
$S_{12} = \frac{2Z_{12n} \left[\frac{R_{01} R_{02}}{Z_{01} Z_{02}} \right]^{1/2}}{(Z_{11n} + 1)(Z_{22n} + 1) - Z_{12n} Z_{21n}}$	$Z_{12n} = \frac{2S_{12} \left[\frac{R_{01} R_{02}}{Z_{01} Z_{02}} \right]^{1/2}}{(1 - S_{11})(1 - S_{22}) - S_{12} S_{21}}$
$S_{21} = \frac{2Z_{21n} \left[\frac{R_{01} R_{02}}{Z_{01} Z_{02}} \right]^{1/2}}{(Z_{11n} + 1)(Z_{22n} + 1) - Z_{12n} Z_{21n}}$	$Z_{21n} = \frac{2S_{21} \left[\frac{R_{01} R_{02}}{Z_{01} Z_{02}} \right]^{1/2}}{(1 - S_{11})(1 - S_{22}) - S_{12} S_{21}}$
$S_{22} = \frac{(Z_{11n} + 1) \left[Z_{22n} \frac{Z_{02}^*}{Z_{02}} \right] - Z_{12n} Z_{21n}}{(Z_{11n} + 1)(Z_{22n} + 1) - Z_{12n} Z_{21n}}$	$Z_{22n} = \frac{(1 - S_{11}) \left[Z_{02}^* + S_{22} \right] + S_{12} S_{21}}{(1 - S_{11})(1 - S_{22}) - S_{12} S_{21}}$
$Z_{11n} = \frac{Z_{11}}{Z_{01}}$	$Z_{12n} = \frac{Z_{12}}{(Z_{01} Z_{02})^{1/2}}$
$Z_{21n} = \frac{Z_{21}}{(Z_{01} Z_{02})^{1/2}}$	$Z_{22n} = \frac{Z_{22}}{Z_{02}}$
$S_{11} = \frac{[1 - Y_{11n} \left[\frac{Z_{01}^*}{Z_{01}} \right]] (1 + Y_{22n}) + Y_{12n} Y_{21n} \left[\frac{Z_{01}^*}{Z_{01}} \right]}{(1 + Y_{11n})(1 + Y_{22n}) - Y_{12n} Y_{21n}}$	$Y_{11n} = \frac{(1 - S_{11}) \left[\frac{Z_{02}^*}{Z_{02}} + S_{22} \right] + S_{12} S_{21}}{\left[\frac{Z_{01}^*}{Z_{01}} + S_{11} \right] \left[\frac{Z_{02}^*}{Z_{02}} + S_{22} \right] - S_{12} S_{21}}$
$S_{12} = \frac{-2Y_{12n} \left[\frac{R_{01} R_{02}}{Z_{01} Z_{02}} \right]^{1/2}}{(1 + Y_{11n})(1 + Y_{22n}) - Y_{12n} Y_{21n}}$	$Y_{12n} = \frac{-2S_{12} \left[\frac{R_{01} R_{02}}{Z_{01} Z_{02}} \right]^{1/2}}{\left[\frac{Z_{01}^*}{Z_{01}} + S_{11} \right] \left[\frac{Z_{02}^*}{Z_{02}} + S_{22} \right] - S_{12} S_{21}}$
$S_{21} = \frac{-2Y_{21n} \left[\frac{R_{01} R_{02}}{Z_{01} Z_{02}} \right]^{1/2}}{(1 + Y_{11n})(1 + Y_{22n}) - Y_{12n} Y_{21n}}$	$Y_{21n} = \frac{-2S_{21} \left[\frac{R_{01} R_{02}}{Z_{01} Z_{02}} \right]^{1/2}}{\left[\frac{Z_{01}^*}{Z_{01}} + S_{11} \right] \left[\frac{Z_{02}^*}{Z_{02}} + S_{22} \right] - S_{12} S_{21}}$
$S_{22} = \frac{(1 + Y_{11n}) \left[1 - Y_{22n} \left[\frac{Z_{02}^*}{Z_{02}} \right] \right] + Y_{12n} Y_{21n} \left[\frac{Z_{02}^*}{Z_{02}} \right]}{(1 + Y_{11n})(1 + Y_{22n}) - Y_{12n} Y_{21n}}$	$Y_{22n} = \frac{\left[\frac{Z_{01}^*}{Z_{01}} + S_{11} \right] (1 - S_{22}) + S_{12} S_{21}}{\left[\frac{Z_{01}^*}{Z_{01}} + S_{11} \right] \left[\frac{Z_{02}^*}{Z_{02}} + S_{22} \right] - S_{12} S_{21}}$
$Y_{11n} = Y_{11} Z_{01}$	$Y_{12n} = Y_{12} (Z_{01} Z_{02})^{1/2}$
	$Y_{21n} = Y_{21} (Z_{01} Z_{02})^{1/2}$
	$Y_{22n} = Y_{22} Z_{02}$
$S_{11} = \frac{\left[h_{11n} - \frac{Z_{01}^*}{Z_{01}} \right] (1 + h_{22n}) - h_{12n} h_{21n}}{(1 + h_{11n})(1 + h_{22n}) - h_{12n} h_{21n}}$	$h_{11n} = \frac{\left[\frac{Z_{01}^*}{Z_{01}} + S_{11} \right] \left[\frac{Z_{02}^*}{Z_{02}} + S_{22} \right] - S_{12} S_{21}}{(1 - S_{11}) \left[\frac{Z_{02}^*}{Z_{02}} + S_{22} \right] + S_{12} S_{21}}$
$S_{12} = \frac{2h_{12n} \left[\frac{R_{01} R_{02}}{Z_{01} Z_{02}} \right]^{1/2}}{(1 + h_{11n})(1 + h_{22n}) - h_{12n} h_{21n}}$	$h_{12n} = \frac{2S_{12} \left[\frac{R_{01} R_{02}}{Z_{01} Z_{02}} \right]^{1/2}}{(1 - S_{11}) \left[\frac{Z_{02}^*}{Z_{02}} + S_{22} \right] + S_{12} S_{21}}$
$S_{21} = \frac{-2h_{21n} \left[\frac{R_{01} R_{02}}{Z_{01} Z_{02}} \right]^{1/2}}{(1 + h_{11n})(1 + h_{22n}) - h_{12n} h_{21n}}$	$h_{21n} = \frac{-2S_{21} \left[\frac{R_{01} R_{02}}{Z_{01} Z_{02}} \right]^{1/2}}{(1 - S_{11}) \left[\frac{Z_{02}^*}{Z_{02}} + S_{22} \right] + S_{12} S_{21}}$
$S_{22} = \frac{(1 + h_{11n}) \left[1 - h_{22n} \left[\frac{Z_{02}^*}{Z_{02}} \right] \right] + h_{12n} h_{21n} \left[\frac{Z_{02}^*}{Z_{02}} \right]}{(1 + h_{11n})(1 + h_{22n}) - h_{12n} h_{21n}}$	$h_{22n} = \frac{(1 - S_{11})(1 - S_{22}) - S_{12} S_{21}}{(1 - S_{11}) \left[\frac{Z_{02}^*}{Z_{02}} + S_{22} \right] + S_{12} S_{21}}$
$h_{11n} = \frac{h_{11}}{Z_{01}}$	$h_{12n} = h_{12} \left[\frac{Z_{02}}{Z_{01}} \right]^{1/2}$
	$h_{21n} = h_{21} \left[\frac{Z_{02}}{Z_{01}} \right]^{1/2}$
	$h_{22n} = h_{22} Z_{02}$
$S_{11} = \frac{A_n + B_n - C_n \left[\frac{Z_{01}^*}{Z_{01}} \right] - D_n \left[\frac{Z_{01}^*}{Z_{01}} \right]}{A_n + B_n + C_n + D_n}$	$A_n = \frac{\left[\frac{Z_{01}^*}{Z_{01}} + S_{11} \right] (1 - S_{22}) + S_{12} S_{21}}{2S_{21} \left[\frac{R_{01} R_{02}}{Z_{01} Z_{02}} \right]}$
$S_{12} = \frac{2 \left[\frac{R_{01} R_{02}}{Z_{01} Z_{02}} \right] (A_n D_n - B_n C_n)}{A_n + B_n + C_n + D_n} = \frac{2(AD - BC)}{A_n + B_n + C_n + D_n}$	$B_n = \frac{\left[\frac{Z_{01}^*}{Z_{01}} + S_{11} \right] \left[\frac{Z_{02}^*}{Z_{02}} + S_{22} \right] - S_{12} S_{21}}{2S_{21} \left[\frac{R_{01} R_{02}}{Z_{01} Z_{02}} \right]}$
$S_{21} = \frac{2}{A_n + B_n + C_n + D_n}$	$C_n = \frac{(1 - S_{11})(1 - S_{22}) - S_{12} S_{21}}{2S_{21} \left[\frac{R_{01} R_{02}}{Z_{01} Z_{02}} \right]}$
$S_{22} = \frac{-A_n \left[\frac{Z_{02}^*}{Z_{02}} \right] + B_n - C_n \left[\frac{Z_{02}^*}{Z_{02}} \right] + D_n}{A_n + B_n + C_n + D_n}$	$D_n = \frac{(1 - S_{11}) \left[\frac{Z_{02}^*}{Z_{02}} + S_{22} \right] + S_{12} S_{21}}{2S_{21} \left[\frac{R_{01} R_{02}}{Z_{01} Z_{02}} \right]}$
$A_n = \frac{AZ_{02}}{(R_{01} R_{02})^{1/2}}$	$B_n = \frac{B}{(R_{01} R_{02})^{1/2}}$
	$C_n = \frac{CZ_{01} Z_{02}}{(R_{01} R_{02})^{1/2}}$
	$D_n = \frac{DZ_{01}}{(R_{01} R_{02})^{1/2}}$

TABLE IV
EQUATIONS FOR THE CONVERSION BETWEEN T PARAMETERS AND NORMALIZED Z, Y, h,
AND ABCD PARAMETERS WITH A SOURCE IMPEDANCE Z_{01} AND LOAD IMPEDANCE Z_{02}

$T_{11} = \frac{(Z_{11n}+1)(Z_{22n}+1)-Z_{12n}Z_{21n}}{2Z_{21n}\left[\frac{R_{01}R_{02}}{Z_{01}Z_{02}}\right]^{1/2}}$	$Z_{11n} = \frac{\left[\frac{Z_{01}}{Z_{02}}\right](T_{11}+T_{12})+(T_{21}+T_{22})}{T_{11}+T_{12}-T_{21}-T_{22}}$
$T_{12} = \frac{(Z_{11n}+1)\left[\frac{Z_{02}}{Z_{02}}-Z_{22n}\right]+Z_{12n}Z_{21n}}{2Z_{21n}\left[\frac{R_{01}R_{02}}{Z_{01}Z_{02}}\right]^{1/2}}$	$Z_{12n} = \frac{2\left[\frac{R_{01}R_{02}}{Z_{01}Z_{02}}\right]^{1/2}(T_{11}T_{22}-T_{12}T_{21})}{T_{11}+T_{12}-T_{21}-T_{22}}$
$T_{21} = \frac{\left[Z_{11n}-\frac{Z_{01}}{Z_{01}}\right](Z_{22n}+1)-Z_{12n}Z_{21n}}{2Z_{21n}\left[\frac{R_{01}R_{02}}{Z_{01}Z_{02}}\right]^{1/2}}$	$Z_{21n} = \frac{2\left[\frac{R_{01}R_{02}}{Z_{01}Z_{02}}\right]^{1/2}}{T_{11}+T_{12}-T_{21}-T_{22}}$
$T_{22} = \frac{\left[\frac{Z_{01}}{Z_{01}}-Z_{11n}\right]\left[Z_{22n}-\frac{Z_{02}}{Z_{02}}\right]+Z_{12n}Z_{21n}}{2Z_{21n}\left[\frac{R_{01}R_{02}}{Z_{01}Z_{02}}\right]^{1/2}}$	$Z_{22n} = \frac{\left[\frac{Z_{02}}{Z_{02}}\right](T_{11}-T_{21})-(T_{12}-T_{22})}{T_{11}+T_{12}-T_{21}-T_{22}}$
$Z_{11n} = \frac{Z_{11}}{Z_{01}}$	$Z_{12n} = \frac{Z_{12}}{(Z_{01}Z_{02})^{1/2}}$
$Z_{21n} = \frac{Z_{21}}{(Z_{01}Z_{02})^{1/2}}$	$Z_{22n} = \frac{Z_{22}}{Z_{02}}$
$T_{11} = \frac{(-1-Y_{11n})(1+Y_{22n})+Y_{12n}Y_{21n}}{2Y_{21n}\left[\frac{R_{01}R_{02}}{Z_{01}Z_{02}}\right]^{1/2}}$	$Y_{11n} = \frac{\left[\frac{Z_{02}}{Z_{02}}\right](T_{11}-T_{21})-(T_{12}-T_{22})}{T_{11}\left[\frac{Z_{01}Z_{02}}{Z_{01}Z_{02}}\right]-T_{12}\left[\frac{Z_{01}}{Z_{01}}\right]+T_{21}\left[\frac{Z_{02}}{Z_{02}}\right]-T_{22}}$
$T_{12} = \frac{(1+Y_{11n})\left[1-Y_{22n}\left[\frac{Z_{02}}{Z_{02}}\right]\right]+Y_{12n}Y_{21n}\left[\frac{Z_{02}}{Z_{02}}\right]}{2Y_{21n}\left[\frac{R_{01}R_{02}}{Z_{01}Z_{02}}\right]^{1/2}}$	$Y_{12n} = \frac{-2\left[\frac{R_{01}R_{02}}{Z_{01}Z_{02}}\right]^{1/2}(T_{11}T_{22}-T_{12}T_{21})}{T_{11}\left[\frac{Z_{01}Z_{02}}{Z_{01}Z_{02}}\right]-T_{12}\left[\frac{Z_{01}}{Z_{01}}\right]+T_{21}\left[\frac{Z_{02}}{Z_{02}}\right]-T_{22}}$
$T_{21} = \frac{\left[Y_{11n}\left[\frac{Z_{01}}{Z_{01}}\right]-1\right](1+Y_{22n})-Y_{12n}Y_{21n}\left[\frac{Z_{01}}{Z_{01}}\right]}{2Y_{21n}\left[\frac{R_{01}R_{02}}{Z_{01}Z_{02}}\right]^{1/2}}$	$Y_{21n} = \frac{-2\left[\frac{R_{01}R_{02}}{Z_{01}Z_{02}}\right]^{1/2}}{T_{11}\left[\frac{Z_{01}Z_{02}}{Z_{01}Z_{02}}\right]-T_{12}\left[\frac{Z_{01}}{Z_{01}}\right]+T_{21}\left[\frac{Z_{02}}{Z_{02}}\right]-T_{22}}$
$T_{22} = \frac{\left[1-Y_{11n}\left[\frac{Z_{01}}{Z_{01}}\right]\right]\left[1-Y_{22n}\left[\frac{Z_{02}}{Z_{02}}\right]\right]-Y_{12n}Y_{21n}\left[\frac{Z_{01}}{Z_{01}}\frac{Z_{02}}{Z_{02}}\right]}{2Y_{21n}\left[\frac{R_{01}R_{02}}{Z_{01}Z_{02}}\right]^{1/2}}$	$Y_{22n} = \frac{\left[\frac{Z_{01}}{Z_{01}}\right](T_{11}+T_{12})+(T_{21}+T_{22})}{T_{11}\left[\frac{Z_{01}Z_{02}}{Z_{01}Z_{02}}\right]-T_{12}\left[\frac{Z_{01}}{Z_{01}}\right]+T_{21}\left[\frac{Z_{02}}{Z_{02}}\right]-T_{22}}$
$Y_{11n} = Y_{11}Z_{01}$	$Y_{12n} = Y_{12}(Z_{01}Z_{02})^{1/2}$
$Y_{21n} = Y_{21}(Z_{01}Z_{02})^{1/2}$	$Y_{22n} = Y_{22}Z_{02}$
$T_{11} = \frac{(-h_{11n}-1)(1+h_{22n})+h_{12n}h_{21n}}{2h_{21n}\left[\frac{R_{01}R_{02}}{Z_{01}Z_{02}}\right]^{1/2}}$	$h_{11n} = \frac{T_{11}\left[\frac{Z_{01}Z_{02}}{Z_{01}Z_{02}}\right]-T_{12}\left[\frac{Z_{01}}{Z_{01}}\right]+T_{21}\left[\frac{Z_{02}}{Z_{02}}\right]-T_{22}}{\left[\frac{Z_{02}}{Z_{02}}\right](T_{11}-T_{21})-(T_{12}-T_{22})}$
$T_{12} = \frac{(h_{11n}+1)\left[1-h_{22n}\left[\frac{Z_{02}}{Z_{02}}\right]\right]+h_{12n}h_{21n}\left[\frac{Z_{02}}{Z_{02}}\right]}{2h_{21n}\left[\frac{R_{01}R_{02}}{Z_{01}Z_{02}}\right]^{1/2}}$	$h_{12n} = \frac{2\left[\frac{R_{01}R_{02}}{Z_{01}Z_{02}}\right]^{1/2}(T_{11}T_{22}-T_{12}T_{21})}{\left[\frac{Z_{02}}{Z_{02}}\right](T_{11}-T_{21})-(T_{12}-T_{22})}$
$T_{21} = \frac{\left[\frac{Z_{01}}{Z_{01}}-h_{11n}\right](1+h_{22n})+h_{12n}h_{21n}}{2h_{21n}\left[\frac{R_{01}R_{02}}{Z_{01}Z_{02}}\right]^{1/2}}$	$h_{21n} = \frac{-2\left[\frac{R_{01}R_{02}}{Z_{01}Z_{02}}\right]^{1/2}}{\left[\frac{Z_{02}}{Z_{02}}\right](T_{11}-T_{21})-(T_{12}-T_{22})}$
$T_{22} = \frac{\left[h_{11n}-\frac{Z_{01}}{Z_{01}}\right]\left[1-h_{22n}\left[\frac{Z_{02}}{Z_{02}}\right]\right]+h_{12n}h_{21n}\left[\frac{Z_{02}}{Z_{02}}\right]}{2h_{21n}\left[\frac{R_{01}R_{02}}{Z_{01}Z_{02}}\right]^{1/2}}$	$h_{22n} = \frac{T_{11}+T_{12}-T_{21}-T_{22}}{\left[\frac{Z_{02}}{Z_{02}}\right](T_{11}-T_{21})-(T_{12}-T_{22})}$
$h_{11n} = \frac{h_{11}}{Z_{01}}$	$h_{12n} = h_{12}\left[\frac{Z_{02}}{Z_{01}}\right]^{1/2}$
$h_{21n} = h_{21}\left[\frac{Z_{02}}{Z_{01}}\right]^{1/2}$	$h_{22n} = h_{22}Z_{02}$
$T_{11} = \frac{A_n+B_n+C_n+D_n}{2}$	$A_n = \frac{\left[\frac{Z_{01}}{Z_{01}}\right](T_{11}+T_{12})+(T_{21}+T_{22})}{2\left[\frac{R_{01}R_{02}}{Z_{01}Z_{02}}\right]}$
$T_{12} = \frac{A_n\left[\frac{Z_{02}}{Z_{02}}\right]-B_n+C_n\left[\frac{Z_{02}}{Z_{02}}\right]-D_n}{2}$	$B_n = \frac{T_{11}\left[\frac{Z_{01}Z_{02}}{Z_{01}Z_{02}}\right]-T_{12}\left[\frac{Z_{01}}{Z_{01}}\right]+T_{21}\left[\frac{Z_{02}}{Z_{02}}\right]-T_{22}}{2\left[\frac{R_{01}R_{02}}{Z_{01}Z_{02}}\right]}$
$T_{21} = \frac{A_n+B_n-C_n\left[\frac{Z_{01}}{Z_{01}}\right]-D_n\left[\frac{Z_{01}}{Z_{01}}\right]}{2}$	$C_n = \frac{T_{11}+T_{12}-T_{21}-T_{22}}{2\left[\frac{R_{01}R_{02}}{Z_{01}Z_{02}}\right]}$
$T_{22} = \frac{A_n\left[\frac{Z_{02}}{Z_{02}}\right]-B_n-C_n\left[\frac{Z_{01}Z_{02}}{Z_{01}Z_{02}}\right]+D_n\left[\frac{Z_{01}}{Z_{01}}\right]}{2}$	$D_n = \frac{\left[\frac{Z_{02}}{Z_{02}}\right](T_{11}-T_{21})-(T_{12}-T_{22})}{2\left[\frac{R_{01}R_{02}}{Z_{01}Z_{02}}\right]}$
$A_n = \frac{AZ_{02}}{(R_{01}R_{02})^{1/2}}$	$B_n = \frac{B}{(R_{01}R_{02})^{1/2}}$
	$C_n = \frac{CZ_{01}Z_{02}}{(R_{01}R_{02})^{1/2}}$
	$D_n = \frac{DZ_{01}}{(R_{01}R_{02})^{1/2}}$

TABLE V
EQUATIONS SHOWING THE CONVERSIONS BETWEEN Z , Y , h , AND $ABCD$ PARAMETERS

$Z_{11} = \frac{Y_{22}}{Y_{11}Y_{22}-Y_{12}Y_{21}}$	$Y_{11} = \frac{Z_{22}}{Z_{11}Z_{22}-Z_{12}Z_{21}}$	$Z_{11} = \frac{h_{11}h_{22}-h_{12}h_{21}}{h_{22}}$	$h_{11} = \frac{Z_{11}Z_{22}-Z_{12}Z_{21}}{Z_{22}}$
$Z_{12} = \frac{Y_{11}Y_{22}-Y_{12}Y_{21}}{Y_{11}Y_{22}-Y_{12}Y_{21}}$	$Y_{12} = \frac{Z_{11}Z_{22}-Z_{12}Z_{21}}{Z_{11}Z_{22}-Z_{12}Z_{21}}$	$Z_{12} = \frac{h_{12}}{h_{22}}$	$h_{12} = \frac{Z_{12}}{Z_{22}}$
$Z_{21} = \frac{Y_{11}Y_{22}-Y_{12}Y_{21}}{Y_{11}Y_{22}-Y_{12}Y_{21}}$	$Y_{21} = \frac{Z_{11}Z_{22}-Z_{12}Z_{21}}{Z_{11}Z_{22}-Z_{12}Z_{21}}$	$Z_{21} = \frac{h_{21}}{h_{22}}$	$h_{21} = \frac{Z_{21}}{Z_{22}}$
$Z_{22} = \frac{Y_{11}Y_{22}-Y_{12}Y_{21}}{Y_{11}Y_{22}-Y_{12}Y_{21}}$	$Y_{22} = \frac{Z_{11}}{Z_{11}Z_{22}-Z_{12}Z_{21}}$	$Z_{22} = \frac{1}{h_{22}}$	$h_{22} = \frac{1}{Z_{22}}$
$Z_{11} = \frac{A}{C}$	$A = \frac{Z_{11}}{Z_{21}}$	$Y_{11} = \frac{1}{h_{11}}$	$h_{11} = \frac{1}{Y_{11}}$
$Z_{12} = \frac{AD-BC}{C}$	$B = \frac{Z_{21}Z_{22}-Z_{12}Z_{21}}{Z_{21}}$	$Y_{12} = \frac{-h_{12}}{h_{11}}$	$h_{12} = \frac{-Y_{12}}{Y_{11}}$
$Z_{21} = \frac{1}{C}$	$C = \frac{1}{Z_{21}}$	$Y_{21} = \frac{h_{21}}{h_{11}}$	$h_{21} = \frac{Y_{21}}{Y_{11}}$
$Z_{22} = \frac{D}{C}$	$D = \frac{Z_{22}}{Z_{21}}$	$Y_{22} = \frac{h_{11}h_{22}-h_{12}h_{21}}{h_{11}}$	$h_{22} = \frac{Y_{11}Y_{22}-Y_{12}Y_{21}}{Y_{11}}$
$Y_{11} = \frac{D}{B}$	$A = \frac{-Y_{22}}{Y_{21}}$	$h_{11} = \frac{B}{D}$	$A = \frac{h_{12}h_{21}-h_{11}h_{22}}{h_{21}}$
$Y_{12} = \frac{BC-AD}{B}$	$B = \frac{Y_{21}}{Y_{21}}$	$h_{12} = \frac{AD-BC}{D}$	$B = \frac{-h_{11}}{h_{21}}$
$Y_{21} = \frac{-1}{B}$	$C = \frac{Y_{12}Y_{21}-Y_{11}Y_{22}}{Y_{21}}$	$h_{21} = \frac{-1}{D}$	$C = \frac{-h_{22}}{h_{21}}$
$Y_{22} = \frac{A}{B}$	$D = \frac{-Y_{11}}{Y_{21}}$	$h_{22} = \frac{C}{D}$	$D = \frac{h_{11}}{h_{21}}$

between T parameters and Z , Y , h , and $ABCD$ parameters. Tables III and IV provide the conversions from S and T parameters to the normalized Z , Y , h , and $ABCD$ parameters, respectively. From Tables III and IV, it is easy to see that if Z_{01} and Z_{02} are real, the conversions become those shown in many of the references cited, e.g., [2], [4], [7], [8], [11], [12], [14], [15]. Finally, Table V shows the conversions between Z , Y , h , and $ABCD$ parameters while Table VI shows the conversions between S and T parameters. These are included to make the table of conversions in this paper complete.

IV. VERIFICATION

Using PSPICE, a SPICE based circuit analysis program, a lumped element model of an NE32000 HEMT was analyzed. The netlist was taken from the NEC databook and is shown below:

```

g1 5 6 3 4 0.045
lg 1 2 0.1nh
rg 2 3 2
cgs 3 4 0.2pf
cgd 3 5 0.016pf
cdg 5 4 6.7ff
ri 4 6 4
rs 6 7 3.5
ls 7 10 0.03nh
rds 5 6 200
cds 5 6 7.2ff
rd 5 8 4
ld 8 9 0.09nh.

```

By properly configuring a source at first port 1 then port 2, and opening and shorting out the other port, PSPICE will provide the complex voltages and currents required to calculate the Z , Y , h , and $ABCD$ parameters. Tables VII and VIII show the voltages and currents from PSPICE under the conditions listed in those tables. The Z , Y , h , and $ABCD$ parameters are calculated from these using (1)-(4) and are shown in Table IX.

The NE32000 lumped element model was also analyzed using Super Compact. For no particular reason, I chose to

TABLE VI
EQUATIONS SHOWING THE CONVERSIONS BETWEEN S AND T PARAMETERS

$S_{11} = \frac{T_{21}}{T_{11}}$	$T_{11} = \frac{1}{S_{21}}$
$S_{12} = \frac{T_{11}T_{22}-T_{12}T_{21}}{T_{11}}$	$T_{12} = \frac{-S_{22}}{S_{21}}$
$S_{21} = \frac{1}{T_{11}}$	$T_{21} = \frac{S_{11}}{S_{21}}$
$S_{22} = \frac{-T_{12}}{T_{11}}$	$T_{22} = \frac{S_{12}S_{21}-S_{11}S_{22}}{S_{21}}$

calculate the S parameters for the NE32000 in a system with a source impedance, Z_{01} , equal to $70+j30$ and load impedance, Z_{02} , equal to $25-j35$ at the single frequency of 10 GHz. The results of the Super Compact analysis are shown in Table X.

If a person uses the Z , Y , h , or $ABCD$ parameters of Table IX, in the equations of Table I, with $Z_{01} = 70+j30$ and $Z_{02} = 25-j35$, they will find that the calculated S parameters agree with those from Super Compact. In a like fashion, using the S parameters of Super Compact in the other equations in Table I will result in Z , Y , h , and $ABCD$ parameters shown in Table IX.

V. CONCLUSION

This paper developed the equations for converting between the various common 2-port parameters, Z , Y , h , $ABCD$, S , and T . The equations are derived from the definitions of the various 2-port parameters, the definition of a_j and b_j , and basic transmission line theory. As a result, the equations are completely general and are valid for complex and unique source and load impedances.

The validity of these results is shown by first calculating S parameters from Z , Y , h , and $ABCD$ parameters for an NE32000 HEMT in a system with $Z_S = 70 + j 30$ and $Z_L = 25 - j 35$. These results agreed with the S parameters produced by Super Compact. Also, beginning with the S parameters from Super Compact, the Z , Y , h , and $ABCD$ parameters are calculated using the equations developed. The results are the same as those calculated from the voltages and currents produced by PSPICE.

TABLE VII
VOLTAGES AND CURRENTS FOR THE NE3200 HEMT AT 10 GHz WITH THE SOURCE AT PORT 1. THE VOLTAGES AND CURRENTS ARE DEFINED IN FIG. 1

$I_2 = 0$ (Port 2 Open Circuited)		$V_1 = 1 + j 0$		$V_2 = 0$ (Port 2 Short Circuited)	
I_1	V_2	I_1	I_2	I_1	I_2
8.844E-03 + j 2.371E-02	-8.181E+00 + j 5.615E+00	2.010E-03 + j 1.292E-02	4.018E-02 - j 1.071E-02		

TABLE VIII
VOLTAGES AND CURRENTS FOR THE NE3200 HEMT AT 10 GHz WITH THE SOURCE AT PORT 2. THE VOLTAGES AND CURRENTS ARE DEFINED IN FIG. 1

$I_1 = 0$ (Port 1 Open Circuited)		$V_2 = 1 + j 0$		$V_1 = 0$ (Port 1 Short Circuited)	
I_2	V_1	I_2	V_1	I_1	I_1
8.032E-03 + j 1.119E-03	9.661E-02 + j 1.869E-02	3.949E-03 + j 1.402E-03	4.741E-05 - j 1.286E-03		

TABLE IX
*Z, Y, h, AND ABCD PARAMETERS FOR THE NE3200 HEMT AT 10 GHz. THESE PARAMETERS
WERE CALCULATED FROM THE VOLTAGES AND CURRENTS IN TABLES VII AND VIII USING (1)–(4)*

	11	12	21	22
<i>Z</i>	1.380E+01 - j 3.702E+01	1.212E+01 + j 6.395E-01	9.518E+01 + j 3.803E+02	1.221E+02 - j 1.701E+01
<i>Y</i>	2.010E-03 + j 1.292E-02	4.741E-05 - j 1.286E-03	4.018E-02 - j 1.071E-02	3.949E-03 + j 1.402E-03
<i>h</i>	1.176E+01 - j 7.557E+01	9.661E-02 + j 1.869E-02	-3.370E-01 - j 3.162E+00	8.032E-03 + j 1.119E-03
<i>A</i>	<i>B</i>		<i>C</i>	<i>D</i>
<i>ABCD</i>	-8.309E-02 - j 5.703E-02	-2.324E+01 - j 6.194E+00	6.173E-04 - j 2.474E-03	3.332E-02 - j 3.127E-01

TABLE X
SUPER COMPACT RESULTS FOR THE NE32000 HEMT

$Z_S = 70 + j 30$								
MICROWAVE HARMONICA PC V1.06 File: ne320-l.ckt 25-FEB-92 21:42:46								
Freq	MS11	PS11	MS21	PS21	MS12	PS12	MS22	MS21
GHz	mag	deg	mag	deg	mag	deg	mag	dB
10.000	0.665	-121.4	2.194	118.3	0.068	45.3	0.796	-12.4
								6.82

ACKNOWLEDGMENT

The author would like to thank Dr. Ulrich Rohde and Dr. Ray Pengelly of Compact Software for the use of Microwave Harmonica. He also wishes to acknowledge as his Lord and Savior Jesus Christ, and thank Him for His love and guidance.

REFERENCES

- [1] D. C. Youla, "On scattering matrices normalized to complex port numbers," *Proc. IRE*, vol. 49, p. 1221, July 1961.
- [2] S. Y. Liao, *Microwave Circuit Analysis & Amplifier Design*. Englewood Cliffs, NJ: Prentice-Hall, 1987, pp. 471-472.
- [3] P. I. Somlo and J. D. Hunter, *Microwave Impedance Measurement*. (Electrical Measurement Ser.: No. 2), IEE 1985, p. 23.
- [4] R. S. Carson, *High-Frequency Amplifiers*, 2nd ed. New York: Wiley 1982, p. 200.
- [5] R. W. Beatty and D. M. Kerns, "Relationships between different kinds of network parameters, not assuming reciprocity or equality of the waveguide or transmission line characteristic impedances," *Proc. IEEE*, vol. 52, p. 84, Jan. 1964.
- [6] ———, "Correction to 'Relationships between different kinds of network parameters, not assuming reciprocity or equality of the waveguide or transmission line characteristic impedances,'" *Proc. IEEE*, vol. 52, p. 426, Apr. 1964.
- [7] Hewlett-Packard, "S-Parameter techniques for faster, more accurate network design," Appl. Note 95-1, Palo Alto, CA, Feb. 1967.
- [8] G. D. Vendelin, A. M. Pavio, and U. L. Rohde, *Microwave Circuit Design Using Linear and Nonlinear Techniques*. New York: Wiley, 1990, pp. 16-17.
- [9] D. M. Kerns and R. W. Beatty, *Basic Theory of Waveguide Junctions and Introductory Microwave Network Analysis*. Elmsford, NJ: Pergamon, 1967, pp. 136-139.
- [10] D. M. Pozar, *Microwave Engineering*. Reading: MA: Addison-Wesley 1990, p. 235.
- [11] *Microwave Systems News*, The Microwave System Designer's Handbook, 5th ed., vol. 17, no. 8, July 1987, p. 229.
- [12] S. F. Adam, *Microwave Theory and Applications*. Englewood Cliffs, NJ: Prentice-Hall, 1969, p. 89.
- [13] L. J. Giacoletto, Ed., *Electronics Designers' Handbook*, 2nd Ed. New York: McGraw-Hill, 1977, pp. 5.77-5.79.
- [14] G. Gonzalez, *Microwave Transistor Amplifiers: Analysis and Design*. Englewood Cliffs, NJ: Prentice-Hall, 1984, pp. 24-25.
- [15] R. Soares, Ed., *GaAs MESFET Circuit Design*. Butler, WI: Artech 1988, pp. 92-93.
- [16] P. A. Rizzi, *Microwave Engineering: Passive Circuits*. Englewood Cliffs, NJ: Prentice-Hall, 1988, p. 538.

Dean A. Frickey (S'76-M'82) was born in Sheridan, WY on March 10, 1958. He received the B.S. and M.S. degrees in electrical engineering from the South Dakota School of Mines and Technology, Rapid City in 1980 and 1981, respectively. He is pursuing, part-time, the Ph.D. degree in electrical engineering through the University of Idaho, Moscow.

He spent one year with the Boeing Military Airplane Company, Seattle, WA, in a systems analysis group before becoming involved in microwave technology at Raytheon Missile Systems Division, Tewksbury, MA, where he spent 6 years mostly involved in the analysis and design of hybrid microwave integrated circuits, but with some time spent working with W-Band IMPATT diodes. In November 1989, he joined EG&G Idaho, which operates the Idaho National Engineering Laboratory. His research interests are in microwave theory and applications.

- [7] D. Nghiem, J. T. Williams, and D. R. Jackson, "A general analysis of propagation along multiple-layer superconducting stripline and microstrip transmission lines," *IEEE Trans. Microwave Theory Tech.*, vol. 39, no. 9, pp. 1553-1565, Sept. 1991.

Comments on "Conversions Between S, Z, Y, h, ABCD, and T Parameters which are Valid for Complex Source and Load Impedances"

Roger B. Marks and Dylan F. Williams

In his recent paper,¹ Frickey presents formulas for conversions between various network matrices. Four of these matrices (Z , Y , h , and $ABCD$) relate voltages and currents at the ports; the other two (S and T) relate wave quantities. These relationships depend on the definitions of the waves themselves in terms of voltage and current. Frickey's results are based on an unconventional definition of the waves, whose resulting properties are unfamiliar to most microwave engineers. As a result, application of his formulas can easily lead to catastrophic errors.

The scattering and transmission matrices of classical microwave circuit theory (e.g., [1]-[3]) relate the complex amplitudes of the counterpropagating traveling waves in a transmission line. These modal waves are solutions of Maxwell's equations whose dependence on the axial coordinate z is $e^{\pm i\gamma z}$, where γ is the propagation constant. Ratios of the traveling wave amplitudes can be measured by classical slotted line techniques or with a network analyzer using a thru-reflect-line (TRL) calibration [4].

The classical circuit theory also allows the possibility of renormalizing the traveling waves by introducing a reference impedance Z_{ref} that may differ from the characteristic impedance Z_o . The resulting quantities form the basis of a renormalized scattering matrix. For instance, the renormalized reflection coefficient (one-port scattering matrix) Γ of a load of impedance Z_{load} , using a reference impedance Z_{ref} , is simply

$$\Gamma = \frac{Z_{load} - Z_{ref}}{Z_{load} + Z_{ref}} = \frac{Z_{load}/Z_{ref} - 1}{Z_{load}/Z_{ref} + 1}. \quad (1)$$

This familiar form is the basis of the Smith Chart, which provides a convenient graphical method of transforming between the reflection coefficient and the normalized load impedance Z_{load}/Z_{ref} , which, as shown by (1), uniquely determines Γ .

Instead of traveling waves, Frickey [1] makes use of parameters that Youla [5] defines and calls "waves"; a form of these parameters known as "power waves" has previously been applied to microwave circuits [6]. In spite of the terminology, Youla's parameters have little in common with waves. For instance, they do not depend exponentially or even monotonically on z [4]. Furthermore, the

¹Manuscript received August 12, 1994.

The authors are with the National Institute of Standards and Technology, Boulder, CO 80303 USA.

IEEE Log Number 9408572.

¹D. A. Frickey, *IEEE Trans. Microwave Theory Tech.*, vol. 42, pp. 205-211, Feb. 1994.

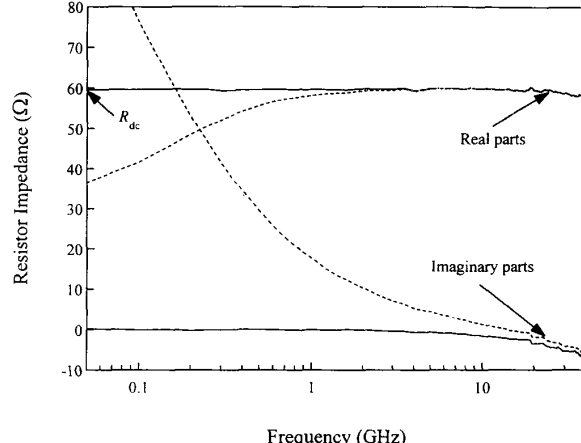


Fig. 1. The impedance of a small lumped resistor calculated, using $Z_{ref} = Z_o$, from scattering parameters measured by the multiline TRL calibration. The solid curves are calculated from (1), the dashed curves from (2).

properties of Youla's parameters differ fundamentally from those of the renormalized traveling waves. For example, Youla's reflection coefficient $\hat{\Gamma}$ is

$$\hat{\Gamma} = \frac{Z_{load} - Z_{ref}^*}{Z_{load} + Z_{ref}} = \frac{Z_{load}/Z_{ref} - Z_{ref}^*/Z_{ref}}{Z_{load}/Z_{ref} + 1}. \quad (2)$$

Since (1) does not apply, the Smith Chart is *inapplicable* to Youla's parameters. In fact, $\hat{\Gamma}$ is not even uniquely determined by Z_{load}/Z_{ref} , as is Γ . As an illustration, the renormalized reflection coefficient of a short circuit ($Z_{load} = 0$) is always $\Gamma = -1$, regardless of reference impedance Z_{ref} . In contrast, (2) shows that Youla's reflection coefficient of a short is equal *not* to -1 but to $-Z_{ref}^*/Z_{ref}$, which has magnitude 1 but is not generally real.

No microwave instrumentation or calibration known to us measures Youla's waves [4]. Thus, the equations of the above paper cannot be used to determine impedance parameters from measured scattering parameters. To illustrate, we used the multiline TRL calibration [7] to measure the scattering parameters of a small lumped resistor (with measured dc resistance $R_{dc} = 59.3 \Omega$) embedded in a coplanar waveguide. We measured the characteristic impedance Z_o of the transmission line using the technique of [8] and [9]. In applying (1) and (2), we made use of the fact that $Z_{ref} = Z_o$, a condition which, as is well known, is mandated by the TRL calibration [4], [10]. We determined the resistor impedance Z_{load} first using (1). The result, shown in the solid curves of Fig. 1, closely tracks the resistor's anticipated behavior: the real part is approximately 59Ω , and the imaginary part is small, approaching zero approximately linearly at low frequencies. When we instead used (2) to calculate Z_{load} , under the assumption that the measured reflection coefficient is actually $\hat{\Gamma}$, we found an anomalous result (dashed curves of Fig. 1).

Due to the unconventional definition of Youla's waves, they can easily lead to erroneous results. For example, consider the simple flow graph of Fig. 2. When the two devices are joined at a reflectionless connector, we generally assume that, as long as the reference impedances at adjoining ports are identical, we can model the circuit by using the simple boundary conditions

$$b_3 = a_2 \quad (3)$$

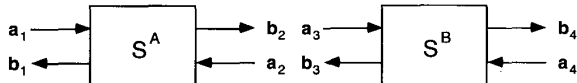


Fig. 2. Signal flow graph of cascaded two-ports.

and

$$a_3 = b_2. \quad (4)$$

In the classical waveguide circuit theory, these conditions arise directly from the continuity of the voltage and current. They are so fundamental as to be intuitive, and they form the basis of signal flow graph analysis and indeed of circuit modeling in general. However, when a and b are Youla's waves, the boundary conditions (3) and (4) do not apply. In other words, Youla's waves are not subject to signal flow graph analysis. A corollary is that Frickey's defined transmission matrices, formed from the scattering parameters using his Table VI, do not function as transmission matrices. In other words, let us denote the transmission matrix of A by T^A , that of B by T^B , and that of the circuit AB by T^{AB} . A functional transmission matrix must satisfy the condition that $T^A T^B = T^{AB}$. However, algebraic manipulation of Frickey's expressions for the transmission matrix in terms of voltage-current parameters confirms that, for his definitions

$$T^A T^B \neq T^{AB}. \quad (5)$$

Equality in (5) holds true only when the reference impedances on adjoining ports are complex conjugates, a restriction with numerous negative implications. This result of the above paper demonstrates that the counterintuitive nature of Youla's waves can easily lead to serious errors.

In the above paper, Frickey compares his results to those of a commercial simulator. From that comparison, it appears that the simulator also defines scattering parameters in terms of Youla's parameters. This suggests caution in the use of scattering parameters based on a complex reference impedance.

An alternative to Youla's theory is the general waveguide circuit theory of [4], which preserves the essential features of the classical theory while allowing for complex characteristic and reference impedances.

REFERENCES

- [1] R. E. Collin, *Foundations for Microwave Engineering*. New York: McGraw-Hill, 1966.
- [2] N. Marcuvitz, *Waveguide Handbook*. New York: McGraw-Hill, 1951.
- [3] D. M. Kerns and R. W. Beatty, *Basic Theory of Waveguide Junctions and Introductory Microwave Network Analysis*. Oxford: Pergamon, 1967.
- [4] R. B. Marks and D. F. Williams, "A general waveguide circuit theory," *J. Res. Natl. Inst. Stand. Technol.*, vol. 97, pp. 533-561, Sept.-Oct. 1992.
- [5] D. C. Youla, "On scattering matrices normalized to complex port numbers," *Proc. IRE*, vol. 49, p. 1221, July 1961.
- [6] K. Kurokawa, "Power waves and the scattering matrix," *IEEE Trans. Microwave Theory Tech.*, vol. MTT-13, pp. 194-202, Mar. 1965.
- [7] R. B. Marks, "A Multiline Method of Network Analyzer Calibration," *IEEE Trans. Microwave Theory Tech.*, vol. 39, pp. 1205-1215, July 1991.
- [8] R. B. Marks and D. F. Williams, "Characteristic impedance determination using propagation constant measurement," *IEEE Microwave and Guided Wave Lett.*, vol. 1, pp. 141-143, June 1991.
- [9] D. F. Williams and R. B. Marks, "Transmission line capacitance measurement," *IEEE Microwave and Guided Wave Lett.*, vol. 1, pp. 243-245, Sept. 1991.
- [10] Specifying Calibration Standards for Use with the HP 8510 Network Analyzer, Hewlett-Packard Product Note 8510-5, Mar. 1986.

Reply to Comments on "Conversions Between S , Z , Y , h , $ABCD$, and T Parameters which are Valid for Complex Source and Load Impedances"

D. A. Frickey

I would like to thank Mr. Marks and Mr. Williams for pointing out the error in using the definition of a_j and b_j in the above paper¹ as I was unaware of the implications involved. Also, I would like to thank the authors for bringing to my attention their work in [1].

REFERENCES

- [1] R. B. Marks and D. F. Williams, "A general waveguide circuit theory," *J. Res. Natl. Inst. Stand. Technol.*, vol. 97, pp. 533-561, Sept.-Oct. 1992.
- Manuscript received October 12, 1994.
The author is at Idaho Falls, ID 83406 USA.
IEEE Log Number 9408573.
- ¹D. A. Frickey, *IEEE Trans. Microwave Theory Tech.*, vol. 42, pp. 205-211, Feb. 1994.

Comments on "An Equivalent Transformation for the Mixed Lumped Lossless Two-port and Distributed Transmission Line"

R. Finkler and R. Unbehauen

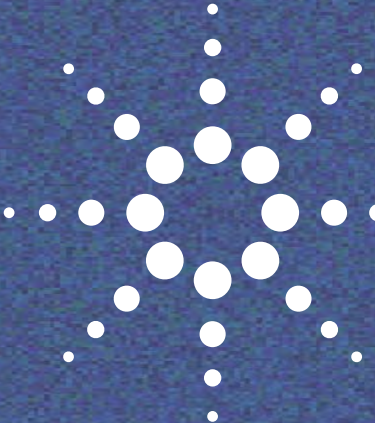
Stimulated by previous articles [1]-[4] by the authors of the above paper,¹ we have done related research. In doing so, we have found additional results and synthesis applications ([5], parts also in [6]) that we would like to communicate here briefly.

In [6] and (more conveniently in [5]) we gave formulas for the transformation of the D section with l'Hospital's rule already incorporated, so that no indefinite expressions such as 0/0 (cf. p. 277, text between (80) and (81)) occur. According formulas for the other sections are also given in [5], [6]. These formulas seem to be more suited for the use in the synthesis applications described below.

The equivalent transformation treated in the Theorem in Section V of the above paper, which we in accordance to the idiomatic usage in [1], [2] and due to [7] called extended Levy transformation, can also be performed numerically. This can be done by solving a system of ordinary differential equations, where the line length l is the independent variable and the coefficients of the numerators of the lumped lossless two-port chain matrix elements are the functions to be determined. Reference [5] contains some additional theorems on the asymptotic behavior of this transformation for $l \rightarrow \infty$.

Manuscript received August 22, 1994.
The authors are with the Lehrstuhl für Allgemeine und Theoretische Elektrotechnik, Universität Erlangen-Nürnberg, D 91058 Erlangen, Germany.
IEEE Log Number 9408574.

¹I. Endo, Y. Nemoto, and R. Sato, *IEEE Trans. Microwave Theory Tech.*, vol. 42, pp. 272-282, Feb. 1994.

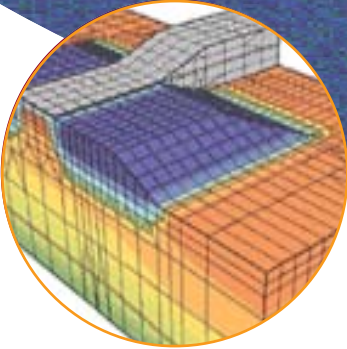


Solutions for

Securing Successful First-Pass Component Design

Understanding X-Parameter Nonlinear Measurements

Application Note



Overview

At one time, linear systems and components were designed using a patchwork of instrumentation and measurements. This approach was quickly replaced by scattering parameters (S-parameters), which unified the multiple instruments and measurements and enabled just one instrument, the network analyzer, to make measurements like gain, isolation and match with a single connection. For more than 40 years, S-parameters have stood as one of the most important of all the foundations of microwave theory and techniques. They are related to familiar measurements such as S_{11} input match, S_{22} output match, S_{21} gain/loss, and S_{12} isolation, and can be easily imported into electronic simulation tools. Today, S-parameters are commonly used to analyze and model the linear behavior of RF and microwave components. Unfortunately, current industry trends toward increasing energy efficiency, higher output power and longer battery life are forcing many linear devices to operate in a nonlinear fashion. Measuring this behavior requires a solution that is much more deterministic in nature.

Problem

While extremely useful and powerful, S-parameters are only defined for small-signal linear systems. With the communications revolution forcing active components like power amplifiers (PAs) into more and more strongly nonlinear regimes of operation, engineers are now forced to use a new set of patchwork solutions for measuring a component's nonlinear attributes. Essentially, they make linear assumptions by taking S-parameters and applying nonlinear figures of merit (e.g., ACPR and gain compression). Relying on this incomplete set of information means that the engineer has to perform extensive and costly empirical-based iteration of their designs, adding substantial time and cost to the design process. To quickly, accurately and more deterministically design nonlinear components at high frequencies, today's engineers require the ability to properly measure nonlinear behavior, as well as a unifying model (similar to an S-parameter, but for nonlinear components) that can take this behavioral information into simulation and design.



Agilent Technologies

Solution

By doing for nonlinear components and systems what S-parameters do for their linear counterparts, X-parameters* offer engineers an answer to this dilemma. X-parameters represent a new category of nonlinear network parameters for deterministic, high-frequency design and are used for characterizing the amplitudes and relative phase of the nonlinear behavior of components. Unlike S-parameters, they are applicable to both large-signal and small-signal conditions, and can be used for linear and nonlinear components. They correctly characterize impedance mismatches and frequency mixing behavior to allow accurate simulation of cascaded nonlinear X-parameter blocks (e.g., amplifiers and mixers), in design.

In contrast to S-parameters, X-parameters represent and analyze the nonlinear behavior of RF/MW components in a much more robust and complete manner. As the logical, mathematical extension of S-parameters under large-signal operating conditions, they are driven into saturation (the real-word operating environment for many components) and then measured under these conditions. When making this measurement, no knowledge is used or required concerning the internal circuitry of the device under test (DUT). Rather, the measurement is a stimulus response model of the voltage waves (Figure 1). In other words, the absolute amplitude and cross frequency relative phase of the fundamental, and the generated distortion products, are accurately measured and represented by X-parameters. Corresponding X-parameter-based behavioral models are created from this information and can be used with calibrated measurement tools to derive different figures of merit (e.g., ACPR, compression and EVM) (Figure 2). These fast, accurate models can take into account a range of different variables including source and load impedance, among other things.

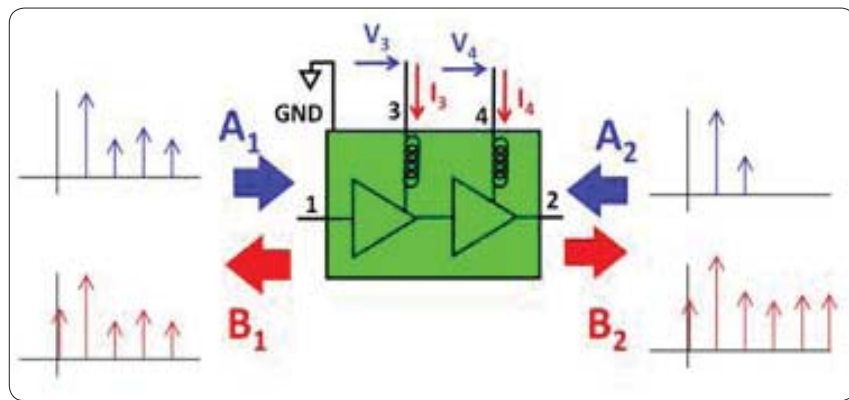


FIGURE 1: The X-parameter model for the multi-stage amplifier in this example is formulated in the frequency domain and maps incident waves (A) to scattered waves (B). Because the complete knowledge of magnitude and phase of incident and scattered waves at all harmonics is exactly equivalent to complete knowledge of the time-domain waveform, the full nonlinear input-output characteristics of the device are captured.

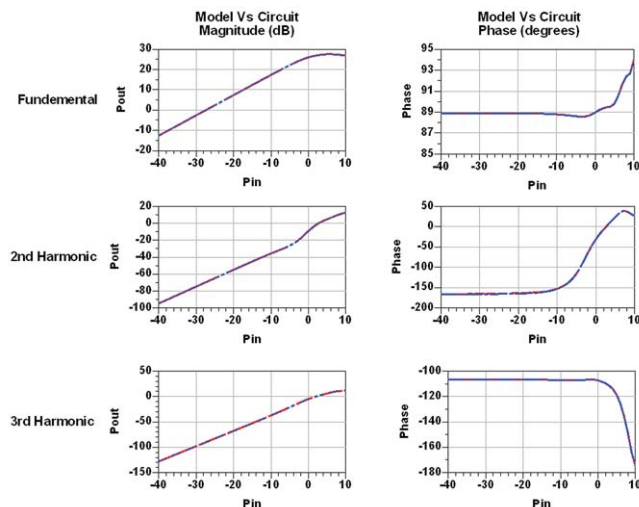


FIGURE 2: The X-parameters are shown here overlaid on actual circuit-level PA results. As is evident, the X-parameters accurately correlate with the actual circuit.

Generating X-Parameters

X-parameters can be obtained in one of two ways: generated from a circuit-level design in Agilent Technologies' Advanced Design System (ADS) software or measured using the Nonlinear Vector Network Analyzer (NVNA) software running inside the Agilent Technologies' PNA-X network analyzer (Figure 3).

To generate the X-parameters from a circuit-level schematic, first create the schematic in ADS. Once the schematic is complete, information regarding frequency, bias, temperature, and other important parameters is entered into the X-Parameter Generator. This tool takes the circuit-level design and computes the X-parameters for a component or module that can be used

in an ADS, harmonic balance or circuit envelope simulation. The X-Parameter Generator is very flexible and can generate X-parameter models of nonlinear, multi-port components with multi-tone stimulus, as well as simulation under load-pull conditions.

Obtaining quick and accurate X-parameters through measurement requires the use of Agilent's NVNA. It measures the X-parameters of the DUT, which can then be imported into the ADS simulator or displayed like S-parameters. To measure the X-parameters the NVNA uses its two internal RF sources to drive the DUT with a large signal tone to set the large signal operating point of the device and at the same time applies a small signal tone at the appropriate frequencies and phases.

Careful control of the phase and amplitude of these signals is therefore critical (Figure 4). Measuring the amplitudes and phases of the scattered waves under these conditions allows for the identification of X-parameters. These parameters provide the engineer with information on such things as device gain and match, while the device is operating in either a linear or nonlinear state.

The accurate and robust nature of X-parameters makes them extremely useful for engineers trying to better understand the nonlinear behavior of their active components. Whether created or measured, these X-parameters can be easily imported into ADS and then dropped into a component or system to start the design process or for use with simulation.

Other key features and benefits of X-parameters include:

- Extensible beyond $50\ \Omega$. While network analyzers are inherently $50\ \Omega$ devices, the extensibility of X-parameters enables components to be measured beyond this point (e.g., a PA at $3\ \Omega$). This can be done by either placing a matching circuit between the network analyzer and the DUT, or by employing a load pull tuner. In addition, since the X-Parameter Generator in ADS has no limits on the number of ports, power or frequency it can handle, it is able to deal with complicated designs involving multiple ports (e.g., 3-port devices), tones and biases (e.g., mixers), as well as arbitrary topology. In the future, such capabilities will also be available in the NVNA to make the physical measurements of X-parameters.
- High power. X-parameters are currently targeted at active devices, like PA's, that commonly exhibit strong nonlinear behavior. The NVNA can make high power X-parameter measurements (e.g., GAN and 10, 100 and 250 watt devices), even if the base network analyzer configuration can only handle 1 watt. The flexibility of Agilent's PNA-X hardware has enabled measurements to be made to 100, and even 250 watts.

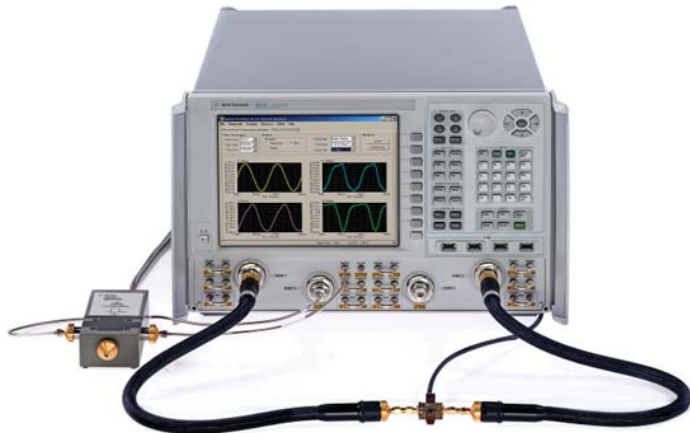


FIGURE 3: Agilent's NVNA software, for use with the PNA-X network analyzer, establishes a new industry standard in RF/MW nonlinear network analysis from 10 MHz to 50 GHz. It allows the engineer to deterministically measure X-parameters.



FIGURE 4: The NVNA requires a simple procedure using a power meter, phase reference and vector calibration standard to analytically remove the systematic errors from the measurements.

Summary of Results

With active components continuing to be driven into nonlinear operation, the need for fast and accurate measurement of that nonlinear behavior becomes all the more urgent. As a logical extension of S-parameters to include nonlinear effects, accurate and robust X-parameters represent the ideal solution to this dilemma. Whether created from measurement or ADS simulation, they offer speed and convenience analogous to the well-known linear S-parameters. Resulting X-parameter-based behavioral models can be quickly and easily dropped into simulation and used to deterministically design the most robust components and systems in the shortest amount of time and with the highest degree of accuracy.



The Power of X

The Agilent X-Parameters and PNA-X Microwave Network Analyzer with the NVNA software are key products in Agilent's comprehensive Power of X suite of products. These products grant engineers the power to gain greater design insight, speed manufacturing processes, solve tough measurement problems, and get to market ahead of the competition.

Offering the best combination of speed and scalability, and created and supported by renowned worldwide measurement experts, Agilent's X products are helping engineers bring innovative, higher performing products to emerging markets around the globe.

To learn more about Agilent's suite of X products please visit:
www.agilent.com/find/powerofx.

Related Applications

- Semiconductor process design
- Semiconductor IC design and validation of active components
- Base station PA design and validation
- Military active component design and validation

Related Agilent Products

- W2305 X-Parameter Generator
- W2200 ADS Core
- Nonlinear Vector Network Analyzer

Remove all doubt

For more information on repair and calibration services, go to:

www.agilent.com/find/removealldoubt

www.agilent.com
www.agilent.com/find/powerofx

For more information on Agilent Technologies' products, applications or services, please contact your local Agilent office. The complete list is available at:

www.agilent.com/find/contactus

Americas

Canada	(877) 894-4414
Latin America	305 269 7500
United States	(800) 829-4444

Asia Pacific

Australia	1 800 629 485
China	800 810 0189
Hong Kong	800 938 693
India	1 800 112 929
Japan	0120 (421) 345
Korea	080 769 0800
Malaysia	1 800 888 848
Singapore	1 800 375 8100
Taiwan	0800 047 866
Thailand	1 800 226 008

Europe & Middle East

Austria	43 (0) 1 360 277 1571
Belgium	32 (0) 2 404 93 40
Denmark	45 70 13 15 15
Finland	358 (0) 10 855 2100
France	0825 010 700*
	*0.125 €/minute
Germany	49 (0) 7031 464 6333
Ireland	1890 924 204
Israel	972-3-9288-504/544
Italy	39 02 92 60 8484
Netherlands	31 (0) 20 547 2111
Spain	34 (91) 631 3300
Sweden	0200-88 22 55
Switzerland	0800 80 53 53
United Kingdom	44 (0) 118 9276201
Other European Countries:	www.agilent.com/find/contactus

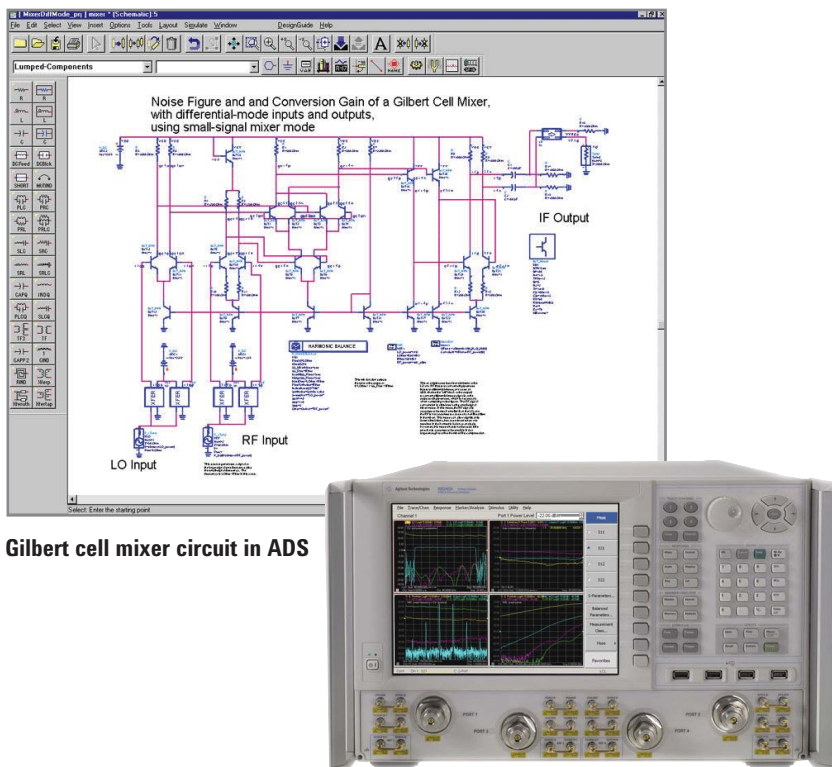
Revised: October 1, 2009

Product specifications and descriptions in this document subject to change without notice.

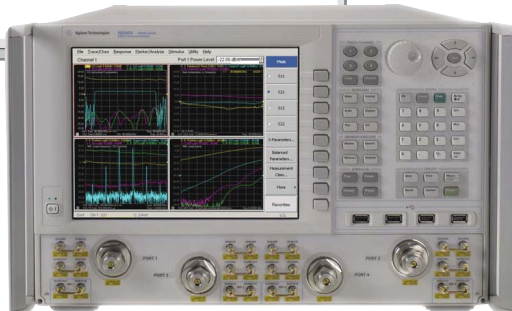
© Agilent Technologies, Inc. 2010

Printed in USA, January 6, 2010

5990-5151EN



Gilbert cell mixer circuit in ADS



PNA-X network analyzer



Agilent Technologies

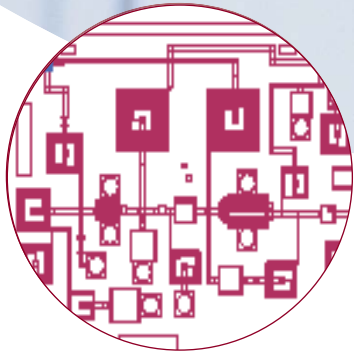


Solutions for

Sharing Accurate, IP-Protected Nonlinear RF Behavioral Models

Generating X-parameters from Circuit-level Designs

Application Note



Overview

X-parameters^{*} represent a new category of nonlinear network parameters for high-frequency design and are used for characterizing the amplitudes and relative phase of harmonics generated by the nonlinear behavior of components. Developed and introduced by Agilent Technologies, X-parameters are applicable to both large-signal and small-signal conditions, and for linear and nonlinear components. They correctly characterize impedance mismatches and frequency mixing behavior to allow accurate simulation of cascaded nonlinear X-parameter blocks (e.g., amplifiers and mixers), in wireless design. X-parameters play a key role in the development of active devices like the power amplifier (PA) and mixers—critical components in today's wireless designs.

Problem

Designing and testing wireless communications systems like the wireless handset at the system level can be challenging. Using circuit-level designs and models in hierarchical RF-system simulation and trade-off analysis, for example, is slow and cumbersome. Further complicating matters, behavioral models do not accurately represent a circuit's nonlinear behavior in phase and magnitude at all harmonics. The challenge is no less complex for the component/device designer supplying their Intellectual Property (IP) to the system designer/integrator. Traditionally, the designer would have to wait until a physical hardware prototype of their circuit-level design was available before sending it to the system designer/integrator for evaluation within their system. It may take several months for the chip to be manufactured and several more to properly characterize it across different operating parameters. Finding a way to share the performance of their circuit-level design with the system designer/integrator, instead of waiting for a physical prototype, represents a significant competitive advantage not only for the designer vying for an early design win, but also for the system designer/integrator hoping to deliver their product to market ahead of the competition.



Agilent Technologies

Solution

A fast, accurate behavioral model based on X-parameters generated from a circuit-level design, offers an ideal way for the designer to share the performance of their circuit-level design with the system design/integrator, prior to the availability of a physical prototype. Using these models, the system designer/integrator can evaluate overall system performance and conduct trade-off analysis—earlier in the design cycle and much faster than if they were working with circuit-level designs. Because the X-parameter-based models are accurate and characterized over the same set of parameters that would be used to characterize the actual physical device, system designers/integrators also have a higher degree of confidence that the chip will work within the system the first time. Some of the key benefits of this approach include:

- **Simulation speed up and accuracy.**

X-parameter models enable faster hierarchical design analysis, and system simulation and verification than circuit-level models. They also provide unprecedented accuracy of nonlinear behavior in phase and magnitude at all harmonics. Fully functional behavioral models with the ability to accurately simulate measurements like IMD (IP3/TOI), PAE, spurs, and higher-order harmonics can be cascaded, load-pulled and account for mismatches.

- **Sharing IP-protected designs.**

X-parameter models provide a convenient way for design houses to protect their IP. The models essentially encapsulate the composite design, modeling it in an X-parameter representation that offers more protection of the design information than encrypting. The ability to share IP in real time speeds ongoing communication between design houses and system designers/integrators, enabling design houses to secure design wins before physical parts are available. It also significantly reduces chip, package and system design iterations. Minimizing hardware respins saves cost and speeds time-to-market for products with increased accuracy and therefore better specifications.

Generating X-parameters

Until recently, the ability to create fast, accurate behavioral models based on X-parameters generated from a circuit-level design did not exist. X-parameters could only be obtained through Agilent's Nonlinear Vector Network Analyzer (NVNA) software running inside its PNA-X microwave network analyzer. Now though, X-parameters can also be generated from a circuit-level design in Agilent's Advanced Design System (ADS) software—an Electronic Design Automation (EDA) platform specifically engineered to generate X-parameter models of multi-port, nonlinear components or devices under load-pull conditions (Figure 1).

X-parameters are generated using the ADS X-Parameter Generator, which takes an ADS circuit-level design and creates X-parameters that can be used in an ADS linear, harmonic balance or circuit envelope simulation. The resulting X-parameter-based, nonlinear behavioral models are fast, drop-in useable and accurate.

The process for generating X-parameters is simple and straightforward. It begins with the creation of a circuit-level schematic in ADS. Once the schematic is complete, information regarding frequency, bias, temperature, and other important parameters is entered into the X-Parameter Generator. In turn, it creates X-parameters. ADS simulation of the X-parameters then extracts the corresponding X-parameter-based behavioral model.

A key benefit of using the X-Parameter Generator in ADS is that with no limits on the number of ports, power or frequency it can handle, it is able to deal with complicated designs involving multiple ports and biases (e.g., mixers), as well as arbitrary topology.

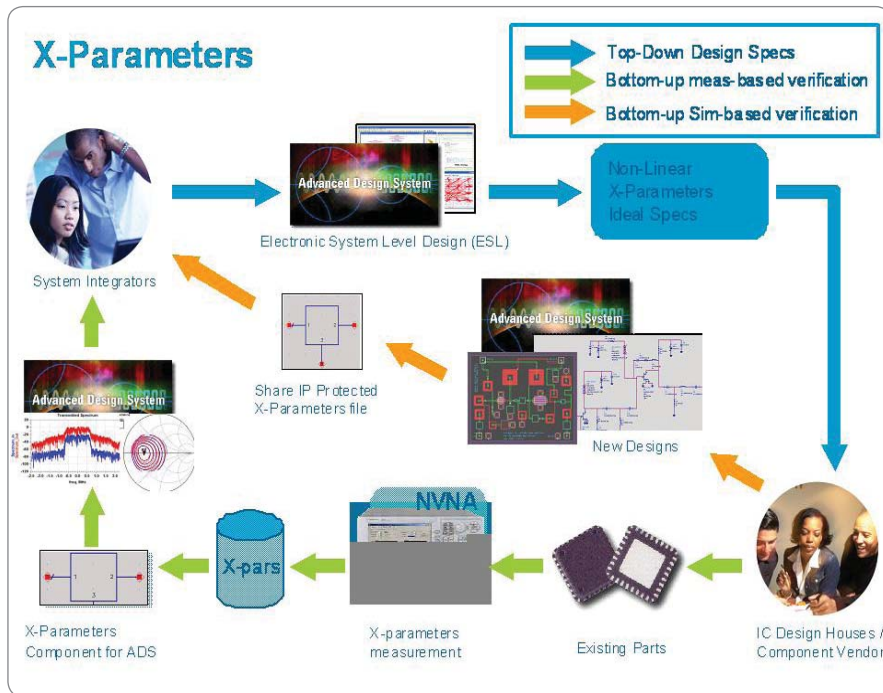


FIGURE 1: X-parameters can now be created from measurement or ADS simulation with the same speed and convenience as the well-known linear S-parameters. When generated from ADS circuit-level models, the resulting nonlinear behavioral models can be confidently used to speed system-level design.

Active Device Example

Using the ADS X-Parameter Generator, it is a straightforward process to create X-parameter models that can be analyzed and quickly distributed as secure IP to system designers/integrators. Consider the example of an LTE PA design as shown in Figure 2. To extract the X-parameters model for the device from simulation, the designer must first set up the ADS X-Parameter Generator (Figure 3). X-parameters are then created, producing an X-parameter-based model that can be distributed as IP (Figure 4). In one real-life scenario, this process allowed a designer to go from software download to a distributable X-parameter model in less than 10 minutes. The simulation of the amplifier with a complex LTE signal took just a few seconds. Without ADS and the X-Parameter Generator, the design would not have had IP protection and, at the system level, would have taken much longer to simulate—making it very difficult for the system engineer to conduct multi-simulation trade-off analysis.

Summary of Results

X-parameters represent a very useful and competitive technology for both design houses and system designers/integrators alike. This technology is now all the more powerful given the ability to generate X-parameters from circuit-level designs using Agilent's X-Parameter Generator in ADS. This critical capability enables design houses to secure early design wins and system designers/integrators to deliver products to market ahead of the competition.



The Power of X

The Agilent X-Parameters and PNA-X Microwave Network Analyzer are key

products in Agilent's comprehensive Power of X suite of products. These products grant engineers the power to gain greater design insight, speed manufacturing processes, solve tough measurement problems, and get to market ahead of the competition.

Offering the best combination of speed and scalability, and created and supported by renowned worldwide measurement experts, Agilent's X products are helping engineers bring innovative, higher-performing products to emerging markets around the globe. To learn more about Agilent's suite of X products please visit:

www.agilent.com/find/powerofx.

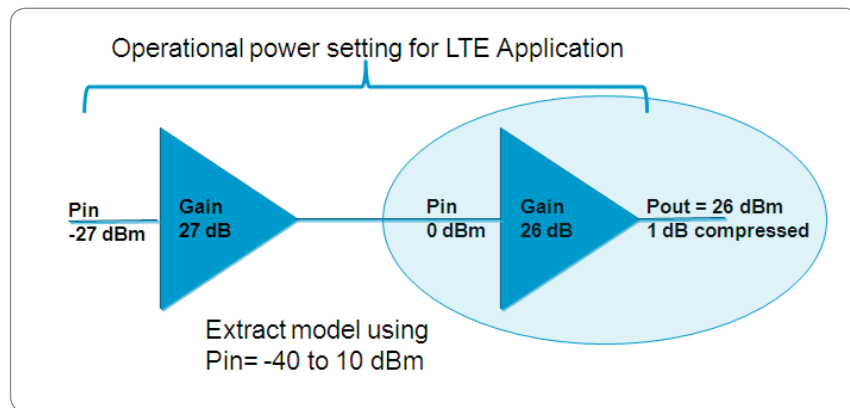


FIGURE 2: Agilent's ADS and X-Parameter Generator can be used to extract an X-parameters model for the second stage of two cascaded MMIC PAs.

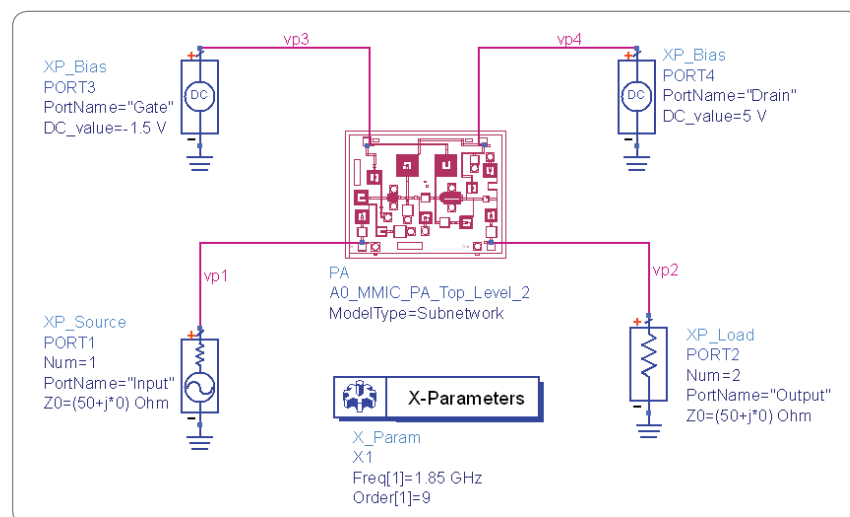


FIGURE 3: Prior to simulating the parameters, the engineer must set up the different parameters, such as bias, frequency and temperature.

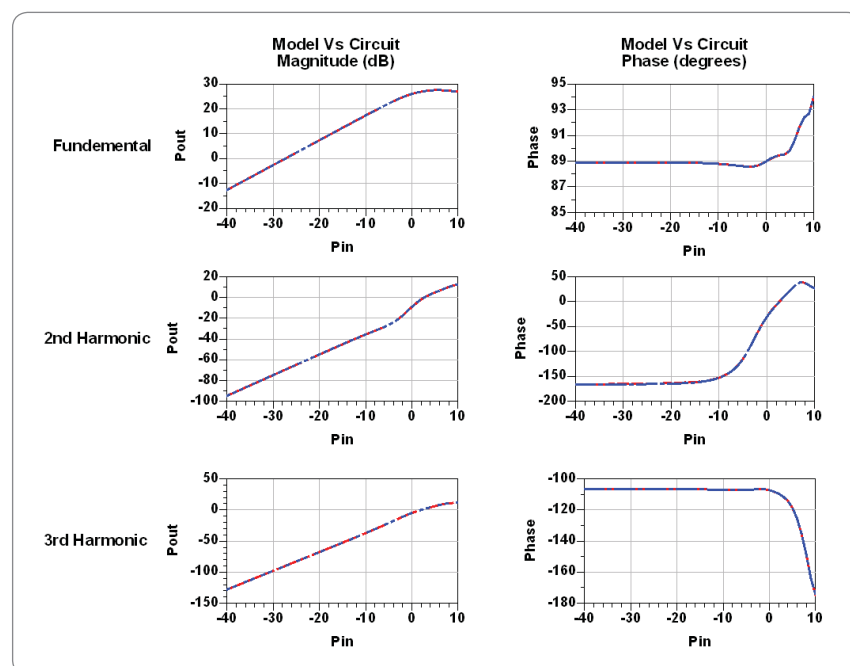


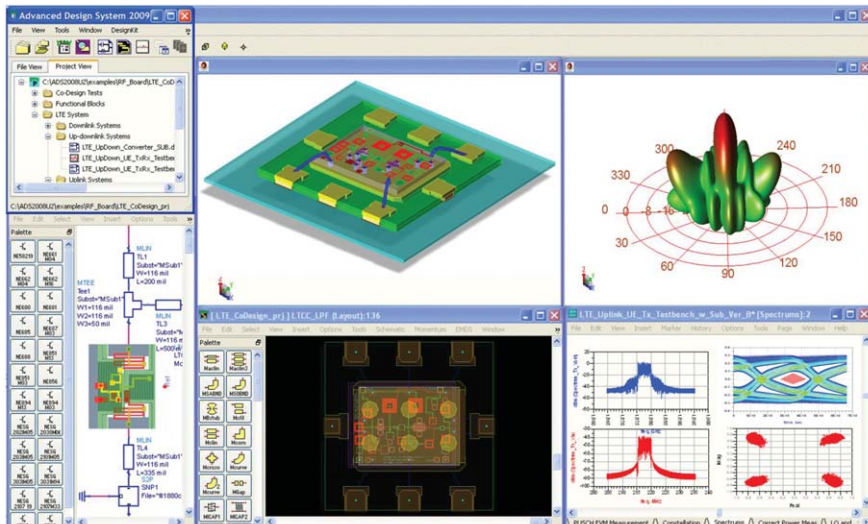
FIGURE 4: The X-parameter-based model is shown here overlaid on actual circuit-level PA results.

Related Applications

- Aerospace/defense
- Consumer wireless
- Generate X-parameters for handset/basestation PAs
- Generate X-parameters for amplifiers, mixers or any nonlinear device

Related Agilent Products

- W2305 X-Parameter Generator
- W2200 ADS Core
- Nonlinear Vector Network Analyzer



W2200 ADS Core

Remove all doubt

For more information on repair and calibration services, go to:

www.agilent.com/find/removealldoubt



Agilent Email Updates

www.agilent.com/find/emailupdates

Get the latest information on the products and applications you select.



Agilent Direct

www.agilent.com/find/agilentdirect

Quickly choose and use your test equipment solutions with confidence.

www.agilent.com

www.agilent.com/find/powerofx

For more information on Agilent Technologies' products, applications or services, please contact your local Agilent office. The complete list is available at:

www.agilent.com/find/contactus

Americas

Canada	(877) 894-4414
Latin America	305 269 7500
United States	(800) 829-4444

Asia Pacific

Australia	1 800 629 485
China	800 810 0189
Hong Kong	800 938 693
India	1 800 112 929
Japan	0120 (421) 345
Korea	080 769 0800
Malaysia	1 800 888 848
Singapore	1 800 375 8100
Taiwan	0800 047 866
Thailand	1 800 226 008

Europe & Middle East

Austria	01 36027 71571
Belgium	32 (0) 2 404 93 40
Denmark	45 70 13 15 15
Finland	358 (0) 10 855 2100
France	0825 010 700*
	*0.125 €/minute
Germany	07031 464 6333
Ireland	1890 924 204
Israel	972-3-9288-504/544
Italy	39 02 92 60 8484
Netherlands	31 (0) 20 547 2111
Spain	34 (91) 631 3300
Sweden	0200-88 22 55
Switzerland	0800 80 53 53
United Kingdom	44 (0) 118 9276201
Other European Countries:	www.agilent.com/find/contactus

Revised: July 2, 2009

Product specifications and descriptions in this document subject to change without notice.

© Agilent Technologies, Inc. 2009

Printed in USA, September 4, 2009

5990-4628EN

*X-parameters is a trademark of Agilent Technologies



Agilent Technologies

**Class Notes, 31415 RF-Communication Circuits
Autumn 2005**

Chapter IV

NOISE and DISTORTION

Jens Vidkjær

NB 232 rev.Sep.2005

Contents

IV Noise and Distortion	1
IV-1 Sources and Basic Properties of Electrical Noise	2
Thermal Noise	2
Example IV-1-1 (noise in a RC circuit, noise bandwidth) ..	4
Shot Noise	6
Flicker or 1/f Noise	8
Other Noise Sources in Electronics	10
Characterizing and Combining Noise Sources	11
Man-Made Noise	13
IV-2 Noise in Semiconductor Devices	15
Noise in Diodes	15
Noise in Bipolar Transistors	17
Example IV-2-1 (minimum noise in bipolar transistors) ..	18
Noise in Field Effect Transistors	22
IV-3 Noise Characterization of Two-Ports	25
Noise Figure	25
Example IV-3-1 (noise figure measurement)	28
Noise Temperature of Two-Ports	29
Noise in Cascaded Two-Ports	30
Example IV-3-2 (link budget)	31
Noise Representation in Two-Ports	33
Minimum Noise Conditions	36
Constant Noise Figure Circles	37
Example IV-3-3 (noise figure circles in Y-plane)	39
Example IV-3-4 (noise figure circles in Smith chart)	42
IV-4 Distortion in Almost Linear Circuits	47
Single Signal Distortions	48
Distortions with Two Signals	52
Intercept Points	56
Sensitivity and Dynamic Range	59
Problems	62
References and Further Reading	66
Index	69

IV Noise and Distortion

Linear amplification for a wide range of signal levels is crucial in many RF applications. Electronic circuits may be designed to show linearity over large operating ranges, but eventually the condition ceases at both high and low drive levels as demonstrated by the typical amplifier characteristic in Fig.1.

When at low levels the output flattens to constancy regardless of input, we have reached the so-called noise floor. Its major causes are thermal motions and quantized current flows in the circuit components, which add a random fluctuation to the deterministic output signals. When noise and signal become equal in size, we are close to the borderline below which the output is useless. It is a common design challenge to push the noise floor to an acceptable minimum in a given application, and it is one of the major objectives of the present section to provide the background and present techniques for doing so.

In the opposite range of input drives the amplifier performance degenerates due to nonlinearities in the circuit, commonly introduced by the large signal operation of transistors or other electron devices. At the ultimate edge the output may saturate to constancy but in most applications the limit for acceptable performance is reached long before that. There are many occasions where we highly benefit from nonlinear operation of electronic circuits but presently we focus on failures that arise when linearity is expected. Transmission of a signal through a nonlinear device is accompanied by formation of deterministic distortion components at frequencies which differ from the input signal frequencies. Filtering may remove some of these new components, known as spurious responses, but others are so close to the original ones that they seriously influence the signal processing that succeeds amplification, detection for instance. We shall consider various forms of nonlinear distortions and their characterization in the last section of this chapter.

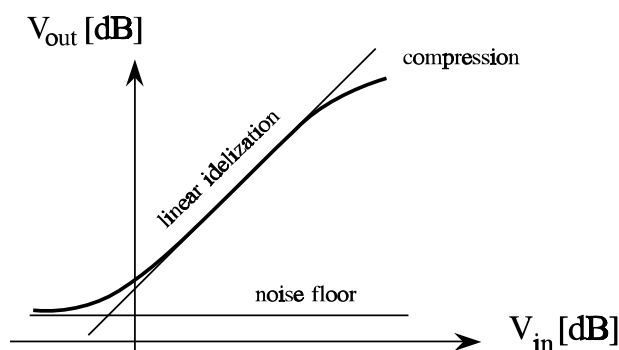


Fig.1 Typical input-output characteristic of an amplifier designed for linear applications.

IV-1 Sources and Basic Properties of Electrical Noise

A voltage or current carrying a signal includes in practice both the desired deterministic signal and disturbing components, which again may be either deterministic or random. The latter encompasses terms that are completely unavoidable on basis of fundamental physical principles, and they are always referred to as noise. Solving practical problem, moreover, other non-ideal contributions may be included under the noise term, particularly if the statistical means and properties that apply to physical noise remain usable. The basic origins and properties of electrical noise are presented in this first section with the aim of providing a foundation for our subsequent discussion of noise in electronic devices and circuits.

Thermal Noise

Thermal motion of the electrons in a resistor causes a fluctuating noise voltage across the terminals. The voltage has Gaussian distribution around a mean value of zero. If the resistor is in thermal equilibrium with its surroundings at temperature T [K], the two-sided spectral density of the mean squared noise voltage is given by,

$$S_v(\omega) = 2R \frac{h\omega/2\pi}{e^{h\omega/2\pi kT} - 1} \approx 2kTR \quad - \text{ where}$$

Planck's constant: $h = 6.6260755 \cdot 10^{-34}$ [Js], (1)

Boltzman's constant: $k = 1.380658 \cdot 10^{-23}$ [J/K].

The first frequency dependent expression is included to indicate that there is a natural upper frequency roll-off in spectral density, even though it suffices for most practical purposes to use the last - frequency independent - approximation. Around room temperature 300 K we have $kT/h=6.44$ THz, so here it is the bandwidth of circuit embodying the resistor that impose restrictions on the resultant noise. In a frequency band of Δf Hz around any frequency $\omega_0=2\pi f_0$ fairly below the kT/h bound, thermal noise provides a fluctuation voltage v_n that still has zero mean value and a variance, i.e. mean squared value, given by¹

$$\overline{v_n^2} = 2 \times \frac{1}{2\pi} \int_{\omega_0-\pi\Delta f}^{\omega_0+\pi\Delta f} S_v(\omega) d\omega = 2 S_v(\omega_0) \Delta f = 4kTR\Delta f \quad [V^2]. \quad (2)$$

1) The overline notation has a long tradition in noise literature for both time averaging like $\langle v_n^2 \rangle$ in common notation or statistical averaging - expectation - like $E[v_n^2]$. Most noise processes we consider are ergodic with equal time and ensemble averages and the overline notation is maintained below unless it leads to ambiguity.

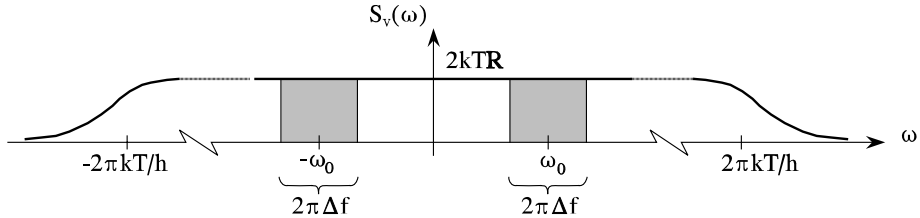


Fig.2 Double-sided power spectral density of thermal noise from a resistor. The mean squared voltage from frequency interval Δf is the hatched area divided by 2π .

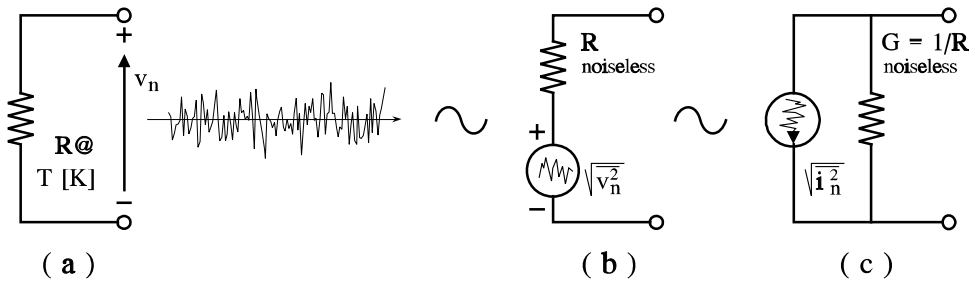


Fig.3 Circuit schematic representations of thermal noise from a resistor. The square roots are often omitted for clarity although the noise generators still represent RMS (root mean square) voltages or currents.

Incorporating thermal noise from a resistor in a circuit diagram is often done as shown by Fig.3(b). The noise is accounted for separately by the RMS voltage generator and the resistor R is assumed noiseless. Translated to the Norton equivalent form in Fig.3(c), the corresponding short-circuit noise current is given by

$$\frac{\overline{i_n^2}}{R^2} = \frac{\overline{v_n^2}}{R^2} = 4kTG\Delta f \quad [A^2], \quad (3)$$

where conductance G equals $1/R$. It is superfluous in most cases to orient the noise voltage or current generators as it is done in the figures. On the other hand this makes no harm, so the orientations are maintained since we later shall consider situations that requires signs. Regarding equivalent circuits that incorporates noise sources of the types above, there is a tacit assumption that if we are going to measure a noise voltage, ideal filtering must precede the instrument. Fig.4 shows the simplest case, where a resistor is the only circuit component.

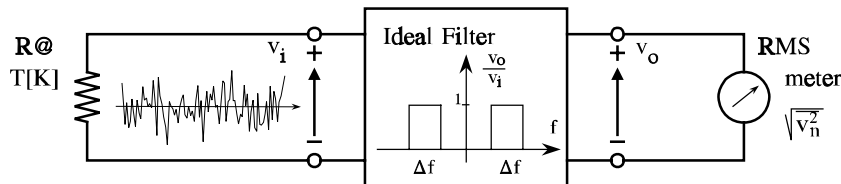


Fig.4 Hypothetical setup for noise voltage measurement corresponding to Fig.3. Substituting with practical filters Δf represents the so-called noise bandwidth.

The available noise power N_{av} from the equivalent circuits in Fig.3(b) and (c) is independent of the resistance value and given by,

$$N_{av} = \frac{\overline{v_n^2}}{4R} = kT\Delta f \quad [W]. \quad (4)$$

Thermal noise is sometimes called Johnson noise after its discoverer. The physical and mathematical descriptions were provided by Nyquist, who also proved that any electrical system in thermal equilibrium has an open circuit thermal noise voltage corresponding to the real part of the impedance, equivalently a short-circuit current corresponding to the real part of the admittance. Both cases agree with the available power expression from Eq.(4).

$$Z(\omega_0) = R(\omega_0) + jX(\omega_0) : \quad \overline{v_{nZ}^2} = 4kTR(\omega_0)\Delta f \quad \Rightarrow \quad N_{av} = \frac{\overline{v_{nZ}^2}}{4Re\{Z(\omega_0)\}} = kT\Delta f, \quad (5)$$

$$Y(\omega_0) = G(\omega_0) + jB(\omega_0) : \quad \overline{i_{nY}^2} = 4kTG(\omega_0)\Delta f \quad \Rightarrow \quad N_{av} = \frac{\overline{i_{nY}^2}}{4Re\{Y(\omega_0)\}} = kT\Delta f. \quad (6)$$

It is assumed here that the frequency interval Δf is small enough to assume constancy of the impedance or admittance across the interval, alternatively that Δf represents the so-called noise bandwidth, which is exemplified below. Cases that can be described by the method above include noise from magnetization losses in inductors and transformers, noise due to dielectrical losses in transmission lines, noise from the radiation and reception resistance in antennas, microphones or other transducers. For a more genuine discussion of these and many other basic topics, the reader should consult ref's [1] and [2], which are collections of fundamental papers on noise in electrical circuits.

Example IV-1-1 (noise in a RC circuit, noise bandwidth)

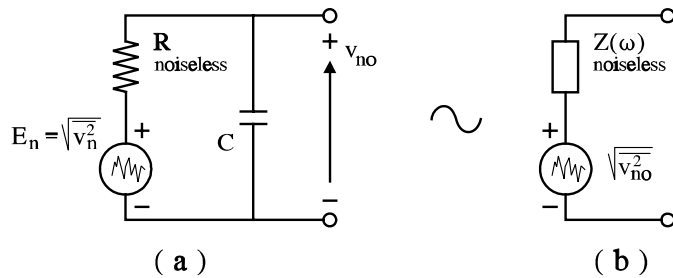


Fig.5 Calculation of RC circuit noise from (a), transfer function $H(j\omega)=v_{no}/E_n$, and (b) directly from Eq.(5).

Consistency of the above results is demonstrated below by considering the RC network in Fig.5(a). It has the output impedance

$$Z_o(\omega) = R(\omega) + jX(\omega) = \frac{R/j\omega C}{R + 1/j\omega C} = \frac{R}{1 + \omega^2\tau^2} - \frac{jR\omega\tau}{1 + \omega^2\tau^2}, \quad \text{where } \tau = RC. \quad (7)$$

The mean-squared output noise voltage per unit bandwidth follows directly from Eq.(5),

$$\overline{\frac{v_{no}^2}{\Delta f}} \Big|_{\omega_0} = 2S_{vo}(\omega_0) = \frac{4kTR}{1 + \omega_0^2\tau^2} \quad (8)$$

A leading factor of two is required in the equation above to let $S_{vo}(\omega)$ be a double-sided spectrum. We shall see that the same result follows from the resistor noise representation in Fig.5(a) where $H(j\omega)$ is the transfer function from voltages E_n to voltage v_{no} . This is a usual voltage division, which in absolutely squared form provides

$$H(j\omega) = \frac{v_{no}}{E_n} = \frac{1/j\omega C}{R + 1/j\omega C} = \frac{1}{1 + j\omega\tau} \Rightarrow |H(j\omega)|^2 = \frac{1}{1 + \omega^2\tau^2} \quad (9)$$

$$\overline{\frac{v_{no}^2}{\Delta f}} \Big|_{\omega_0} = 2S_{no}(\omega_0) = 2|H(j\omega_0)|^2 S_n(\omega_0) = \frac{4kTR}{1 + \omega_0^2\tau^2}$$

i.e. the same result as the one obtained by Eq.(8). Including all frequencies, it is furthermore seen, that the total mean-squared voltage from a RC circuit is independent of the resistance value,

$$\overline{v_{no,tot}^2} = \frac{1}{2\pi} \int_0^\infty 2S_{no}(\omega) d\omega \stackrel{u = \omega\tau}{=} \frac{4kTR}{2\pi\tau} \int_0^\infty \frac{du}{1+u^2} = \frac{kT}{C}, \quad (10)$$

since the last definite integral is $\pi/2$. The noise output voltage is also the voltage across the capacitor, which therefore holds a thermal noise mean energy of size

$$\overline{E_C} = \frac{1}{2} C \overline{v_{no,tot}^2} = \frac{1}{2} kT. \quad (11)$$

This result shows agreement with classic statistical thermodynamics. A system in thermal equilibrium with its surroundings at an absolute temperature T has an energy of $1/2kT$ per degree of freedom, i.e. number of state variables required to describe the system. The RC circuit needs only one - the capacitor voltage.

The so-called noise bandwidth is illustrated by Fig.6 for the RC circuit. It is the bandwidth that provides the same available noise power from a uniform distribution at peak level as the power actually available from the entire, frequency dependent distribution. The noise-bandwidth W_N spans the interval from $-W_N$ to W_N , so the hatched rectangle has an area equal to the area beneath the actual spectral density curve. Using the result from Eq.(10), the noise-bandwidth in radians per second becomes

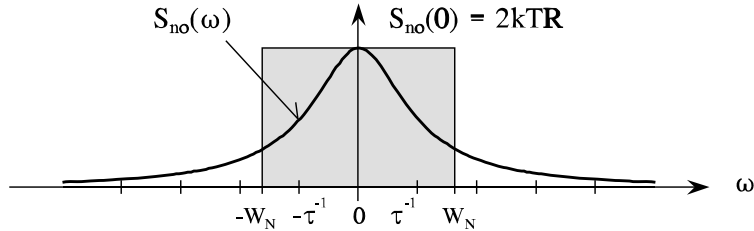


Fig.6 Noise bandwidth W_N in a RC-circuit. The hatched area corresponds to the total area beneath the spectral density curve, $S_{no}(\omega)$.

$$2 W_N S_{no}(0) = 2 \int_0^{\infty} S_{no}(\omega) d\omega \quad \Rightarrow \quad W_N = \frac{2 \pi k T / C}{4 k T R} = \frac{\pi}{2} \frac{1}{\tau} . \quad (12)$$

In an RC circuit the noise bandwidth is seen to be $1/2\pi = 1.56$ times greater than the usual 3dB (half power) bandwidth, which is the inverse of the time constant $\tau = RC$.

Example IV-1-1 end

Shot Noise

If the current through a device is the net effect of many single events that occur randomly, but with a mean rate \bar{N}_I events per second, the double-sided power spectrum of current fluctuations around the mean current is given by Carson's theorem, [4] sec.2.2.c,²

$$S_I(\omega) = \bar{N}_I E [|p_I(\omega)|^2] , \quad (13)$$

Here, $p_I(\omega)$ represents Fourier transforms of pulse shapes that contributes to the current. Taking expectation of the absolutely squared transform conducts averaging over the ensemble in cases that includes different pulse shapes. As a simple illustration we consider one electron, which is injected into the depletion region in a pn-junction, where it moves across the region at mean velocity v_e [m/s]. The width of the region is d , so $T_d = d/v_e$ [s] is the mean time of traversing the region. While in move the electron causes a current pulse of height q/T_d [A] through the bulk-regions and circuitry that connects the two sides of the depletion region. Being rectangular each current pulse has the $\sin x/x$ shaped Fourier transform

$$p_I(t) = \begin{cases} \frac{q}{T_d}, & -\frac{T_d}{2} \leq t \leq \frac{T_d}{2} \\ 0, & \text{otherwise} \end{cases} \quad \Rightarrow \quad p_I(\omega) = q \frac{\sin(\omega T_d/2)}{\omega T_d/2} \quad (14)$$

electron charge: $q = 1.60207 \cdot 10^{-19}$ [C]

2) Note that to find the spectrum of a random binary signal in section I-3, a similar expression was used in slightly weaker form due to the constant bit-rate.

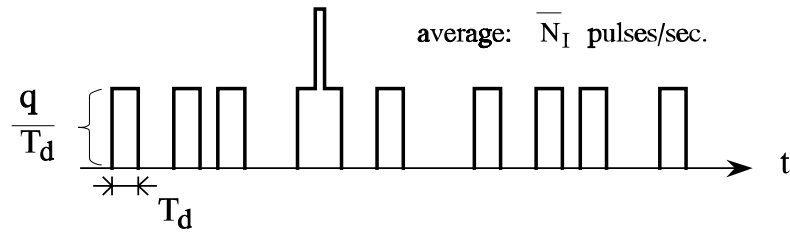


Fig.7 Train of pulses, each representing the transition of one electron across the depletion region in a pn-junction.

A train of electron pulses sums up to the DC current $I = qN_I$. Substituting I into Eq(13), the doublesided spectrum for current fluctuations becomes

$$S_I(\omega) = qI \left[\frac{\sin(\omega T_d/2)}{\omega T_d/2} \right]^2 \underset{f \ll 1/T_d}{\approx} qI. \quad (15)$$

Thus, the total mean squared noise current from the fluctuations in a frequency band Δf around $\omega_0 = 2\pi f_0$ is given by

$$\overline{i_I^2} = 2 \times \frac{1}{2\pi} \int_{\omega_0 - \pi \Delta f}^{\omega_0 + \pi \Delta f} S_I(\omega) d\omega \underset{f_0 \ll 1/T_p}{\approx} 2qI\Delta f. \quad (16)$$

The last, approximated result is called Schottky's theorem. It represents the limit where $T_d \rightarrow 0$, so each current contribution is an impulse - a shot - of weight q and a flat spectrum in concordance with the $1/T_d$ frequency bound for the approximation. The frequency independent simplification suffices for most practical application of devices that exhibits shot noise, for instance Schottky barrier and pn junction diodes or bipolar transistors where the time carriers are in drift across depletion regions commonly are considerably shorter than the transit time through neutral bulk regions [3].

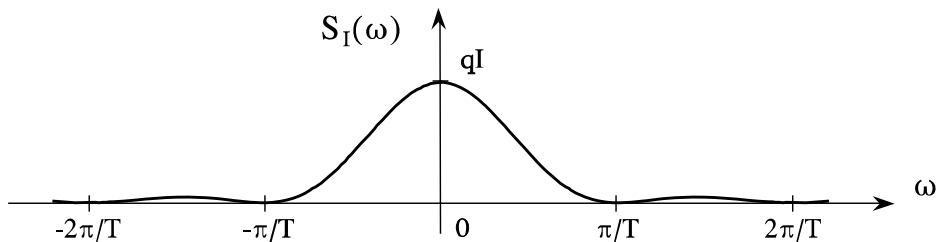


Fig.8 Spectrum of a mean squared shot noise current. In a pn-junction T is the transit time of carriers across the depletion region.

Flicker or 1/f Noise

While the types of noise considered above were ascribed to specific and well understood noise mechanism, the term flicker or 1/f noise is distinguished solely from the shape of the spectral density,

$$S_f(\omega) = \frac{C}{|\omega|^\alpha}, \quad \text{where } \alpha \approx 1 \quad (17)$$

The numerator C depends commonly upon the device biasing, but it is independent of frequency. This type of noise is observed in most electronic devices, passive as well as active, although the extent may vary by orders of magnitude between different types. Among transistors, MOSFET's are in the high flicker noise end and BJT's are in the low end. Considering resistors, bulk carbon and carbon film types are the noisiest while metal film or wirewound resistors have low flicker noise.

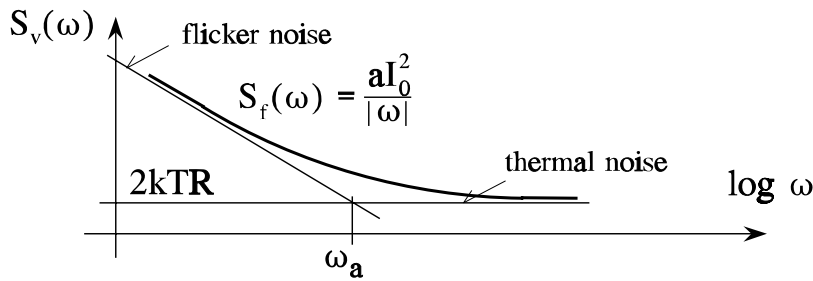


Fig.9 Spectrum including flicker noise for the mean squared noise voltage across a carbon resistor. I_0 is the DC current through the resistor.

To exemplify flicker noise we start considering the noise voltage across a carbon resistor. In addition to the flat thermal noise spectrum we get an 1/f shaped contribution as sketched in Fig.9. Observations show that the level of flicker noise is proportional to the square of the DC current through the resistor, an influence that may be understood if we associate the 1/f noise with random resistance fluctuations δR around a mean value R_0 ,

$$R = R_0 + \delta R \quad (18)$$

Applying DC current I_0 , the voltage across the resistor and especially the mean squared noise voltage are given by

$$v = v_0 + \delta v = R_0 I_0 + \delta R I_0 \Rightarrow \overline{\delta v^2} = \overline{\delta R^2} I_0^2. \quad (19)$$

The spectrum of the mean squared voltage fluctuations originates here from a 1/f spectrum in the mean squared resistance fluctuations. Note that the DC current only is required to observe the noise but not for controlling the underlying mechanisms of resistance fluctuations.

Although flicker noise basically is a low frequency phenomenon, low frequency parameter fluctuations might get substantial influence on RF circuit performances. Applying a sinusoidal current $I_c \cos \omega_c t$ in the carbon resistor case gives the voltage components

$$v = v_1 + \delta v = R_0 I_c \cos \omega_c t + \delta R I_c \cos \omega_c t. \quad (20)$$

The last term holds the noise, but it is no longer a stationary random variable but a cyclo-stationary one of period $T_c = 2\pi/\omega_c$. The resultant power spectrum for the mean squared voltage is given by

$$S_v(\omega) = \frac{R_0^2 I_c^2}{4} \delta(\omega_c) + \frac{R_0^2 I_c^2}{4} \delta(-\omega_c) + \frac{I_c^2}{4} S_{Rf}(\omega + \omega_c) + \frac{I_c^2}{4} S_{Rf}(\omega - \omega_c). \quad (21)$$

The two first terms account for the sinusoidal carrier in v_1 . If $S_{Rf}(\omega)$ denotes the mean square 1/f shaped spectrum of the stationary random variable δR , the noise portion of the resultant spectrum is shifted in frequency to fringe the carrier. Suppose we have two signals represented by carriers I_{c1} and the nearby but much smaller I_{c2} , which is the one we subsequently want to separate by filtering and detect. From the above relationship and the sketch in Fig.10, we see that the flicker noise induced by the large carrier may overwhelm the signal to be found and the succeeding filtering becomes difficult. So despite its basic low-frequency outset, flicker noise may be critical also at RF frequencies.

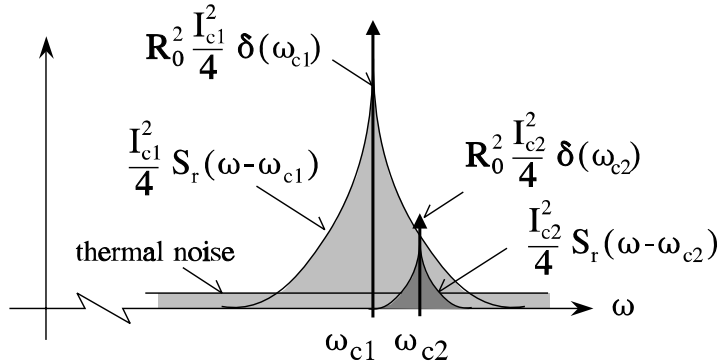


Fig.10 Noise and signal components when two RF signals are inflicted by parameter flicker noise like resistance fluctuations in carbon resistors. Only the positive frequency parts from Eq.(21) are shown.

Flicker noise contribution to the mean squared noise voltage in a frequency interval from f_l to f_u by the 1/f relationship gives

$$\overline{v_f^2} = 2 \times \frac{C}{2\pi} \int_{2\pi f_l}^{2\pi f_u} \frac{d\omega}{\omega} = 2 C \log f_u - 2 C \log f_l, \quad (22)$$

Both limits, $f_u \rightarrow \infty$ or $f_l \rightarrow 0$, make unrealistic advancements towards infinity. A closer look on details in the spectrum must therefore depart from $1/f$ in the limits. In the high end the spectrum must roll off faster than $1/f$, for example like $1/f^2$ above a certain frequency f_l . Correspondingly the spectrum must grow slower than $1/f$ when f goes towards zero. A constant spectrum below a certain frequency f_l would be appropriate. For most practical noise calculations we have commonly no detailed knowledge about these matters. If the bandwidth of interest spans the whole frequency range of flicker noise, a safe choice on the upper bound is to use f_u above the limit frequency f_a where thermal noise becomes dominant as indicated by Fig.9. The low bound f_l could be chosen so low that we are no longer willing to spent time observing consequences of the noise, alternatively $1/f_l$ could be taken as the length of the longest message that is processed separately in a communication system.

There are many physical origins of flicker noise in electronic components and devices. The cause in resistors might be fluctuations in the mobility of the carriers that convey the current. In semiconductors, flicker noise also accompanies the generation and recombination process of free carriers. Often phenomena that deteriorate normal device performance, for instance uncontrolled oxide traps and surface states in transistors, contribute dominantly to flicker noise. In new device types this noise may be excessive, but commonly it levels off when the corresponding technology matures. Flicker noise in semiconductor devices manifests itself both directly as noise currents or voltages, but it also contributes to parameter fluctuations. The transconductance, for instance, might get an $1/f$ spectrum, so the modulating property that was illuminated for bulk resistors by Eq.(21) and Fig.10 applies to transistors as well. Consult refs. [1] and [4] chap.8 to gain more insight into the physics behind $1/f$ noise. A discussion of common basic aspects of the flicker noise may be found in ref.[5].

Other Noise Sources in Electronics

The three noise types we have considered are far the most prominent in RF circuits. They are also typical from the point of view, that we have covered three basic forms, the unavoidable flat spectrum thermal noise, the bias current dependent shot noise with approximately flat spectrum, and finally flicker noise whose dominant low-frequency spectrum transforms to RF and smear out signal spectra. There are other types and sources of noise. Most of them can hardly be distinguished from the types above in experimental data. For the same reason, noise models in circuit simulator programs are concentrated around our basic types. If other sources are present in the circuit, they are taken into account by parameter adjustments. However, some specific noise contributions are so frequently referred to in literature that they need a few comments.

Generation-recombination noise accompanies the random processes of generating and recombining carriers in electronic devices. If one mechanism dominates the process, for instance a well defined trap, the corresponding noise gets a spectrum of shape,

$$S_{gr}(\omega) = K \frac{\tau}{1 + \tau^2 \omega^2} \quad (23)$$

Here τ is the lifetime of carriers. Factor K depends typically on bias currents. It is seen that the high frequency asymptote decays with the square of frequency, so it is much steeper than in flicker noise. However, many different processes of widely separated lifetimes are usually engaged in generation and recombination of carriers in semiconductor devices. Their joint effect approximates the 1/f spectral density of flicker noise [4].

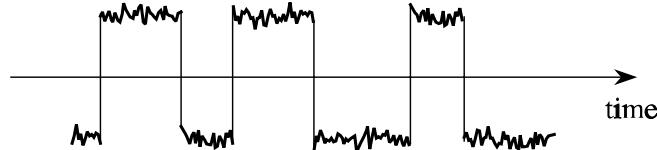


Fig.11 Typical time-domain burst noise waveshape

Burst noise is a special form of generation-recombination noise with spectral density like Eq.(23). This noise is sorted out due to its characteristic wave shape like the one in Fig.11, but the basic mechanisms of the pronounced jumps are not completely understood [4]. Burst noise is sometime called popcorn noise after the sound the waveshape produces in a loudspeaker. Like flicker and other noise types with low-frequency spectral dominance, burst noise gets significance in RF if it controls device parameter variations.

Avalanche noise follows the avalanche effect in reverse biased pn-junctions. If the field is sufficiently high, free carriers may gain the energy that is necessary to produce new electron hole pairs by impact ionization. The total current is still made by a sequence of random events, so the noise is a shot noise of the type in Eq.(16). However, the current in the noise expression under reverse bias is not the saturation current I_S , which we might extract from the characteristic of the forward biased junction, but instead the actual and commonly much greater experimental reverse current that includes avalanching.

Characterizing and Combining Noise Sources

The power spectral density functions are the direct way of specifying a noise source, either $S_v(\omega)$ [V^2/Hz] for a voltage source or $S_i(\omega)$ [A^2/Hz] for a current source. Data sheets give often the square root of twice the densities that are shown, for instance the functions

$$V_n(f) = \sqrt{2 S_v(2\pi f)} \left[\frac{V}{\sqrt{Hz}} \right] \quad \text{or} \quad I_n(f) = \sqrt{2 S_i(2\pi f)} \left[\frac{A}{\sqrt{Hz}} \right] \quad (24)$$

Assuming flat spectrum, we get the RMS voltage or current from the noise source by multiplying the $V_n(f)$ or the $I_n(f)$ function by the square root of the frequency interval or the noise bandwidth in the measurements.

Instead of the direct specification above, noise sources of any kind are sometimes compared to the idealized flat spectrum thermal noise from resistors, which was defined by

either Eq.(2) or Eq.(3) for voltage and current respectively. There are two approaches here. The first one requires that the noise source has an output impedance or admittance with positive real part. An effective noise temperature T_{eff} for the one-port is now defined as the temperature that an impedance equal to the one-port impedance must have to give thermal noise equal to the observed noise. If a one-port has impedance $Z_1(\omega_0)$ and mean squared noise voltage or current equal to either \bar{v}_1^2 or \bar{i}_1^2 in the frequency interval Δf around ω_0 , the noise temperature becomes

$$T_{eff} = \frac{\bar{v}_{ol}^2}{4 k \operatorname{Re}\{Z_1(\omega_0)\} \Delta f} \quad \text{or} \quad T_{eff} = \frac{\bar{i}_{sl}^2}{4 k \operatorname{Re}\{Y_1(\omega_0)\} \Delta f}. \quad (25)$$

Another way of characterizing a noise source is to specify the resistance R_n or the conductance G_n that provide thermal noise equal to the observed source. This is particularly useful when the source is given solely in the form of either a RMS voltage or a RMS current generator at a given temperature. R_n and G_n are called the noise resistance and the noise conductance respectively. If the observed noise in frequency interval Δf is either \bar{v}_1^2 or \bar{i}_1^2 , the corresponding noise resistance or conductance are

$$R_n = \frac{\bar{v}_{ol}^2}{4 k T \Delta f} \quad \text{or} \quad G_n = \frac{\bar{i}_{sl}^2}{4 k T \Delta f}. \quad (26)$$

It should be emphasized that R_n and G_n are noise level parameters, which are not required to be recognizable as resistors or conductances in an equivalent circuit, although this will be the case, if the noise is thermal and the temperature has been agreed upon. The temperature is often the reference temperature of 290 [K], which is a part of the noise figure definition for two-ports to be discussed below in section IV-3 on page 25.

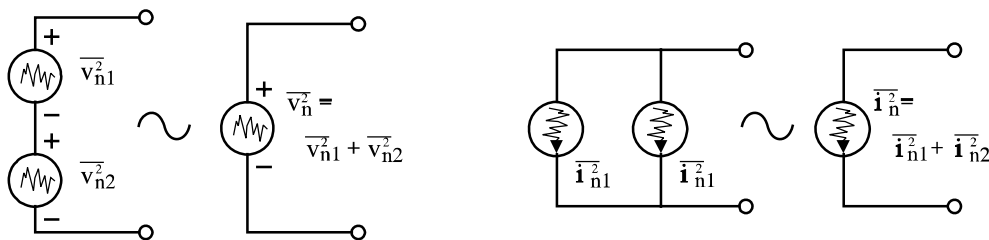


Fig.12 Combining uncorrelated noise sources. The mean square of the resultant voltage or current is the sum of the two original mean squared quantities.

The combined effect of two series connected noise voltage sources - two paralleled noise current sources behave similarly - must be calculated on a mean-squared basis to yield

$$\bar{v}_n^2 = \overline{|v_{n1} + v_{n2}|^2} = \bar{v}_{n1}^2 + \bar{v}_{n2}^2 + 2 \overline{v_{n1} v_{n2}} = \bar{v}_{n1}^2 + \bar{v}_{n2}^2 + 2 \rho \sqrt{\bar{v}_{n1}^2 \bar{v}_{n2}^2}. \quad (27)$$

Here ρ is a correlation coefficient between the two sources. With time averaging it is defined

$$\rho \equiv \frac{\langle v_1 v_2 \rangle}{\sqrt{\overline{v_{n1}^2} \overline{v_{n2}^2}}} \quad (28)$$

This coefficient is confined to the interval $[-1 \leq \rho \leq 1]$.

Uncorrelated noise sources have a zero-valued correlation coefficient, so the mean square of the result becomes the sum of mean squares from the two original sources as indicated by Fig.12. Imagining that the two original sources are thermal noise from resistors R_1 and R_2 at the same temperature, the result above makes sense since their series connection is the sum of the resistors and the mean squared noise is proportional to the resistance value. If the sources are characterized by noise resistances, the combined effect in Eq.(27) corresponds to the sum of the noise resistances. Finally, if the noise sources refer to the same real part impedance, the combined result also corresponds to adding noise temperatures.

While noise contributions from independent origins are uncorrelated, correlated noise generators often result when noise from a common physical origin is sensed at different places in a network. We shall see below that the equivalent input and output noise sources in device models may be correlated. In network calculation it is often convenient to use cross spectra, which might be complex even with real valued noise signals. To make circuit computations in frequency domain a corresponding complex correlation coefficient is

$$c \equiv \frac{S_{21}(\omega_0)}{\sqrt{S_1(\omega_0) S_2(\omega_0)}} = \frac{\overline{v_1 v_2^*}}{\sqrt{\overline{v_1^2} \overline{v_2^2}}} \quad (29)$$

The last form is often seen in literature. Like deterministic signal whose components may be represented by complex phasors in frequency response calculations, noise contributions from a narrow frequency band around a given frequency may be represented by random phasors for transmission computations. In analogy with deterministic phasors we should use $\rho = \text{Re}\{c\}$ when translating back to the time domain version in Eq.(27).

Man-Made Noise

Man-made noise is often encountered in the reception of radio signals, which may be equivalenced as sketched in Fig.13. The antenna has impedance Z_a which resembles a bandpass characteristic around a center frequency. Besides radio signals, which are indicated by the v_s voltage source, noise contributions of various nature are received. They are included in the circuit by the mean square voltage $\overline{v_n^2}$. The level of noise depends very much upon the application that guided the antenna design.

In mobile communication antennas are often omnidirectional and a considerable amount of noise from all directions may be picked up. Fig.14 - from ref.[6] through

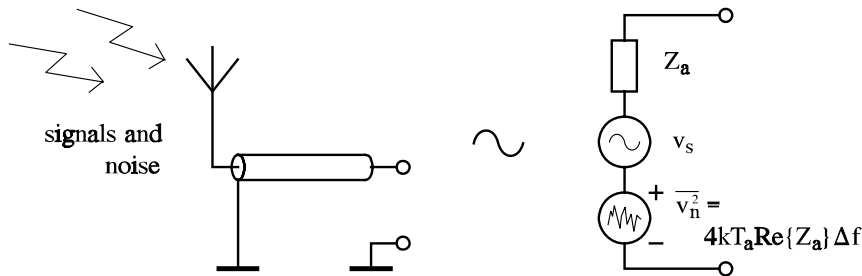


Fig.13 Equivalent circuit for radio signal reception

ref.[7] - shows the nature and relative significance of the received noise quantities as function of frequency. The left scale gives the noise temperature of the antenna impedance. As seen, both types of urban area man-made noise - from city center and suburbs - dominate the entire frequency range of practical interest for mobile communications (approx. 10 MHz to 2 GHz). Man-made noise includes terms like ignition noise from cars or radiation due to switching in industrial controllers and power regulators. At much lower levels we have the natural sources antenna noise, i.e. noise from galaxies, sun activity, and atmospheric motions. Finally, the curve termed "typical receiver" shows how much the electronic circuitry of a conventional receiver adds to the noise temperature of the antenna. It should be clear from this figure that in mobile communications, there is no need to spend a lot of efforts in squeezing receiver noise towards ultimately low limits when man-made noise from the environment is the most significant part of input noise.

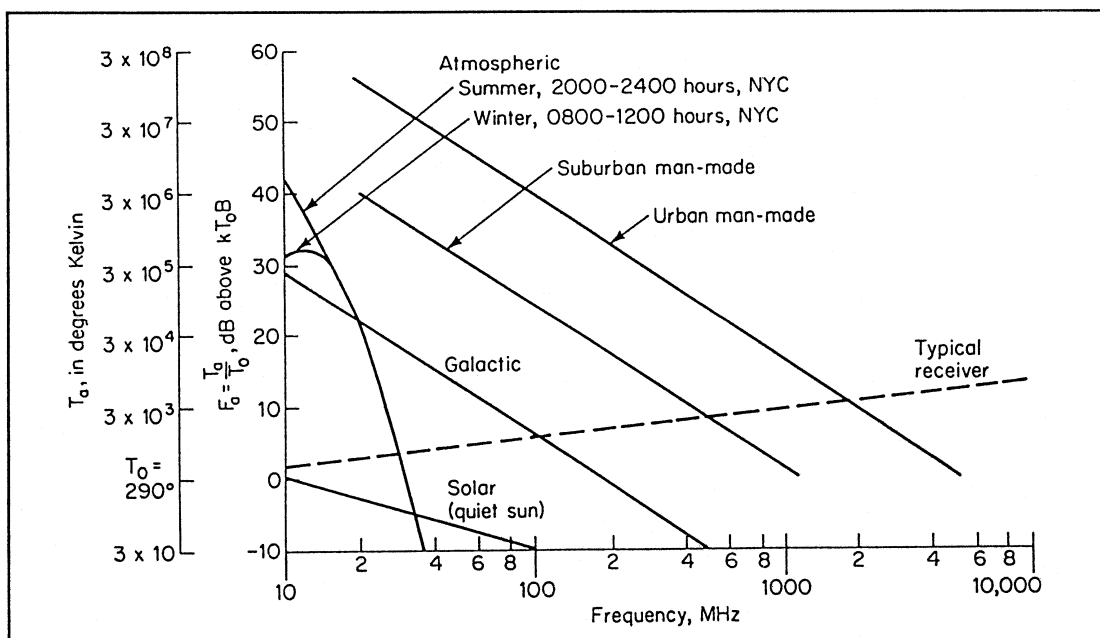


Fig.14 Typical noise components at the antenna terminal in mobile communications (omnidirectional reception). From ref.[6].

IV-2 Noise in Semiconductor Devices

Two ingredients are required to keep control with the noise level in electronic designs. The first one is noise models for the components and devices, the second is systematic approaches for characterizing and constructing circuits that include noise. We address the models in this section, which gives a survey of the most important noise contributions in common RF devices. Beyond this limited scope, the reader should consult the literature on devices, noise, and modeling, for instance [4],[8],[9],[10], or [11].

Noise in Diodes

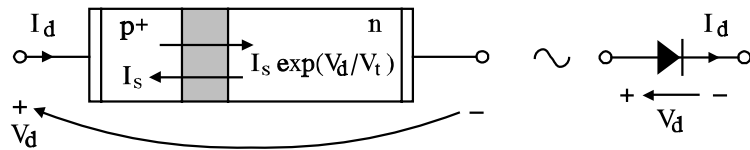


Fig.15 Short p+n-junction. Hole injections across the depletion regions are the only contributions that are included in the idealized model.

A short p⁺n diode is considered. The p region is doped more heavily than the n region, so the current is dominated by holes. Assuming ideal conditions, the current through the diode is given by

$$I_d = I_s (e^{V_d/V_t} - 1) = I_s e^{V_d/V_t} - I_s, \quad V_t = kT/q. \quad (30)$$

The first bias dependent term represent flow of holes injected from the p+ region. The second opposing term is a current of holes injected from the n region. At zero bias, i.e. V_d=0, the two terms balance. Under forward bias the first term dominates and gives the exponential voltage to current relationship. Under reverse bias the resultant current approaches the constant -I_s, which for small signal silicon diodes typically is in the femto ampere range. Injection from the two sides of the depletion region are statistically independent and implies both full shot noise. The mean squared noise current is therefore

$$\overline{i_{dn}^2} = 2qI_s e^{V_d/V_t} \Delta f + 2qI_s \Delta f \quad (31)$$

A large signal model for an ideal diode is shown in Fig.16(a). Linearized small-signal descriptions includes the differential conductance of the diode,³

$$g_d = \frac{dI_d}{dV_d} = \frac{I_s}{V_t} e^{V_d/V_t} \quad (32)$$

3) At high frequencies, diode capacitances should be paralleled. They are left out here for clarity since they introduce no new noise aspects.

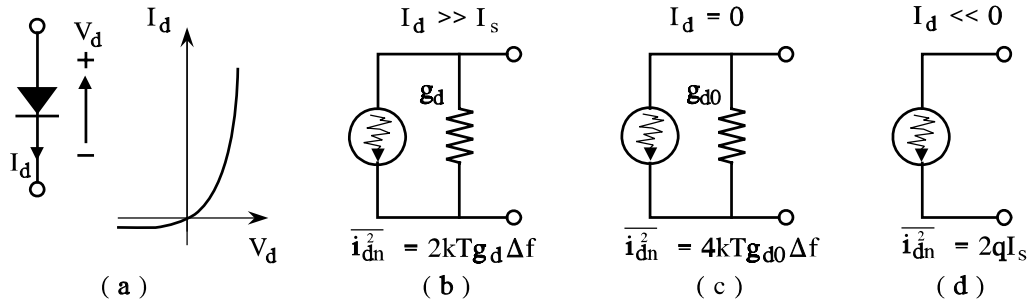


Fig.16 Small-signal noise equivalent circuits for diode in large forward (b), zero (c), and reverse bias (d). $I_d(V_d)$ from Eq.(35) may replace I_s in reverse breakdown.

Using the common assumption that the exponential term dominates the current under forward bias, the conductance and the noise expressions above approximate to,

$V_d > 0$:

$$I_d(V_d) \approx I_s e^{V_d/V_t} \Rightarrow g_d \approx \frac{I_d(V_d)}{V_t} \Rightarrow \overline{i_{dn}^2} \approx 2qI_d(V_d)\Delta f = 2kTg_d\Delta f. \quad (33)$$

To get the last expression, parameter V_t was rewritten kT/q . Comparing with thermal noise from Eq.(3), a conducting diode shows only half the noise that a conductance of similar size provides in thermal equilibrium. In terminology of noise temperatures, the diode conductance has as noise temperature that is half the physical temperature. The difference between the conductor and the diode regarding noise is that a forward biased diode is not in thermal equilibrium. To illustrate this point further it is seen that at zero bias, where diode is in thermal equilibrium, we avoid approximations and get directly from Eq.(31) a result that is in agreement with the thermal noise equation,

$$\underline{\underline{V_d = 0}} : \quad g_d = g_{d0} = \frac{I_s}{V_t}, \quad \overline{i_{dn}^2} = 4qI_s\Delta f = 4kTg_{d0}\Delta f. \quad (34)$$

Under moderate reverse bias the ideal pn-diode model tends to have no significant conductance, and the noise corresponds to the shot noise associated with the saturation current I_s as sketched in Fig.16(d). At greater reverse biases this description may be too simple for practical purposes, as the reverse current raises significantly beyond I_s . Although it still may be small, the excessive reverse current includes start of Zener and avalanche breakdowns, phenomena that are accompanied by shot noise processes themselves. To complete a noise calculation, an expression including all reverse currents must be provided, for instance using the so-called Miller or avalanche multiplier, M_{av} . It is often stated empirically, [12]. Keeping orientations from Fig.16(a), reverse DC and noise characteristics are now written

$V_d < 0$:

$$I_d(V_d) = I_s [1 + M_{av}(V_d)], \quad M_{av}(V_d) = \left[1 - \left(\frac{-V_d}{V_{av}}\right)\right]^{-N_{av}}, \quad \overline{i_n^2} = 2qI_d(V_d)\Delta f. \quad (35)$$

The multiplier rises towards infinity when $-V_d$ is approaching the breakdown voltage V_{av} , which is a positive parameter. The exponent N_{av} is another positive parameter that falls in the range from approximately 2 to 7.

Noise in Bipolar Transistors

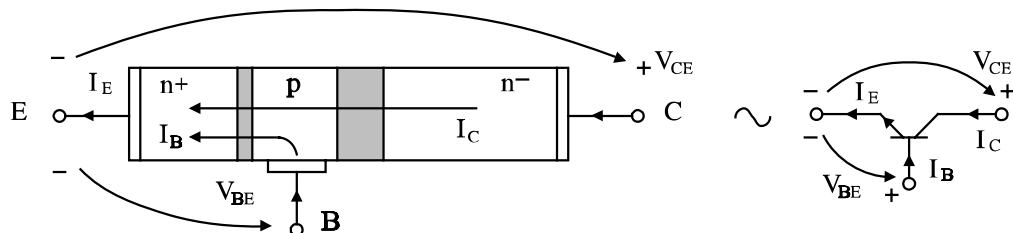


Fig.17 Structure of npn bipolar junction transistor (BJT). The dominant part of the bias currents I_C and I_B are carried by electrons.

Under normal, forward biased operation, the most significant current in a npn transistor consists of electrons that are emitted into the base which they traverse before they eventually are collected after drift through the collector-basis junction. This is the collector terminal current I_C in the sketch of Fig.17. Its noise component is dominated completely by shot noise. The base current I_B is more composite, but in most cases, it is dominated by a flow of holes injected from the base into the emitter, i.e. the mechanism that controls the current gain β . It is a process completely equivalent to emitting electrons to I_C , so that part of the base current shows shot noise. In addition, the base current may contain contributions from carrier recombinations in the base, in the depletion regions, and possibly at surface traps, so the base current may contain flicker and burst noise components in the low frequency part of the spectrum. Noise components, which are associated with I_C and I_B , are included in a transistor equivalent circuit like Fig.18 by the mean squared currents $\overline{i_{nc}^2}$ and $\overline{i_{nb}^2}$. Without flicker and burst noise, the noise sources in this diagram are given by

$$\overline{i_{nc}^2} = 2qI_C\Delta f, \quad \overline{i_{nb}^2} = 2qI_B\Delta f, \quad \overline{v_{nbb}^2} = 4kTR_{BB}\Delta f, \quad (36)$$

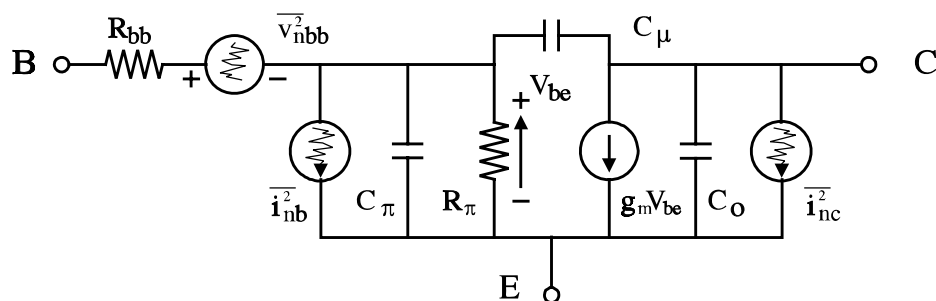


Fig.18 Dominant noise sources in a BJT under forward bias. v_{nbb}^2 is thermal while i_{nb}^2 and i_{nc}^2 are shot noise contributions.

where the noise voltage v_{nbb}^2 is thermal noise from the base series resistance R_{BB} . This noise may be the dominant noise contribution, so a major objective in RF transistor design is to reduce the base resistance, both for the sake of reducing noise, but also to keep the bandwidth large.

If flicker and burst noise are important in an application, a standard way of inclusion is the following extension of i_{nb}^2 , cf. ref.[13],p.271,

$$\overline{i_{nb}^2} = 2qI_B\Delta f + K_f \frac{I_B^{a_f}}{f} \Delta f + K_b \frac{I_B}{1 + (f/f_c)^2} \Delta f, \quad (37)$$

where K_f and a_f are parameters for flicker noise and K_b , f_c describes burst noise separately, cf. Eq.(23). Note, this model assumes an observation bandwidth Δf , which is small compared to the operating frequency f . Then it is unnecessary to integrate the frequency dependent denominators over the Δf interval as it was done in Eq.(22).

Example IV-2-1 (minimum noise in bipolar transistors)

The relative significance of the different noise sources in a transistor coupling may be studied by their contributions to the output mean square short circuit current. In this example, we consider noise in the mid-frequency range of the transistor, which means that we are sufficiently low in frequency to disregard all the capacitors in the equivalent circuit, Fig.19, but high enough in frequency to ignore possible flicker and burst noise terms. Besides the internal transistor noise generators, the noise from the generator resistance, R_g , is included by v_{ng}^2 . The total short circuit output noise current gets a term from each source,

$$\overline{i_{no}^2} \Big|_{total} = \overline{i_{no}^2} \Big|_{v_{ng}} + \overline{i_{no}^2} \Big|_{v_{nbb}} + \overline{i_{no}^2} \Big|_{i_{nb}} + \overline{i_{no}^2} \Big|_{i_{nc}}, \quad (38)$$

As the noise sources are uncorrelated, the different terms are found from the diagram applying the corresponding source one by one

$$\begin{aligned} \overline{i_{no}^2} \Big|_{v_{ng}} &= \overline{v_{ng}^2} \mathbf{g}_m^2 \left[\frac{\mathbf{R}_\pi}{\mathbf{R}_\pi + \mathbf{R}_{bb} + \mathbf{R}_g} \right]^2, & \overline{i_{no}^2} \Big|_{v_{nbb}} &= \overline{v_{nbb}^2} \mathbf{g}_m^2 \left[\frac{\mathbf{R}_\pi}{\mathbf{R}_\pi + \mathbf{R}_{bb} + \mathbf{R}_g} \right]^2, \\ \overline{i_{no}^2} \Big|_{i_{nb}} &= \overline{i_{nb}^2} \mathbf{g}_m^2 \left[\frac{\mathbf{R}_\pi (\mathbf{R}_{bb} + \mathbf{R}_g)}{\mathbf{R}_\pi + \mathbf{R}_{bb} + \mathbf{R}_g} \right]^2, & \overline{i_{no}^2} \Big|_{i_{nc}} &= \overline{i_{nc}^2}. \end{aligned} \quad (39)$$

The ratio of the total mean square short circuit output current over the component that originates from the generator resistor alone is a common measure of noise performance, the so-called noise figure F. We shall discuss its interpretation intensively in next section. For now we just calculate to get

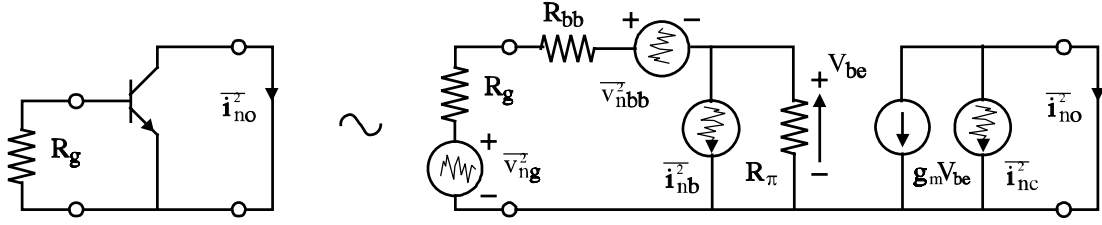


Fig.19 Equivalent circuit for calculating mid-frequency output mean square short circuit current in a bipolar transistor.

$$\begin{aligned}
 F \equiv \frac{\overline{i_{no}^2}}{\overline{i_{no}^2}} \Big|_{total} &= 1 + \frac{\overline{i_{no}^2}}{\overline{i_{no}^2}} \Big|_{v_{nbb}} + \frac{\overline{i_{no}^2}}{\overline{i_{no}^2}} \Big|_{i_{nb}} + \frac{\overline{i_{no}^2}}{\overline{i_{no}^2}} \Big|_{i_{nc}} \\
 &= 1 + \frac{\overline{v_{nbb}^2}}{\overline{v_{ng}^2}} + \frac{\overline{i_{nb}^2}}{\overline{v_{ng}^2}} (R_{bb} + R_g)^2 + \frac{\overline{i_{nc}^2}}{\overline{v_{ng}^2}} \frac{1}{g_m^2} \left[1 + \frac{R_{bb} + R_g}{R_\pi} \right]^2
 \end{aligned} \quad (40)$$

To express bias dependencies, we introduce the bipolar transistor parameter relationships

$$g_m = \frac{I_C}{V_t}, \quad R_\pi = \frac{\beta}{g_m} = \frac{\beta V_t}{I_C}, \quad V_t = \frac{k T}{q}. \quad (41)$$

where β is the common emitter DC current gain, which is supposed to be constant in the calculations. It is furthermore assumed that possible recombination currents are a small part of the base current, so β is also the scaling between the shot noises from I_C and I_B , i.e.

$$\overline{i_{nc}^2} = 2 q I_C \Delta f, \quad \overline{i_{nb}^2} = 2 q I_B \Delta f = \frac{1}{\beta} 2 q I_C \Delta f = \frac{\overline{i_{nc}^2}}{\beta}. \quad (42)$$

Finally we introduce the two thermal noise terms from the generator and the base series resistors respectively,

$$\overline{v_{ng}^2} = 4 k T R_g \Delta f, \quad \overline{v_{nbb}^2} = 4 k T R_{bb} \Delta f. \quad (43)$$

Inserting the relationships above into Eq.(40), the noise figure may be expressed as a function of the collector bias current I_C to read

$$F = \left(1 + \frac{1}{\beta} \right) \left(1 + \frac{R_{bb}}{R_g} \right) + \frac{1}{2 R_g} \left[\frac{V_t}{I_C} + \frac{(R_{bb} + R_g)^2}{\beta V_t} \left(1 + \frac{1}{\beta} \right) I_C \right]. \quad (44)$$

The factor in brackets has terms that are inversely and directly proportional to I_C . For a given generator resistance R_g , we seek the collector current that minimizes noise figure F,

$$\frac{\partial F}{\partial I_C} = \frac{1}{2R_g} \left[-\frac{V_t}{I_C^2} + \frac{(R_{bb} + R_g)^2}{\beta V_t} \left(1 + \frac{1}{\beta} \right) \right] = 0, \quad \Rightarrow \quad (45)$$

$$I_{C,minF} = \frac{V_t}{R_{bb} + R_g} \frac{\beta}{\sqrt{\beta + 1}} \approx \frac{V_t \sqrt{\beta}}{R_{bb} + R_g}. \quad (46)$$

At the minimizing $I_{C,minF}$ current, the noise figure becomes

$$F_{I_{min}} = \left(1 + \frac{1 + \sqrt{\beta + 1}}{\beta} \right) \left(1 + \frac{R_{bb}}{R_g} \right). \quad (47)$$

Considered isolated, the last result suggests use of a high generator resistance to keep the noise figure down. Simultaneously, however, Eq.(46) dictates a low collector current. The transconductance $g_m = \text{Re}\{y_{21}\}$ is proportional to the collector current, so a small I_C implies a small power gain in an amplifier. This is our first mentioning of a common problem in design considerations including noise, namely that conditions for low noise figure and high gain differ, so a trade-off between the two has to be made.

Keeping the collector current fixed, there must be a generator resistance that minimizes the noise figure. The first term in Eq.(44) reduces while its second term eventually will grow with increasing R_g . Rearranging the equation gives the noise figure expression

$$F = \left(1 + \frac{1}{\beta} \right) \left[1 + \frac{I_C R_{bb}}{\beta V_t} + \left(R_{bb} + \frac{I_C R_{bb}^2}{2 V_t \beta} + \frac{V_t \beta}{2 I_C (1 + \beta)} \right) \frac{1}{R_g} + \frac{I_C}{2 \beta V_t} R_g \right]. \quad (48)$$

Minimum in the noise figure requires

$$\frac{\partial F}{\partial R_g} = \left(1 + \frac{1}{\beta} \right) \left[- \left(R_{bb} + \frac{I_C R_{bb}^2}{2 V_t \beta} + \frac{V_t \beta}{2 I_C (1 + \beta)} \right) \frac{1}{R_g^2} + \frac{I_C}{2 \beta V_t} \right] = 0, \quad \Rightarrow \quad (49)$$

$$R_{g,minF} = \sqrt{R_{bb}^2 + R_{bb} \frac{2 \beta V_t}{I_C} + \frac{\beta^2 V_t^2}{I_C^2 (1 + \beta)}}, \quad (50)$$

which finally provides

$$F_{R_{min}} = \left(1 + \frac{1}{\beta} \right) \left[1 + \frac{I_C}{\beta V_t} (R_{bb} + R_{g,minF}) \right]. \quad (51)$$

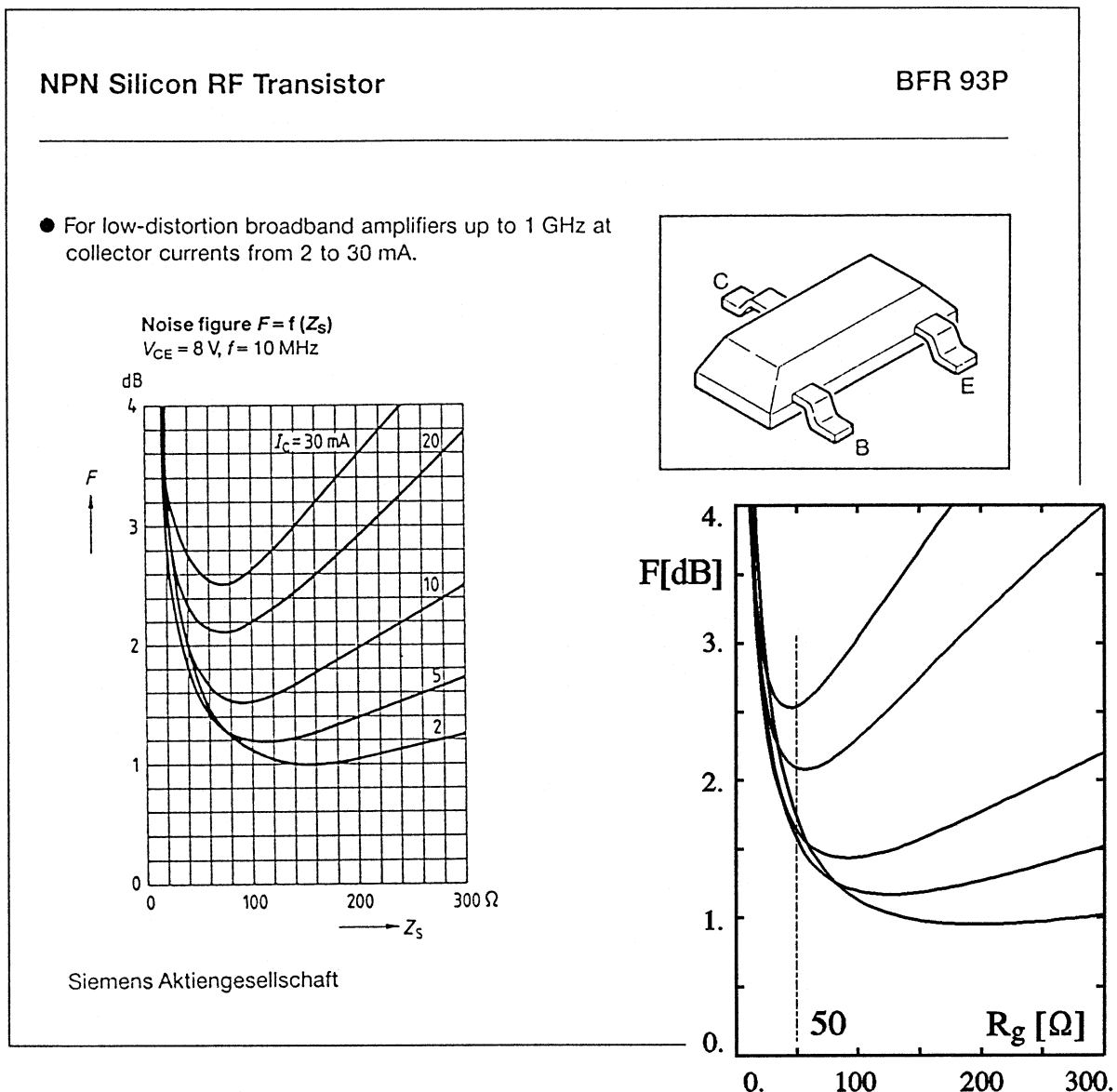


Fig.20 Extract from Siemens RF and Microwave Transistors and Diodes Data Book 1990/91 exemplifying low-frequency noise figures. The insert demonstrates similar theoretical results.

A practical example of the two types of noise figure minima may be observed in the data book extract in Fig.20. With a fixed generator resistor R_g of 50Ω (Z_s in data), there is a minimum in the noise figure between the $I_C = 2\text{mA}$ and 5mA curves. Keeping the collector currents fixed, the noise figure curves indicate the minimizing generator resistance very distinctly. The example here is a RF transistor usable to 1GHz. The noise figure in the extract apply to 10MHz, and we should expect that the simple low to middle frequency equivalent circuit from Fig.19 apply to the data. To investigate the question we search pairs of β, R_{bb} that satisfy corresponding $F_{R,\min}, R_{g,\min F}$ readings from the curves. The process was conducted numerically requiring Eqs.(48) and (51) to fit the data. Table I summarizes the results and, as seen, neither β nor R_{bb} are completely constant. However they follow expectable variations,

Table I Parameters for transistor data in Fig.20. β and R_{bb} are fitted to reproduce $F_{R,min}$ and $R_{g,minF}$ in the data.

I_C [mA]	$F_{I,min}$ [dB]	$R_{g,minF}$ [Ω]	β	R_{bb} [Ω]
30.	2.5	70.	85.	11.5
20.	2.1	75.	90.	12.0
10.	1.5	90.	110.	13.0
5.	1.2	120.	95.	13.5
2.	1.0	155.	75.	14.0

cf.ref's [13] p.70 or [9] p.56, where the current gain often has a maximum before the high current rating of the transistor (50 mA for BFR93) due to high injection across the emitter base junction. High injection also increases conductivity in the base beneath the emitter area, which reduces the base series resistance. The third but less direct consequence of high injection is the fact that despite β and R_{bb} are adjusted to fit the minimum conditions, complete coincidence between data and theoretical curves are not achieved. The reason is the transconductance g_m is reduced compared to the ideal value of I_C/V_t by a factor that approaches one half. Even with this precautions, the simplified theoretical results are qualitatively correct and accurate enough for initial designs, especially taking into account that the base series resistance R_{bb} is a parameter that commonly not is accurately known. As a matter of fact, noise measurements and identification like the example here is suggested as a method to determine the base series resistance experimentally, cf. ref.[9] p.291.

Example IV-2-1 end

Noise in Field Effect Transistors

The basic operation of junction and metal gate field effect transistors, JFET's or MESFET's - are that the resultant conductance of a semiconductor region in a channel between the drain and source terminals is modulated primarily by the gate to source voltage but also by the drain to source voltage. The mechanism of modulation is that a region of the channel beneath the gate junction or electrode is depleted from mobile carriers under control of the gate to channel voltage. The depleted region - sketched by the hatched area in Fig.21 - cannot conduct current. Due to the voltage drop along the channel it narrows to practically zero in the drain end under normal biasing to pinched operation, which is the only condition we consider. JFETs and MESFETs are our vehicles for presentation. The physics of MOSFET's is quite different and more involved regarding the formation of a conducting channel under the isolated gate, but in small-signal and noise respects, there are no needs to make major distinctions between MOSFET's and other FET types, so the discussion below applies to all types of field effect transistors.

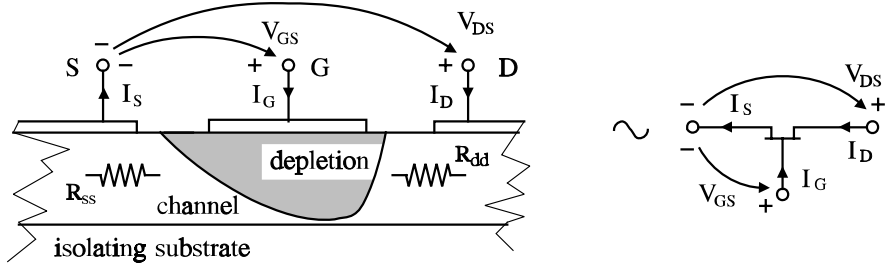


Fig.21 Structure of field effect transistor (MESFET or junction FET). Channel noise originates from thermal and flicker noise in the undepleted part of the channel.

Being a voltage controlled conductance the major noise mechanisms in field effect transistor are thermal noise and flicker noise of various origins. An equivalent circuit that includes most of the contributions that are suggested in literature is shown by Fig.22. The series noise voltages are associated with bulk regions outside the channel. They are commonly assumed independent of bias and obey simple thermal noise rules, i.e.

$$\overline{v_{ngg}^2} = 4 k T R_{gg} \Delta f, \quad \overline{v_{ndd}^2} = 4 k T R_{dd} \Delta f, \quad \overline{v_{nss}^2} = 4 k T R_{ss} \Delta f. \quad (52)$$

The series resistances to the channel may include flicker noise in proportion to the square of the drain current. It is, however, difficult to identify the series resistances explicitly. The effect of a small source resistor R_{ss} is a reduction of the transconductance that is seen from the device terminals by a denominator equal to $(1+g_m R_{ss})$. At the drain side the small resistance R_{dd} is series connected to a high output impedance from the active part of the transistor. Without detailed knowledge about processing of the transistor, the effects of channel series resistances may be accounted for by the remaining part of the equivalent circuit.

Thermal and flicker noise from the undepleted part of the channel is described by the i_{nd}^2 noise current in the equivalent circuit. There is a close connection between transconductance and channel conductance. If the transistor is biased for a given g_m , the thermal noise and flicker noise that arise from channel conductance may be included by the two terms,

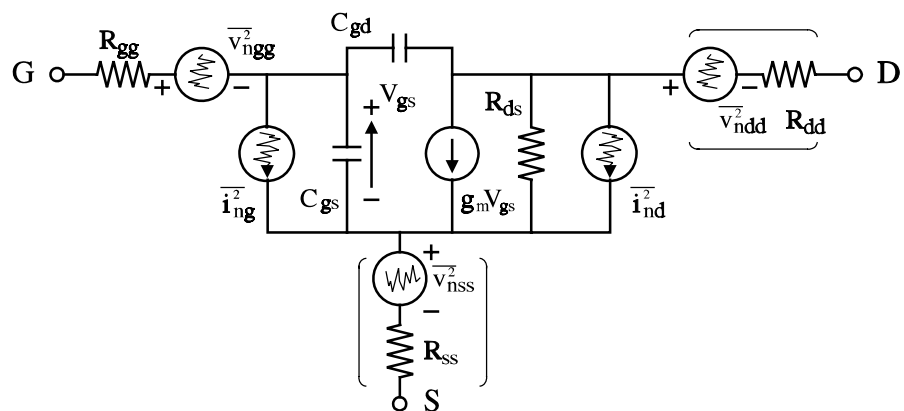


Fig.22 FET noise. i_{nd}^2 , channel noise incl. flicker. i_{ng}^2 , leakage shot and induced noise. Series resistances and noise sources in parentheses are often omitted.

$$\overline{\dot{i}_{nd}^2} = \overline{\dot{i}_{nd,thermal}^2} + \overline{\dot{i}_{nd,flick}^2} = \frac{2}{3} \times 4kT g_m \Delta f + K_{ch} \frac{I_D^{a_{ch}}}{f} \Delta f. \quad (53)$$

The weight factor of 2/3 in front of the thermal noise term is a result of averaging noise contributions along the channel. The last term holds flicker noise characterized by parameters K_{ch} and the drain current exponent, a_{ch} , which may be close to two. Like the similar modeling in bipolar transistors, it is assumed that the Δf bandwidth is small compared to frequency f . Otherwise we must again conduct an integration over the observation bandwidth as it was done in Eq.(22).

There are two highly different contributions to the gate noise current, $\overline{\dot{i}_{ng}^2}$. The first contributions arises because voltage fluctuations from the channel noise also appear as fluctuations in voltage across the depletion region. It forces a capacitively induced gate current through the circuit that is connected to the gate electrode. Secondly, a possible small gate DC leakage current I_G implies shot-noise like the noise from a reverse biased diode given through Eq.(35) above.

$$\overline{\dot{i}_{ng}^2} = \overline{\dot{i}_{ng,induced}^2} + \overline{\dot{i}_{ng,shot}^2} = 0.25 \times 4kT \frac{(\omega C_{gs})^2}{g_m} \Delta f + 2q |I_G| \Delta f. \quad (54)$$

Like in drain noise, the leading factor in the channel induced term represents an averaging of the coupling effect along the channel. Its actual value differs somewhat in literature, partly according to the FET type under investigation, partly due to different ways of defining and including terms, cf. ref's [4]p.91, [9]p.245, and [14]. The value of .25 is chosen halfway between the figures in the first two references. The capacitive nature of the term is emphasized by proportionality between the mean squared induced noise current and the squared susceptance of the gate capacitance, in turns to the squared frequency. Originating from the same noise sources in the channel that formerly gave the first term in Eq.(53), the induced gate noise and the drain noise are correlated having the correlation coefficient

$$c = \frac{\overline{\dot{i}_{ng,induced} \dot{i}_{nd,thermal}^*}}{\sqrt{\overline{\dot{i}_{ng,induced}^2} \overline{\dot{i}_{nd,thermal}^2}}} = j 0.4. \quad (55)$$

We shall see below that it is important to keep track on correlations between noise sources when the noise properties of composite circuits are determined.

IV-3 Noise Characterization of Two-Ports

Small-signal parameters like y or s -parameters provide concentrated characterization of building blocks in electronic circuit that may contain many components. The parameters are both measurable under well defined conditions and directly suitable in design of deterministic signal handling. The number of independent noise sources inside electronic components and subcircuits requires equally simple and concentrated approaches with respect to noise characterization and design for low noise properties. The noise figure fulfill this need and is the most common way of specifying electronic devices with respect to noise. Noise temperature is an alternative or supplement to the noise figure and both concepts are considered in details below. Like the small-signal parameters presentation in the foregoing chapter, the discussion is concentrated on the important two-port case. The corresponding multiport properties may be found elsewhere in literature, for instance ref's [15] or [16].

Noise Figure

At a given frequency the noise figure concentrates the effect of all internal noise sources of a two-port that is driven by a signal generator into a single figure F , the so-called noise figure⁴. The basic definition is, [17],

$$F = \frac{N_{out,tot}/\Delta f}{N_{out,g0}/\Delta f} = \frac{\text{total available output noise power per unit bandwidth}}{\text{available output noise power per unit bandwidth caused by the generator admittance or impedance @ 290[K]}} \quad (56)$$

It is assumed in measurements that the noise powers $N_{out,tot}$ and $N_{out,g0}$ are determined in a bandwidth, which is sufficiently narrow to take the underlying noise spectra constant, so the noise figure becomes independent of bandwidth. To emphasize this assumption, F above is sometimes referred to as the spot noise figure to be distinguished from the bandwidth dependent so-called average noise figure [17]. The available output powers are independent of the actual loading of the two-port and this property conveys to the noise figure. However, the generator impedance or admittance is significant to the way by which internal noise sources contribute to the output. In consequence, a noise figure F for a two-port is meaningless without a specification of the corresponding generator impedance or admittance. In this

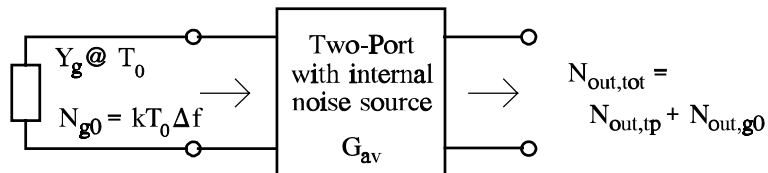


Fig.23 Two-Port with internal noise sources. Y_g is kept at the reference temperature $T_0=290K$. $N_{out,tp}$ is the effect of the internal two-port noise sources.

4) Some authors distinguish between noise factor F and the db-scaled noise figure $NF=10.\log(F)$. No such distinctions between terms are made below but, clearly, it is always pointed out whether we are using dB scale or not.

context the generator impedance or admittance is a remedy for noise characterization of the two-port. To get unambiguous two-port noise figures, the generator must be settled at a reference temperature, which by definition is set to $T_0 = 290$ K.

Subdividing the total output noise into terms stemming from sources internal to the two-port and from the generator admittance, as indicated in Fig.23, yields

$$N_{out,tot} = F N_{out,g0} = N_{out,tp} + N_{out,g0} \quad \Rightarrow \quad (57)$$

$$N_{out,tp} = (F - 1) N_{out,g0} = (F - 1) G_{av} N_{g0} = (F - 1) G_{av} k T_0 \Delta f$$

Comparing the upper and lower part shows that the two-ports own contribution to the output noise is a fraction $(F-1)/F$ of the total output noise. In the last sequence above, the generator contribution is referred back to the input through the available power gain G_{av} , which - like the noise figure - is independent of the two-port load and therefore particularly useful in noise calculations. If also the two-port noise is referred to the input side and called $N_{in,tp}$, we get

$$N_{out,ip} = G_{av} N_{in,ip} \quad \Rightarrow \quad N_{in,ip} = (F - 1) k T_0 \Delta f \quad (58)$$

If there are no significant internal noise sources, the minimum value of a two-port noise figure is one. This is the case with circuits build from ideal lossless, passive components that do not radiate or receive radio signals.

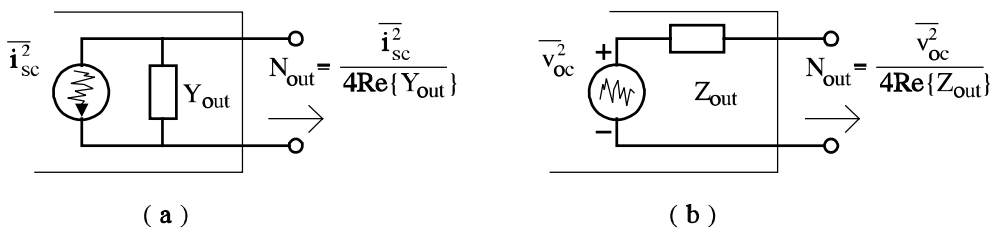


Fig.24 Noise equivalent circuit for the output side of a two-port in a) Norton and b) Thevenin equivalent forms.

The output from the two-port may be described by either a Norton or a Thevenin equivalent circuit as shown in Fig.24. In the first case the available output noise power is given by the real part of the output admittance in conjunction with the squared noise short-circuit current i_{sc}^2 . The output admittance depends on the two-port parameters and the generator admittance as we saw in Chap.III, p.6. To calculate the noise figure according to the definition, the short circuit noise current must be available in two versions, $i_{sc|tot}^2$ representing the joint effect of all noise contributions in the two-port and the generator network, and $i_{sc|g0}^2$ holding the output noise short-circuit current caused by generator admittance or impedance alone. In duality, the Thevenin equivalent in Fig.24(b) expresses available output noise powers in terms of the two-port output impedance and the squared noise open-circuit voltage, either the total, $v_{oc|tot}^2$, or the contribution from the generator alone, $v_{oc|g0}^2$. Output admittances or impedances cancel when taking ratios of available powers in the two equivalent representations, so the noise figure is expressed solely in ratios of squared noise short-circuit currents or open-circuit voltages,

$$F = \frac{\overline{i_{sc}^2} \Big|_{tot}}{\overline{i_{sc}^2} \Big|_{Y_g}} = \frac{\overline{v_{oc}^2} \Big|_{tot}}{\overline{v_{oc}^2} \Big|_{Z_g}} \quad (59)$$

These results - sometimes called Van der Ziels equations [18] - are highly useful for computing noise figures in composite networks, for instance device models as it was anticipated by example IV-2-1 on page 18. The effects of separate noise sources are combined by accumulating their contributions to the short-circuit current or open-circuit voltage. This way of calculating noise figures free us from the crucial problem that the concept of available power at the output of the two-port implicitly assumes positive real parts of the output admittance or impedance. If the two-port is potentially unstable, this condition may not be satisfied. Nevertheless the two-port may still be useful in practice if it is properly loaded. By the equations above the noise figure of the two-port may also be calculated and it is still independent of the actual load.⁵

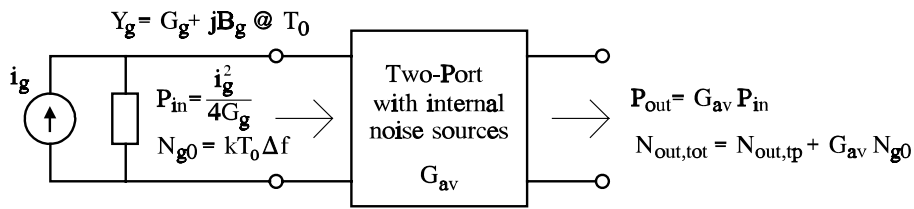


Fig.25 Noisy two-port connected to a signal source. P_{in} , P_{out} are available signal powers, and N_{Yg} , $N_{out,tot}$ are the available noise powers at either side of the two-port.

Noise figures may also be expressed in terms of signal to noise ratios, SNR's, at the input and output side of two-ports. Applying a signal source of admittance Y_g and available signal power P_{in} to the input side of a two-port as shown by Fig.25, we get a development from the formalized definition in Eq.(56) that reads

$$F = \frac{N_{out,tot}}{N_{out,g0}} = \frac{P_{in}N_{out,tot}}{P_{in}G_{av}N_{g0}} = \frac{P_{in}/N_{g0}}{P_{out}/N_{out,tot}} = \frac{SNR_{in,0}}{SNR_{out}} . \quad (60)$$

Here G_{av} is the available power gain of the two-port that is driven by a generator of admittance Y_g and P_{out} is the available signal output power. Since the noise figure cannot be smaller than one, the noise figure may be considered as the divisor by which a signal to noise ratio is deteriorated in passage through the two-port

$$SNR_{out} = \frac{1}{F} SNR_{in,0} . \quad (61)$$

5) The more formalistic approach of extending noise figure definitions to encompass two-ports that get negative output conductance or resistance is given in [15] or [16].

This way of interpreting noise figures may be useful when it is adequate to have the generator impedance at reference temperature $T_0=290\text{K}$ as assumed by the noise figure definition. If this is not the case, a so-called effective noise figures satisfying the SNR conditions above at a given temperature, is sometimes introduced. However, in such cases it makes more sense to use the concept of two-port noise temperatures, which are described in the next paragraph.

Example IV-3-1 (noise figure measurement)

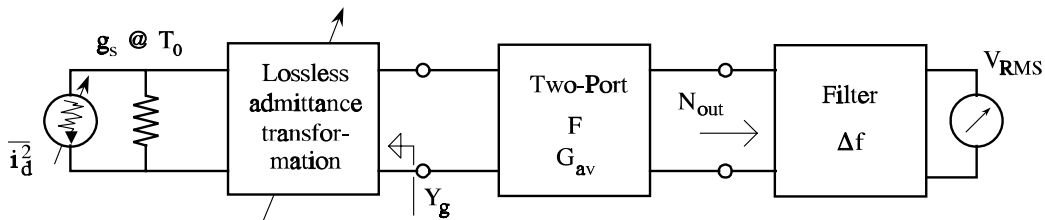


Fig.26 Setup for noise figure measurement. The adjustable noise current source is typically a diode where the noise is directly controlled by the dc-current.

A principle for measuring two-port noise figures is shown in Fig.26. The generator admittance for the noise figure to be measured is provided by an impedance transforming network, which is assumed to be lossless. The available noise power out of the transformer equals the available power from the source. The source includes a conductance g_s held at the reference temperature and an additional, adjustable noise current generator \bar{i}_d^2 . The output noise power N_{out} is the portion of the available output power within the noise-bandwidth Δf of the filter that connects to and RMS voltmeter. The squared meter reading is proportional to N_{out} . Two readings are required to measure a noise figure. First the noise generator \bar{i}_d^2 is kept at zero and we get the output reading $V_{RMS,0}$. Second, the noise generator is adjusted to double the output power, i.e. to a reading 3dB or $\sqrt{2}$ above the first one, i.e.

$$\begin{aligned} \underline{\text{step 1 :}} \quad V_{RMS,0} &\sim N_{out,0} = G_{av} F k T_0 \Delta f \\ \underline{\text{step 2 :}} \quad V_{RMS} &= \sqrt{2} V_{RMS,0} \sim 2 N_{out,0} = G_{av} F k T_0 \Delta f + G_{av} \frac{\bar{i}_d^2}{4 g_s} \end{aligned} \quad (62)$$

By this procedure the two terms in the last reading are equal. The adjustable noise source is often a diode where the dc-current controls the squared noise current, cf.Eq.(33), so we get

$$F = \frac{\bar{i}_d^2}{4 k T_0 g_s \Delta f} \underset{\text{diode}}{=} \frac{I_D}{2 g_s V_t}, \quad \text{where } V_t = \frac{k T_0}{q} \approx 25,0 \text{ mV} \quad (63)$$

The last noise figure expression shows that a DC-meter, which measure the diode current I_D , may be calibrated directly in noise figures.

Example IV-3-1 end

Noise Temperature of Two-Ports

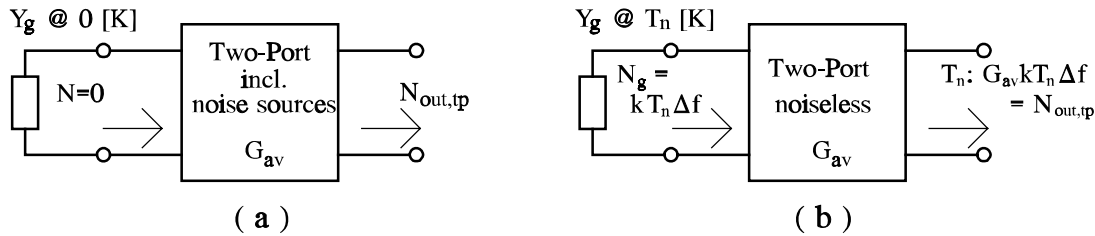


Fig.27 Noise temperature of two-port, T_n . The noise generated inside the two-port in (a) is ascribed to the generator admittance at temperature T_n in (b).

An effective noise temperature was introduced for one-ports by Eq.(25) as a method of specifying its available noise power. Without regards to the actual noise sources, the noise temperature was the temperature in Kelvin of the one-port, had all noise been of thermal origin. In extension, the noise temperature of a two-port driven from a generator is defined as the temperature of the generator if the entire noise contribution from inside the two-port is ascribed to thermal noise from the generator impedance or admittance, cf.[17]. The conditions are depicted in Fig.27, where in (a) the source hypothetically is kept at zero Kelvin, so the available output noise power comes solely from internal sources of the two-port. Assuming no internal noise sources, the noise temperature T_n provides the same output noise power if the temperature of the generator admittance is raised to T_n [K]. Like noise figures, the noise temperature of a two-port needs a specification of the pertinent generator admittance or impedance. Using Eq.(58), the relationship between the two noise characterizations becomes,

$$N_{out,ip} = G_{av}(F - 1)kT_0\Delta f = G_{av}kT_n\Delta f \Rightarrow \begin{cases} T_n = (F - 1)T_0, & (a) \\ F = 1 + \frac{T_n}{T_0}. & (b) \end{cases} \quad (64)$$

where T_0 still is the reference temperature 290 [K].

If the effective noise temperature of the generator admittance in Fig.27 is T_g before any connection to the two-port, the generator itself contributes to the output available power by an amount we call $N_{out,g}$. Including noise from the two-port, the total output available noise power is expressed

$$N_{out,tot} = N_{out,tp} + N_{out,g} = G_{av} k T_n \Delta f + G_{av} k T_g \Delta f = G_{av} k (T_n + T_g) \Delta f . \quad (65)$$

Thus, the two noise temperatures are added to express the total, resultant noise. It is this additive property that makes noise temperatures a convenient tool for noise calculations handling other temperatures than the noise figure reference T_0 .

Noise in Cascaded Two-Ports

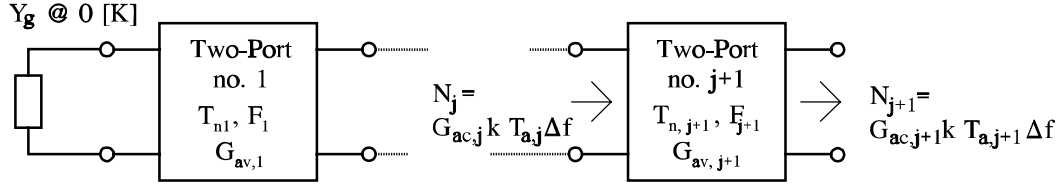


Fig.28 Input and output available noise powers around port no. $j+1$ in a chain of noisy two-ports. $G_{av,j}$ is the accumulated available gain and $T_{a,j}$ is the accumulated noise temperature.

If more two-ports are cascaded, the first one will usually be the most significant with respect to noise figure or noise temperature for the whole chain. To see this, we calculate the contribution from the $j+1$ 'th two-port in the chain. The preceding j ports present an available noise power N_j at the input to port number $j+1$. Like the first expression in Eq.(64), N_j is related to the accumulated noise temperature $T_{a,j}$ and accumulated available gain $G_{aa,j}$ through

$$N_j = G_{aa,j} k T_{a,j} \Delta f, \quad \text{where} \quad G_{aa,j} = G_{av,1} G_{av,2} \cdots G_{av,j}. \quad (66)$$

Seen from the $j+1$ 'th two-port, the product $G_{aa,j} T_{a,j}$ is also the effective generator noise temperature. To include the noise that is generated by this port, a noise temperature $T_{n,j+1}$ must be added to yield

$$N_{j+1} = G_{av,j+1} k \left[G_{aa,j} T_{a,j} + T_{n,j+1} \right] \Delta f = G_{av,j+1} k \left[G_{aa,j} (T_{a,j} + \Delta T_{a,j}) \right] \Delta f. \quad (67)$$

By the last rewriting the noise contribution from two-port number $j+1$ is considered as an increment of the accumulated noise temperature from the j 'th to the $j+1$ 'th step. Equating terms gives

$$\Delta T_{a,j} = \frac{T_{n,j+1}}{G_{aa,j}}. \quad (68)$$

Including the recursion for the gains, the development in noise temperature when two-ports are cascaded is given by

$$T_{n,chain} = T_{n,1} + \frac{T_{n,2}}{G_{av,1}} + \frac{T_{n,3}}{G_{av,1} G_{av,2}} + \frac{T_{n,4}}{G_{av,1} G_{av,2} G_{av,3}} \cdots + \frac{T_{n,j+1}}{G_{av,1} G_{av,2} \cdots G_{av,j}} \cdots. \quad (69)$$

Translating to noise figures, repeated use of Eq.(64) provides

$$T_{n,chain} = T_0 (F_{chain} - 1), \quad T_{n,j} = T_0 (F_j - 1) \Rightarrow \quad (70)$$

$$F_{chain} = F_1 + \frac{F_2 - 1}{G_{av,1}} + \frac{F_3 - 1}{G_{av,1} G_{av,2}} + \frac{F_4 - 1}{G_{av,1} G_{av,2} G_{av,3}} \dots + \frac{F_{j+1} - 1}{G_{av,1} G_{av,2} \dots G_{av,j}} \dots . \quad (71)$$

The last expression is called Friis' formula for cascaded two-ports [19]. Equations (69) and (71) show that if the first two-port in a chain has sufficient gain, the noise temperature or noise figure of the first stage dominate the whole chain.

Example IV-3-2 (link budget)

The radio link system in Fig.29 operates in QPSK modulation and transmits the bit sequence b_k at rate $R_b=8.2$ Mbps. The total attenuation from the transmitter output to the RF amplifier input is 137 dB. All components are supposed to be matched. The antenna has noise temperature $T_{ant}=195$ K and the RF amplifier has noise figure $F=6.5$ dB. Find the transmitter output power P_{tr} that gives the bit error rate $BER=10^{-6}$ after demodulation.

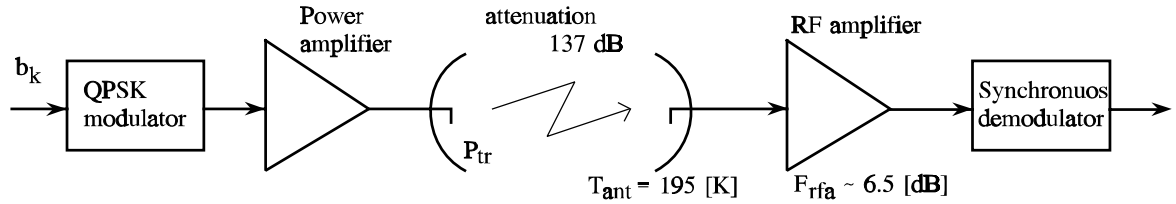


Fig.29 Block diagram for a radio link.

Bit error rates in QPSK-modulation corresponds to PSK-PRK modulation, which was discussed in chap.I, where Fig.I-29 provides the signal to noise ratio per bit, BER,

$$BER = Q\left(\sqrt{\frac{2 E_b}{\eta}}\right) = 10^{-6} \quad \Rightarrow \quad (72)$$

$$\frac{E_b}{\eta} = \frac{E_b}{k T_{eff}} = 10.5 [dB] \sim 11.2 . \quad (73)$$

The noise power spectral density is held in $\eta=kT_{eff}$ with T_{eff} being the total effective noise temperature at the RF-amplifier input. To find T_{eff} , the amplifier noise figure is converted to noise temperature T_{rfa} by Eq.(64)(a). We get

$$T_{eff} = T_{ant} + T_{rfa} , \quad T_{rfa} = T_0 (F_{rfa} - 1) , \quad F_{rfa} \sim 6.5 [dB] \sim 4.47 \Rightarrow \quad (74)$$

$$T_{rfa} = 290 (4.47 - 1) = 1006. [K] , \quad T_{eff} = 195 + 1006 = 1201 [K] .$$

From Eq.(73), the required energy per bit at the receiver input is

$$E_b = 11.2 \cdot k T_{eff} = 11.2 \cdot 1.381 \cdot 10^{-23} [Ws/K] \cdot 1201 [K] = 1.858 \cdot 10^{-19} [Ws]. \quad (75)$$

To calculate the corresponding input power, we recall that in QPSK the symbol time is twice the input bit period. However, two bits are simultaneously transmitted in quadrature, so the necessary input power is the ratio of the bit energy over the input bit period, i.e.

$$P_{in} = E_b R_b = 1.858 \cdot 10^{-19} \cdot 8.2 \cdot 10^6 = 1.523 \cdot 10^{-12} [W]. \quad (76)$$

Taking attenuation from transmitter to receiver into account, the transmitter power becomes

$$D \sim 137 [dB] \sim 5.01 \cdot 10^{13} \Rightarrow \quad (77)$$

$$\underline{P_{tr}} = P_{in} D = 1.523 \cdot 10^{-12} \cdot 5.01 \cdot 10^{13} = \underline{76.30 [W]}.$$

Suppose the transmitter amplifier has a maximum undistorted output of $P_{tr}=40[W]$, and the receiver is improved by inserting a low noise amplifier, LNA, of 6 dB gain in front of the receiver as shown in Fig.30. Find the noise figure requirement F_{LNA} to the low-noise amplifier, if the resultant BER should remain unchanged.

Unaffected BER requires unaffected signal to noise ratio at the detector or equivalently, that the total effective noise temperature at the receiver input is reduced by the same factor as is the input power, i.e.

$$T_{eff,new} = T_{eff} \frac{P_{tr,new}}{P_{tr}} = 1201 \cdot \frac{40}{76.30} = 629.6 [K]. \quad (78)$$

Subtracting antenna noise temperature from $T_{eff,new}$ gives the noise temperature T_{cas} of the two cascaded amplifiers, which is expressed through Eq.(69). Therefore,

$$T_{cas} = T_{LNA} + \frac{T_{amp}}{G_{LNA}} = T_{eff,new} - T_{ant} = 629.6 - 195 = 434.6 [K], \quad (79)$$

$$G_{LNA} \sim 6 [dB] \sim 3.98 \Rightarrow T_{LNA} = 434.6 - 1006 / 3.98 = 181.8 [K].$$

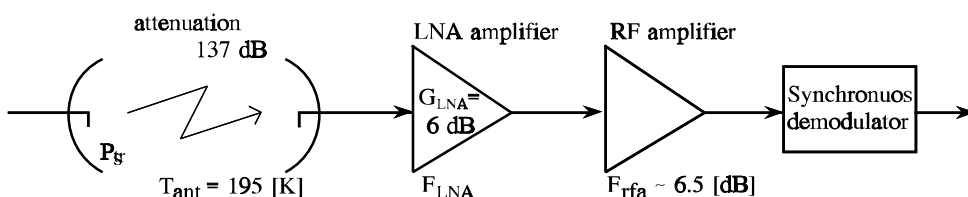


Fig.30 Inclusion of a low-noise amplifier, LNA, in front of the receiver from Fig.29.

Calculating back to noise figure by Eq.(64)(b) yields the LNA noise figure requirement,

$$\underline{F_{LNA}} = 1 + \frac{T_{LNA}}{T_0} = 1 + \frac{181.8}{290} = \underline{1.627} \sim \underline{2.11 [dB]} . \quad (80)$$

Example IV-3-2 end

Noise Representation in Two-Ports

Noise figures and temperatures are suitable for calculating the type of noise performance required in system design, for instance signal-to-noise ratio degradations and bit error rates. Like gain functions, noise figure and temperature depends on the operating conditions of the two-port in the form of either admittance or impedance of the driving generator. It is desirable, therefore, to have a more basic noise characterization that is self-contained and from which questions about the best way of using a given two-port regarding noise may be investigated.

Terminal currents are the dependent variables in conventional y-parameter small-signal characterization of two-ports, so in this representation it is natural to include noise properties by paralleling noise currents across the two ports as shown in Fig.31. The two noise generators represent the joint contributions from all noise sources inside the two-port to the short-circuit terminal noise currents. An internal noise source may contribute to the short-circuit currents at both the input and the output side of the two-port, so the two equivalent representations $\overline{i_{n1}^2}$ and $\overline{i_{n2}^2}$ may be correlated. The noise current i_{n1} and i_{n2} have real power spectra $S_1(\omega)$ and $S_2(\omega)$ respectively. They are normalized to 1Ω . In a bandwidth Δf around center frequency f_0 the two noise sources are characterized by the noise conductances $G_{n1}(f_0)$ and $G_{n2}(f_0)$ defined through the spectra

$$\begin{aligned} G_{n1}(f_0) : \overline{i_{n1}^2} &= 2S_1(\omega_0)\Delta f = 4kT_0G_{n1}(f_0)\Delta f , \\ G_{n2}(f_0) : \overline{i_{n2}^2} &= 2S_2(\omega_0)\Delta f = 4kT_0G_{n2}(f_0)\Delta f . \end{aligned} \quad (81)$$

Using noise conductances G_{n1} and G_{n2} is a convenient method of quantifying noise levels, but observe that the figures are not ascribed to any particular circuit elements. The correlation coefficient between the input and the output noise is defined by

$$c = \frac{\overline{i_{n1} i_{n2}^*}}{\sqrt{\overline{i_{n1}^2} \overline{i_{n2}^2}}} = \frac{S_{21}(\omega_0)}{\sqrt{S_1(\omega_0) S_2(\omega_0)}} , \quad (82)$$

where $S_{21}(\omega)$ is the cross spectrum between the input and the output noise currents. Even when the power spectra for the two currents are real, their cross spectrum may be complex,

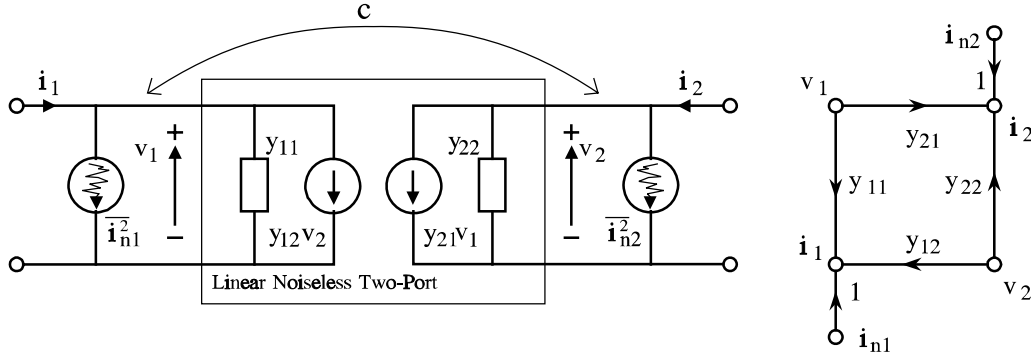


Fig.31 Noise representation in a linear two-port by two short-circuit noise currents. The possible correlation is expressed through the complex coefficient c .

and so does the correlation coefficient c . Four parameters are therefore required to describe the noise properties of the two-port at a given frequency, G_{n1} , G_{n2} , $\text{Re}\{c\}$, and $\text{Im}\{c\}$.

The representation in Fig.31 may be useful in basic noise analysis, for instance of device models where the short-circuit noise currents at either port and their possible correlation often are obtained easily. In signal calculations, however, it is desirable to let all noise contributions refer to the input side of the two port. A common representation is here to use a series noise voltage and a shunt noise current as shown by Fig.32, where γ denotes the correlation coefficient between the noise generators [20]. We may establish the connection between the two representations by setting their terminal short-circuit noise currents equal to each other. The flow graphs illuminate this process and give

$$\left. \begin{array}{l} \text{input port, } i_1 : \quad i_{n1} = i_{n,tot} - y_{11}v_n, \quad (a) \\ \text{output port, } i_2 : \quad i_{n2} = -y_{21}v_n, \quad (b) \end{array} \right\} \Rightarrow \left\{ \begin{array}{l} i_{n,tot} = i_{n1} - \frac{y_{11}}{y_{21}}i_{n2}, \quad (c) \\ v_n = -\frac{1}{y_{21}}i_{n2}. \quad (d) \end{array} \right. \quad (83)$$

Before setting up the relationship between correlations in the two representations, the shunt current $i_{n,tot}$ is split into a part i_n that is completely uncorrelated with v_n and a part that is

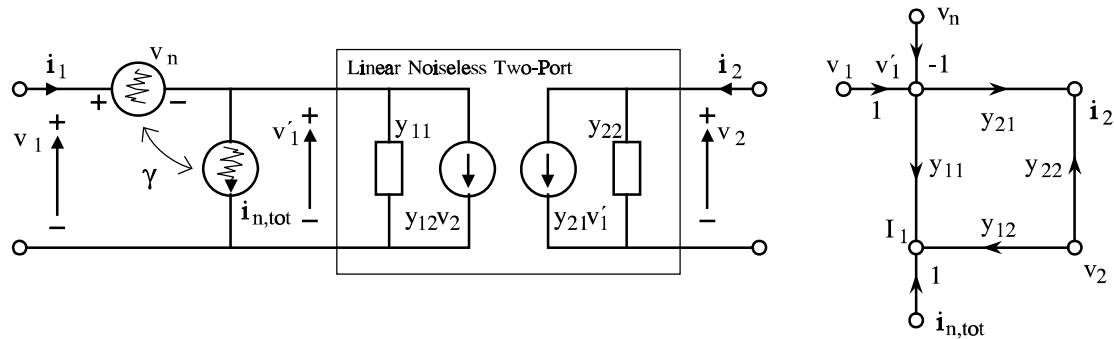


Fig.32 Linear two-port noise representation referred to the input port. Series noise voltage and shunt noise current may be dependent with complex correlation coefficient γ .

fully correlated. The last one follows v_n by a constant, complex scale factor that has dimension of admittance and therefore is denoted Y_{cor} .⁶ We get

$$\mathbf{i}_{n,tot} = \mathbf{i}_n + Y_{cor} v_n \quad \text{where} \quad \overline{\mathbf{i}_n^* v_n^*} = 0 \quad \Rightarrow \quad \gamma \equiv \frac{\overline{\mathbf{i}_{n,tot} v_n^*}}{\sqrt{\overline{v_n^2} \overline{\mathbf{i}_{n,tot}^2}}} = Y_{cor} \sqrt{\frac{\overline{v_n^2}}{\overline{\mathbf{i}_{n,tot}^2}}} , \quad (84)$$

so Y_{cor} may substitute for the γ correlation coefficient. Equations (82) and (83)(a-b) provide

$$\begin{aligned} \overline{\mathbf{i}_{n2}^* \mathbf{i}_{n1}} &= -y_{21}^* \left(\overline{v_n^* \mathbf{i}_{n,tot}} - y_{11} \overline{v_n^2} \right) = -y_{21}^* \left(Y_{cor} - y_{11} \right) \overline{v_n^2} = \frac{-1}{y_{21}} \left(Y_{cor} - y_{11} \right) \overline{\mathbf{i}_{n2}^2} \Rightarrow \\ Y_{cor} &= y_{11} - y_{21} \frac{\overline{\mathbf{i}_{n1} \mathbf{i}_{n2}^*}}{\overline{\mathbf{i}_{n2}^2}} = y_{11} - y_{21} c \sqrt{\frac{\overline{\mathbf{i}_{n1}^2}}{\overline{\mathbf{i}_{n2}^2}}} . \end{aligned} \quad (85)$$

Like the first equivalent circuit, the one with noise referred to the input port may be characterized by equivalent noise components, resistance R_n to describe the series noise voltage and conductance G_n to describe the uncorrelated part of the shunt current. They are defined and - by comparing equivalent circuits - related to the previous parameters in Eq.(81) through

$$\begin{aligned} R_n : \quad \overline{v_n^2} &= 4kT_0 R_n(f_0) \Delta f , \quad G_n : \quad \overline{\mathbf{i}_n^2} = 4kT_0 G_n(f_0) \Delta f , \\ \text{where } R_n &= \frac{G_{n2}}{|y_{21}|^2} . \quad \text{where } G_n = G_{n1} + G_{n2} \frac{|y_{11} - Y_{cor}|^2}{|y_{21}|^2} . \end{aligned} \quad (86)$$

Four parameters are again used to characterize the noise performance of the two-port, R_n , G_n , and the two components of Y_{cor} . A direct representation of these noise parameters is shown in Fig.33(b). Due to the parallelling of two admittances of opposite sign, the port gives no loading to signal transmissions, but a short-circuit on either port will carry the full squared noise current, $\overline{\mathbf{i}_{n,tot}^2}$, while the opposite open port shows the squared noise voltage $\overline{v_n^2}$.

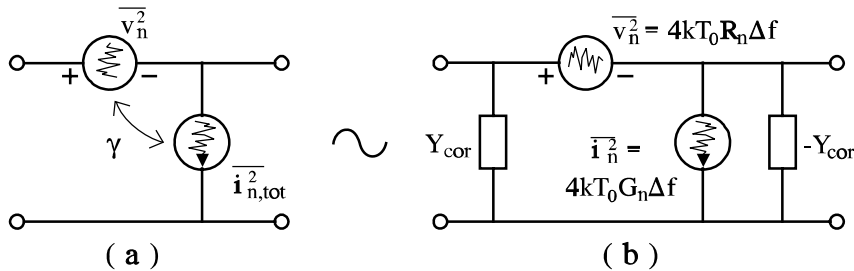


Fig.33 Equivalent representation of a noisy two-port specified by parameters R_n , G_n , and the noiseless correlation admittance Y_{cor}

6) Be aware that the correlation admittance Y_{cor} is not uniquely defined in the literature. Here we follow the definition in [20].

Minimum Noise Conditions

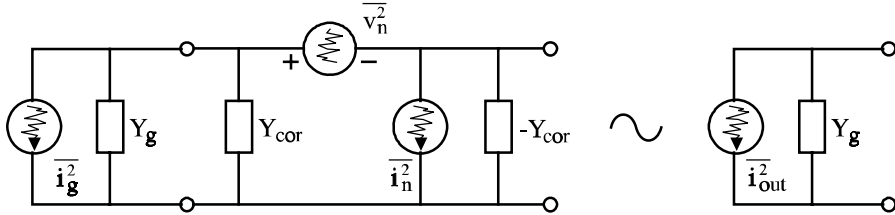


Fig.34 Equivalent circuit for calculating the noise figure of a two-port connected to a source, which by definition must have the reference temperature $T_0=290[\text{K}]$.

Concentrating the noise characterization to the input side of a two-port means that the rest of the port is noiseless as indicated in Fig.32. A noiseless two-port has noise figure equal to one and, according to the cascading rule in Eq.(71), this will not influence the noise figure when the two port is connected to a generator. To investigate the noise figure of the complete two-port, it suffices to consider the generator and the noise input equivalent parts that are shown in Fig.34. The definition of the noise figures assumes that the generator admittance $Y_g=G_g+jB_g$ has settled at the reference temperature T_0 , so its squared noise current becomes

$$\overline{i_g^2} = 4kT_0G_g(f_0)\Delta f. \quad (87)$$

Now, Eq.(59) can be used to calculate the noise figure by taking ratios between short-circuit contributions. We get

$$\begin{aligned} F &= \frac{\overline{i_{out}^2}|_{tot}}{\overline{i_{out}^2}|_{Y_g}} = \frac{\overline{i_g^2} + \overline{i_n^2} + \overline{v_n^2}|Y_g + Y_{cor}|^2}{\overline{i_g^2}} \\ &= 1 + \frac{G_n}{G_g} + \frac{R_n}{G_g} [(G_g + G_{cor})^2 + (B_g + B_{cor})^2], \end{aligned} \quad (88)$$

where the last equation includes the noise parameters from Eq.(86) and the components of the complex correlation admittance $Y_{cor}=G_{cor}+jB_{cor}$. To find the generator admittance Y_{nfo} that minimizes the noise figure, it is readily seen, that one requirement toward minimizing the noise figure is to use a generator susceptance, which cancels the correlation susceptance. This is called noise tuning, i.e.

$$\underline{\text{Noise Tuning}} : \quad B_g = B_{nfo} = -B_{cor}. \quad (89)$$

The conductance that simultaneously minimizes the noise figure is found by setting the partial derivative of Eq.(88) with respect to generator conductance equal zero,

$$\frac{\partial F}{\partial G_g} \Bigg|_{B_g=-B_{cor}} = \frac{1}{G_g^2} (G_g^2 R_n - G_{cor}^2 R_n - G_n) = 0 \quad \Rightarrow \quad G_g = G_{nfo} = \sqrt{\frac{G_n}{R_n} + G_{cor}^2}. \quad (90)$$

The 2nd order derivative becomes $2R_n G_{nfo}^2 / G_g^3$, which is positive if G_g is positive, so the result above gives a minimum in noise figure. Simultaneous use of the two conditions is called noise matching, where

$$\underline{\text{Noise Matching}} : \quad Y_g = Y_{nfo} \equiv G_{nfo} + jB_{nfo} = \sqrt{\frac{G_n}{R_n} + G_{cor}^2 - jB_{cor}}. \quad (91)$$

The corresponding minimum noise figure is found by inserting Y_{nfo} into Eq.(88),

$$\begin{aligned} F_{min} &= 1 + \frac{R_n}{G_{nfo}} \left[\frac{G_n}{R_n} + (G_{nfo} + G_{cor})^2 \right] = 1 + \frac{R_n}{G_{nfo}} \left[2G_{nfo}^2 + 2G_{nfo}G_{cor} \right] \\ &= 1 + 2R_n(G_{cor} + G_{nfo}). \end{aligned} \quad (92)$$

Substituting this result back into Eq.(88), the noise figure with an arbitrary generator admittance is written

$$\begin{aligned} F &= 1 + \frac{R_n}{G_g} \left[\frac{G_n}{R_n} + G_g^2 + G_{cor}^2 + 2G_gG_{cor} + (B_g - B_{nfo})^2 + 2G_gG_{nfo} - 2G_gG_{nfo} \right] \\ &= 1 + \frac{R_n}{G_g} \left[2G_gG_{cor} + 2G_gG_{nfo} \right] + \frac{R_n}{G_g} \left[(G_g - G_{nfo})^2 + (B_g - B_{cor})^2 \right] \\ &= F_{min} + \frac{R_n}{G_g} |Y_g - Y_{nfo}|^2. \end{aligned} \quad (93)$$

Note, in this form four parameters are still needed to characterize the noise properties of the two-port, namely F_{min} , R_n , and the two components G_{nfo} , B_{nfo} of the generator admittance Y_{nfo} that minimizes the noise figure.

Constant Noise Figure Circles

Commonly the optimum generator admittance with respect to noise for a transistor differs from the choice that would be optimal regarding gain and stability considerations alone. The designer must compromise between the two concerns. An aid to decisions is to map contours of constant noise figures. They constitute a system of circles with centers in y_{gcn} and radii g_{cn} , where

$$y_{gcn} = Y_{nfo} + \frac{F - F_{min}}{2R_n}, \quad g_{cn} = \sqrt{\left(\frac{F - F_{min}}{2R_n}\right)^2 + \frac{G_{nfo}}{R_n}(F - F_{min})}. \quad (94)$$

These expressions are verified by observing that a circle of center y_{gcn} and radius g_{cn} in the complex Y_g -plane is described by

$$|Y_g - y_{gcn}|^2 = Y_g Y_g^* + y_{gcn} y_{gcn}^* - Y_g^* y_{gcn} - Y_g y_{gcn}^* = g_{cn}^2. \quad (95)$$

Expanding the noise figure in Eq.(93) with the circle expression in mind, using $G_g = \frac{1}{2}(Y_g + Y_g^*)$, gives temporarily

$$\begin{aligned} |Y_g - Y_{nfo}|^2 &= Y_g Y_g^* + Y_{nfo} Y_{nfo}^* - Y_g Y_{nfo}^* - Y_g^* Y_{nfo} = \frac{F - F_{\min}}{2R_n} (Y_g + Y_g^*) \Rightarrow \\ Y_g Y_g^* - Y_g \left(Y_{nfo}^* + \frac{F - F_{\min}}{2R_n} \right) - Y_g^* \left(Y_{nfo} + \frac{F - F_{\min}}{2R_n} \right) &= -Y_{nfo} Y_{nfo}^*. \end{aligned} \quad (96)$$

By this step the center y_{gcn} in Eq.(94) is identified from the coefficients to either Y_g or Y_g^* . To complete the circle requirement and get the radius, we add $y_{gcn} y_{gcn}^*$ to both sides of the last equation, i.e.

$$\begin{aligned} g_{cn}^2 &= Y_g Y_g^* - Y_g y_{gcn}^* - Y_g^* y_{gcn} + y_{gcn} y_{gcn}^* = y_{gcn} y_{gcn}^* - Y_{nfo} Y_{nfo}^* \\ &= \left(Y_{nfo} + \frac{F - F_{\min}}{2R_n} \right) \left(Y_{nfo}^* + \frac{F - F_{\min}}{2R_n} \right) - Y_{nfo} Y_{nfo}^* = \left(\frac{F - F_{\min}}{2R_n} \right)^2 + \frac{G_{nfo}}{R_n} (F - F_{\min}). \end{aligned} \quad (97)$$

The set of parameters containing the minimum noise figure F_{\min} , the series noise equivalent resistance R_n , and the optimal generator admittance Y_{nfo} , or the equivalent sets based on the generator reflection coefficient, are becoming more and more common in device data sheets. The relationship between the two forms is straightforward to establish, albeit it needs a little algebra. Reflection coefficients for impedances and admittances were introduced in Chap.II sec.8. With reference impedance Z_0 , which is real, the generator and optimum admittances are expressed by their reflection coefficients through

$$Y_g = \frac{1}{Z_0} \frac{1 - \Gamma_g}{1 + \Gamma_g}, \quad Y_{nfo} = \frac{1}{Z_0} \frac{1 - \Gamma_{nfo}}{1 + \Gamma_{nfo}} \Rightarrow \quad (98)$$

$$\left\{ \begin{array}{l} |Y_g - Y_{nfo}|^2 = \frac{1}{Z_0^2} \left| \frac{(1 - \Gamma_g)(1 + \Gamma_{nfo}) - (1 - \Gamma_{nfo})(1 + \Gamma_g)}{(1 + \Gamma_g)(1 + \Gamma_{nfo})} \right|^2 = \frac{4}{Z_0^2} \frac{|\Gamma_g - \Gamma_{nfo}|^2}{|1 + \Gamma_g|^2 |1 + \Gamma_{nfo}|^2}, \\ G_g = \frac{|Y_g + Y_g^*|}{2} = \frac{1}{2Z_0} \left| \frac{(1 - \Gamma_g)(1 + \Gamma_g^*) + (1 - \Gamma_g^*)(1 + \Gamma_g)}{(1 + \Gamma_g)(1 + \Gamma_g^*)} \right| = \frac{1}{Z_0} \frac{1 - |\Gamma_g|^2}{|1 + \Gamma_g|^2}. \end{array} \right. \quad (99)$$

Inserting into the last expression from Eq.(93) yields

$$F = F_{\min} + \frac{4R_n}{Z_0} \frac{\left| \Gamma_g - \Gamma_{nfo} \right|^2}{\left(1 + |\Gamma_g|^2 \right) \left(1 + \Gamma_{nfo} \right)^2}. \quad (100)$$

Moving from admittance plane to reflection plane is represented by the Smith chart. The underlying transformation maps circles into circles, so contours of constant noise figures in an admittance plane become also a system of circles in a reflection plane or a Smith chart. To get the corresponding centers and radii we rewrite Eq.(100) to read

$$\Gamma_g \Gamma_g^* + \Gamma_{nfo} \Gamma_{nfo}^* - \Gamma_g \Gamma_{nfo}^* - \Gamma_g^* \Gamma_{nfo} = \left(1 + \Gamma_g \Gamma_g^* \right)^2 N, \\ \text{where } N = \frac{F - F_{\min}}{4R_n/Z_0} \left| 1 + \Gamma_{nfo} \right|^2 \Rightarrow \quad (101)$$

$$\Gamma_g \Gamma_g^* + \frac{\Gamma_{nfo} \Gamma_{nfo}^*}{1+N} - \Gamma_g \frac{\Gamma_{nfo}^*}{1+N} - \Gamma_g^* \frac{\Gamma_{nfo}}{1+N} = N + \frac{\Gamma_{nfo} \Gamma_{nfo}^*}{(1+N)^2} - \frac{\Gamma_{nfo} \Gamma_{nfo}^*}{(1+N)^2}. \quad (102)$$

Like the previous computation in Eq.(96), it is the Γ_g and Γ_g^* coefficients that determine the center of the circle. The radius is adjusted accordingly afterwards. Above in Eq.(102) this is anticipated by adding and subtracting the upcoming center term in absolutely squared form at the right hand side. Rearranging this equation gives the constant noise figure circles,

$$\left| \Gamma_g - \Gamma_{gcn} \right|^2 = \rho_{cn}^2 : \quad \Gamma_{gcn} = \frac{\Gamma_{nfo}}{1+N}, \\ \rho_{cn} = \sqrt{N + \frac{|\Gamma_{nfo}|^2}{(1+N)^2} - \frac{|\Gamma_{nfo}|^2}{1+N}} = \sqrt{\frac{N^2 + N \left(1 - \left| \Gamma_{nfo} \right|^2 \right)}{1+N}}. \quad (103)$$

Here centers and radii are denoted Γ_{gcn} and ρ_{cn} respectively. The noise figures for the circles are expressed through the quantity N that was defined in Eq.(101).

Example IV-3-3 (noise figure circles in Y-plane)

Fig.35 shows constant noise figure circles for two collector bias currents in a generator admittance plane for a bipolar transistor, BFR91A. All centers of the circle system in each figure have equal imaginary parts, which is in agreement with the first equation in (94), where the second non-constant term is real.

Philips Semiconductors

Product specification

NPN 6 GHz wideband transistor

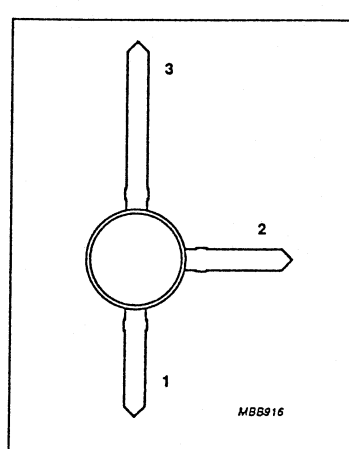
BFR91A

FEATURES

- Low noise
- Low intermodulation distortion
- High power gain
- Gold metallization.

PINNING

PIN	DESCRIPTION
Code: BFR91A/02	
1	base
2	emitter
3	collector



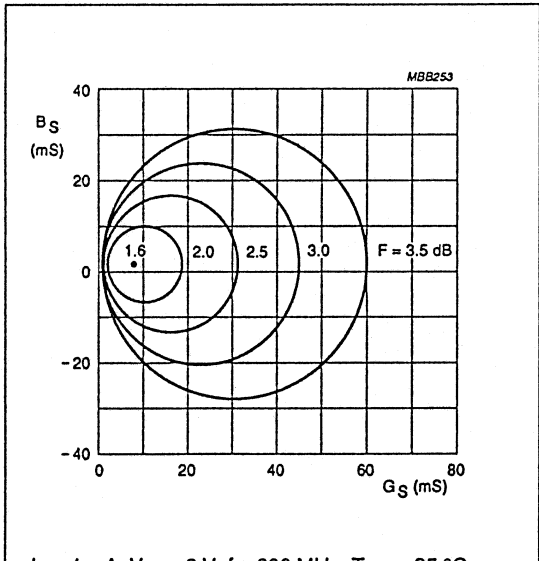
DESCRIPTION

NPN transistor in a plastic SOT37 envelope primarily intended for use in RF wideband amplifiers.

A SOT54 (TO-92) version (ref: ON4185) is available on request.

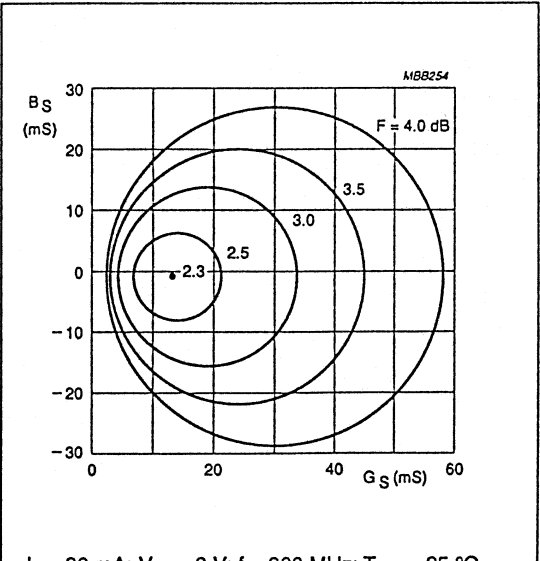
PNP complement is BFQ23.

Fig.1 SOT37.



$I_C = 4 \text{ mA}$; $V_{CE} = 8 \text{ V}$; $f = 800 \text{ MHz}$; $T_{amb} = 25^\circ \text{C}$.

Fig.12 Noise circle figure.



$I_C = 30 \text{ mA}$; $V_{CE} = 8 \text{ V}$; $f = 800 \text{ MHz}$; $T_{amb} = 25^\circ \text{C}$.

Fig.13 Noise circle figure.

Fig.35 Extract from Philips Data Handbook, SC14 RF Wideband Transistors, Video Transistors and Modules, 1993.

In design considerations it is sometimes convenient to use the primary equivalent two-port input noise parameters R_n , G_n , and $Y_{cor}=G_{cor}+jB_{cor}$ from Fig.33(b). Calculating backwards from F_{min} and $Y_{nfo}=G_{nfo}+jB_{nfo}$, keeping R_n and using Eqs.(92),(91), provides

$$G_{cor} = (F_{min} - 1) / 2 R_n - G_{nfo}, \quad B_{cor} = -B_{nfo}, \quad G_n = R_n (G_{nfo}^2 - G_{cor}^2). \quad (104)$$

Table II Extraction of noise equivalent circuit parameters for BFR91A from data in Fig.35

I_C, V_{CE}	4 mA, 8 V	30 mA, 8 V
F_{min}	1.6 dB ~ 1.45	2.3 dB ~ 1.70
G_{nfo}	8.0 mS	13.5 mS
B_{nfo}	1.7 mS	-0.75 mS
g_{cn}	29.4 mS	28.1 mS
$F @ g_{cn}$	3.5 dB ~ 2.24	4.0 dB ~ 2.51
R_n	17.4 Ω	22.6 Ω
G_{cor}	4.96 mS	1.97 mS
B_{cor}	-1.7 mS	0.75 mS
G_n	0.68 mS	4.04 mS
$g_m/2\beta = I_C/0.026/180$	0.85 mS	6.41 mS
$G_{n,tot} = G_n + Y_{cor} ^2 R_n$	1.16 mS	4.14 mS

While F_{min} and Y_{cor} are directly recognized in the above figures, R_n must be calculated from a circle radius g_{cn} and the corresponding noise figure. By Eq.(94) we get

$$R_n = \frac{G_{nfo}(F - F_{min})}{2 g_{cn}^2} \left[1 + \sqrt{1 + \left(\frac{g_{cn}}{G_{nfo}} \right)^2} \right]. \quad (105)$$

Table II summarizes data that are deduced from the two systems of circles in Fig.35 by the expressions above. The first five rows contain direct readings and the next four hold parameters of the input equivalent circuit. The two bottom rows are included to illuminate the results where first the $g_m/2\beta$ value is the idealized value of G_n . To see this we recall from Eqs.(83),(84) that G_n controls an uncorrelated source, which according to the discussions on page 17 is the shot noise associated with the base current in the transistor. Using $I_B = I_C/\beta$ we get from Eq.(36)

$$\overline{i_{nb}^2} = 2 q \frac{I_C}{\beta} \Delta f = 4 k T G_n \Delta f \quad \Rightarrow \quad G_n = \frac{I_C}{2 \beta V_t} = \frac{g_m}{2 \beta} \quad (106)$$

Table entries correspond to a typical $\beta=90$ value from the data sheets and $V_t=26mV$. They are relatively close to the extracted G_n 's. It is supposed that the observed overestimation in the

check values are caused by reductions of the actual transistor conductances due to high injections. The last row indicate the significance of correlation by showing the value of G_n that correspond to the total input noise shunt current. Especially in the low current case the difference and thereby the correlation is pronounced. This is in agreement with the fact that the transistor input impedance is relatively high at low currents where the input noise voltage source encompasses the effect of the collector noise current if the generator impedance is low.

Example IV-3-3 end

Example IV-3-4 (noise figure circles in Smith chart)

Fig.36 shows noise circles in Smith chart representing generator impedances. There are two system of circles. The closed ones at the right hand side are the noise figure circles corresponding to Eq.(103). The four corresponding noise parameters are also given. The other system includes circular arcs,⁷ where the input impedance provide constant gain if the transistor is matched conjugatedly at the output port, i.e. curves of constant available power gain. Transforming to admittance or impedance form, the noise parameters are

$$F_{\min} = 2.[dB] \sim 1.58, \quad R_n = 50 \cdot 2.6 = 130 \Omega, \quad \Gamma_{nfo} = 0.74 \angle 8^\circ = 0.733 + j0.103 \Rightarrow \quad (107)$$

$$Y_{nfo} = \frac{1}{50} \frac{1 - \Gamma_{nfo}}{1 + \Gamma_{nfo}} = 3.00 - j1.37 [mS] \quad \sim \quad Z_{nfo} = 1/Y_{nfo} = 276. + j126. [\Omega].$$

At the particular bias and frequency, the transistor is potentially unstable and cannot be simultaneously matched at both ports with respect to power. This is the reason why the Smith chart is divided by a so-called stability circle. Generator impedances map into output impedances of negative real parts in the unstable region. The arc of highest gain, which is shown in the figure, is 11.2dB. It is called MSG and equals is the maximum stable gain $G_{ms} = |y_{21}/y_{12}| = |s_{21}/s_{12}|$ that was introduced in chap.III, p.13.

The Smith chart in the example shows that it is possible to construct a stable amplifier of gain equal to G_{ms} with a noise figure slightly below 3dB. Sacrificing gain, the optimum noise figure of 2dB may be achieved with an available power gain of approximately 8dB. To see the further consequences of such a choice we need small-signal parameters for the transistor. In the present case they are transformed from data sheet s-parameters to read

$$\mathbf{Y}_{tr} = \begin{Bmatrix} \mathbf{g}_{11} + j\mathbf{b}_{11} & \mathbf{g}_{12} + j\mathbf{b}_{12} \\ \mathbf{g}_{21} + j\mathbf{b}_{21} & \mathbf{g}_{22} + j\mathbf{b}_{22} \end{Bmatrix} = \begin{Bmatrix} 2.33 + j4.73 mS & -0.014 - j2.09 mS \\ 21.3 - j17.9 mS & 0.154 + j3.46 mS \end{Bmatrix}. \quad (108)$$

7) It is proven in most literature on RF amplifiers, for instance [8] or chap.III ref's [5], [6], that curves of constant power gain constitute a systems of circles in either Smith charts or impedance and admittance planes.

Philips Semiconductors	Product specification																		
NPN 5 GHz wideband transistor																			
BFT25A																			
<p>FEATURES</p> <ul style="list-style-type: none"> • Low current consumption (100 µA - 1 mA) • Low noise figure • Gold metallization ensures excellent reliability. 	<p>PINNING</p> <table border="1" style="width: 100%; border-collapse: collapse; text-align: center;"> <thead> <tr> <th>PIN</th> <th>DESCRIPTION</th> </tr> </thead> <tbody> <tr> <td colspan="2" style="text-align: center;">Code: V10</td> </tr> <tr> <td>1</td> <td>base</td> </tr> <tr> <td>2</td> <td>emitter</td> </tr> <tr> <td>3</td> <td>collector</td> </tr> </tbody> </table> <p>Top view MSB003</p>	PIN	DESCRIPTION	Code: V10		1	base	2	emitter	3	collector								
PIN	DESCRIPTION																		
Code: V10																			
1	base																		
2	emitter																		
3	collector																		
<p>DESCRIPTION</p> <p>The BFT25A is a silicon npn transistor, primarily intended for use in RF low power amplifiers, such as pocket telephones and paging systems with signal frequencies up to 2 GHz.</p>	<p>Fig.13 Noise circle figure.</p>																		
<table border="1" style="width: 100%; border-collapse: collapse; text-align: center;"> <thead> <tr> <th>f (MHz)</th> <th>V_{CE} (V)</th> <th>I_c (mA)</th> </tr> </thead> <tbody> <tr> <td>1000</td> <td>1</td> <td>1</td> </tr> </tbody> </table> <p>Noise Parameters</p> <table border="1" style="width: 100%; border-collapse: collapse; text-align: center;"> <thead> <tr> <th>F_{min} (dB)</th> <th colspan="2">Gamma (opt)</th> <th>R_n/50</th> </tr> <tr> <th>(dB)</th> <th>(mag)</th> <th>(ang)</th> <th></th> </tr> </thead> <tbody> <tr> <td>2</td> <td>0.74</td> <td>8</td> <td>2.6</td> </tr> </tbody> </table>	f (MHz)	V _{CE} (V)	I _c (mA)	1000	1	1	F _{min} (dB)	Gamma (opt)		R _n /50	(dB)	(mag)	(ang)		2	0.74	8	2.6	
f (MHz)	V _{CE} (V)	I _c (mA)																	
1000	1	1																	
F _{min} (dB)	Gamma (opt)		R _n /50																
(dB)	(mag)	(ang)																	
2	0.74	8	2.6																

Fig.36 Extract from Philips Data Handbook, SC14 RF Wideband Transistors, Video Transistors and Modules, 1993.

Highest gain with minimum noise figure is achieved when the load y_L equals the complex conjugated of the transistor output admittance using the optimal noise figure generator admittance Y_{nfo} at the input port. We get

$$y_{12}y_{21} = (-0.014 - j2.09)(21.3 - j17.6) = -37.7 - j44.3 [mS]^2 = 58.2 [mS]^2 \angle -130^\circ. \quad (109)$$

$$\begin{aligned} y_L^* &= y_{out} = y_{22} - \frac{y_{12}y_{21}}{y_{11} + Y_{nfo}} = (0.154 + j3.46) - \frac{(-37.7 - j44.3)}{(2.23 + j4.73) + (3.00 - j1.37)} \\ &= 8.96 + j6.21 [mS] \quad \sim \quad z_L = 1/y_L^* = 75.4 + j52.3 [\Omega]. \end{aligned} \quad (110)$$

The corresponding available gain and the stability factor in augmented estimation are

$$\begin{aligned} G_{av} &= \left| \frac{y_{21}}{y_{11} + Y_{nfo}} \right|^2 g_{nfo} = \frac{21.3^2 + 17.9^2}{(2.33 + 3.00)^2 + (4.73 - 1.37)^2} \frac{3.00}{8.96} = 6.53 \sim 8.15 [dB], \\ K_{aug} &= \frac{2(g_{11} + g_{nfo})(g_{22} + g_L) - Re\{y_{12}y_{21}\}}{|y_{12}y_{21}|} = \frac{2(2.33 + 3.00)(0.154 + 8.96) + 37.7}{58.2} = 2.32. \end{aligned} \quad (111)$$

The gain becomes a little more than 8 dB in agreement with Fig.36, where the point of optimum noise figure is slightly above this gain arch. The K-factor is far below the ideal of five that makes a parameter insensitive amplifier, so one of the penalties of getting minimum noise figure with most gain from this transistor is that the resultant amplifier may be difficult to tune. Another drawback is that the input port becomes highly mismatched. The input admittance and impedance of the amplifier are

$$\begin{aligned} y_{in} &= y_{11} - \frac{y_{12}y_{21}}{y_{22} + y_L} = (2.33 + j4.73) - \frac{(-37.7 - j44.3)}{(0.154 + j3.46) + (8.96 - j6.21)} \\ &= 4.78 + j10.33 [mS] \quad \sim \quad z_{in} = 1/y_{in} = 36.9 - j79.7 [\Omega], \end{aligned} \quad (112)$$

which implies a mismatching of

$$\begin{aligned} M_{mch} &= \frac{4G_{nfo}g_{in}}{\left| Y_{nfo} + y_{in} \right|^2} = \frac{4 \cdot 3.00 \cdot 4.78}{(3.00 + 4.78)^2 + (-1.37 + 10.3)^2} = 0.408, \\ |\Gamma| &= \sqrt{1 - M_{mch}} = 0.770 \Rightarrow SWR = 7.68. \end{aligned} \quad (113)$$

According to the previous discussion in chap.III,p.15 ff., the mismatch pertains at either side of any lossless input matching network. Therefore, it will also be present at the input port to any amplifier designed to minimum noise figure with most gain around this transistor. The mismatch is rather high and may be impractical. To lower it we may either reduce gain, sacrifice noise figure, or both. As an example, applying an ohmic load of 50Ω in parallel with a capacitor of 15.9pF ($y_L=20\text{mS}+j10\text{mS}$) provides gain - transducer gain as the output port is no longer matched - and stability factor that are calculated using

$$\begin{aligned} (y_{11} + Y_{nfo})(y_{22} + y_L) &= [(2.33 + 3.00) + j(4.73 - 1.37)][(0.154 + 20.0) + j(3.56 + 10)] \\ &= 62.2 + j140. \end{aligned} \quad (114)$$

$$G_{tr} = \left| \frac{y_{21}}{(y_{11} + y_{nfo})(y_{22} + y_L) - y_{12}y_{21}} \right|^2 4g_{nfo}g_L = \frac{(21.3^2 + 17.9^2)4 \cdot 3.00 \cdot 20.0}{(62.2 + 37.7)^2 + (140. + 44.3)^2} = 4.25 \sim 6.21 [dB], \quad (115)$$

$$K_{aug} = \frac{2(g_{11} + g_{nfo})(g_{22} + g_L) - Re\{y_{12}y_{21}\}}{|y_{12}y_{21}|} = \frac{2(2.33 + 3.00)(0.154 + 20.0) + 37.7}{58.2} = 4.34.$$

The corresponding input admittance and mismatching properties are

$$y_{in} = y_{11} - \frac{y_{12}y_{21}}{y_{22} + y_L} = 2.33 + j4.73 - \frac{-37.7 - j44.3}{20.154 + j13.46} = 4.64 + j5.38 [mS]. \quad (116)$$

$$M_{mch} = \frac{4g_{nfo}g_{in}}{\left| y_{nfo} + y_{in} \right|^2} = \frac{4 \cdot 3.00 \cdot 4.64}{(3.00 + 4.64)^2 + (-1.37 + 5.38)^2} = 0.748, \quad (117)$$

$$|\Gamma| = \sqrt{1 - M_{mch}} = 0.502 \Rightarrow SWR = 3.01.$$

In this case we maintain the minimum noise figure and obtain an amplifier that has improved the input mismatch at the expense of gain. Another choice with the same ohmic load could be to optimize gain letting an input matching network provide conjugated matching to the input admittance from Eq.(116). In that case the input power equals the available power, so it is relevant to consider the operational power gain, which yields

$$G_p = \left| \frac{y_{21}}{y_{22} + y_L} \right|^2 \frac{g_L}{g_{in}} = \frac{21.3^2 + 17.9^2}{(0.154 + 20.0)^2 + (3.46 + 10)^2} \frac{20.}{4.64} = 5.68 \sim 7.55 [dB], \quad (118)$$

$$K_{aug} = \frac{2(g_{11} + g_{in})(g_{22} + g_L) - Re\{y_{12}y_{21}\}}{|y_{12}y_{21}|} = \frac{2(2.33 + 4.64)(0.154 + 20.0) + 37.7}{58.2} = 5.48.$$

To find the corresponding noise figure, Eq.(93) is employed with generator admittance equal to the complex conjugated input admittance, i.e.

$$F = F_{min} + \frac{R_n}{g_{in}} \left| y_{in}^* - y_{nfo} \right|^2 = 1.58 + \frac{0.130}{4.64} [(4.64 - 3.00)^2 + (5.38 + 1.37)^2] = 2.11 \sim 3.25 [dB] \quad (119)$$

Clearly, the noise figure increases when the generator admittance differs from the optimal one, instead we achieve higher gain, better stability and no mismatch at the input port.

Example IV-3-4 end

IV-4 Distortion in Almost Linear Circuits

The type of distortion we consider in this section is the so-called nonlinear distortion, i.e. departures from linear input-output relationships of electronic circuits and components. Nonlinear distortion accompanies large drive signals and sets an upper bound on the operation level for proper performance of many intentionally linear circuits.

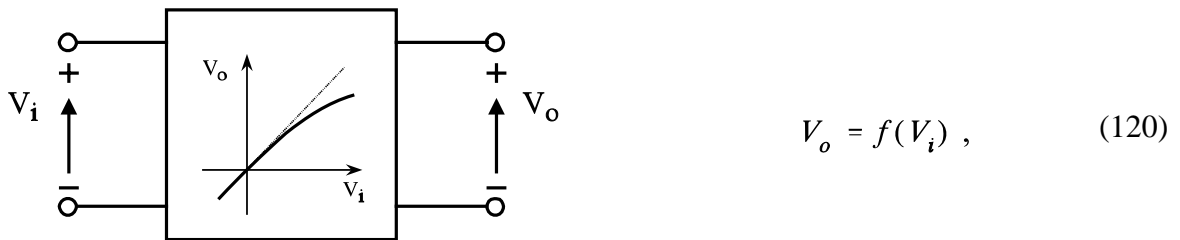


Fig.37 Nonlinear two-port example, a voltage controlled voltage generator circuit.

To fix ideas of a circuit that eventually exhibits nonlinear distortion, the voltage controlled voltage source in Fig.37 is considered. It could be a DC-coupled voltage amplifier with a simple, memoryless input-output relationship like Eq.(120). Taken as a function of the entire input range in V_i , this general form is a large-signal expression, which is commonly not linear. Linear amplification is established in restricted input intervals around the DC biasing point and expressed mathematically by the first order term of a Taylor expansion in the deviation v_i from the bias V_{i0} ,

$$V_o = f(V_{i0} + v_i) = f(V_{i0}) + \frac{df}{dV_i} \Bigg|_{V_{i0}} v_i + \frac{1}{2} \frac{d^2f}{dV_i^2} \Bigg|_{V_{i0}} v_i^2 + \frac{1}{6} \frac{d^3f}{dV_i^3} \Bigg|_{V_{i0}} v_i^3 + \dots \quad (121)$$

Subdividing output into bias and a small-signal part yields

$$V_o = V_{o0} + v_o, \quad \begin{cases} \text{bias term: } V_{o0} = f(V_{i0}), \\ \text{small-signal terms: } v_o = a v_i + b v_i^2 + c v_i^3 + \dots \end{cases} \quad (a) \quad (b) \quad (122)$$

where the a , b , c , and possibly more coefficients of the small-signal polynomial are shorthand notation for the scaled derivatives of the original, large-signal expression,

$$a = \frac{df}{dV_i} \Bigg|_{V_{i0}}, \quad b = \frac{1}{2} \frac{d^2f}{dV_i^2} \Bigg|_{V_{i0}}, \quad c = \frac{1}{6} \frac{d^3f}{dV_i^3} \Bigg|_{V_{i0}}. \quad (123)$$

In an amplifier the a coefficient would be the small signal voltage gain and the higher order terms b and c introduce distortion. To keep distortion low we should select components with small second, third and even higher order expansion terms or hold the signal level low, so powers in v_i stay insignificant. The nonlinear expansion coefficients b , c , etc. refer to DC and

instant voltages or currents. If DC bias is unimportant, a polynomial expansion may express distortion directly in RMS scale, i.e.

$$v_{o,rms} = \frac{v_o}{\sqrt{2}} = a_{rms} v_{i,rms} + b_{rms} v_{i,rms}^2 + c_{rms} v_{i,rms}^3 , \quad (124)$$

where $a_{rms} = a$, $b_{rms} = \sqrt{2} b$, $c_{rms} = 2 c$, $v_{i,rms} = \frac{v_i}{\sqrt{2}}$

One of the most prominent consequences of the nonlinear distortion is the occurrence of deterministic signal components at frequencies that are not present in the input signal. No strictly linear circuits are able to do that and there are several technical utilizations of the property, mixing for instance. In this section we shall, however, concentrate on the different ways in which nonlinear effects may degrade the performance of RF communication circuits and on methods of quantifying this in data sheets.

A precautionary word on the validity of our results is in place. To let the response of a nonlinear circuit be represented by a Taylor series expansion requires that all nonlinearities combine memoryless. This will be the case with algebraic characteristics in ohmic networks, but typically not if the problem includes combinations of linear and nonlinear conductances and reactances. In such cases more powerful but also significantly more laborious methods are required to conduct genuine analytical treatments. Volterra series expansions - introduced in ref's [21] or [22] chap.4 - are suggestions for that purpose. Using these methods we get expansion coefficients corresponding to the a, b, and c's above, which become frequency dependent. However, no more frequency components arise with combined nonlinearities compared to the ones that are demonstrated by Taylor series expansions, which therefore suffice for the present purpose of exploring basic matters. They also suffice in design if the polynomial coefficients are deduced from data that apply to the actual operating frequencies.

Simplifying concerns are also the reason why expansions mostly are limited to encompass third order terms only. Going higher would provide no really new phenomena but a lot more messy algebra.

Single Signal Distortions

Fig.38 shows the single sided frequency components in the amplifier voltages when a single tone input signal drives the circuit that was described by Eq.(122),

$$v_o = a v_i + b v_i^2 + c v_i^3 + \dots \quad \text{where} \quad v_i = A \cos \omega_a t . \quad (125)$$

The frequency components in the output emerge when the trigonometric identities,

$$\cos^2 x = \frac{1}{2} + \frac{1}{2} \cos 2x , \quad \cos^3 x = \frac{3}{4} \cos x + \frac{1}{4} \cos 3x , \quad (126)$$

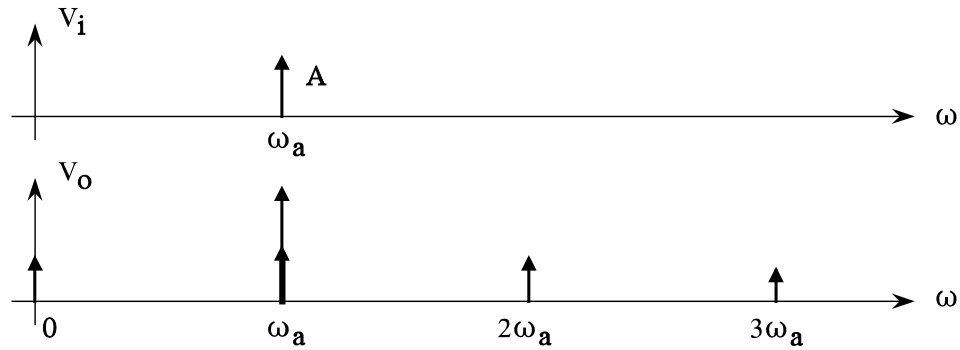


Fig.38 Signal and distortion components when a single tone input signal is applied to a circuit which includes nonlinear components.

are applied to the polynomial input-output relationship. The different terms become

Taylor terms v_o components

$$1st \text{ order : } aA \cos \omega_a t \quad (a)$$

$$2nd \text{ order : } + \frac{1}{2} bA^2 + \frac{1}{2} bA^2 \cos 2\omega_a t \quad (127) \quad (b)$$

$$3rd \text{ order : } + \frac{3}{4} cA^3 \cos \omega_a t + \frac{1}{4} cA^3 \cos 3\omega_a t \quad (c)$$

The first order term is the conventional linear small-signal gain term. The second order term in the Taylor expansion causes a DC contribution and a second harmonic component. Care must be taken, both in circuit analysis and in practical design, to ensure that proper biasing of the component persists even when the quadratic term adds to the DC voltage or current. The third order term produces both a component at the input frequency and a third harmonic component. It is possible in many applications to discard the effects of higher harmonic components by filtering. But it is impossible to remove the distortion component from the signal at the fundamental frequency, so the third order term will always cause distortion. Therefore, third order terms often draw most attention in specifications and data sheets. Actually all odd ordered Taylor expansion terms would contribute to the fundamental signal component, but their significance decrease rapidly with raising order in electronic devices that are intended for linear operation and driven accordingly, so we stay with the third order maximum below.

Including all frequency components, except DC, gives a measure called the total harmonic distortion, K_{THD} , in an amplifier. It includes all components, i.e.

$$V_{o,1} = aA + \frac{3}{4} c A^3, \quad V_{o,2} = \frac{1}{2} b A^2, \quad V_{o,3} = \frac{1}{4} c A^3. \quad (128)$$

$$K_{THD} = \sqrt{\frac{V_{o,2}^2 + V_{o,3}^2 + \dots}{V_{o,1}^2}} = \sqrt{K_2^2 + K_3^2 + \dots}, \quad \text{where}$$

$$K_2 = \frac{V_{o,2}}{V_{o,1}} \approx \frac{1}{2} \left| \frac{b}{a} \right| A, \quad K_3 = \frac{V_{o,3}}{V_{o,1}} \approx \frac{1}{4} \left| \frac{c}{a} \right| A^2, \dots.$$
(129)

The approximations in the distinct second, third, or possible higher harmonic terms like K_2 and K_3 require that the third order term at the signal frequency is small compared to the first order term, i.e. $\frac{3}{4}c/a A^2 \ll 1$. The assumption is necessary for calculating the total distortion from experimental data, because it is difficult to distinguish between fundamental frequency outputs arising from the first and the third order terms in measurements.

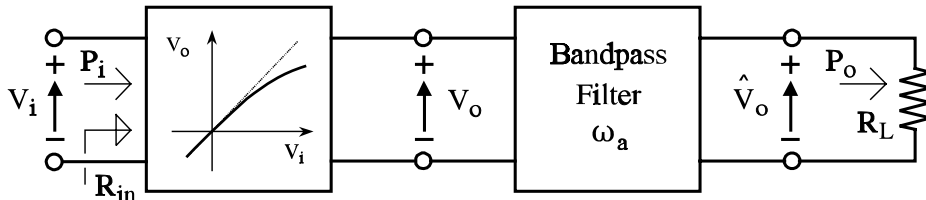


Fig.39 Amplifier or other electronic component followed by a bandpass filter that removes all but signal components around the fundamental frequency.

Removing all but the signal frequency components from the output, as indicated by the setup of Fig.39, leaves the first third order term in Eq.(127)(c) as the only disturbing component in observation. Fig.40 shows a typical shape of the input to filtered output characteristics of amplifiers or transistors, where the output signal falls below the linear extrapolation at higher signal levels. This is called compression and may be characterized by the RMS input drive level, $V_{i,1dB}$, where the compression corresponds to 1dB output signal reduction or, equivalently, an output amplitude reduction by a factor of 0.891 compared to the assumed linear value. In terms of the Taylor series expansion, the compression level becomes

$$\hat{V}_o \Big|_{\omega_a} = aA + \frac{3}{4} c A^3 \xrightarrow[1dB \text{ comprss.}]{=} \frac{3}{4} |c| A^3 \quad |A|_{1dB} = 0.109 |a| A_{1dB} \quad \Rightarrow$$

$$1 \text{ dB compression : } V_{i,1dB} = \frac{A_{1dB}}{\sqrt{2}} = 0.269 \sqrt{\left| \frac{a}{c} \right|} [V_{rms}]. \quad (130)$$

Absolute values of the Taylor coefficients are required above to account for the fact that a and c must be of opposite signs if the resultant output amplitude falls below the linear term. The result is scaled to RMS values, that are common in data sheets and instrument readings.

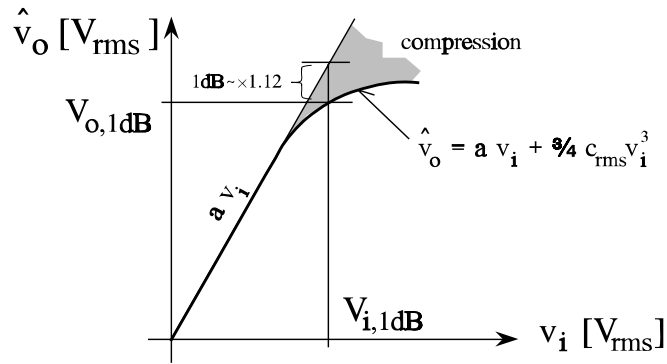


Fig.40 Amplifier characteristics with compression. Coefficients a and c_{rms} must be of opposite signs. Input and output hold fundamental frequency components only.

Instead of referring to the input side, compression specifications refer typically to the output side by giving an output power level and a gain, either the stipulated linear G_{lin} or the actual gain at 1dB compression, G_{1dB} . Backtracking from powers to voltages requires that input and output impedances are defined. Dealing with amplifier blocks this is commonly not a problem whereas transistor data often require careful review before interpretation. For the setup in Fig.39 the powers and the power gains are

$$P_i = \frac{V_{i,rms}^2}{R_{in}} , \quad P_o = \frac{V_{o,rms}^2}{R_L} = G_{lin} P_i \quad \Rightarrow \quad G_{lin} = a^2 \frac{R_{in}}{R_L} . \quad (131)$$

Absolute power indications may be in dBm, decibels relative to 1mW. Translated to dB scales, the linear region of the input-output plot in Fig.41 shows

$$P_i[\text{dBm}] = 10 \log_{10} \left[V_{i,rms}^2 / R_{in} 10^{-3} \right] = 20 \log_{10} V_{i,rms} - 10 \log_{10} R_{in} + 30 , \quad (132)$$

$$P_o[\text{dBm}] = P_i[\text{dBm}] + G_{lin}[\text{dB}] , \quad \text{where} \quad G_{lin}[\text{dB}] = 10 \log_{10} \left[a^2 R_{in} / R_L \right] .$$

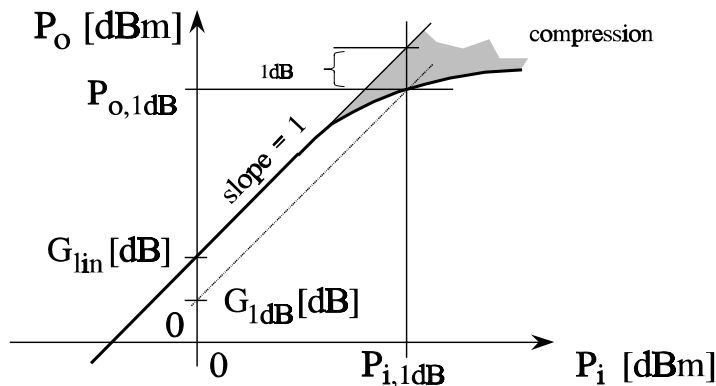


Fig.41 Amplifier characteristics in dB scale. Gains are represented by lines of slope equal to one with values given by the vertical positions.

Inserting the voltage for 1dB compression from Eq.(130), the corresponding input and output powers are expressed,

$$P_{i,1dB}[dBm] = 10 \log_{10} [V_{i,1dB}^2 / R_{in} 10^{-3}] = 10 \log_{10} |a/c| - 10 \log_{10} R_{in} + 18.60, \quad (133)$$

$$P_{o,1dB}[dBm] = P_{i,1dB}[dBm] + G_{lin}[dB] - 1 = 10 \log_{10} |a/c| + 20 \log_{10} a - 10 \log_{10} R_L + 17.60.$$

Distortions with Two Signals

Applying two sinusoids of sufficient amplitudes to an amplifier that eventually becomes nonlinear may produce a multitude of frequency components in the output spectrum. With two tones input to the Taylor expansion,

$$v_o = a v_i + b v_i^2 + c v_i^3 + \dots \quad \text{where} \quad v_i = A \cos \omega_a t + B \cos \omega_b t, \quad (134)$$

we get all the components that are shown below in Fig.42 and Eq.(136). They are calculated from the trigonometric identities in Eq.(126) with supplement of the product formula,

$$\cos x \cos y = \frac{1}{2} \cos(x+y) + \frac{1}{2} \cos(x-y). \quad (135)$$

For illustrating purposes the two input signal components in Fig.42 are chosen with close frequency spacing, which is an important situation in practice. In that case we still refer to the fundamental input frequency in the meaning of the range around ω_a and ω_b . Regarding output components in Eq.(136), the first observation is that all terms generated from a single tone in Eq.(127) are present with unaltered powers of amplitudes for both the ω_a and the ω_b input components. It is also observed that the second order Taylor term causes components around DC and around twice the fundamental input frequency. This is equivalent to the single tone case. There is also resemblance in the third order term, which produces a complex of components in the fundamental frequency range and a complex around third harmonics.

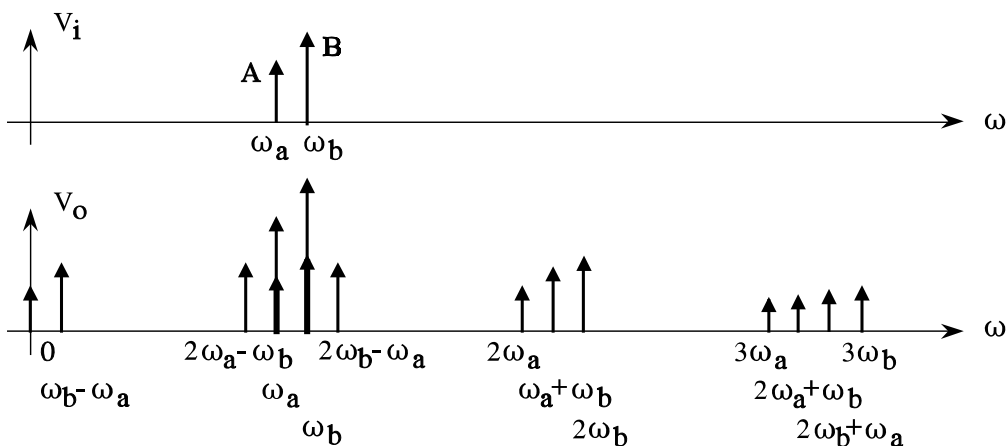


Fig.42 Output signal and distortion components with two-tone signal input to a nonlinear component.

Taylor terms v_o components

$$1st \ order : \quad aA \cos \omega_a t + aB \cos \omega_b t \quad (a)$$

$$2nd \ order : \quad + \frac{1}{2} bA^2 + \frac{1}{2} bB^2 \quad (b1)$$

$$+ \frac{1}{2} bA^2 \cos 2\omega_a t + \frac{1}{2} bB^2 \cos 2\omega_b t \quad (b1)$$

$$+ bAB \cos(\omega_a - \omega_b) t + bAB \cos(\omega_a + \omega_b) t \quad (b2) \quad (136)$$

$$3rd \ order : \quad + \left[\frac{3}{4} cA^3 + \frac{3}{2} cAB^2 \right] \cos \omega_a t + \left[\frac{3}{4} cB^3 + \frac{3}{2} cA^2B \right] \cos \omega_b t \quad (c1)$$

$$+ \frac{1}{4} cA^3 \cos 3\omega_a t + \frac{1}{4} cB^3 \cos 3\omega_b t \quad (c2)$$

$$+ \frac{3}{4} cA^2B \cos(2\omega_a + \omega_b) t + \frac{3}{4} cAB^2 \cos(\omega_a + 2\omega_b) t \quad (c3)$$

$$+ \frac{3}{4} cA^2B \cos(2\omega_a - \omega_b) t + \frac{3}{4} cAB^2 \cos(\omega_a - 2\omega_b) t \quad (c4)$$

News with two tones are the different possibilities for interaction between the two. The second order terms in Eq.(136)(b2) and the third order terms in (c3) and (c4) contain so-called intermodulation products, where especially the last ones may cause troubles if the resultant frequencies hit the desired fundamental frequency range. Moreover, there is a direct cross-coupling between the two signals at their fundamental frequencies through the third order distortions terms in Eq.(136)(c1). The latter have great practical importance in radio receiver design causing blocking and cross-modulation effects, which we shall consider below. Keep in mind here that the cosine functions are indifferent with respect to sign of the arguments, so in comparisons the terms follow signs of the coefficients a, b, and c.

Blocking is a condition that occurs when two signals are present at the input to an amplifier which has a narrow channel selecting bandpass filter in the output port. As sketched in Fig.43(a), the input holds a weak signal, which is the one we are supposed to receive, so its frequency ω_a lies in the passband. The other signal is much stronger. Albeit close in frequency to the desired signal, its frequency ω_b falls outside the passband of the filter. The total output from the passband gets the amplitude,

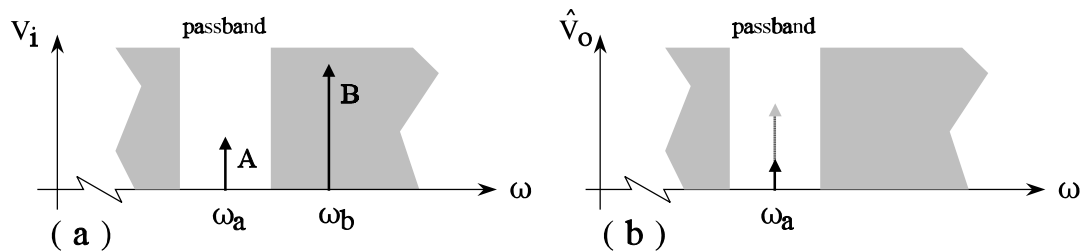


Fig.43 Input and output components illustrating signal desensitization towards blocking.

$$\hat{V}_o \Big|_{\omega_a} = aA + \frac{3}{4}cA^3 + \frac{3}{2}cAB^2 \underset{\text{small } A}{\approx} aA \left(1 - \frac{3}{2} \left| \frac{c}{a} \right| B^2 \right). \quad (137)$$

It is assumed that the A signal is so small, that its own third order distortion term may be ignored. When it is also supposed that the nonlinearity is of compression type, so the a and c coefficients have opposite signs, the last expression clearly shows that the undesirable B signal controls the size of the received signal. Blocking is the condition where the received signal disappears, i.e. $\hat{V}_o = 0$ in Eq.(137). The corresponding RMS value of the B signal is

$$\underline{\text{Blocking}} : B_{block} = \sqrt{\frac{2}{3} \left| \frac{a}{c} \right|} \Rightarrow V_{block} = \frac{B_{block}}{\sqrt{2}} = 0.577 \sqrt{\left| \frac{a}{c} \right|} [V_{rms}]. \quad (138)$$

The situation where the received signal still is present, but significantly reduced by the neighboring signal - like Fig.43(b) - is sometime called desensitization.

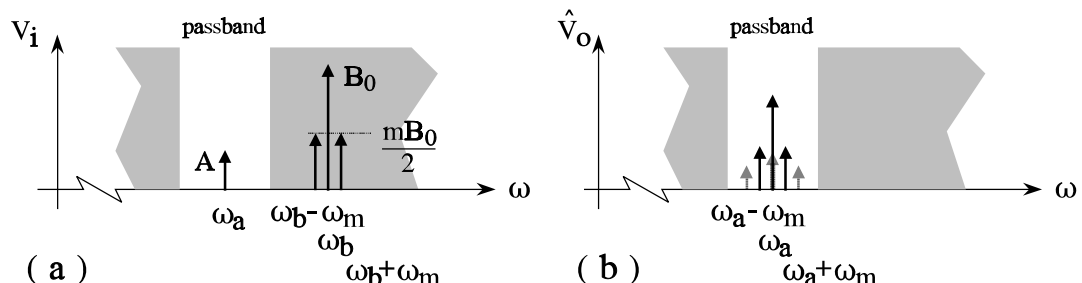


Fig.44 Input and output components illustrating cross-modulation. The selected ω_a signal is inflicted by the modulation of a neighboring but undesired channel around ω_b .

Cross modulation is the situation where the modulation in a large out-of-band signal transfers to a smaller signal in reception. For clarity the latter signal is represented by the unmodulated carrier at frequency ω_a . We suppose that the B signal is amplitude modulated by a low frequency sinusoid at ω_m with modulation index m , which is smaller than one,

$$B = B_0 (1 + m \cos \omega_m t). \quad (139)$$

The squared value of disturbing signal is approximated,

$$\mathbf{B}^2 = \mathbf{B}_0^2 \left(1 + \frac{m^2}{2} + 2m \cos \omega_m t + \frac{m^2}{2} \cos 2\omega_m t \right) \underset{m \ll 1}{\approx} \mathbf{B}_0^2 (1 + 2m \cos \omega_m t). \quad (140)$$

where it is assumed again that the signal to be received is small enough to let its own distortion be ignored on insertion into Eq.(136)(c1). The resultant passband output gets thereby a form that clearly shows transfer of modulation from the B signal to the A signal with a resultant modulation index \hat{m} ,

$$V_o|_{passb.} = aA + \frac{3}{2} c A \mathbf{B}^2 = aA \left(1 + 3m \mathbf{B}_0^2 \frac{c}{a} \cos \omega_m t \right) = aA (1 + \hat{m} \cos \omega_m t). \quad (141)$$

A common way of specifying cross modulation is to give the RMS voltage of the disturbing out-of-band carrier, which corresponds to 1% overcoupled modulation, i.e.

$$\frac{\hat{m}}{m} = \frac{1}{100} \Rightarrow \mathbf{B}_{0,cm}^2 = \frac{a}{300c}, \quad (142)$$

$$\underline{1\% cross-modulation} : V_{1\%cm} = \frac{\mathbf{B}_{0,cm}}{\sqrt{2}} = 0.0408 \sqrt{\left| \frac{a}{c} \right|} [V_{rms}]. \quad (143)$$

Neighboring input signals interact through the third order terms since they can produce frequency components close or equal to the original ones. Interaction between widely separated frequency components may occur by other terms. An example is interaction between a RF signal of frequency ω_a and a LF signal at ω_b , which is illustrated in Fig.45. Examples are low-frequency components from insufficient smoothing and decoupling of the bias in sensitive amplifiers. The second order terms in Eq.(136)(b2) may be rejoined to give,

$$v_o|_{passb.} = aA \cos \omega_a t + 2bA \mathbf{B} \cos \omega_a t \cos \omega_b t = aA \cos \omega_a t \left(1 + 2 \frac{b}{a} \mathbf{B} \cos \omega_b t \right). \quad (144)$$

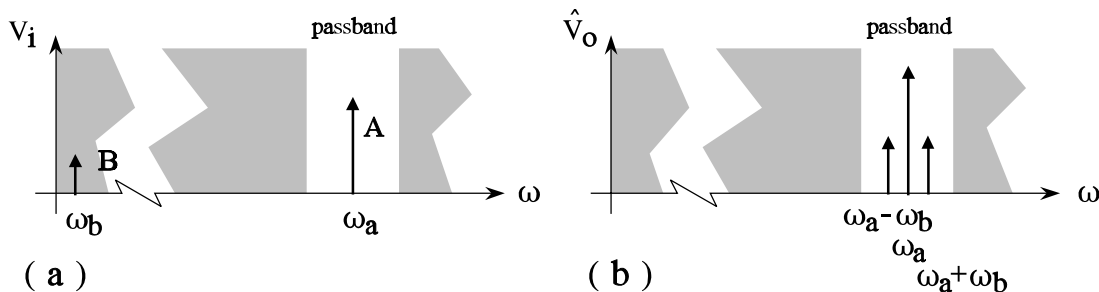


Fig.45 Input and output components illustrating hum-modulation. The low-frequency ω_b signal translates to an amplitude modulation of the RF signal at ω_a .

The last expression demonstrates that the LF signal amplitude modulates the RF signal with an AM modulation index given by

$$\underline{\text{Hum-modulation}} : \quad \hat{m} = 2 \left| \frac{b}{a} \right| B . \quad (145)$$

This phenomenon is sometimes called hum-modulation because it could be heard in many older receivers where it stemmed from the AC supply.

Common in all the examples above is that a signal in the passband and a signal outside enter a device that is nonlinear at large drive levels. The interaction leaves distortion components that cannot be removed by subsequent filtering. To anticipate the thought that we could apply filtering at the input side and avoid all the troubles, it should be recalled that in tunable receivers, bandpass filtering is done in the IF section after the RF signal is transferred to the intermediate frequency by a mixer, cf. Chap.I, Sec.5. In such receivers, the passband indications above must be interpreted as the effect of IF filtering transferred in frequency to the RF band. It should also be mentioned at this point that mixers introduce distortion defects like compression and cross-modulation. They are characterized and quantified by the same concepts we are introducing here for components and amplifiers, the only exception being that input and output fundamental frequencies do not coincide but differ by the frequency of the local oscillator. We shall return to the matters below when mixers are considered explicitly.

Intercept Points

Distortion specifications may be directly related to the practical consequences of intermodulation, for instance by cross-modulation as exemplified by Eq.(143). Recall, however, that all the implications of distortion we have considered express basically the absolute ratio of a higher order expansion term over the fundamental frequency term. A simple and easily interpretable way to get this information experimentally is by so-called intercept points. Below we start concentrating on the most important third order distortion and the associated 3rd order interception point. Afterwards the less frequent second order points, which develop equivalently, cf.[23] chap.10, is summarized briefly.

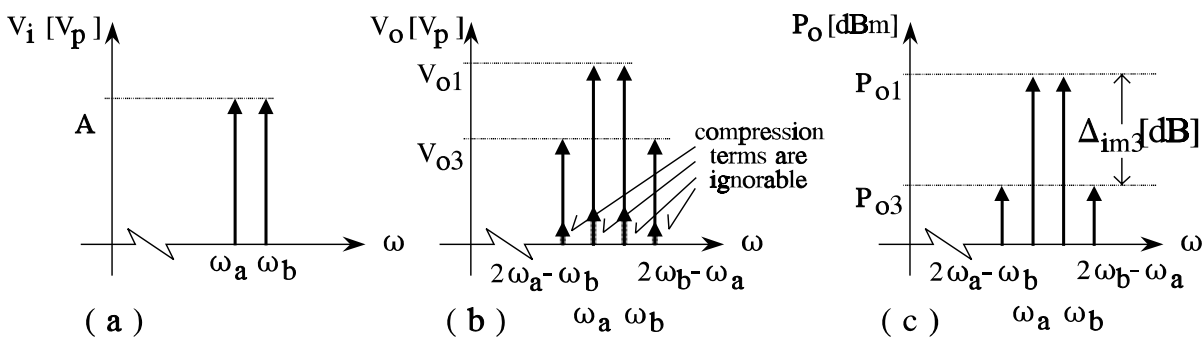


Fig.46 Third order intercept point conditions, (a) equal inputs, sufficiently low to ignore (b) compression terms in outputs. Experimental data are often dBm scaled like (c).

Intercept points are recorded from two-tone setups where the two input amplitudes are equal. Using Eq.(136), B is set equal to A while the frequencies ω_a and ω_b still differ. A picture of this situation preparing third order intercept point determination is shown in Fig.46. The two output components corresponding to the two-tone input are equal if ω_a is sufficiently close to ω_b . We call the corresponding output amplitude V_{o1} . The two intermodulation products at nearby frequencies $2\omega_a - \omega_b$ and $2\omega_b - \omega_a$ are also practically equal in size each of amplitude V_{o3} . With common input amplitudes, $V_{i1}=A=B$, one linear gain term from Eq.(136)(a) and one intermodulation term from Eq.(136)(c4) are

$$V_{o1} = aA, \quad V_{o3} = \frac{3}{4} c A^3. \quad (146)$$

Corresponding powers of input and output components with input and load resistances R_{in} and R_L respectively

$$P_i = \frac{A^2}{2R_{in}}, \quad P_{o1} = \frac{V_{o1}^2}{2R_L} = a^2 \frac{R_{in}}{R_L} P_i, \quad P_{o3} = \frac{V_{o3}^2}{2R_L} = \left(\frac{3}{2} c\right)^2 \frac{R_{in}^3}{R_L} P_i^3. \quad (147)$$

Considered as function of input power P_{in} , the intermodulation term P_{o3} rises much faster than the linear term P_{o1} . Their ratio, often called the intermodulation ratio or - in dB scale - the intermodulation distortion, IMD, is

$$\Delta_{im3}(P_i) = \frac{P_{o1}}{P_{o3}} = \frac{4}{9R_{in}^2} \left(\frac{a}{c}\right)^2 \frac{1}{P_i^2}. \quad (148)$$

The third order intercept point is the stipulated crossing point between P_{o1} and P_{o3} where the intermodulation ratio is one, and input and output powers $P_{i,IP3}$, $P_{o,IP3}$ are

$$\Delta_{im3}(P_{i,IP3}) = 1: \quad P_{i,IP3} = \frac{2}{3R_{in}} \left| \frac{a}{c} \right|, \quad P_{o,IP3} = \frac{2a^2}{3R_L} \left| \frac{a}{c} \right|. \quad (149)$$

Translating the above results to dB scales provide a simple and easily interpretable graphical presentation as seen in Fig.47 where,

$$P_{o1}[dBm] = P_i[dBm] + 10 \log_{10} \left[a^2 R_{in} / R_L \right], \quad (150)$$

$$P_{o3}[dBm] = 3 P_i[dBm] + 10 \log_{10} \left[9c^2 R_{in}^3 / 4R_L \right].$$

When assumptions of no compressions are met, the fundamental frequency term $P_{o1}[dBm]$ grows in direct proportion to $P_i[dBm]$ - slope equal to one - while the third order intermodulation term $P_{o3}[dBm]$ grows linearly, but faster with a slope of three. Above certain drive levels, the assumptions are no longer met and experimental data start falling below the assumptions. P_{o1} is lowered by compression as described formerly on page 50 while lowering

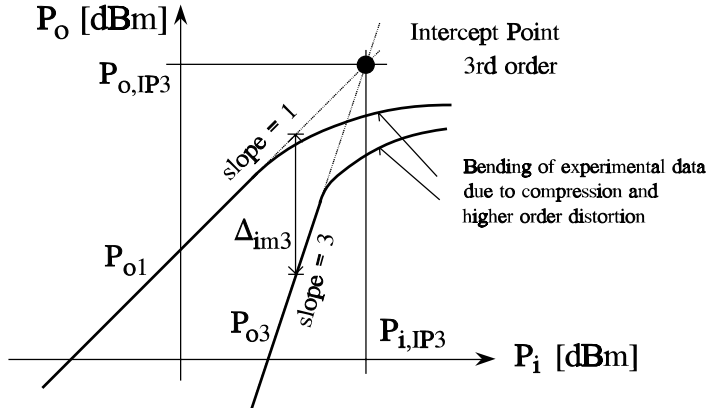


Fig.47 Third order intercept point: Crossing of a fundamental frequency output P_{o1} and a 3rd order intermodulation product, P_{o3} , both in straight line stipulations.

of P_{o3} is caused by odd-numbered higher order terms which we commonly disregard under small signal excitations. Dealing with experimental data that bend as sketched in the figure, it is still easy to draw linear extrapolations and find the intercept point. In dB scale we get

$$\begin{aligned} P_{i,IP3}[dBm] &= 10 \log_{10} |a/c| - 10 \log_{10} R_{in} + 28.24 \\ P_{o,IP3}[dBm] &= 10 \log_{10} |a/c| + 20 \log_{10} a - 10 \log_{10} R_L + 28.24 \end{aligned} \quad (151)$$

Comparing the last result with the 1dB compression output power, $P_{o,1dB}$ from Eq.(133), we must expect that under similar conditions, i.e. same frequency, same bias i.e. same a and c coefficients, and same load impedances, the output power at the intercept points should lie 10.6 dB above the 1dB compression level, if a simple Taylor expansion is quantitatively adequate for the circuit in consideration⁸.

The second order intercept point concerns the intermodulation product of frequency equal to either the sum or the difference of the two input signals, i.e. the first or the second term in Eq.(136)(b2). In analogy with Eqs.(146) to (148), keeping in mind that the input power expressions for P_i and P_{o1} stay unaltered from the third order case, we get,

$$V_{o1} = aA, \quad V_{o2} = bA^2 \quad \Rightarrow \quad P_{o2} = 2b^2 \frac{R_{in}^2}{R_L} P_{in}^2. \quad (152)$$

$$\Delta_{im2}(P_i) = \frac{P_{o1}}{P_{o2}} = \frac{1}{2R_{in}} \left(\frac{a}{b} \right)^2 \frac{1}{P_i} \quad \Rightarrow \quad P_{i,IP2} = \frac{1}{2R_{in}} \left(\frac{a}{b} \right)^2, \quad P_{o,IP2} = \frac{a^2}{2R_L} \left(\frac{a}{b} \right)^2 \quad (153)$$

8) A common violation of the assumption occurs when the output swing is limited by power supply, so the amplifier or device is driven into heavy saturation and/or cut-off. Taylor expansions with three terms are not adequate for characterizing such abrupt events that might include relaxation effects.

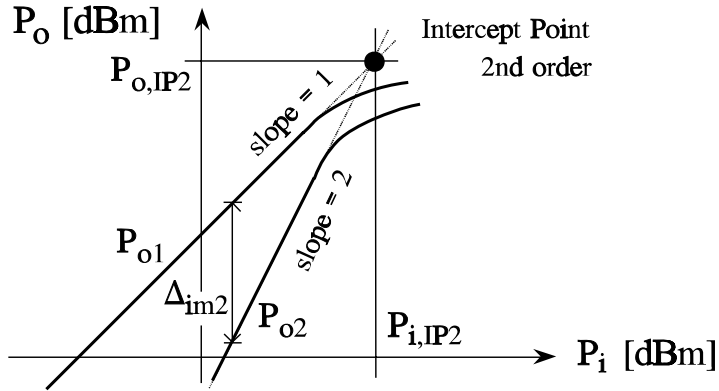


Fig.48 Second order intercept point: Crossing of a fundamental frequency output P_{o1} and a 2nd order intermodulation product, P_{o2} , both in straight line stipulations.

The dB-scaled asymptotes that determines the second order intercept point as shown in Fig.48 are given by

$$\begin{aligned} P_{o1}[dBm] &= P_i[dBm] + 10 \log_{10} \left[a^2 R_{in} / R_L \right], \\ P_{o2}[dBm] &= 2 P_i[dBm] + 10 \log_{10} \left[2 b^2 R_{in}^2 / R_L \right], \end{aligned} \quad (154)$$

and the intercept point gets the coordinates

$$\begin{aligned} P_{i,IP2}[dBm] &= 20 \log_{10} |a/b| - 10 \log_{10} R_{in} + 26.99, \\ P_{o,IP2}[dBm] &= 20 \log_{10} |a/b| + 20 \log_{10} a - 10 \log_{10} R_L + 26.99. \end{aligned} \quad (155)$$

Second order intermodulation products occur at the sum and the difference frequency of the incoming signal. The distance in frequencies between the signal components might be large, so if the a and b Taylor expansion coefficients are frequency dependent it is important to ensure that the second order specifications applies to the problem at hand.

Sensitivity and Dynamic Range

Noise determines a lower boundary for the signal level that may be processed successfully in a communication system. In complete systems it is often the first amplifier stage in the receiver that limits performance. The minimum required signal-to-noise ratio at the amplifier output is called $\text{SNR}_{o,mds}$, where mds stands for minimum discernible signal. Its level depends on system architecture including data rates, modulation, coding, interleaving schemes etc. The corresponding minimum input signal to the amplifier, $P_{i,mds}$, is sometimes called the sensitivity. Besides the required signal-to-noise ratio, it depends on noise bandwidth B_N Hz, on noise temperature of the source impedance T_g , and on noise temperature T_n of the amplifier, equivalently on the noise figure $F=1+T_n/T_0$ from Eq.(64). The level is

$$\frac{P_{o,mds}}{N_o} = \frac{G_{av} P_{i,mds}}{G_{av} k (T_g + T_n) B_N} = SNR_{o,mds} \Rightarrow \quad (156)$$

$$P_{i,mds} = SNR_{o,mds} k (T_g + T_n) B_N = SNR_{o,mds} k T_0 \left(F - 1 + \frac{T_g}{T_0} \right) B_N,$$

where the temporarily included G_{av} is the available power gain of the amplifier. If there is no association to specific system requirements, the acceptable output signal level from an amplifier may be taken equal to its noise output, i.e. using $SNR_{o,mds}=1$. If, furthermore, the source impedance is supposed to be at the reference temperature, $T_g=T_0=290$ K, the minimum discernible level gets a simpler form that sometimes is seen in literature,

$$P_{i,mds0} = P_{i,mds} \Big|_{T_g=T_0, SNR_o=1} = k T_0 F B_N. \quad (157)$$

The dynamic range of an amplifier indicates the span of useful input levels. It is commonly the distance - in decibels - from the minimum discernible signal to the upper bound. Several upper bound criteria are possible, a simple one being the so-called spurious free dynamic range. The upper bound is the input level where the third order intermodulation term P_{o3} passes the noise floor at the amplifier output. The noise floor is taken as the output corresponding to the minimum discernible signal from Eq.(156). Triangle considerations in Fig.49 provide a simple expression for the spurious-free dynamic range,

$$D_{spf}[dB] = P_{i,spf}[dBm] - P_{i,mds}[dBm] = \frac{2}{3} \left\{ P_{i,IP3}[dBm] - P_{i,mds}[dBm] \right\}, \quad (158)$$

where third order modulation is parameterized through the third order input level $P_{i,IP3}$.

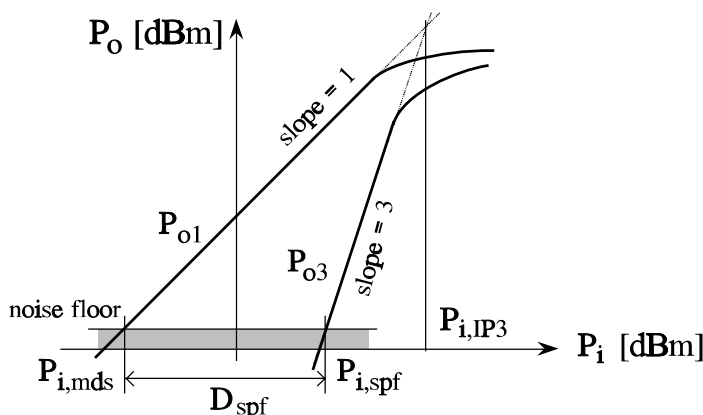


Fig.49 Spurious-free dynamic range, D_{spf} dB, the distance in input power levels where the third order intermodulation and the signal exceed the noise floor respectively.

Alternative dynamic range specifications use upper bound input that gives a minimum intermodulation ratio, for instance 40dB, or a certain amount of gain compression, for instance

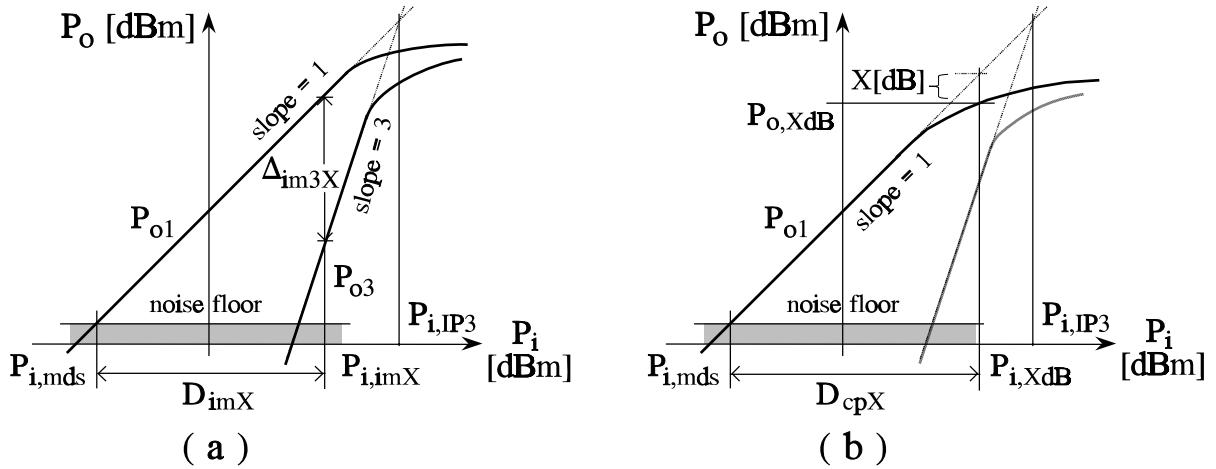


Fig.50 Dynamic range specifications with upper bound set by (a) intermodulation product or (b) compression.

.1 or 1 dB. These two cases are summarized by Fig.50. To express the intermodulation bounded dynamic range, D_{imX} , Eqs.(148),(149) are combined to give the input power for a required intermodulation ratio Δ_{im3X} in terms of the third order intercept point,

$$\Delta_{im3} = \frac{P_{i,IP3}^2}{P_i^2} \quad \Rightarrow \quad P_{i,im3X} = \frac{P_{i,IP3}}{\sqrt{\Delta_{im3X}}} . \quad (159)$$

Now the intermodulation bounded dynamic range is expressed

$$D_{imX}[dB] = 10 \log \left(\frac{P_{i,imX}}{P_{i,mds}} \right) = P_{i,IP3}[dBm] - \frac{1}{2} \Delta_{im3X}[dB] - P_{i,mds}[dBm] . \quad (160)$$

Compression is commonly specified by a single tone test and expressed separately. When the compression levels of specification equals the upper dynamic range bound, the corresponding dynamic is given by

$$D_{cpX}[dB] = P_{i,XdB}[dBm] - P_{i,mds}[dBm] = P_{o,XdB}[dBm] - G_{lin}[dB] + 1 - P_{i,mds}[dBm] . \quad (161)$$

The last expression uses data that refer to the output side, i.e. the output power level at XdB compression and the linear gain G_{lin} prior to compression.

Problems

P.IV-1

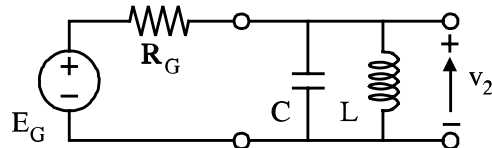


Fig.51

Assume narrowband conditions and show that the noise-bandwidth of the transmission from signal source E_G to v_2 in Fig.51 becomes $\pi/2$ times the 3dB bandwidth like the RC circuit in Example IV-1-1. What is the RMS noise voltage at port 2 if $R_G=50\Omega$ @ 290[K] and the circuit has center frequency $f_0=100$ MHz with 3dB bandwidth $BW_{3dB}=10$ MHz?

P.IV-2

An amplifier, which has ohmic optimal noise admittance, $y_{nfo}=g_{nfo}$, and ignorable input and correlation admittances, $y_{in}, y_{cor} \rightarrow 0$, is driven from a source with ohmic generator admittance at 290[K] where $y_G=g_G < g_{nfo}$. Show and explain the fact that if the input port of the amplifier is shunted by a resistor to provide noise matching, the resultant output SNR decreases compared to the case with no shunting resistance.

P.IV-3⁹

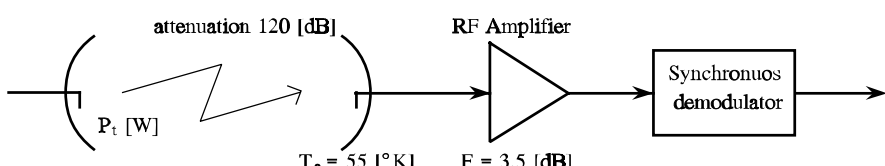


Fig.52

A QPSK signal is transmitted at 45 Mbps rate and is received as shown in Fig.52. The attenuation from the transmitter to the receiver is 120dB and the antenna has the noise temperature $T_a=55^{\circ}\text{K}$. The noise figure of the RF amplifier corresponding to the antenna impedance is $F=3.5$ dB.

Calculate the transmitter power $P_t[\text{W}]$ corresponding to the resultant bit error rates of 10^{-5} , 10^{-6} , and 10^{-7} respectively.

P.IV-4^{9,10}

A satellite transmits from a distance of 36000 kM a 1.2 Mbps QPSK modulated signal on a 12.2 GHz carrier. The transmitter power is 100 W and the satellite

9) Review chap.I pp 24-27 on bit error rates in digital modulations.

10) Review Friis' transmission formula and antenna areas

antenna gain is 27 dB. At the receiver site, the antenna has the noise temperature 52°K and the noise figure of the input amplifier is 2.5 dB at the antenna impedance of 50Ω .

Find the receiver antenna gain and the antenna area that are required to get $\text{BER} < 10^{-4}$. What is the corresponding signal voltage at the receiver amplifier input ?

P.IV-5⁹

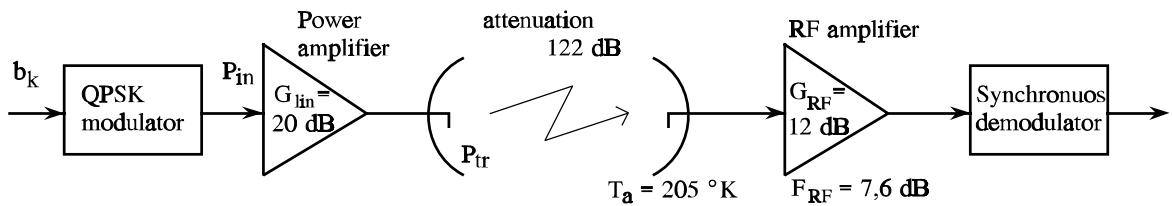


Fig.53

The transmission system in Fig.53 operates in QPSK modulation at rate $R_b = 102$ Mbps. The carrier frequency is $f_0 = 14.2$ GHz and the 122 dB attenuation is from the transmitter output power to the RF amplifier input. It is supposed that all components are matched at impedance level $Z_o = 50\Omega$.

What is the RF amplifier input signal to noise ratio per bit E_b / η if a bit error rate of $\text{BER} = 10^{-6}$ is required ? Find the corresponding transmitter output power.

What are the 1dB compression input and output levels for the transmitter power amplifier if it is supposed that 0.2 dB compression or less has no significant influence on the resultant bit error rate ?

Repeat the above calculations when a low-noise front amplifier is inserted as shown by Fig.54.

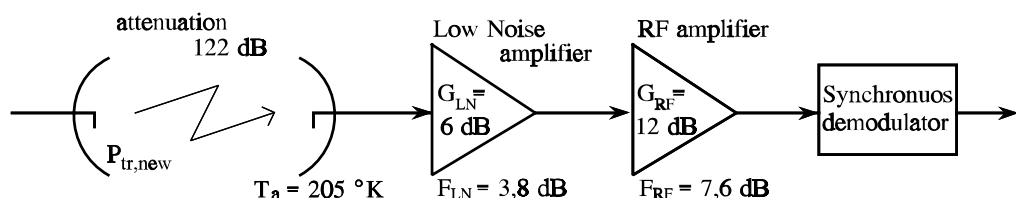


Fig.54

P.IV-6

The transistor in Example IV-3-3, biased by $I_C = 30\text{mA}$ and $V_{CE} = 8\text{V}$, has at 800 MHz the following y-parameters

$$Y_{tr} = \begin{Bmatrix} 12.2 + j4.34 \text{ mS} & -0.262 - j2.71 \text{ mS} \\ -5.42 - j114. \text{ mS} & 0.600 + j7.63 \text{ mS} \end{Bmatrix}. \quad (162)$$

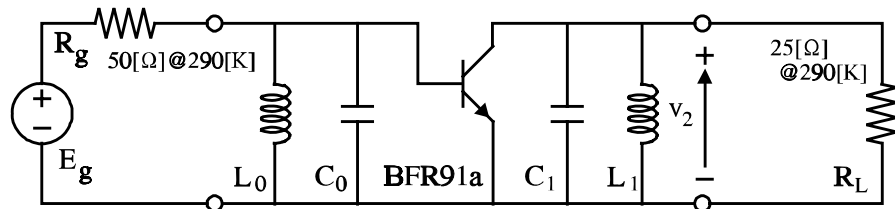


Fig.55

The transistor is driven by a 50Ω impedance and loaded by 25Ω as shown in Fig.6. The input and output resonance circuits are designed independently neglecting feed-back to approximate synchronous tuning around 800 MHz with 3dB bandwidth equal to 80 MHz. It is assumed that the generator and load impedances are at the reference temperature of 290K. Data sheets specify 1dB compression at 36 dBm output power if the transistor is loaded with 75Ω . It is supposed that this level reduces to 28 dBm when the load is 25Ω .

- Verify that it is legal to disregard feed-back effects when the tuning conditions are calculated. Find the operational, the transducer and the available power gains for the amplifiers and explain their differences.
- What is the noise figure of the amplifier ?
- Find the noise bandwidth of the amplifier if it assumed that it corresponds to the synchronously tuned characteristic. What is the total RMS output noise voltage at the amplifier output port ?
- Calculate the amplifier sensitivity in terms of input available power and find the corresponding 50dB 3rd order intermodulation bounded dynamic range.

P.IV-7

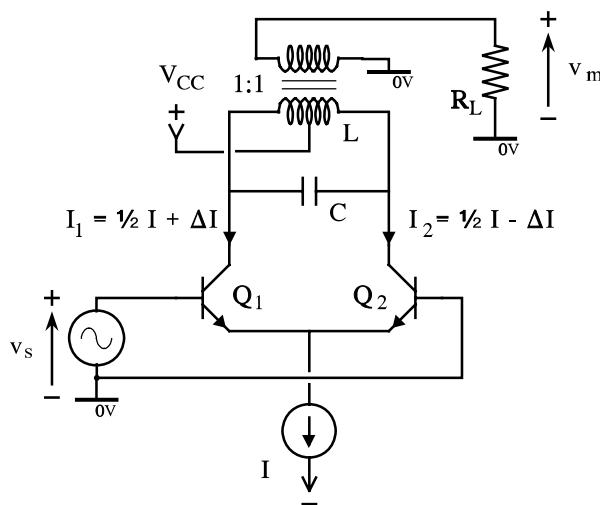


Fig.56

Fig.56 shows a single-tuned differential amplifier that is tuned to center frequency f_o . The differential current is expressed

$$\Delta I = \frac{I}{2} \tanh\left(\frac{v_s}{2V_t}\right), \quad \text{where} \quad V_t = \frac{kT}{q} \approx 25 \text{ [mV]}. \quad (163)$$

The bias current is $I=5\text{mA}$. The input signal is amplitude modulated,

$$v_s = V_s \cos \omega_0 t (1 + m \cos \omega_m t), \quad \omega_0 = 2\pi f_0, \quad \omega_m = 2\pi f_m. \quad (164)$$

The modulation index is $m=1$, and it is assumed that the modulating frequency is so low, that the sideband transistor load impedance is the same as the center frequency impedance. The nonlinear characteristic in Eq.(163) causes distortion in the low-frequency envelope at the output from the amplifier. Derive an expression for the third harmonic contribution K_3 to the total harmonic distortion of the output envelope, the so-called third order modulation distortion. Find the values with $V_s = 1\text{mV}$ and 10mV . Assume that the voltage bias and R_L are chosen to prevent transistor saturation.

References and Further Reading

- [1] M.S.Gupta,ed., Electrical Noise: Fundamentals & Sources, IEEE press, 1977
Includes 22 papers on basic noise properties and extensive bibliographies.
- [2] M.S.Gupta,ed., Selected Papers on Noise in Circuits and Systems, IEEE press, 1988. Includes 13 more papers on noise.
- [3] H.F.Cooke,"Microwave Transistors: Theory and Design", Proc.IEEE, vol.59, pp.1163-1181,Aug.1971, reprinted in [8].
- [4] A.van der Ziel, Noise in Solid State Devices and Circuits, Wiley, NY 1987.
- [5] M.S.Keshner,"1/f Noise",Proc.IEEE, Vol.70, No.3, pp.212-218, March 1982.
- [6] ITT Reference Data for Radio Engineers, Sams, NY, 1968
- [7] W.C.E.Lee, Mobile Communications Engineering, McGraw-Hill NY, 1982
- [8] H.Fukui,ed., Low-Noise Microwave Transistors and Amplifiers, IEEE press, 1981.
Includes 60 papers on device noise and low-noise design.
- [9] H.C.de Graff, F.M.Klaassen, Compact Transistor Modelling for Circuit Design, Springer, Wien-N.Y, 1990.
- [10] Y.P.Tsividis, Operation and Modeling of the MOS Transistor, McGraw-Hill, N.Y. 1988.
- [11] A.van der Ziel, "Noise in Solid-State Devices and Lasers", Proc.IEEE, vol.58,- pp.1178-1206, Aug.1970. Reprinted in [1].
- [12] C.D.Bulucea, D.C.Prisecaru,, "The Calculation of the Avalanche Multiplication Factor in Silicon P-N Junctions Taking into Account the Carrier Generation (Thermal or Optical) in the Space Charge Layer",IEEE trans.,Vol.ED-20,pp.693-701,Aug.1973.
- [13] P.Antognetti, G.Massobrio, eds., Semiconductor Device Modeling with SPICE, McGraw Hill,1988.
- [14] H.Statz,H.A.Hauss,R.A.Pucel,"Noise Characterization of Gallium Arsenide Field-Effect Transistors",IEEE trans. Electron Devices, vol. ED-21,pp.549-562, Sept.1974., reprinted in [8].
- [15] H.A.Haus, R.B.Adler, Circuit Theory of Linear Noisy Networks, Technology Press, Wiley, 1959.
- [16] J.Engberg, S.T.Larsen, Noise Theory of Linear and Nonlinear Circuits, Wiley 1996.
- [17] IRE Standards on Methods of Measuring Noise in Linear Twoports, 1959, Proc.IRE, vol.48, pp.60-68, Jan.1960, included in [8].

- [18] A.van der Ziel, Noise: Sources, Characterization, Measurement, Prentice-Hall N.Y. 1970.
- [19] H.T.Friis,"Noise Figures of Radio Receivers", Proc.IRE vol.32, pp.419-422, July 1944. Reprinted in [8].
- [20] H.Rothe, W.Dahlke, "Theory of Noisy Fourpoles" Proc.IRE, vol.44, pp.811-818, June 1956, reprinted in [8].
- [21] Y.L.Kuo,"Frequency-Domain Analysis of Weakly Nonlinear Networks, "Canned" Volterra Analysis", IEEE Circuit and Systems Magazine, aug.1977, pp.2-8 (part 1), and Oct.1977, pp.2-6 (part 2).
- [22] S.A.Maas, Nonlinear Microwave Circuits, Artech, Boston 1988.
- [23] R.S.Carson, Radio Communications Concepts: Analog, Wiley NY. 1990.

Index

1/f Noise	
see Flicker Noise	8
Avalanche noise	11
Bipolar Junction Transistor, BJT	
see Bipolar Transistor	17
Bipolar Transistor	
noise	17
Blocking	53
Boltzman's Constant	2
Burst noise	11
Carson	
noise theorem	6
Compression	50
Correlation Coefficient	33
FET gate and drain noise	24
Cross Modulation	54
Desensitization	54
Diode	
noise	15
Distortion	
almost linear circuits	47
compression	50
cross modulation	54
hum	55
modulation	65
single tone	48
total harmonic, THD	49
two-tone	52
Dynamic Range	60
compression bounded	60
intermodulation bounded	60
spurious free	60
Electron Charge	6
Field Effect Transistor	
noise	22
Flicker Noise	8
RF effects	9
Generation-Recombination	
noise	10
Hum, Hum-Modulation	56
Intercept Point	56
second order	58
third order	57
Intermodulation	
distortion IMD	57
products	53
ratio	57
Johnson Noise	4
Link Budget	31
Man-Made noise	13
Minimum Noise Figure	37
Modulation	
third order distortion	65
Noise	
avalanche	11
burst	11
flicker or 1/f	8
generation-recombination	10
in bipolar transistors	17
in diodes	15
in field effect transistors, JFET, MESFET, MOSFET	22
Johnson	4
man-made	13
popcorn	11
shot	6
thermal	2
Noise Bandwidth	5
RC-circuit	5
resonance circuit	62
Noise Conductance	12
Noise Factor	25
Noise Figure	25
by noise temperature	29
by open circuit voltages	26
by short circuit currents	26
by signal to noise ratio	27
cascaded two-ports	31
circles in admittance plane	37
circles in reflection plane	39
measurement	28
minimum in bipolar transistors	18
reference temperature	26
two-port minimum	37
Noise Matching	37
Noise of Cascaded Two-Ports	30

Noise Representation	
input equivalent circuit	35
two-ports	33
Noise Resistance	12
Noise Temperature	
by noise figure	29
cascaded two-ports	30
one-port	12
two-port	29
Noise Tuning	36
Nyquist	
noise	4
Planck's Constant	2
Reference Temperature	
noise figure	26
Schottky's theorem	7
Second Order Intercept Point	58
Sensitivity	59
Shot Noise	6
Signal to Noise Ratio	
noise figure relation	27
Spurious Components	1
Thermal Noise	2
Total Harmonic Distortion, THD	49
Two-Ports	
noise representation	33
Two-Tone Distortion	52
Van der Ziels equations	27
Volterra Series	48

Reviewing The Basics Of Microstrip Lines

An understanding of the fundamentals of microstrip transmission lines can guide high-frequency designers in the proper application of this venerable circuit technology.

Leo G. Maloratsky

Principal Engineer

Rockwell Collins, 2100 West Hibiscus Blvd., Melbourne, FL 32901; (407) 953-1729, e-mail: lgmalora@mbnotes.collins.rockwell.com.

PRINTED transmission lines are widely used, and for good reason. They are broadband in frequency. They provide circuits that are compact and light in weight. They are generally economical to produce since they are readily adaptable to hybrid and monolithic integrated-circuit (IC) fabrication technologies at RF and microwave frequencies. To better appreciate printed transmission lines, and microstrip in particular, some of the basic principles of microstrip lines will be reviewed here.

A number of different transmission lines are generally used for microwave ICs (MICs) as shown in Fig. 1. Each type has its advantages

with respect to the others. In Fig. 1, it should be noted that the substrate materials are denoted by the dotted areas and the conductors are indicated by the bold lines.

The microstrip line is a transmission-line geometry with a single conductor trace on one side of a dielectric substrate and a single ground plane on the opposite side. Since it is an open structure, microstrip line has a major fabrication advantage over stripline. It also features ease of interconnections and adjustments.

In a microstrip line, the wavelength, Λ , is given by:

$$\Lambda = \lambda / (\epsilon_{\text{eff}})^{0.5} \quad (1)$$

where:

ϵ_{eff} = the effective dielectric constant, which depends on the dielectric constant of the substrate material and the physical dimensions of the microstrip line, and

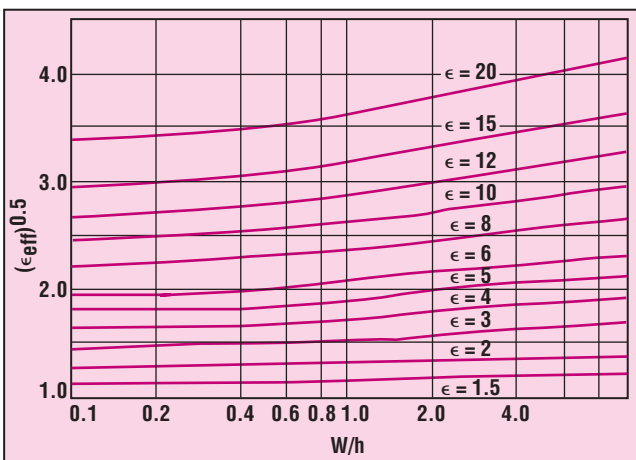
λ = the free-space wavelength.

In a microstrip line, the electromagnetic (EM) fields exist partly in the air above the dielectric substrate and partly within the substrate itself. Intuitively, the effective dielectric constant of the line is expected to be greater than the dielectric constant

Microstrip line	Basic lines		Modifications			
		Microstrip line		Suspended microstrip line		Inverted microstrip line
Stripline		Stripline		Double-conductor stripline		
Suspended stripline		Shielded high-Q suspended stripline		Shielded suspended stripline		Shielded suspended double-substrate stripline
Slotline		Slotline		Antipodal slotline		Bilateral finline
Coplanar waveguide		Symmetrical coplanar line		Shielded coplanar waveguide		
Finline		Finline		Bilateral slotline		Antipodal finline
						Antipodal overlapping finline

1. These are commonly used types of printed transmission lines for MICs.

Microstrip Lines



2. The values of effective dielectric constant are shown for different substrate relative dielectric constants as a function of W/h .

of air (1) and less than that of the dielectric substrate.¹ Various curves for effective dielectric constant are shown in Fig. 2 as a function of physical dimensions and relative dielectric constant.

Referring again to Fig. 1, it should be apparent that a basic (unshielded) microstrip line is not really a practical structure. It is

open to the air and, in reality, it is desirable to have circuits that are covered to protect them from the environment as well as to prevent radiation and EM interference (EMI). Also, the microstrip configurations that have been so far discussed are transversally infinite in extent, which deviates from reality. Covering the basic microstrip configuration with metal top plates on the top and on the sides leads to a more realistic circuit configuration, a shielded microstrip line with a housing (Fig. 1).

The main purposes of the housing or package are to provide mechanical strength, EM shielding, герметизация, and heat sinking in the case of high-power applications. Packaging must protect the circuitry from moisture, humidity, dust, salt spray, and other environmental contaminants. In order to protect the circuit, certain methods of sealing can be used: conductive epoxy, solder, gasket materials, and metallization tape.

An MIC mounted into a housing may be looked on as a dielectrically loaded cavity resonator (Fig. 3, left) with the following inner dimensions: a is the width, l is the length, and H is the height of the enclosure. These dimensions should be selected in a way so that the waveguide modes are below cutoff.

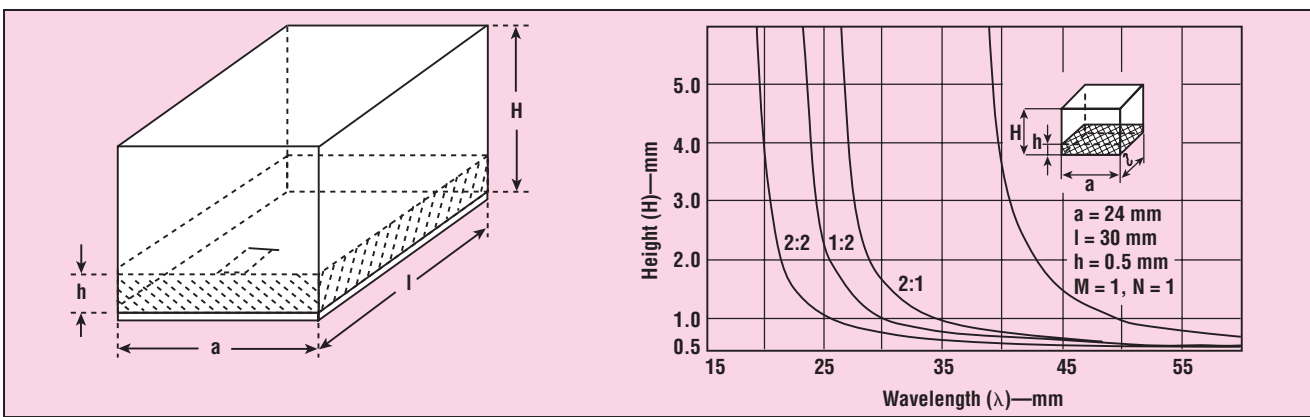
The parasitic modes appear in this resonator if:

$$H = \{h[1 - (1/\epsilon)]R\}I(R - I) \quad (2)$$

where:

$$R = (\lambda_0 / 2)^2 [(M / l)^2 + (N / a)^2] \quad (2a)$$

Transmission line	Q factor	Radiation	Dispersion	Impedance range	Chip mounting
Microstrip (dielectric) (GaAs, Si)	250 100 to 150	Low High	Low	20 to 120	Difficult for shunt, easy for series
Stripline	400	Low	None	35 to 250	Poor
Suspended stripline	500	Low	None	40 to 150	Fair
Slotline	100	Medium	High	60 to 200	Easy for shunt, difficult for series
Coplanar waveguide	150	Medium	Low	20 to 250	Easy for series and shunt
Finline	500	None	Low	10 to 400	Fair



3. Housing dimensions are selected for microstrip circuits (left) to minimize losses. The effects of unfavorable housing height versus wavelength and different parasitic modes is shown (right).

and M and N = positive integers.

From eq. 2, it is possible to obtain the condition of absence of parasitic modes:

$$R - 1 < 0 ; R < 1$$

or

$$\lambda_0^2 < 4 / [(M/1)^2 + (N/a)^2] \quad (3)$$

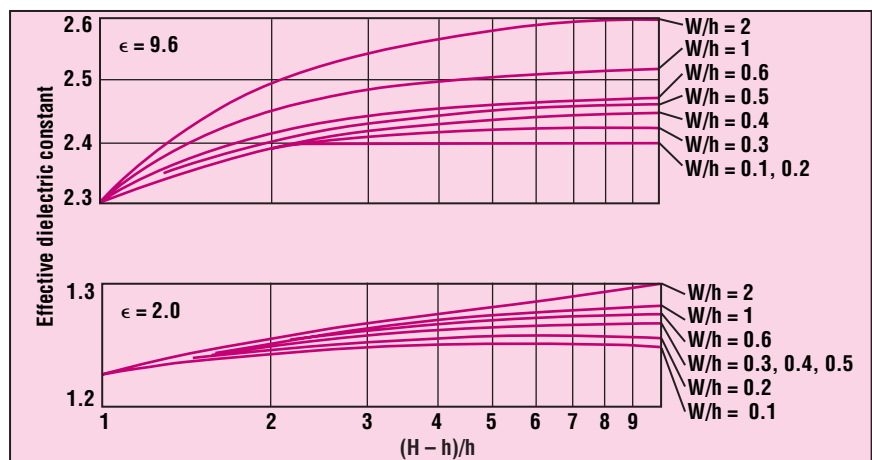
or

$$\lambda_0 < 2 / [(M/1)^2 + (N/a)^2]^{0.5} \quad (4)$$

Equation 4 is known as the condition for wave propagation in a waveguide with dimensions $l \times a$. In the case of this article, it can also be considered the condition for the absence of parasitic modes in a waveguide of cross-section $a \times H$ or $l \times H$. If eq. 4 is not satisfied, parasitic modes can arise, and the height H must be chosen to suppress these modes. Figure 3 (right) illustrates the resulting graphs of unfavorable H versus λ_0 for housing dimensions of $a = 24$ mm, $l = 30$ mm, and dielectric substrate with a dielectric constant of 9.8 and THK of 0.5 mm.

The top and side covers essentially redistribute the field of the more theoretical microstrip and understandably have an influence on the effective dielectric constant.

Figure 4 shows the relationship between the effective dielectric constant and the physical dimensions of the shielded microstrip line for different values of the relative dielectric constant of the substrate material.² In these curves, it has been



4. The effective dielectric constant is shown as a function of the relative dielectric constant and physical dimensions for a shielded microstrip line.

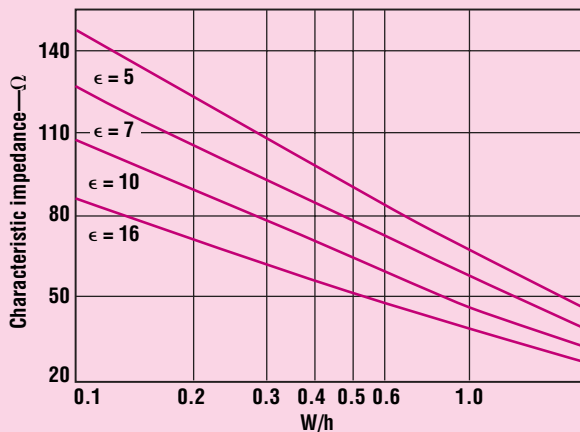
assumed that the side walls are sufficiently spaced so that they only see weak fringing fields and, therefore, have a negligible effect on the effective dielectric constant. The top cover tends to lower the effective dielectric constant (which is consistent with intuition). The top wall enables electric fields in the air above the strip conductor thereby giving the air more influence in determining the propagation characteristics.

The characteristic impedance of a microstrip line may be approximately calculated by assuming that the EM field in the line has a quasi transverse-EM (TEM) nature. The characteristic impedance of a microstrip line can be calculated using the Wheeler equations.^{3,4}

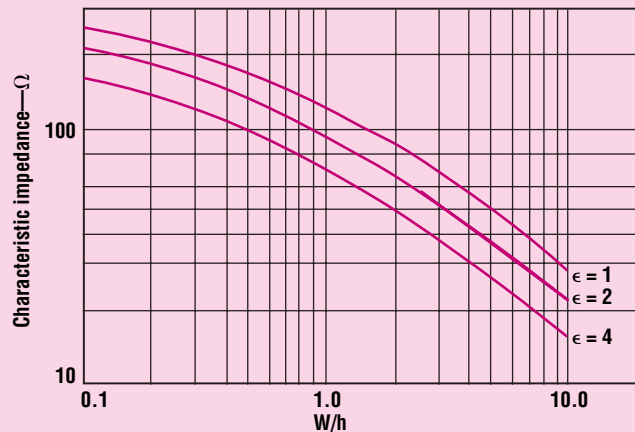
Figure 5 shows the characteristic impedance of microstrip lines for var-

ious geometries and substrates of different relative dielectric constants while Fig. 6 illustrates the relationships between characteristic impedance and the physical dimensions of shielded microstrip lines for two examples: substrates with low (2) and high (9.6) relative dielectric constants.² The top cover tends to reduce the impedance. When the ratio of the distance from the top cover to the dielectric substrate and the substrate thickness $[(H-h)/h]$ is greater than 10, the enclosure effects can be considered negligible. The characteristic impedance range of a microstrip line is 20 to 120 Ω. The upper limit is set by production tolerances while the lower limit is set by the appearance of higher-order modes.

There are three types of losses that occur in microstrip lines: con-

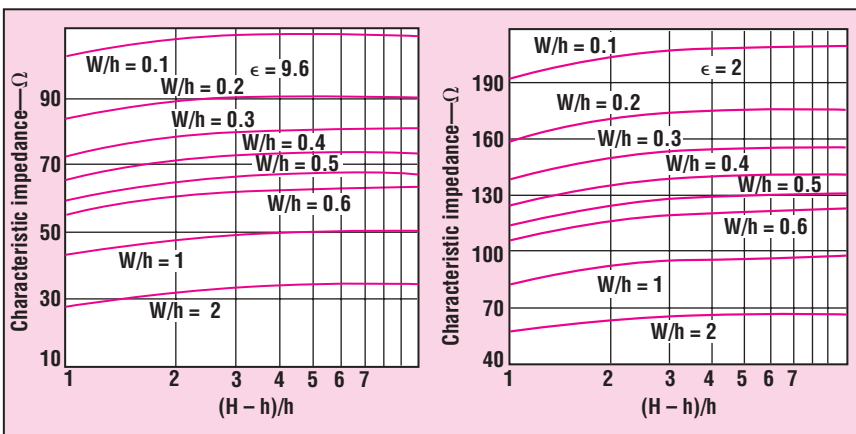


(a)



(b)

5. The characteristic line impedance has been plotted for substrates with high (a) and low (b) dielectric constants.



6. These plots show the relationship between the characteristic impedance and the physical dimensions of microstrip lines using substrates with high (9.6, left) and low (2.0, right) dielectric constants.

ductor (or ohmic) losses, dielectric losses, and radiation losses. An idealized microstrip line, being open to a semi-infinite air space, acts similar to an antenna and tends to radiate energy. Substrate materials with low dielectric constants (5 or less) are used when cost reduction is the priority. Similar materials are also used at millimeter-wave frequencies to avoid excessively tight mechanical tolerances. However, the lower the

dielectric constant, the less the concentration of energy is in the substrate region and, hence, the more are the radiation losses. Radiation losses depend on the dielectric constant, the substrate thickness, and the circuit geometry.

The use of high-dielectric-constant substrate materials reduces radiation losses because most of the EM field is concentrated in the dielectric between the conductive strip and the

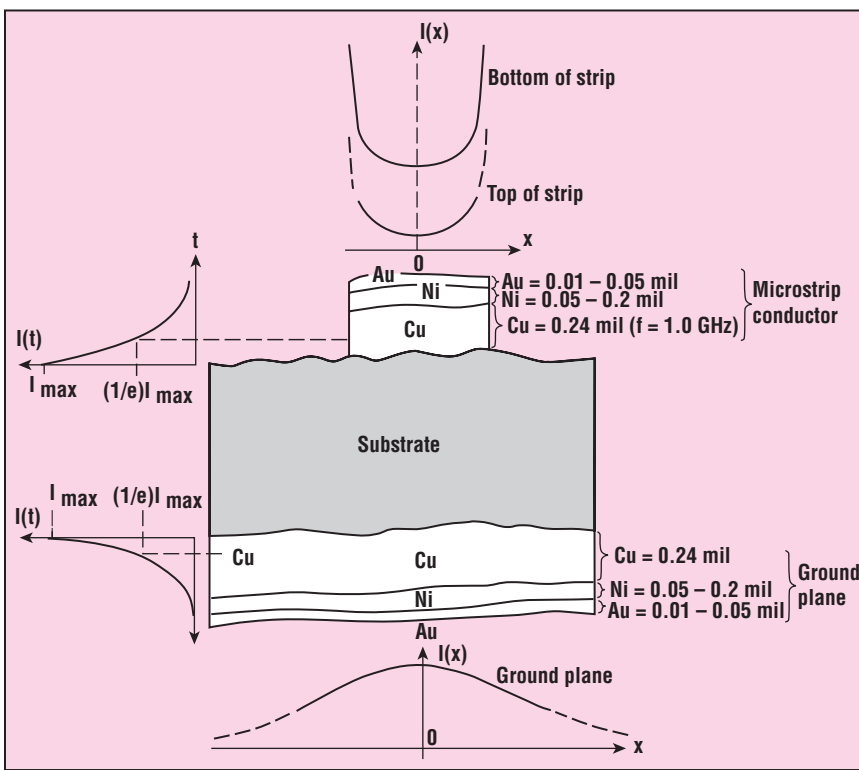
ground plane. The real benefit in having a higher dielectric constant is that the package size decreases by approximately the square root of the dielectric constant. This is an advantage at lower frequencies but may be a problem at higher frequencies.

In most conventional microstrip designs with high substrate dielectric constant, conductor losses in the strip conductor and the ground plane dominate over dielectric and radiation losses. Conductor losses are a result of several factors related to the metallic material composing the ground plane and walls, among which are conductivity, skin effects, and surface roughness. With finite conductivity, there is a non-uniform current density starting at the surface and exponentially decaying into the bulk of the conductive metal. This is the alleged skin effect and its effects can be visualized by an approximation consisting of a uniform current density flowing in a layer near the surface of the metallic elements to a uniform skin depth, δ . The skin depth of a conductor is defined as the distance to the conductor (Fig. 7) where the current density drops to $1/e$ from a maximum current density of I_{max} , or 37 percent of its value at the surface of the conductor.

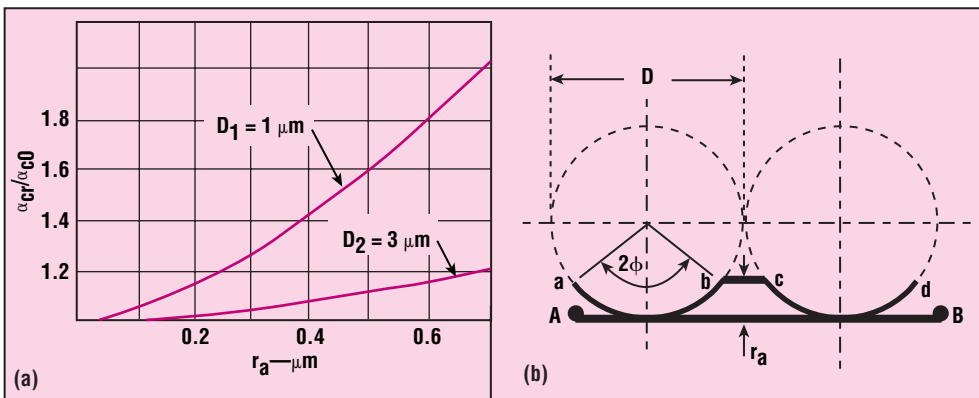
To minimize conductor loss while simultaneously minimizing the amount of metallic material flanking the dielectric, the conductor thickness should be greater than approximately three to five times the skin depth.

In a microstrip line, conductor losses increase with increasing characteristic impedance due to the greater resistance of narrow strips. Conductor losses follow a trend which is opposite to radiation loss with respect to W/h .

The fabrication process of real microstrip devices creates scratches and bumps on the metal surfaces. A cross-section of a microstrip line is shown in Fig. 7. The inside surfaces of the strip conductor and the ground plane facing the substrate repeat the shape of the substrate. The current, concentrated in the metal surface next to the substrate, follows the uneven surface of the substrate and encounters a greater resistance com-



7. This cross-sectional view shows the current distribution across a microstrip conductor and its ground plane.



8. The profile of a substrate's uneven surface (a) shows how surface roughness affects normalized conductor losses (b).

pared to the case of a smooth substrate. As the roughness of the surface increases, the length of the current path increases and, therefore, the losses increase.

Consider a substrate surface which, for example, coincides with the shape of the diamond abrasive material that is used to polish the substrate. The path of the current in conductor segment a-d (Fig. 8a) is shown by the line abcd. For an ideally smooth surface, the length of the current path AB is: $I_{AB} = D_n$ where:

n = the number of diamond abrasives within segment AB.

The ratio of conductor losses in the case of an uneven surface, α_{cr} , to losses in the case of a perfectly smooth surface, α_{c0} ,² is:

$$\frac{\alpha_{cr}}{\alpha_{c0}} = 1 + \arccos [1 - (4r_a/D)] - 2\{(2r_a/D)[1 - (2r_a/D)]\}^{0.5} \quad (5)$$

Using eq. 5, α_{cr}/α_{c0} can be plotted as a function of r_a for $D_1 = 1 \mu\text{m}$ and $D_2 = 3 \mu\text{m}$ (Fig. 8b). Analysis of the resulting functions shows that for smaller diameters, conductor losses in the microstrip line are more dependent on the unevenness of the substrate roughness because the extra path length a surface (or skin) current sees is less. For example, consider a copper (Cu) microstrip line with sapphire substrate where typically the roughness is $1 \mu\text{m}$.⁵ The skin depth at a few gigahertz is $1 \mu\text{m}$ and the loss is increased approximately 60 percent when the surface roughness is taken into account.

To minimize dielectric losses, high-quality, low-loss dielectric substrates, such as alumina, quartz, and sapphire, are typically used in hybrid ICs. For most microstrip lines, conductor losses greatly exceed dielectric losses. However, in monolithic microwave ICs (MMICs), silicon (Si) or GaAs substrates result in much larger dielectric losses (approximately 0.04 dB/mm).⁵

The preceding sections have considered the individual contributions to losses in microstrip by radiation, ohmic, and dielectric effects. These individual loss components are at most first-order perturbations in the

overall EM wave propagation and, consequently, can be combined linearly. To do so, it is convenient to consider the total Q factor, which can be expressed by:

$$1/Q = (1/Q_c) + (1/Q_d) + (1/Q_r)$$

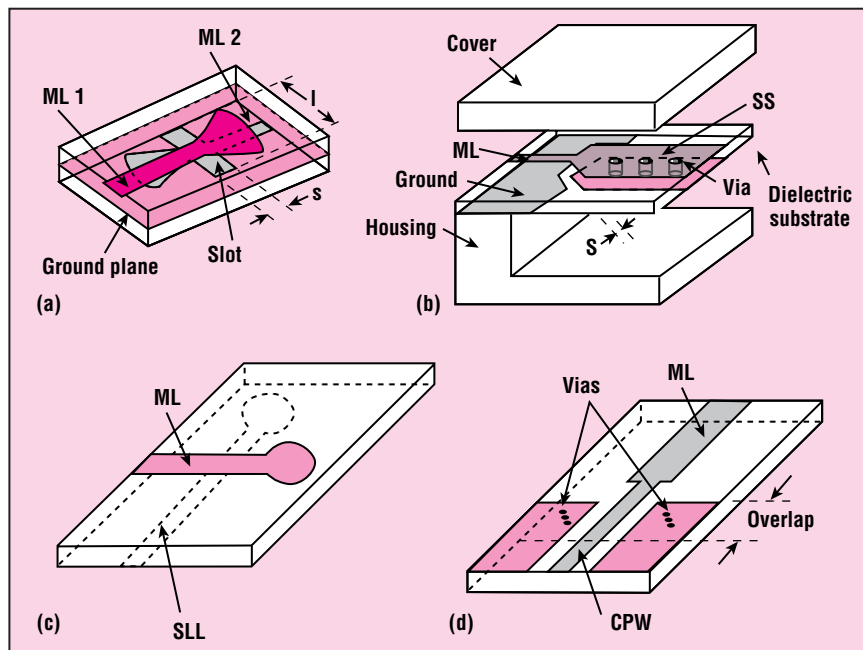
where:

Q_c , Q_d , and Q_r are the quality factors corresponding to the conductor, dielectric, and radiation losses, respectively. The unloaded Q factor of the microstrip line is typically on the order of 250.

CHOOSING DIMENSIONS

For all circuit considerations, a basic approach involves starting with the particular ranges of dimension ratios required to achieve a desired characteristic impedance. Following that, the strip width should be minimized to decrease the overall dimensions, as well as to suppress higher-order modes. It is important to remember, however, that a smaller strip width leads to higher losses.

Factors that affect the choice of substrate thickness are the most contro-



9. Various transitions between microstrip and other circuit structures are possible: microstrip to microstrip (a), microstrip to suspended stripline (b), microstrip to slotted line (c), and microstrip to coplanar waveguide (d).

Microstrip Lines

versial. The positive effects of decreasing substrate thickness are compact circuits, ease of integration, less tendency to launch higher-order modes or radiation, and via holes drilled through the dielectric substrate will contribute smaller parasitic inductances to the overall performance.

However, a decrease in the substrate thickness (h) while maintain-

ing a constant characteristic impedance, Z_0 , must be accompanied by a narrowing of the conductor width, W . Narrowing W leads to higher conductor losses along with a lower Q . Also, for smaller W and h , the fabrication tolerances become more severe. Careless handing of thin substrates can cause stress and strain which can modify the performance of

the substrate.

Microstrip circuit dimensions decrease with increasing substrate dielectric constant. Losses then usually increase because higher dielectric constant materials usually have higher loss tangents, $\tan \delta$, and also because for the same characteristic impedance, reduced conductor line widths have higher ohmic losses. This is a typical conflicting situation between the necessary requirements for small dimensions and low loss. For many applications, lower dielectric constants are preferred since losses are reduced, conductor geometries are larger (and, therefore, more producible), and the cutoff frequency of the circuit increases.

MICROSTRIP TRANSITIONS

The rapid development of high-density modules requires the design of interconnects and transitions, especially for multilayer circuits. Consider useful transitions from microstrip to other printed transition lines. A transition between two microstrip lines (Fig. 9a) can be realized through a slot in the ground plane.

A transition between a microstrip line and a suspended stripline circuit is shown in Fig. 9b.

A transition between a slotline and a microstrip line can be seen in Fig. 9c.^{7,8}

An overlay transition between a microstrip line and coplanar waveguide (CPW) is shown (Fig. 9d).^{9,10} ••

Acknowledgment

The author would like to thank Dr. Paul Chorney who reviewed these materials and provided valuable suggestions.

References

1. H. Sobol, "Application of Integrated Circuit Technology to Microwave Frequencies," *Proceedings of the IEEE*, Vol. 59, 1971, pp. 1200-1211.
2. L.G. Maloratsky, *Miniaturization of Microwave Elements and Devices*, Soviet Radio, Moscow, 1976.
3. H.A. Wheeler, "Transmission-Line Properties of a Strip on a Dielectric Sheet on a Plane," *IEEE Transactions on Microwave Theory & Techniques*, Vol. 25, No. 8, August 1977, pp. 631-647.
4. H.A. Wheeler, "Transmission-Line Properties of Parallel Strips Separated by a Dielectric Sheet," *IEEE Transactions on Microwave Theory & Techniques*, Vol. 13, No. 3, March 1965, pp. 172-185.
5. T.C. Edwards, *Foundations for Microstrip Circuit Design*, Wiley, New York, 1981.
6. K.J. Herrick, J.G. Yook, and P.B. Katehi, "Microtechnology in the Development of Three-Dimensional Circuits," *IEEE Transactions on Microwave Theory & Techniques*, Vol. 46, No. 11, November 1998.
7. S.B. Cohn, "Slot-Line on a Dielectric Substrate," *IEEE Transactions on Microwave Theory & Techniques*, Vol. 17, 1969, pp. 768-778.
8. J.S. Izadian and S.M. Izadian, *Microwave Transition Design*, Artech House, Norwood, MA, 1988.
9. M. Hougart and C. Aury, "Various Excitation of Coplanar Waveguides," *IEEE MTT-S International Microwave Symposium Digest*, 1979.
10. J. Burke and R.W. Jackson, "Surface-to-Surface Transition via Electromagnetic Coupling of Microstrip and Coplanar Waveguide," *IEEE Transactions on Microwave Theory & Techniques*, Vol. 37, No. 3, March 1989, pp. 519-525.

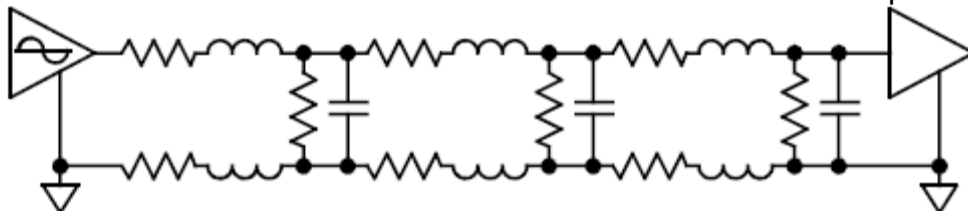
RF / Microwave PC Board Design and Layout

Base Materials for High Speed, High Frequency PC Boards – Rick Hartley

<http://www.gsl.net/va3iul/>

RF / Microwave Design – Basics

- Unlike digital, analog signals can be at any voltage and current level (between their min & max), at any point in time.
- Standard analog signals are assumed to be between DC and a few hundreds of MHz.
- RF/Microwave signals are one frequency or a band of frequencies imposed on a very high frequency carrier.
- RF/Microwave Circuits are designed to pass signals within band of interest and filter energy outside that range.
- Signal band can be narrow or wide.
 - Narrow band circuits usually have pass band less than 1 MHz.
 - Broad band circuits pass a range of frequencies up to tens of MHz.
- When digital and microwave exist in the same unit, pass bands of microwave circuits usually fall (by design) outside the harmonic range of the digital signals.
- RF / Microwave PC Board layout simply follows the “Laws of Physics”-
- When laws of physics can't be followed, know what compromises are available.
- Microwave signals are very sensitive to noise, ringing and reflections and must be treated with great care.
- Need complete impedance (Z_0) matching (50 ohm out/ 50 ohm line/ 50 ohm in).
 - Minimizes Return Loss / VSWR.
- A Transmission Line is any pair of wires or conductors used to move energy from point A to point B, usually of controlled size and in a controlled dielectric to create controlled impedance (Z_0).



$$\text{Evenly Distributed } R, L, G \text{ & } C - Z_0 = \sqrt{\frac{R}{G} + \frac{j\omega L}{j\omega C}}$$

- Inductance (L) is determined by the loop function of signal and return path.
 - Small spacing (tight loop) creates high flux cancellation, hence low inductance.
- Capacitance (C) is function of signal spacing to the return path.
 - Small spacing creates high capacitance.
- Since small spacing (tight loop) creates low L & high C, and since:
 - $Z_0 = \sqrt{L/C}$, small spacing creates low Z_0 .
- Additionally, Z_0 is function of signal conductor width & thickness and a function of the DK dielectric constant (ϵ_r) of the material surrounding the lines.
- Sometimes dielectric surrounding transmission line isn't constant (outer layer trace on PCB).
 - DK above trace is Air ($= 1.0008$).
 - DK below trace is FR4 (approx = 4.1).
 - Effective Relative Er ($\epsilon_{r,\text{eff}}$) is 3 to 3.25.
- Signal return currents follow the path of least impedance (in high frequency circuits that = path of least inductance).

- Whenever we neglect to provide a low impedance return path for RF / Microwave signals, they WILL find a path.
- It may NOT be what we had in mind.
- Signal Wavelength -
 - Wavelength (λ) of a signal is the distance it travels in the time of one cycle.
- For a signal traveling in free space -
 - $\lambda = c / f$ (speed of light) / f (frequency), ($\lambda = 11.78''/\text{nsec}$ at 1GHz = 11.78")
- Signal in a higher dielectric - $\lambda = c / [f \cdot (1 / \sqrt{\epsilon_r})]$
- Signal critical length
 - How long a PCB trace can be before we MUST pay attention to impedance control?
 - Function of frequency (1/16th wavelength)

$$L_{critical} = \frac{c}{f} \cdot \frac{1}{\sqrt{\epsilon_{eff}}} \cdot \frac{1}{16}$$

At 1 GHz = approx .425" (microstrip- FR4)

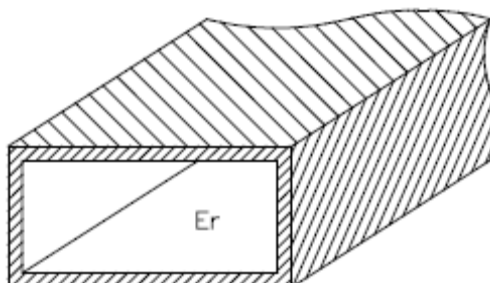
At 1 GHz = approx .375" (stripline - FR4)

Signal Loss / Noise

- Reflections -
 - Return Loss / VSWR
- Skin Effect -
 - Increased resistance of PCB trace due to decreased cross sectional area.
 - In analog circuits above 100 MHz.
 - Skin depth - 0.000822" @ 10 MHz and 0.000026" @ 10 GHz.
- Loss Tangent -
 - Dielectric Loss caused by molecular structure of board material.
 - In analog circuits above 200 MHz.
 - PTFE's far better than FR4.
- Energy Coupling-
 - Cross Talk.
 - Noise Induction.

Line Types and Impedance (Z_0)

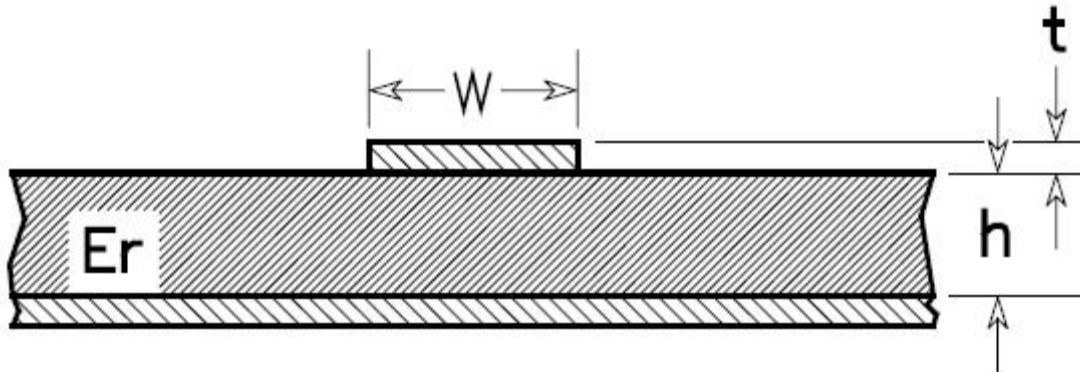
- Waveguide



- Uses air as transmission medium and side walls of tube as return path.
- Won't support energy propagation below cutoff frequency.
- Works best at ultra high frequencies with millimeter wavelengths.
- With an air dielectric, signals propagate at the speed of light.
- Very low loss due to smooth side walls and the air dielectric.
- Ultra low loss with high density, ultra smooth coating on walls.
- In very high power applications, uses solid dielectric to prevent voltage arcing.
- Signal traces longer than critical length (1/16 λ in DK) need impedance control to prevent return loss due to reflections.

- Shorter circuit elements don't require impedance control, but it usually does NO harm.
- Don't bother to Z_0 control, short lines if it will create a problem (ie- DFM – Design for Manufacturing).
- Impedance (L/C)-
 - Lower ϵ_r materials - net higher impedance traces and faster propagation times per given trace width & trace-to-ground separation.
 - As trace width increases, trace impedance decreases (thickness has min effect).
 - As trace spacing from ground increases, impedance increases.

Microstrip



$$Z_0 = \frac{120\pi}{2.0\sqrt{2.0}\pi\sqrt{\epsilon_r+1.0}} \ln \left\{ 1.0 + \frac{4.0h}{w'} \left[\frac{14.0 + 8.0/\epsilon_r}{11.0} \frac{4.0h}{w'} \right. \right. \\ \left. \left. + \sqrt{\left(\frac{14.0 + 8.0/\epsilon_r}{11.0} \right)^2 \left(\frac{4.0h}{w'} \right)^2 + \frac{1.0 + 1.0/\epsilon_r}{2.0} \pi^2} \right] \right\} (\Omega)$$

where: $w' = w + \Delta w'$

$$\Delta w' = \Delta w \left(\frac{1.0 + 1.0/\epsilon_r}{2.0} \right)$$

**(Replace Er
with Eeff)**

$$\frac{\Delta w}{t} = \frac{1.0}{\pi} \ln \left[\frac{4e}{(t/h)^2 + \left(\frac{1/\pi}{w/t + 1.1} \right)^2} \right]$$

$$Z_0 = \frac{60}{\sqrt{\epsilon_{eff}}} \bullet \ln \left(\frac{8h}{w} + \frac{w}{4h} \right) \quad \text{if} \quad \frac{w}{h} < 1$$

otherwise

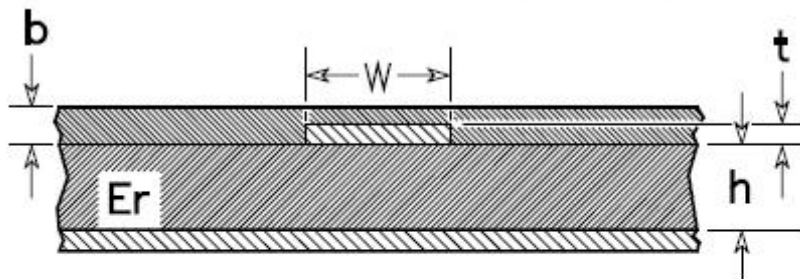
$$Z_0 = \frac{120\pi}{\sqrt{\epsilon_{eff}}} \bullet \frac{1}{\left(\frac{w}{h} + 1.393 + 0.677 \bullet \ln \left(\frac{w}{h} + 1.444 \right) \right)}$$

$$\varepsilon_{eff} = \frac{\varepsilon_r + 1}{2} + \frac{\varepsilon_r - 1}{2} \left[\frac{1}{\sqrt{1 + \frac{12h}{w}}} + 0.04 \left(1 - \frac{w}{h}\right)^2 \right] \text{ if } \frac{w}{h} < 1$$

otherwise

$$\varepsilon_{eff} = \left[\frac{\varepsilon_r + 1}{2} + \frac{\varepsilon_r - 1}{2} \left[\frac{1}{\sqrt{1 + \frac{12h}{w}}} \right] \right]$$

Embedded Microstrip

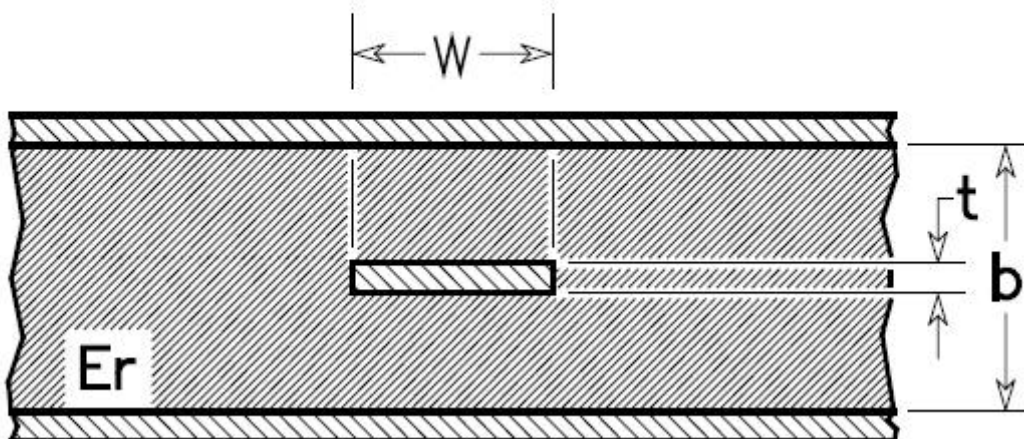


Multiply Zo (from Microstrip) by -

$$\frac{\varepsilon_{eff}}{\varepsilon_{eff} \cdot e^{(-2.0b/h)} + \varepsilon_r [1.0 - e^{(-2.0b/h)}]}$$

Can use w/Soldermask over Microstrip (Often NOT Needed)

Centered Stripline



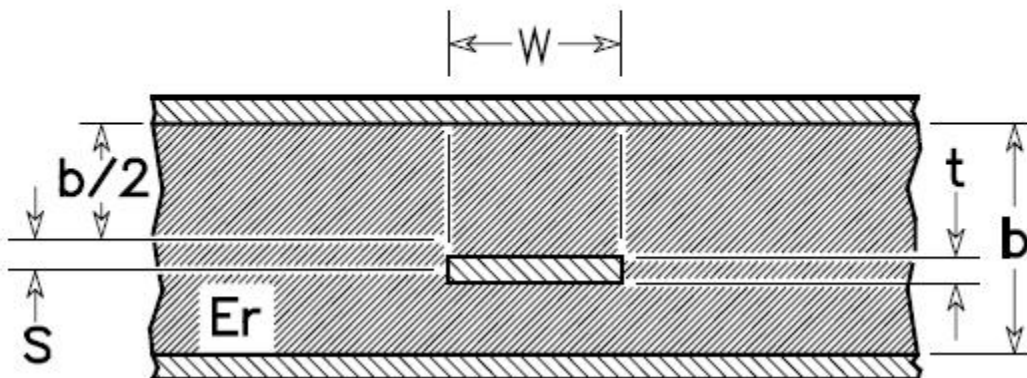
$$Z_0 = \frac{120\pi}{2.0\pi\sqrt{\epsilon_r}} \ln \left\{ 1.0 + \frac{4.0(b-t)}{\pi w'} \left[\frac{8.0(b-t)}{\pi w'} + \sqrt{\left(\frac{8.0(b-t)}{\pi w'} \right)^2 + 6.27} \right] \right\}$$

where: $b = 2.0h + t$

$$w' = w + \frac{\Delta w}{t} t$$

$$\frac{\Delta w}{t} = \frac{1.0}{\pi} \ln \left[\frac{e}{\sqrt{\left(\frac{1}{2.0(b-t)/t+1} \right)^2 + \left(\frac{.25\pi}{w/t+1.1} \right)^m}} \right]$$

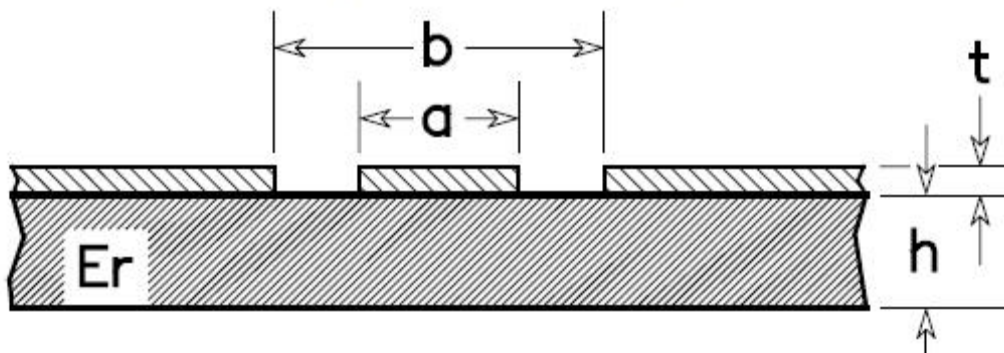
Off-Center stripline



Microstrip verses Stripline

- Microstrip has lower loss-tangent problem.
- Microstrip has faster propagation time.
- Stripline has better immunity to crosstalk.
- Stripline has better EMI characteristics.

Coplanar Waveguide



- 'b' should be less than $\lambda/2$ for best performance.
- Ground must extend greater than $5x'b'$ on either side of trace 'a'.
- Lower loss-tangent than Microstrip (signals couple mostly through air).
- Higher skin-effect losses (fields concentrate on edges of trace and grounds).

- May need to strap grounds together on either side of trace, every 1/20th wavelength.
- Only need one side of board to be accessible.
- No plated holes needed,
- Can narrow trace to match component leads.
- CPW allows variation of trace width, or spacing-to-ground or dielectric thickness to control Z_0 .
- Z_0 of CPW decreases as dielectric thickness increases.
- CPW produces smaller trace per given Z_0 than Microstrip.

$$Z_0 = \frac{30.0\pi}{\sqrt{\epsilon_{eff,t}}} \cdot \frac{K(kt')}{K(kt)} \quad k_1 = \frac{\sinh\left(\frac{\pi a_t}{4.0h}\right)}{\sinh\left(\frac{\pi b_t}{4.0h}\right)}$$

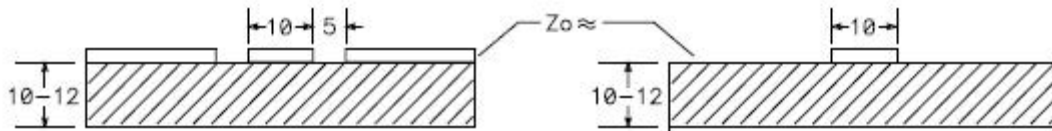
$$\epsilon_{eff,t} = \epsilon_{eff} - \frac{\epsilon_{eff} - 1.0}{\frac{(b-a)/2.0}{0.7t} \cdot \frac{K(k)}{K'(k)} + 1.0} \quad k_1' = \sqrt{1.0 - k_1^2}$$

$$\epsilon_{eff} = 1.0 + \frac{\epsilon_r - 1.0}{2.0} \cdot \frac{K(k)K(k_1)}{K(k)K(k_1')} \quad a_t = a + \frac{1.25t}{\pi} \left[1.0 + \ln\left(\frac{4.0\pi a}{t}\right) \right]$$

$$k_t = \frac{a_t}{b_t} \quad k = \frac{a}{b} \quad b_t = b - \frac{1.25t}{\pi} \left[1.0 + \ln\left(\frac{4.0\pi a}{t}\right) \right]$$

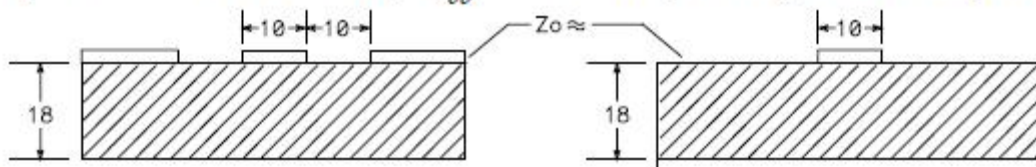
$$k_t' = \sqrt{1.0 - k_t^2} \quad k' = \sqrt{1.0 - k^2}$$

CPW verses Microstrip



$$\epsilon_r = 4.2 - Z_0 = 76 (\epsilon_{eff} = 2.44 \text{ (CPW)} \& 3.02 \text{ (MS)})$$

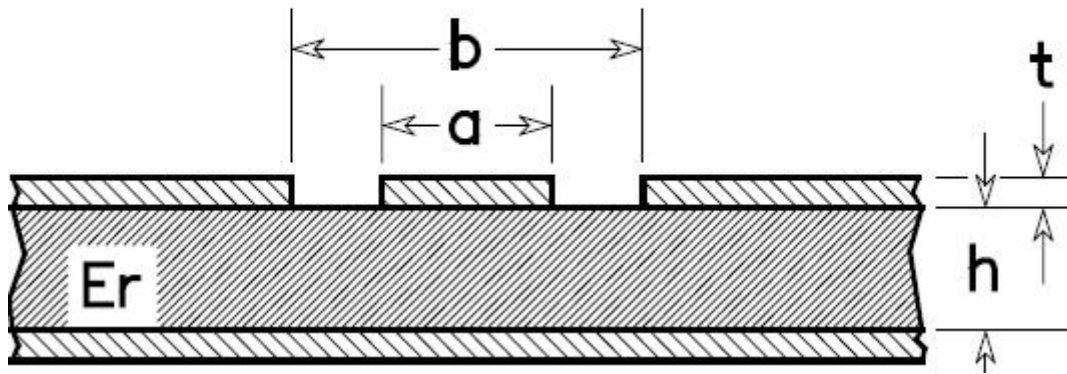
$$\epsilon_r = 2.5 - Z_0 = 94 (\epsilon_{eff} = 1.66 \text{ (CPW)} \& 1.96 \text{ (MS)})$$



$$\epsilon_r = 4.2 - Z_0 = 94 (\epsilon_{eff} = 2.45 \text{ (CPW)} \& 2.95 \text{ (MS)})$$

$$\epsilon_r = 2.5 - Z_0 = 115 (\epsilon_{eff} = 1.68 \text{ (CPW)} \& 1.92 \text{ (MS)})$$

Coplanar Waveguide w/Ground



- In Reality, Microstrip transmission line in the RF / Microwave arena is CPWG.

$$Z_0 = \frac{120\pi}{2.0\sqrt{\epsilon_{eff}}} \cdot \frac{1.0}{\frac{K(k)}{K(k')} + \frac{K(k1)}{K(k1')}} \quad k = a/b$$

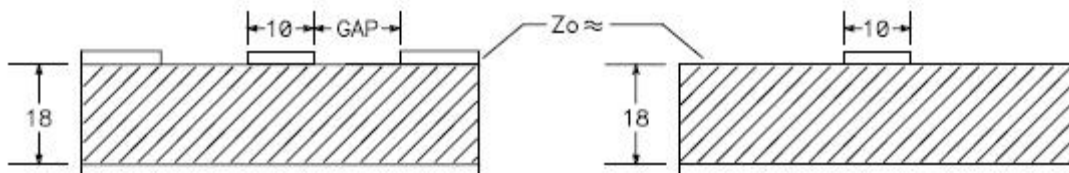
$$k' = \sqrt{1.0 - k^2}$$

$$\epsilon_{eff} = \frac{1.0 + \epsilon_r \frac{K(k')}{K(k)} \frac{K(k1)}{K(k1')}}{1.0 + \frac{K(k')}{K(k)} \frac{K(k1)}{K(k1')}} \quad k1' = \sqrt{1.0 - k1^2}$$

$$k1 = \frac{\tanh\left(\frac{\pi a}{4.0h}\right)}{\tanh\left(\frac{\pi b}{4.0h}\right)}$$

- To avoid Microstrip mode, $h > b$ and left & right ground extend away from 'a' by more than 'b'.
- Zo of CPWG is increased as dielectric thickness increases. Opposite of CPW.
- If 'h' is large, CPW and CPWG behave in similar fashion.

CPWG verses Microstrip



$$\epsilon_r = 4.2 - Z_0 = 94 \text{ Ohms (At Gap = 30)}$$

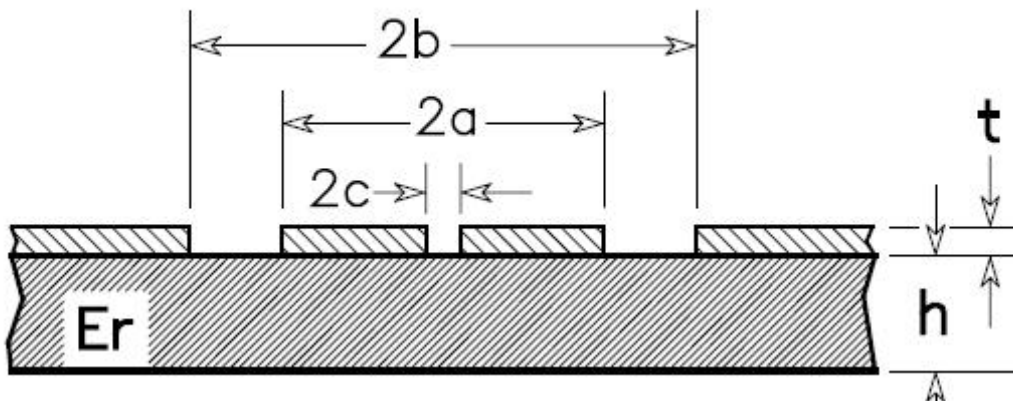
$$(\epsilon_{eff} = 2.92 \text{ (CPWG) and } 2.95 \text{ (MS)})$$

$$\epsilon_r = 2.5 - Z_0 = 115 \text{ Ohms (At Gap = 27)}$$

$$(\epsilon_{eff} = 1.89 \text{ (CPWG) & } 1.92 \text{ (MS)})$$

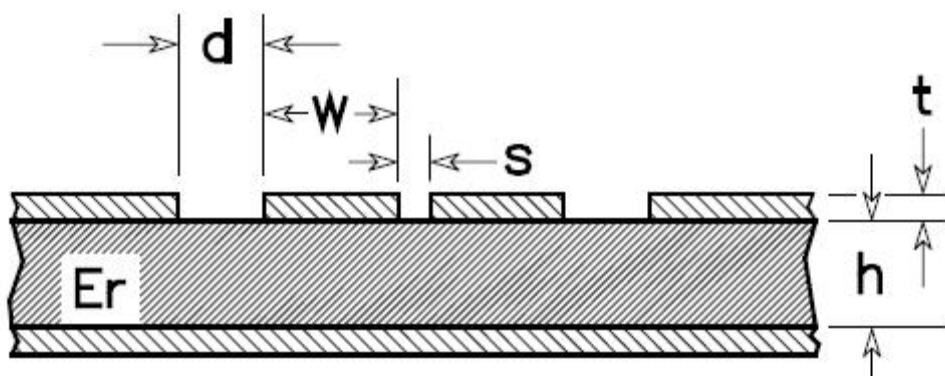
- Beyond gaps shown above, CPWG is like Microstrip.

Edge Coupled CPW (CP Differential Pair)



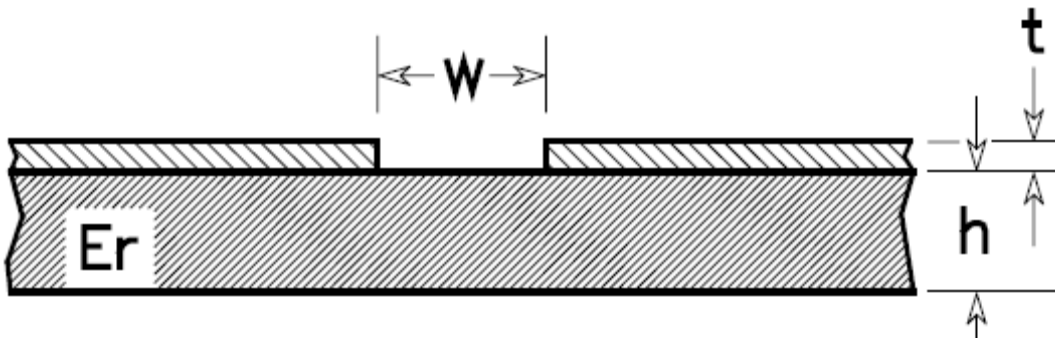
- Gives an extra degree of Signal-to-Noise isolation over standard CPW. (w/o plane, fields are large).

Edge Coupled CPWG (CP Diff Pair w/Grnd)



- Much better field containment than coupled CPW. Better yet in edge couple Stripline.

Slotline



- Acts like Waveguide with air dielectric.

Other Configurations

- 3 Line Coplanar Strip w & w/o Ground.
- Microstrip w/ limited width plane (and/or) limited width dielectric.
- Metal plate or shield covered CPW/CPWG.
- Metal plate or shield covered slotline.
- Offset CPW or CPWG.

Zo Calculations

- Use equations given or Wadell or Gupta.
- Use H.P. AppCAD (DOS and/or Windows).
- Use Rogers Corp. MWI (Dr R. Trout).
- Buy Field Solver (2D or 3D) Based Zo Calculator (i.e.- POLAR Ltd.)
- Don't use Equations or Calcs for Dig Layout that Don't Comp for Coplanar Effects.

Tpd, Capacitance and Inductance calculations (for all previous configurations)

$$Tpd = \sqrt{\epsilon_{eff} / c} (\text{spd of light})$$

$$C = Tpd / Z_0$$

$$L = Z_0^2 \times C \text{ (or } Tpd \times Z_0)$$

Integral Components

- Components can be designed into the PC board utilizing the right configuration of lines and shapes to form:
 - Inductors
 - Capacitors
 - Couplers (similar to transformer)
 - Resistors (very small value)
 - Filters
- Capacitor formed by 2 copper plates separated by PCB dielectric (free component)

$$C = \epsilon_r \times \epsilon_0 \times (A/h)$$

Where: ϵ_r - DK of PCB Material

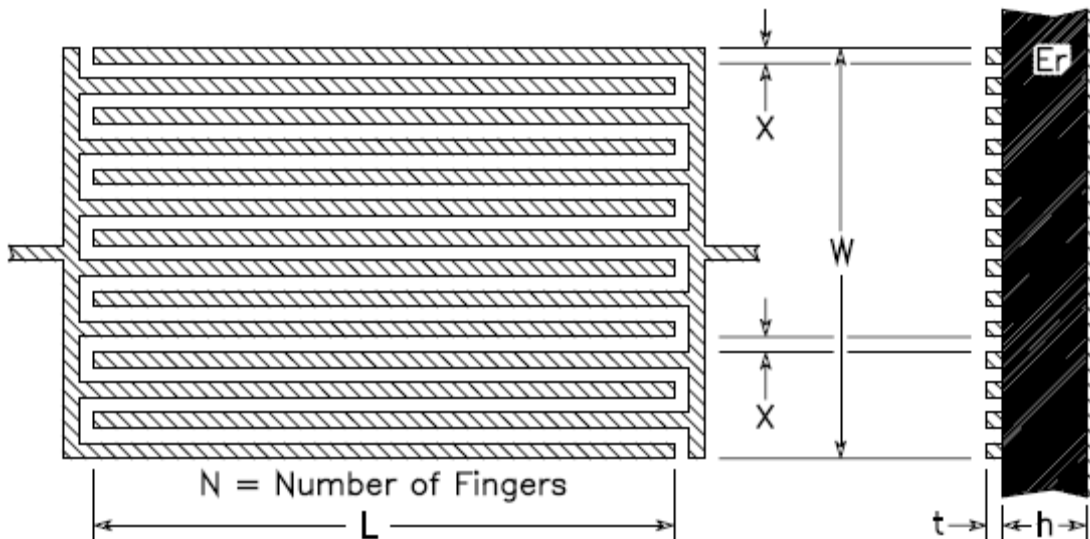
ϵ_0 - Permittivity of Space

$(2.25 \times 10^{-13} \text{ ferrads/in.})$

A - Area of Plate ($L \times W$)

h - Dielectric Thickness

- Interdigital Capacitor



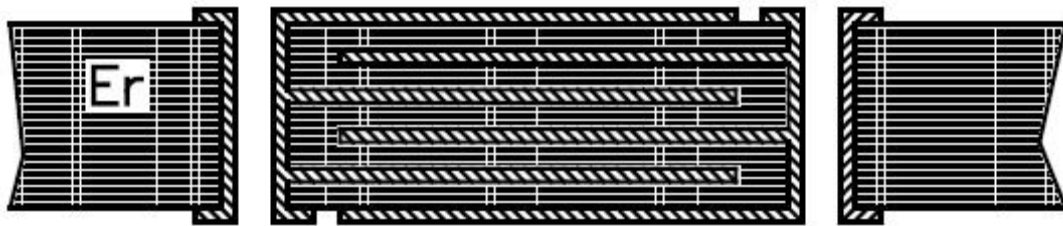
$$C_2 = \frac{\varepsilon_r + 1.0}{w} L [(N - 3.0) A1 + A2] \text{ (pF / in)}$$

$$A1 = \left[0.3349057 - 0.15287116 \left(\frac{t}{X} \right) \right]^2$$

$$A2 = \left[0.50133101 - 0.22820444 \left(\frac{t}{X} \right) \right]^2$$

(Equation valid for $h > w/N$)

- Multilayer Capacitor



$$C = \frac{0.229 \varepsilon_r A (n - 1.0)}{d} \text{ (pF)}$$

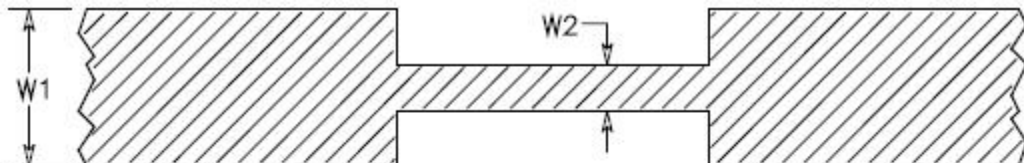
where:

A = area of planes in square inches

n = number of conductor layers

d = plate spacing

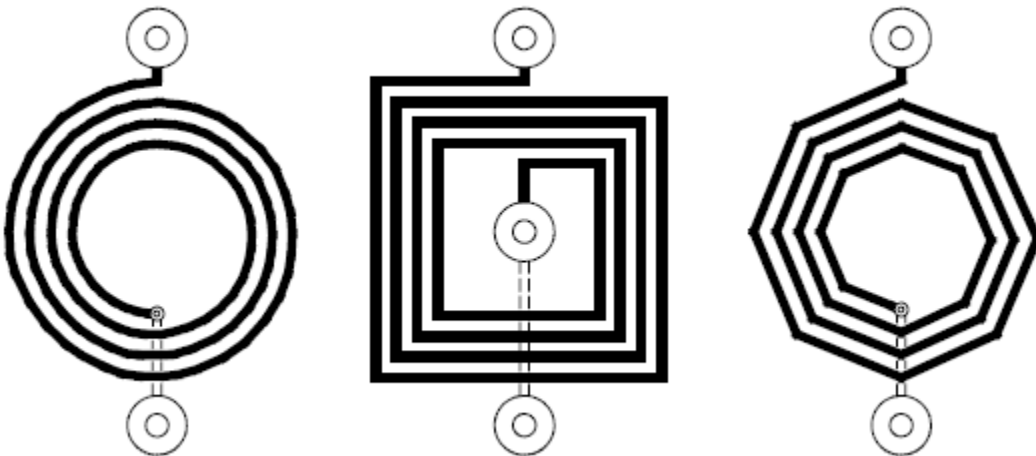
- Inductor- inline inductor is formed by a very thin, high-impedance trace.



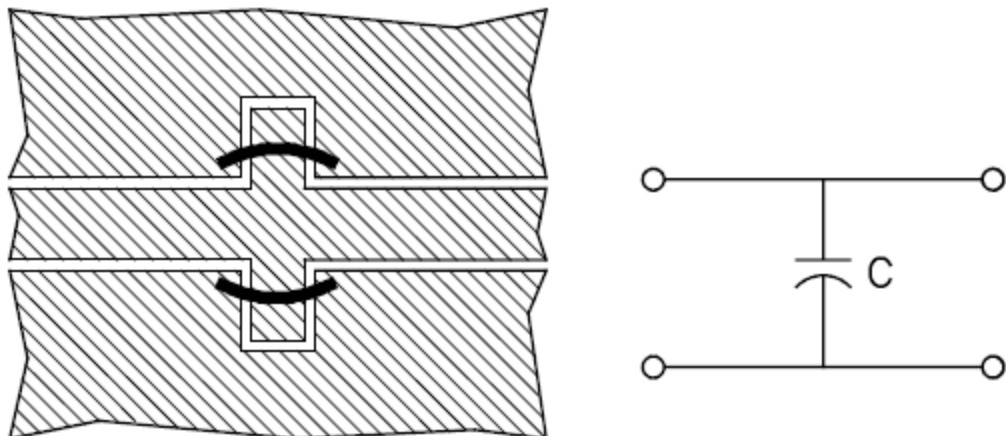
◆ Length Must be Shorter than Critical Length to Prevent Reflections. Can Remove Plane(s) to Boost Inductance.

◆ $L = Z_o^2 \times C$ or $T_{pd} \times Z_o$ (Many Equations available. This is Extremely Accurate.)

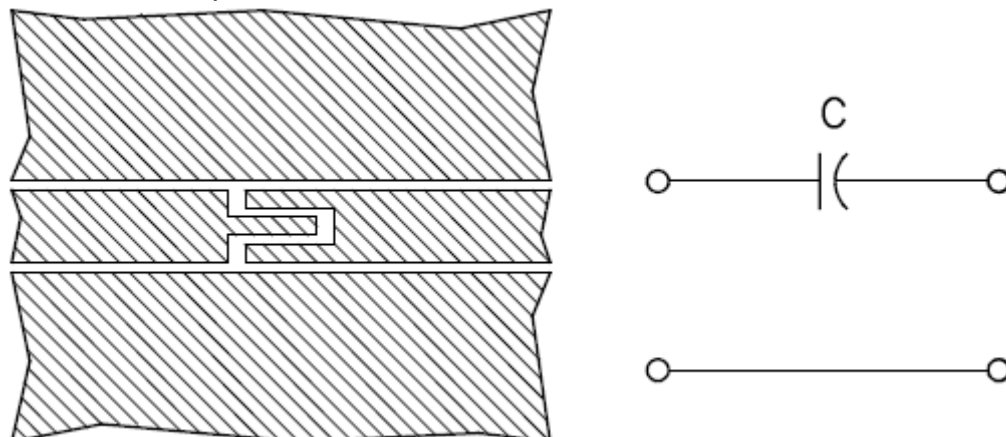
- Spiral Inductors



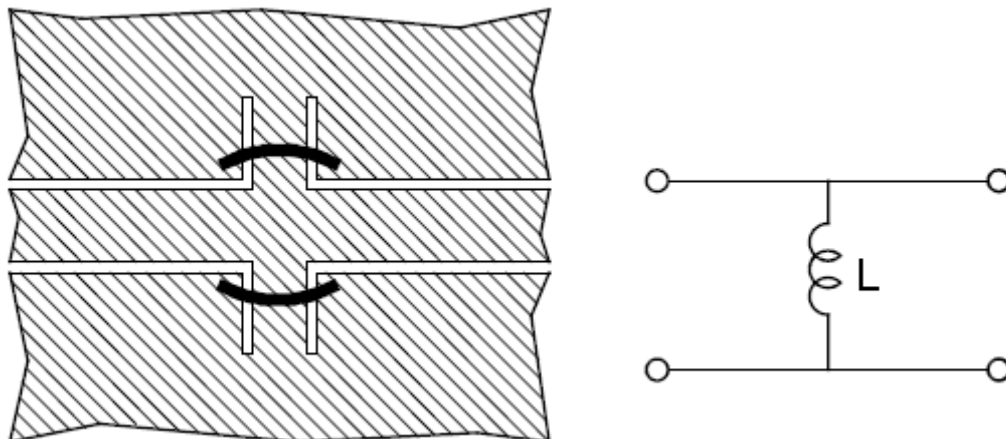
- CPW & CPWG Shunt Capacitor



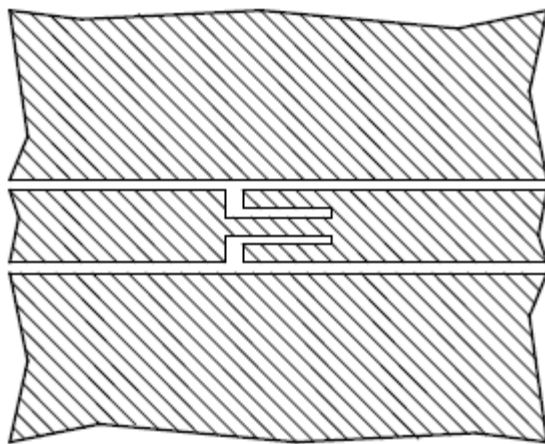
- CPW & CPWG Series Capacitor



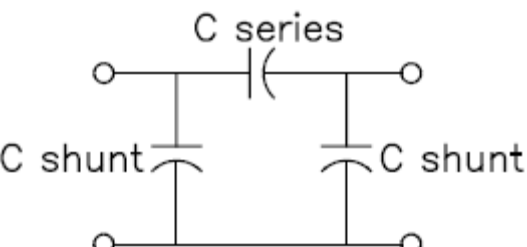
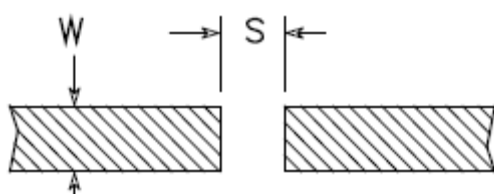
- CPW & CPWG Shunt Inductor



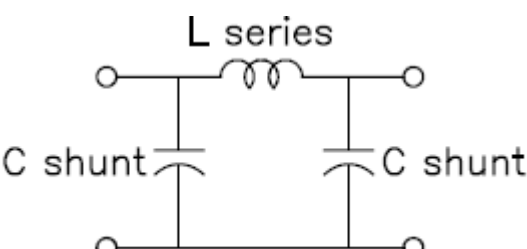
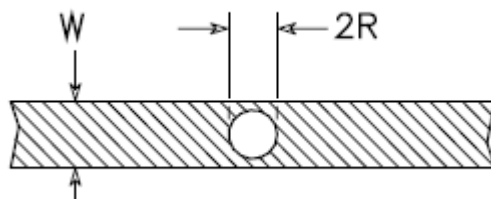
- CPW & CPWG Series Inductor



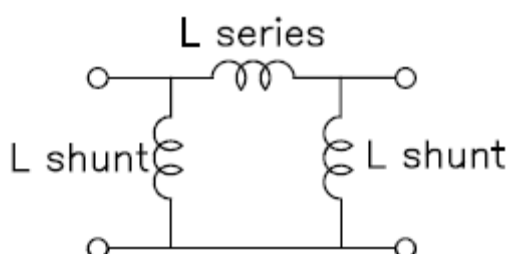
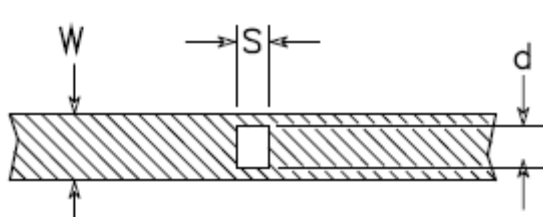
- Gap in Centered Stripline Conductor



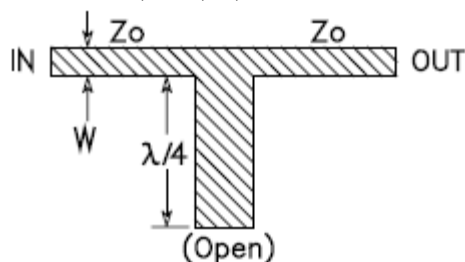
- Round Hole in Centered Stripline



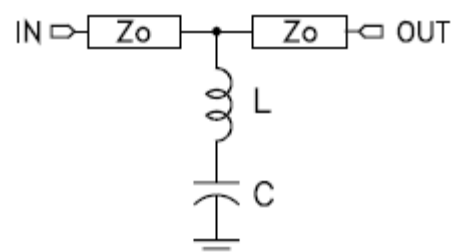
- Rectangular Hole in Centered Stripline



- Filters can be made from the L & C circuit elements discussed.
 - $\lambda/4$ Stub is series resonant circuit at frequency.
 - Circuit shorts to ground at $\lambda/4$, $3/4\lambda$, etc.
 - Open circuit at DC, $\lambda/2$, λ , etc.



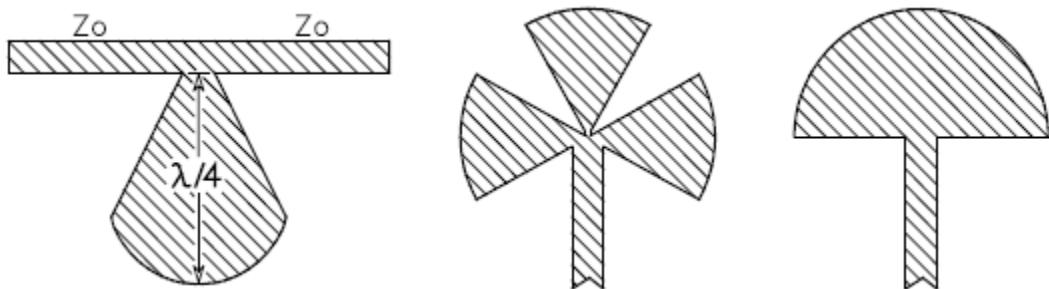
Microstrip Open-Stub



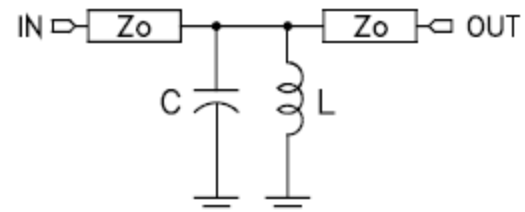
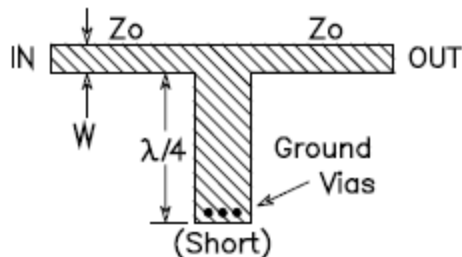
Microstrip Open-Stub Equivalent Circuit at Resonant Frequency

- $2W$ wide for high-Q and to prevent reflections
- Open Stubs (one just shown) have narrow frequency over which they short to ground.

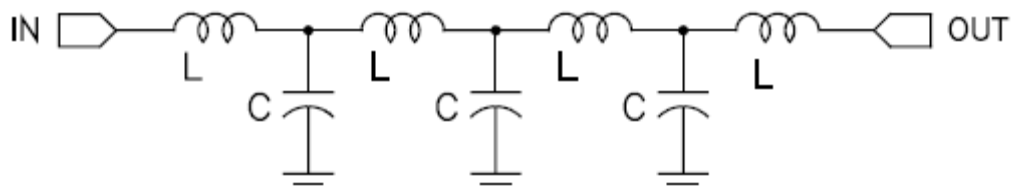
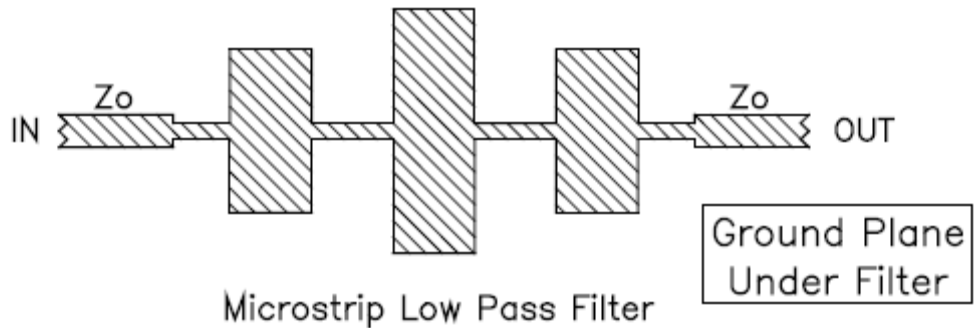
- Flaring the Stub increases frequency response.



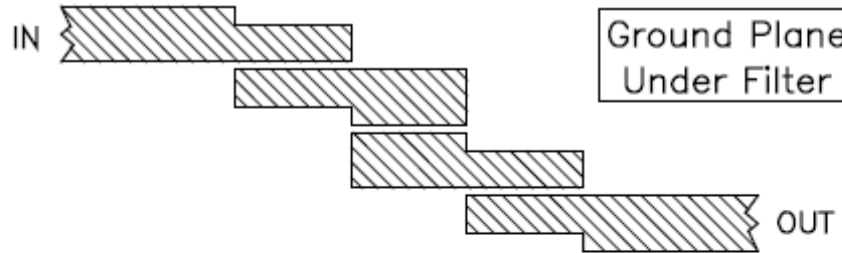
- $\lambda/4$ Stub, shorted to ground, is parallel resonant filter at frequency of interest.
- Circuit shorts to ground at DC, $\lambda/2$, λ , etc.
- Open circuit at $\lambda/4$, $3/4 \lambda$, etc.



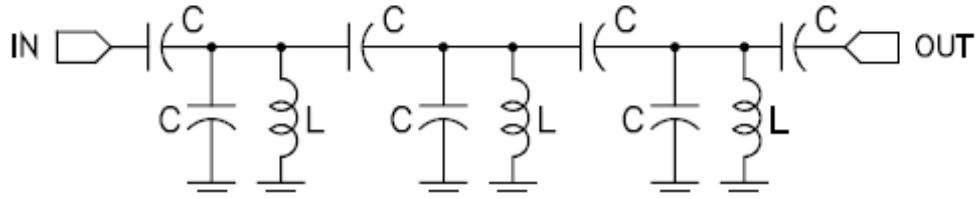
- Low Pass Filter



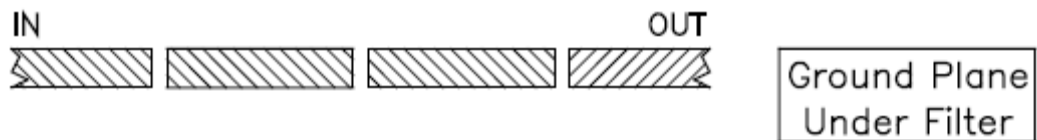
- Edge Coupled Band Pass Filter



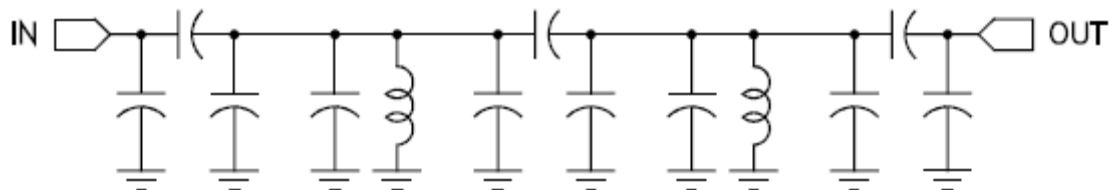
Microstrip Band Pass Filter (Edge Coupled)



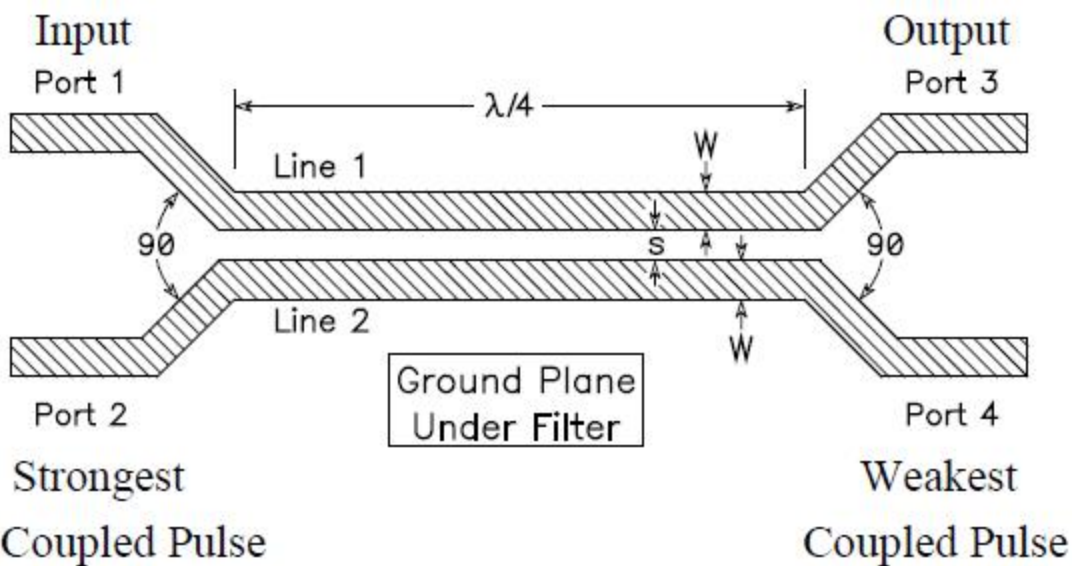
- End Coupled Band Pass Filter



Microstrip Band Pass Filter (End Coupled)



- Directional Coupler



- Directional Coupler can be used as:
 - A Filter at $\lambda/4$ Frequencies.
 - Non loading method to transfer energy to another circuit.
 - A method to monitor power send to Port 3.
 - Closed loop feedback control.
 - A non-loading way to measure a signal with an oscilloscope.

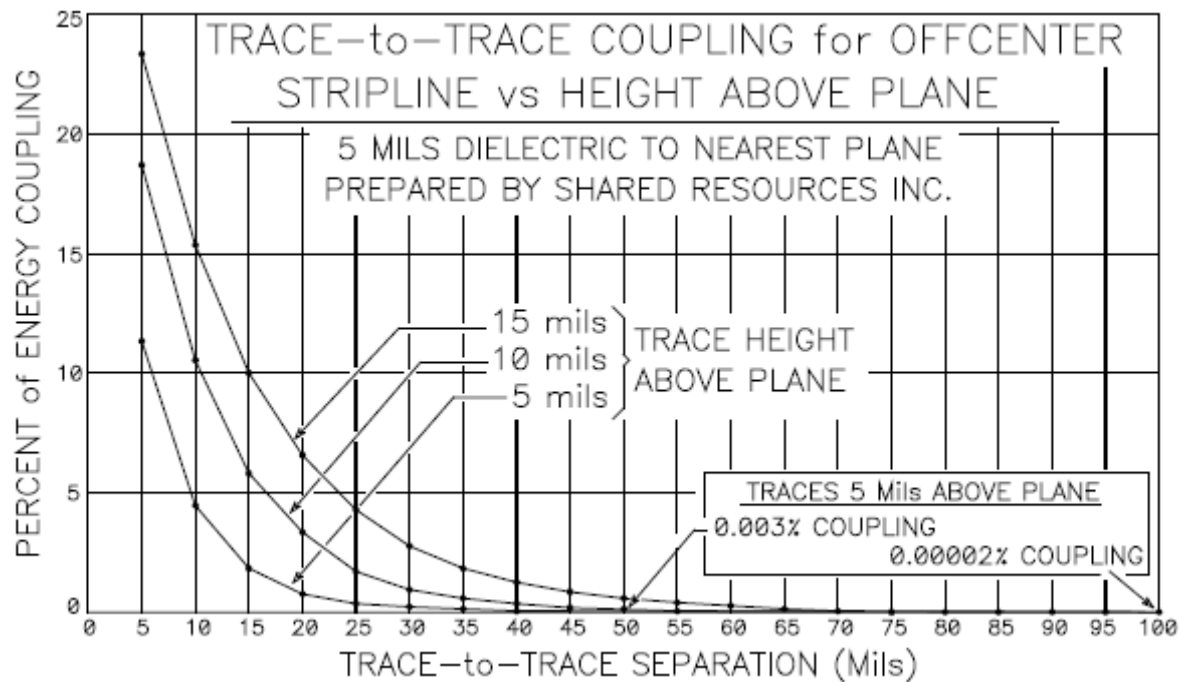
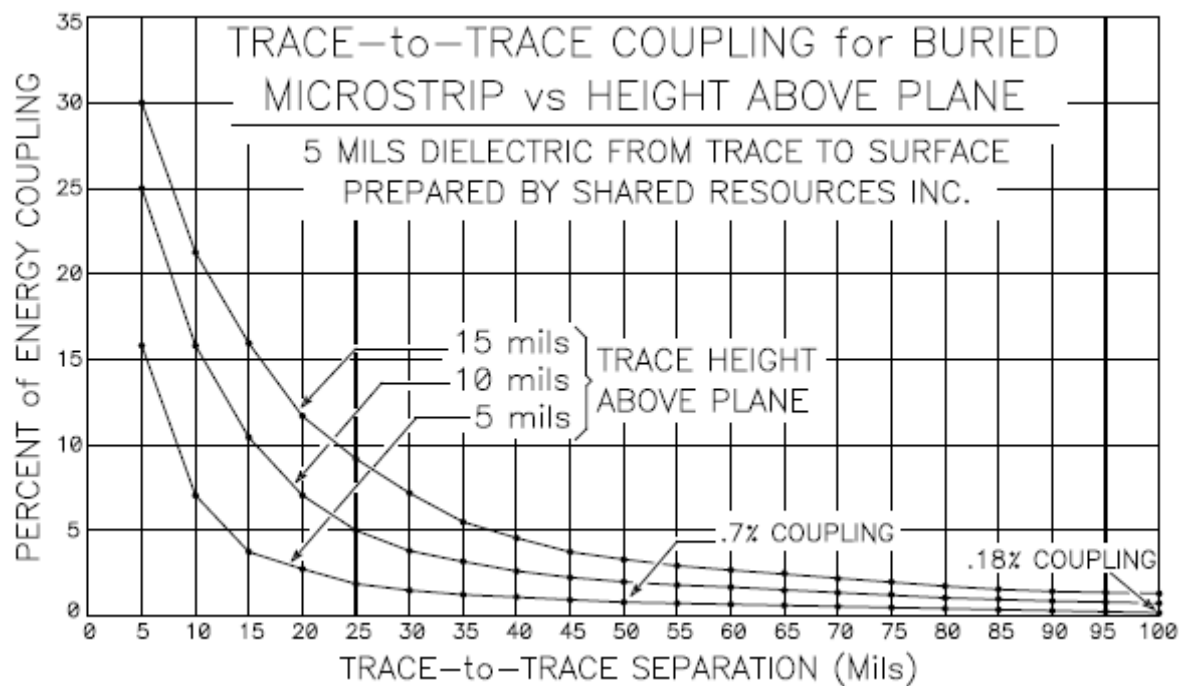
Strongest
Coupled Pulse

Weakest
Coupled Pulse

- Resistors
 - Impractical when made from PCB copper.
 - Requires extremely long lines to achieve
 - Resistance of a few ohms.
- One Exception -
 - When very small 'R' is needed to measure a very large current.

Layout Techniques and Strategies

- Low level analog, RF/Microwave and digital sections must be separated.
- Divide RF/Microwave section into circuit groups (VCO, LO, Amps, etc.).
- Place high frequency components first, to minimize length of each RF route (orientation for function more critical than DFM).
- Place Highest Frequency Components nearest Connectors.
- Don't Locate Unrelated Outputs and Inputs Near Each Other. Especially Multi-Stages Winding Back on One Another.
- When Either the Output or Input to Amplifiers Must be Long, Choose the Output.
- Remember, Trace Impedance (Z_0) is a Critical Factor in the Effort to Control Reflections.
- Impedance must Match Driver and Load.
- In Traces Shorter than $1/20^{\text{th}} \lambda$ Long, Z_0 Matching is usually Not Important.
- When Pull-up Resistors or Inductors are used on the Outputs of Open Collector Devices, Place the Pull-up Component Right At the Output Pin it's Pulling.
- Also, make certain to decouple the Pull-up, in Addition to the Main Power Pins of the IC.
- Inductors have Large Magnetic Fields Around Them-
 - They Should Not be Placed Close Together, when In Parallel (Unless Intent is to have Their Magnetic Fields Couple).
 - Separate Inductors by One (1) Times Body Height (Min) -(OR)-
 - Place Perpendicular to One Another.
- Keep "ALL" Routes Confined to the Stage or Section to which they are Assigned-
 - Digital Traces in the Digital Section. Period.
 - Low Level Analog in Low Level Analog.
 - RF / Microwave in RF / Microwave Section.
 - Don't Route Traces into Adjoining Sections.
- Short RF Traces should be on Component Side of Board, Routed to Eliminate Vias.
- Next Layer Below RF Traces to be Ground.
- Minimizing Vias in RF Path Minimizes Breaks in Ground Plane(s)-
 - Minimizes Inductance.
 - Helps Contain Stray Electric & Magnetic Fields.
- Controls Lines can be Long, but Must Route Away from RF Inputs.
- RF / Microwave Lines Must be Kept Away From One Another By Min Distances to Prevent Unintended Coupling & Crosstalk.
- Minimum Spacing is a Function of How Much Coupling is Acceptable.



- When Circuit MUST Loop Back on Itself and Outputs end up Near Inputs –
 - Place Ground Copper (20 H Wide) Between Sections, Most specifically Between Inputs and Outputs.

- Use 20 H Wall if Copper is Less than 20 H Wide.
 - Attach Ground Copper to Board Planes Every 1/20th Wavelength of Principal Frequency.

- Use Same Methods when Unrelated Inputs and Outputs Must Be Near One Another.

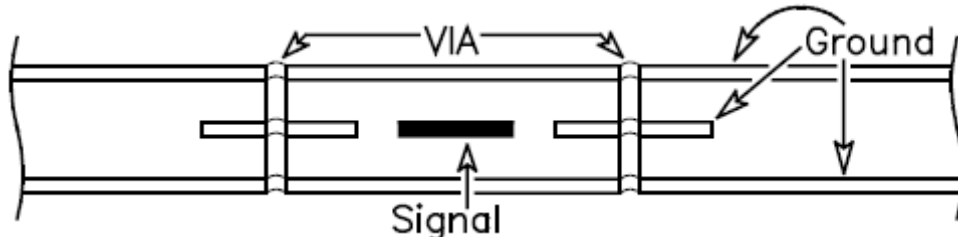
- In Multilayer Boards, When Signals Must Change layer, Route in Layer Pairs -
Layer 1 Signals Reference Ground on Layer 2.

When Direction Change Needed, Via Signal to Layer 3.

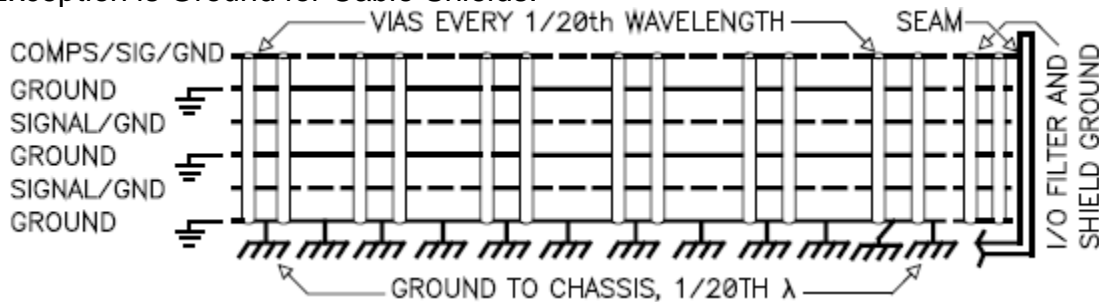
- i.e.: First Four(4) Layers of a Board

- Layer 1 (Signal - X Direction)
- Layer 2 (Ground Plane)
- Layer 3 (Signal - Y Direction)
- Layer 4 (Ground Plane)

- Components Connecting to Ground
 - Flood Component Lead with Surface Ground. (Let Soldermask or Mask Dam Define Pad).
 - Ground Vias as Close to Component Lead as Possible. Preferably ON Component Lead.
 - Multiple Vias (3, 4, etc.) Reduce Inductance and Help Eliminate Ground Bounce.
 - Direct Connection. No Thermal Vias.
 - Must attempt to permit Proper Solder Reflow.
- Ground: All Designs, 2 Layer or Multilayer –
 - Unused Areas of Every Layer to be Poured with Ground Copper.
 - Ground Copper and All Ground Planes through Board to be Connected with Vias Every $1/20^{\text{th}}$ - Wavelength Apart (Where Possible).
 - Vias Closer than $1/20^{\text{th}} \lambda$ are Better.
 - Very Critical Circuits - Vias Closer than $1/20^{\text{th}} \lambda$ Help Reduce Noise.
 - Direct Connect Vias. No Thermal Vias.
 - 'Copper Pours' Too Small to have Vias Must be Removed (Can Act as Antenna).
 - Arrange Poured Ground Around Signals to Completely Surround Signals

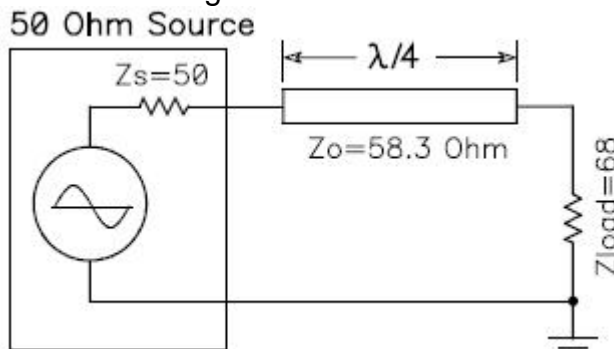


- Ground Vias to Include Picket Fencing at Edge of Board. In Very Critical Circuits, Plate Board Edge.
- By Maintaining Isolation Between Circuits, Do Not Split Ground Plane.
- Attach Ground to Case Continuously.
- One Exception is Ground for Cable Shields.



- Mismatched Source and Load Impedance:

- If Line can be $\lambda/4$ Long

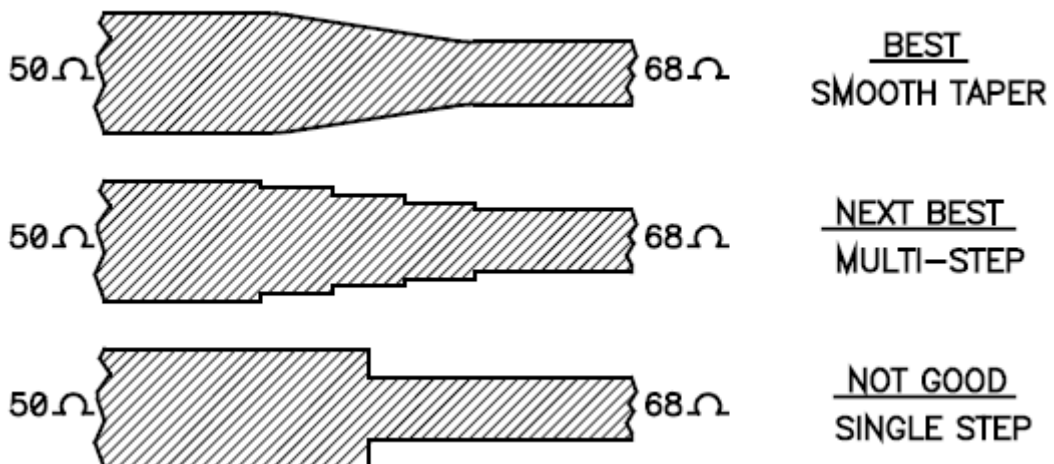


$$\begin{aligned}
 Z_0 &= \sqrt{Z_s \cdot Z_{\text{load}}} \\
 &= \sqrt{50 \times 68} \\
 &= \sqrt{3400} \\
 &= 58.3 \Omega
 \end{aligned}$$

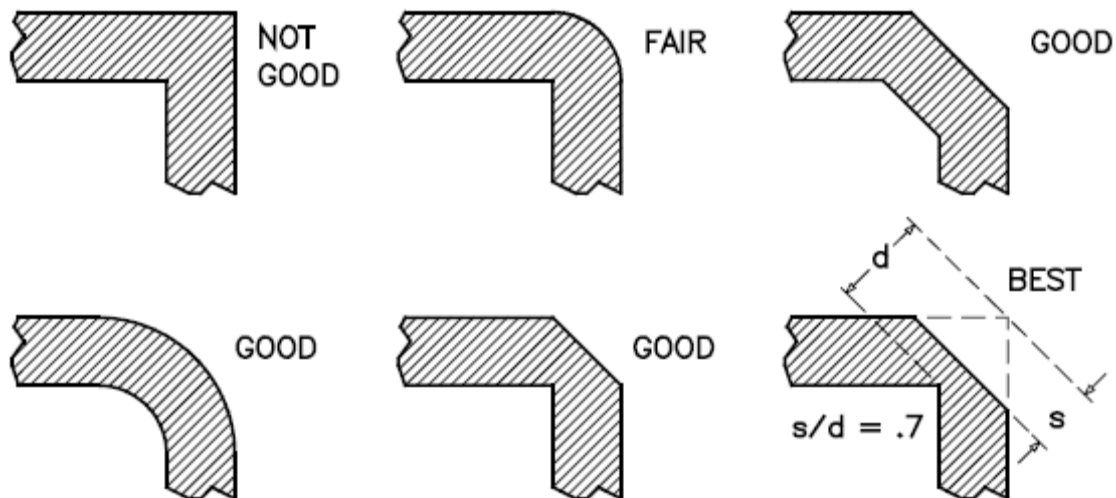
- ($\lambda/4$ is Calculated From Frequency of Source and Eeff of the Transmission Line.)

- Mismatched Source and Load Impedance:

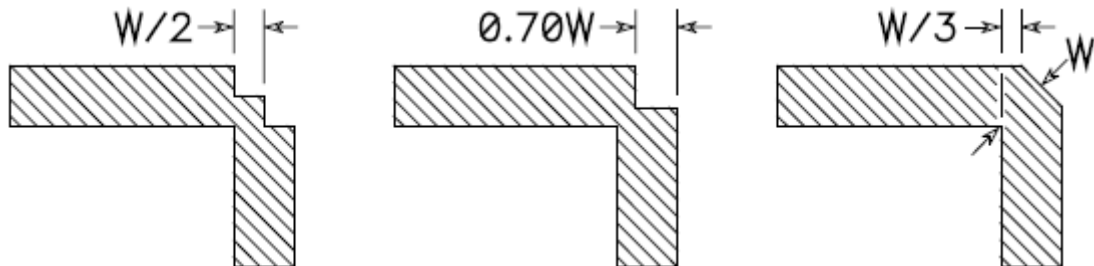
- If Line Can NOT be $\lambda/4$ Long -



- Trace Corners

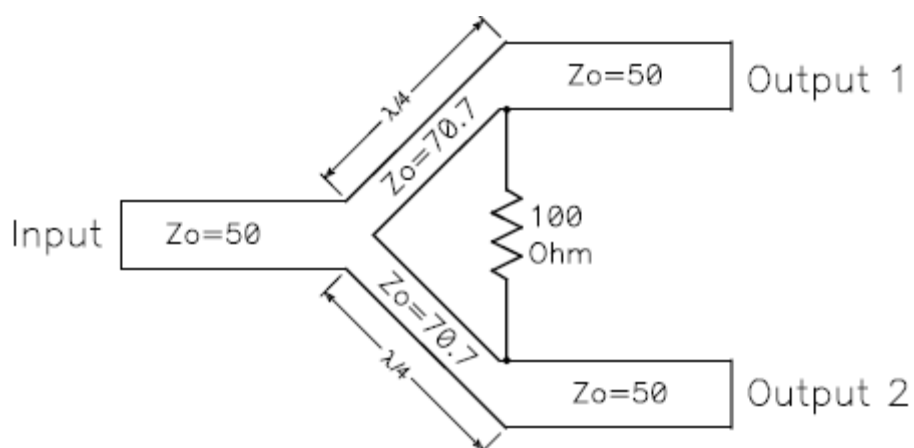


- Others Considered Fair to Good

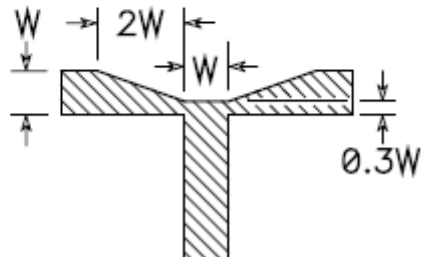
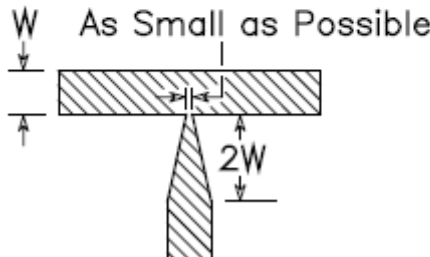
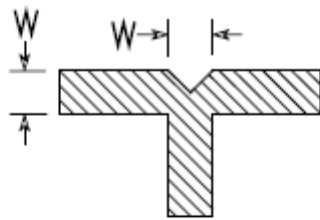
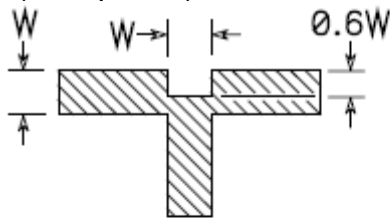


- 'T'-Junctions:

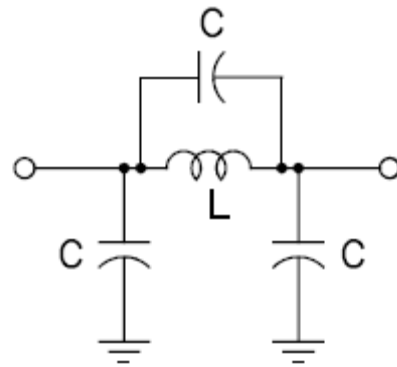
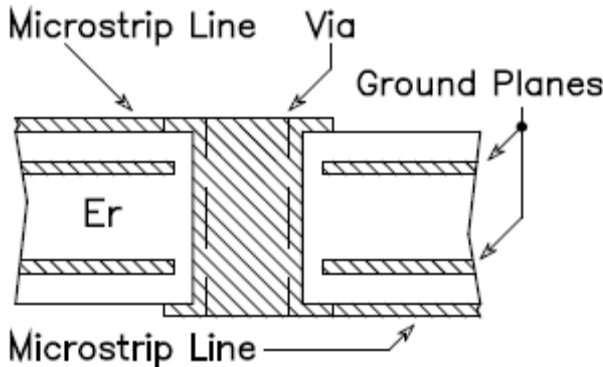
- Ideal is the Wilkinson Splitter



- 'T'-Junctions (Acceptable):



- Impedance of Vias



- Copper Patches can be placed Next to Signal Traces to Create Attachment Points for Wire or Solder to Create Tuning 'C' or 'L'

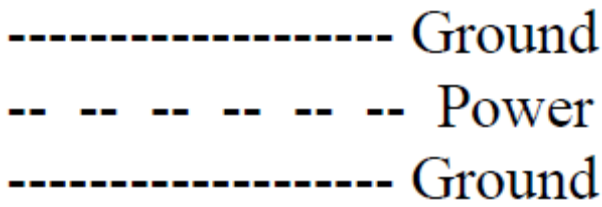


- Long Microstrip Traces can be Antenna for Radiation of EMI or Reception of Noise.
- Ideal Trace Antenna is 1/4 Wavelength Long.
- In Designs where Stripline is available, Keep Outer Layer Traces under Critical Length.

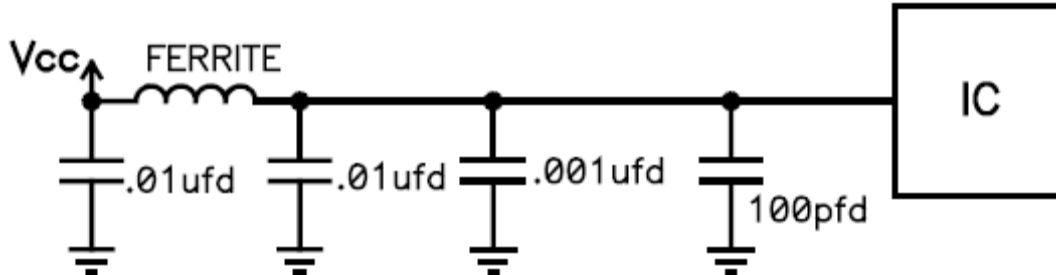
Power Bus

- Route Power in 2 Layer Board (Microstrip, CPW or CPWG) (Only Plane is Ground).
- In Multilayer Boards Power Can be Plane if One(1) Voltage or Split Plane if Several Voltages.
- In Multilayer Board with Many Voltages, Power is Usually Routed on One (1) or more Layers.
- When Routed, Make Power Grid if two(2) or more Layers are used. Grid Most Closely Emulates Behavior of a Plane.
- Due to Self Resonance of Decoupling Caps, selected to match Frequency of Operation, Wide Routes work as well in Analog Circuits to distribute Power as do Planes.

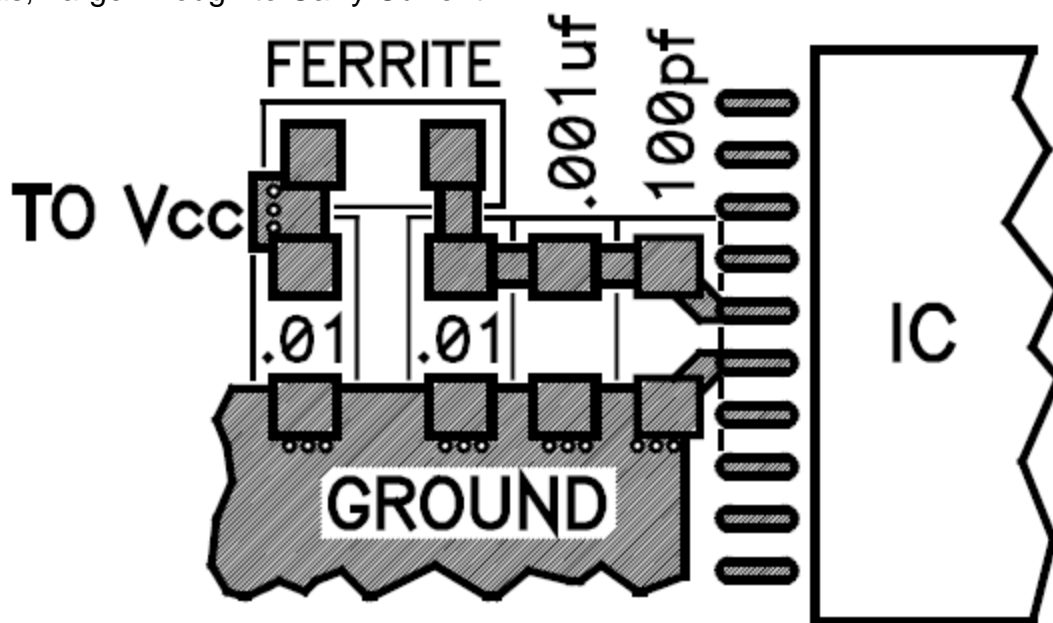
- Power is generally routed between Power Ground Planes to help Lower Noise Coupling in Power Bus.



- Ground Planes are **Always** Continuous. (Only Split at Front Panel for Cable Shields and Filters).
- Power Decoupling Consists of Low Pass Filter with Several Capacitors to Cover a Broad Range of Frequencies and Currents-



- Select Capacitors in Low Pass Filter so Smallest Value has Self Resonance of Operating Frequency of Circuit.
- Largest Value selected to carry Maximum Current Drawn by IC.
- Capacitors Progress Upward in Value in Steps of 10 Times.
- Place Caps w/ Smallest Value Near IC, then Next Largest Value, etc.
- Place Smallest Value Capacitor **AT** Power and Ground Pins of IC.
- Ideally, Capacitors are in Parallel with Power & Ground Pins of IC.
- When Not Possible, Place Smallest Value Capacitor at Power Pin of IC and as Near Ground Pin as Possible.
- Attach Caps w/ Wide Traces & Gnd Floods.
- Many Vias, Large Enough to Carry Current.



Board Stack-Up

- In 2 Layer Boards, Dielectric Will be Tightly Controlled (And Usually Not $.062"$).
- Dielectrics of $.015\text{-}.025"$ Thick, Common.
- In ALL Designs, One Ground Plane MIN.

- In CPW, to create Continuous Ground, Strap Across Sig Lines From Ground to Ground.
- In Microstrip / CPWG, Pour Ground on Sig Side, w/ Continuous Ground Opposite Side.
- In Multilayer Board, have Ground on Every Other Layer.
- Signals Located on Either Side of Ground Plane Must Cross at Right Angles.
(Planes give 60 dB of Isolation of Currents on Either Side. 60 dB May Not be Enough in RF / Microwave Circuit, Hence Right Angle Routing.)
- Remember, Route in Layer Pairs.
- Typical High Layer Count Board

Layer 1	-----	Devices, Short Signals, Ground
Layer 2	-----	Ground Plane
Layer 3	-----	Signals, Ground Pour
Layer 4	-----	Ground Plane
Layer 5	-----	Signals, Ground Pour
Layer 6	-----	Ground Plane
Layer 7	-----	Power Plane or Power Routes
Layer 8	-----	Ground Plane
Layer 9	-----	Signals, Ground Pour
Layer 10	-----	Ground Plane
Layer 11	-----	Signals, Ground Pour
Layer 12	-----	Ground Plane

- When RF Stages Located on Opposite Sides of a Board, Blind Vias May Be Needed in Each Stage to Effectively Create Back-to-Back Boards

Layer 1	-----	Devices, Short Signals, Ground
Layer 2	-----	Ground Plane
Layer 3	-----	Signals, Power, Ground Pour
Layer 4	-----	Ground Plane
Layer 5	-----	Ground Plane
Layer 6	-----	Signals, Power, Ground Pour
Layer 7	-----	Ground Plane
Layer 8	-----	Devices, Short Signals, Ground

Signal Attenuation

- Increases or Decreases Pulse Amplitude
 - 1) Reflections (Return Loss / VSWR - Critical).
 - 2) Signal Cross Talk (Critical in RF).
 - 3) Reference Voltage Accuracy (Critical in RF).
 - 4) Power Bus Noise (Minimal- Filtered).
 - 5) Ground/Vcc Bounce (Minimal in RF).
 - 6) Skin Effect (Resistive Loss in Conductor).
 - 7) Loss Tangent (Property of PCB Dielectric).

Skin Effect

- Increases Resistive Signal Loss (Adds Heat).
- Losses Increase with Increased Frequency.
- Amplitude Loss in Analog Circuits.
- Most effected by Line Width and Length.
- Can be a problem above 10's of MHz in Analog circuits.

$$R = \frac{\rho \cdot \text{Length}}{\text{AREA}_{\text{eff}}}$$

$$\rho = 6.787 \times 10^{-7} \text{ ohm-in}$$

$$\rho = 1.724 \times 10^{-5} \text{ ohm-mm}$$

$$\text{AREA}_{\text{eff}} = 2(w+t) \cdot SD$$

w - Trace Width

t - Trace Thickness

$$SD = \frac{2.6}{\sqrt{f}}$$

SD - Skin Depth in Inches

f - Frequency in Hertz

$$SD = \frac{66}{\sqrt{f}}$$

SD - Skin Depth in mm

f - Frequency in Hertz

- “R” from equation is ONLY Accurate for Centered Stripline configuration.
- “R” of all other Transmission Line configurations must be adjusted due to ‘Proximity Effect’.
 - Microstrip (50 to 75 ohm) - Multiply “R” by 1.70
 - Embedded Microstrip (50-75) - Multiply “R” by 1.85
 - Offset Stripline -
 - Adjust “R” based on Factor Determined by Percent of Offset from Center (OR)
 - Adjust Percent of Attenuation of Signal based on Percent of Coupling to Nearest Plane.
- Attenuation of the Signal is a Function of ‘Skin Effect’ Resistance and Current in the Transmission Line.

$$\text{Atten(volts)} = R \bullet I$$

Where - $I = \frac{V_{\text{DRIVER}}}{Z_{\text{O}_{\text{LOADED}}}}$

$$\text{Atten(dB)} = \frac{2R \bullet 3dB}{Z_{\text{O}_{\text{LOADED}}}}$$

Loss Tangent ($\tan(\delta)$)

- Loss of Signal into PCB Material (Increases Heat).
- Function of Molecular Structure of PCB Material.
- Losses Increase with Increased Frequency.
- Amplitude Loss in Analog Circuits.
- Worse in FR4 (Alternative Materials available).
- Material Selection- Weigh Performance and Price.
- Can be problem above tens of MHz in Analog circuit.

- The amount a signal is attenuated from Loss Tangent can be determined with the equation

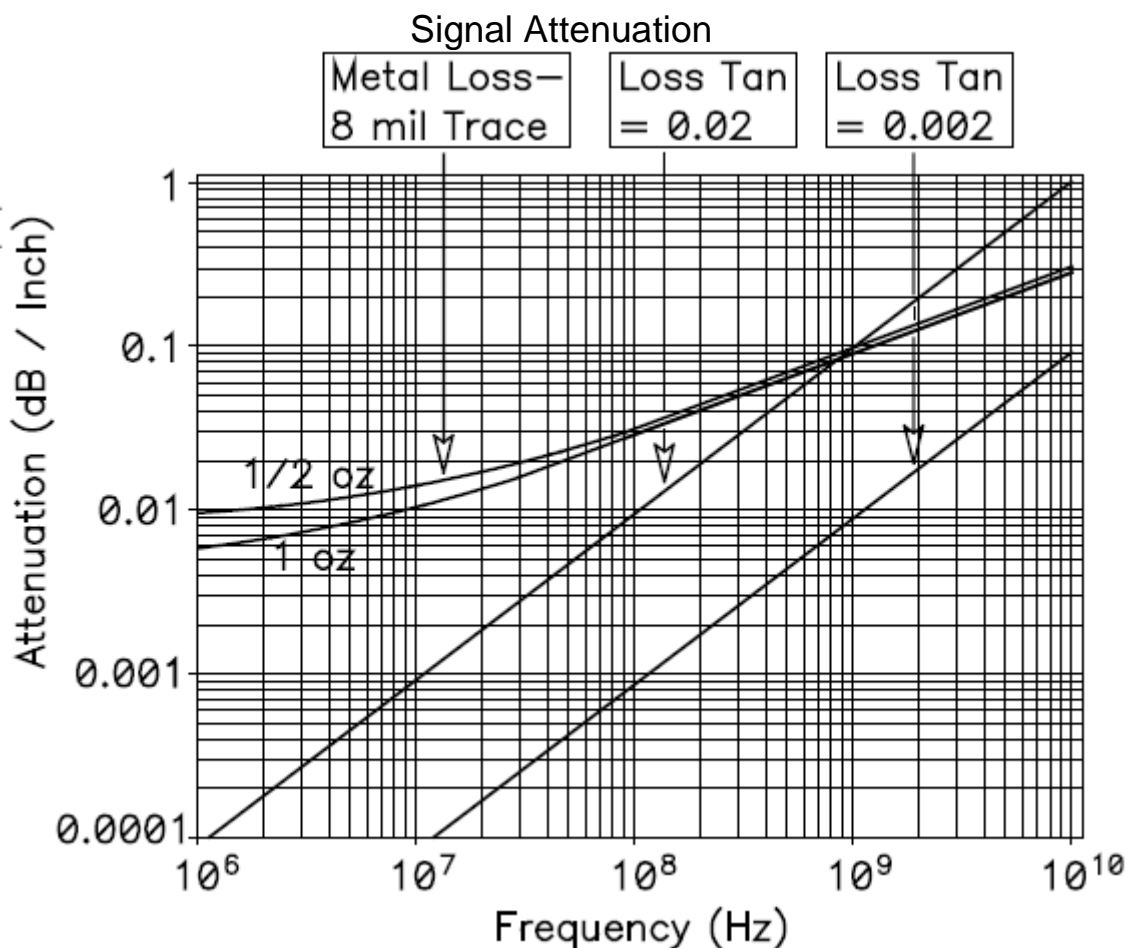
$$\alpha = 2.3f \cdot \tan(\delta) \cdot \sqrt{\epsilon_{eff}}$$

Where : α = Attenuation in dB / Inch.

f = Frequency in GHz.

$\tan(\delta)$ = Loss Tangent of Material.

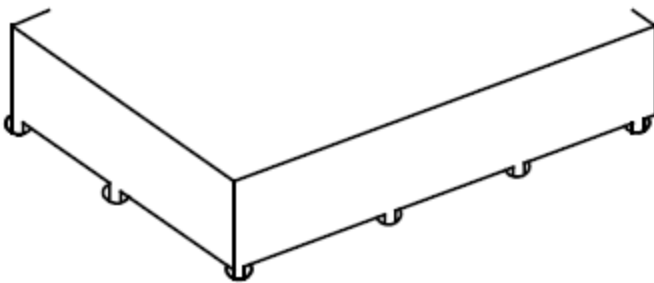
ϵ_{eff} = Effective Relative Er of Material.
(Er for Stripline)



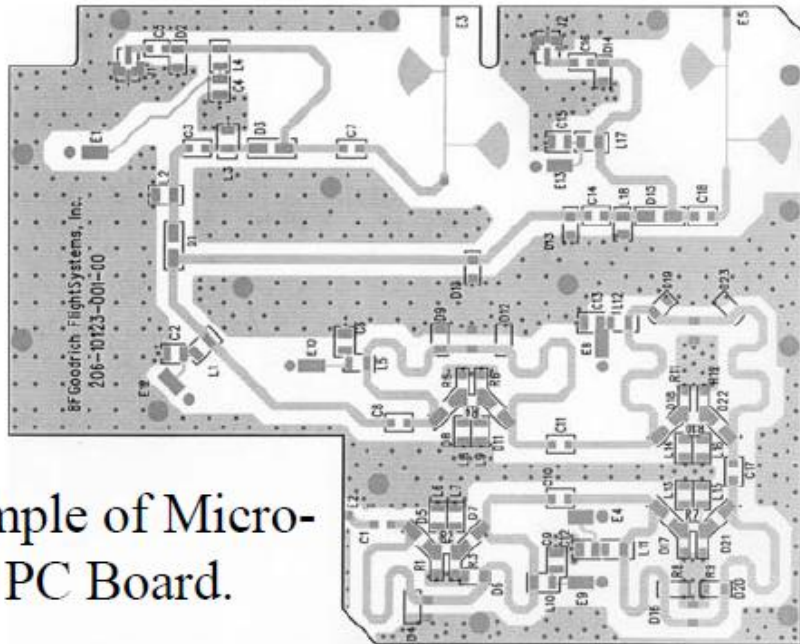
Shields and Shielding

- Use a Metal Can, Grounded Shield when -
 - Circuits are so Close Together that Noise Coupling Naturally Occurs.
 - EMI is Extreme and Cannot be Contained.
 - Circuit is So Sensitive that Normal, Ambient EMI Levels affect Performance.
- Problems! Shields -
 - Use up Valuable Board Space.
 - Are Expensive.
 - Make Trouble Shooting and Repair Very Difficult.
- Shield Cost -
 - Least Expensive is Off-the-Shelf.
 - Next Lowest Cost is Photo Etched.

- Resolve Trouble Shooting / Repair Issues-
 - Tabs Every 1/20th λ instead of Continuous Connection to Ground on Circuit Board.



- § Traces Running out of Shielded Area to be Routed on Inner Layers, if possible.
- § When Routing from Shield Area on Same Layer as Shield, have a Minimum Opening in Shield Side Wall.
- § Cable Exiting Shield Must have 360 degree Attachment of Cable Shield to Metal Can.
- § Avoid Other Openings in Shields.
- § Open Soldermask Under Shield Edges enough to allow Good Solder Attachment of Shield Walls to Ground Plane.
- § Alternative to Soldered Shield- Make Case Lid with Fins/Vanes Long enough to Reach PCB Surface and Contact Ground to Create Compartments inside Enclosure.



PC Board Materials

- § Don't Use FR4 in High Power Circuits or Broad Band Applications (Loss & Er).
- § Dielectric Loss (Loss Tangent) causes as much as 1/2 Signal Loss in 3" Trace Run over Thick Dielectrics in FR4 at 12 GHz.
- § Resistive Loss, Especially Skin Effect, Can be High at Frequencies Above 500 MHz. In Very Sensitive Circuits, even Small Losses Can Create Big Problems.

Board Fab and Assembly

- § Teflon Based Materials used in Many RF/ Microwave Circuits Require Fab Houses which Specialize in Such Materials.
- § Items Like Tetra-Etch are Essential in the Fabrication of Plated Holes.
- § Items such as Large Ground Planes, Flooded Ground Pins of Parts and Multiple Vias On or Near Component Pads force Very Special Attention to Solder Profiles During Assembly.

Base Materials for High Speed, High Frequency PC Boards

Introduction

Two questions often asked, "Will a circuit board made of FR4 laminate work for my High Speed or High Frequency design?" and, "If FR4 isn't OK, where do I turn?" The answers to these questions are specific to each individual circuit and can only be answered through analysis of the characteristics of FR4 versus other material choices, relative to the demands of the circuit's noise budget.

This article will outline the material parameters that affect circuit performance and give some direction about how to decide when to choose the correct material for any specific application. For those people who don't have simulation tools to help calculate the effect of material parameters, a few equations and a graph are included. Near the end of the article is a list of some of the materials available, followed by links to their specifications.

One of the major goals of this article is to provide information that allows designers and engineers to select a material for every PCB application that optimizes both performance and cost.

Circuit Types

There are two basic types of circuits that fall under the heading of high frequency, RF / Analog (aka-RF/Microwave) and High Speed digital. Each of these has their own unique requirements, which have spawned two distinct classes of materials.

RF/Analog circuits usually process precision and/or low level signals. Hence these circuits require much tighter control of parameters pertaining to signal losses. The two losses of greatest concern are losses caused by signal reflections, due to impedance mismatch or impedance changes and the loss of signal energy into the dielectric of the material. Some critical applications also need to focus on losses due to 'Skin Effect'.

Impedance variations result from two things, material parameters that vary with changes in frequency or temperature and variations in the processes at the fabricator. The amount of signal lost into the dielectric is a function of the material's characteristics. Skin effect can be partially controlled through choice of copper type in or on the PC board.

Material choice can have a major impact on all these sources of energy loss. As a result materials geared to the RF/Analog domain tightly control parameters such as Dielectric Thickness, Dielectric Constant (ϵ_r/DK), Loss Tangent ($\tan(\delta)$) and even copper type. In contrast digital circuits can tolerate much greater signal loss and still function. Losses are important in the digital domain as well but because of very broad noise margins of digital ICs, usually don't affect circuit performance until they become a very significant portion of the noise budget. This most often occurs at very high operating frequencies. Also digital circuits are generally very complex and dense and often require very large, high layer count boards. This tends to put the emphasis for digital materials on process capabilities and cost. These needs have spawned the second group of materials, geared to digital applications.

PCB Materials Development

Through the several decades prior to the 1990's many high-end laminates were developed for use in RF/Analog circuits, mostly for military applications. Most of these materials are expensive and only a few work well for multilayer boards. Fortunately most of the RF/Analog circuits for which they were developed have low complexity and generally don't require high layer count boards. During that same period virtually all digital circuits and most low frequency analog circuits utilized the spectrum of FR4 base materials.

Through the 1990's and into this century we have seen a shift in the focus of high frequency and high speed circuitry. As the commercial end of the RF/analog industry has dramatically increased in size, attention has been sharply drawn to the need to produce high end RF/Analog laminates without the 'high end' price tag.

At the same time many digital circuits for telecomm equipment and computers are being pushed into the realm of frequencies where losses can be significant. In today's sub-one nanosecond rise time digital circuits, where clock frequencies are in the hundreds of MHz, the selection of base materials and prepgs used in the laminate structure can play a role in the success or failure of the overall system performance.

Material Parameters

There are a number of material parameters and characteristics important to the overall success of any circuit board. There are 4 parameters that generally affect signal losses:

- Er
- Dielectric Thickness
- Line Width
- Loss Tangent
- There is also a fifth issue that can cause significant losses at some frequencies, Skin Effect.

To gain true control of high speed and high frequency signals, all of these must be considered.

Er (ϵ_r)

- Relative permittivity is a measure of the effect an insulating material has on the capacitance of a conductor embedded in the material or surrounded by it. It is also a measure of the degree to which an electromagnetic wave is slowed down as it travels through the insulating material.
- The higher the relative permittivity, the slower a signal travels on a trace, the lower the impedance of a given trace geometry and the larger the stray capacitance along a transmission line.
- Given a choice, lower dielectric constant is nearly always better.
- Relative permittivity varies with frequency in all materials. In some materials the variation is small enough that it can be ignored even in very sensitive applications.
- Some materials, like FR4, have broad variations in Er with changes in frequency.
- Changes in Er can be a serious problem in broadband analog circuits. Two common problems are changes in transmission line impedance and changes in signal velocity as the circuit operates across its entire frequency range.
- Impedance changes cause reflections of signal energy that affect circuit performance and often create circuit malfunction.
- Changes in signal velocity will result in phase distortion.
- Broadband RF and microwave circuits usually need to be fabricated from materials with low and fairly constant Er.
- Changes in Er with frequency can also affect digital circuits.
- The greatest effect is to cause errors between calculated and measured impedance. Most suppliers of FR4 laminate measure Er at 1 MHz. If impedance is calculated using an Er measured at 1 MHz and the resulting circuit board's impedance is measured using a TDR with rise time set somewhere between 50 and 150 psec, the resulting impedance measurement will be different than the calculated impedance by as much as 5 to 6%. Engineers and designers need to determine correct values of Er for the board material, at operating frequency. With that knowledge impedance calculations can be made using Er at the frequency of operation and at the test frequency so the effects can be compensated for problems won't develop.
- Another area involving Er that can have major impact is an ultra-fast switching application where low Er is necessary to ensure rapid propagation of signals. In these situations, be they analog or

digital, materials must be selected that offer the operating characteristics required. There are a number of materials designed for analog circuits with low and stable ϵ_r . There are also several materials designed for the digital arena that offer a fairly low and stable ϵ_r .

- Another potential concern for sensitive analog circuits is the ‘Coefficient of Thermal Expansion relative to Permittivity’ (CTEr). If the circuit will operate in a broad temperature changing environment attention may need to be paid to CTER.

Dielectric Thickness and Trace Width

Both of these parameters play a key role in transmission line impedance. Control of each is necessary during fabrication of the board, with the greatest degree of control needed for high frequency analog circuits. How much these parameters vary is a function of both process control by the fabricator and selection of the base material.

- A 20% change in dielectric thickness (trace height above the power or ground plane) can cause as much as a 12% change in impedance (Z_0). As dielectric thickness increases, Z_0 increases. This becomes especially critical with very thin dielectric layers. Due to resin type, glass or filler type and glass/filler-to resin ratios, some materials are much easier to maintain control of dielectric thickness than others. A tolerance on dielectric thickness is generally listed on the data sheets or in the specifications for the various materials.
- A 20% change in trace width can cause as much as a 10% change in impedance. As width increases, Z_0 decreases. Control of trace width is both a function of process control by the board fabricator and to some degree the type of copper used on the base material.

Printed circuit copper comes in two forms, rolled sheets and electrodeposited (ED) sheets. Each has advantages and disadvantages. The contribution each makes to skin effect is discussed later. Rolled copper is made by cold forming, with heavy steel rollers, thick copper sheets into sheets thin enough to use on a PC board. Rolled copper has mechanical stresses built into it by the rolling process and excellent flatness on both surfaces. This flatness coupled with the high mechanical stresses cause rolled copper to be more prone to delaminate than ED copper, from the base resin. The advantage of the high density and flat surfaces of rolled copper is better control of etching, hence very tight control of trace width.

Electrodeposited (ED) copper is formed by turning a metal drum in a solution of copper sulfate. The copper/liquid is contained in a tank called a plating cell. As the negatively charged drum rotates through the solution in the positively charged cell, copper migrates to the drum surface and forms as an even copper deposition. At the top of the rotation, the copper is pulled off the drum as a foil sheet. The thickness of the copper is a function of charge potential between the cell & drum and the speed of the drum. ED copper has no internal stresses. Additionally it has one smooth surface (the drum surface) and one surface filled with little, spiked bumps known as dendrites. The rough, low density and no stress nature of ED copper (compared to rolled copper) makes it less prone to delaminate but also makes it more difficult to etch precisely.

- The effect on impedance, caused by the difference in etch capability between rolled and ED copper, would barely be noticed in a typical digital circuit.
- The difference can be significant in an analog circuit needing precise impedance control.

The current spectrum of materials designed for digital applications are all supplied with ED copper. Among the spectrum of analog based materials, most offer rolled or ED copper.

- Copper thickness plays a minor role in the impedance of a transmission line.
- A 20% change in copper thickness will cause only a 3% change in Z_0 . This secondary effect, coupled with the ability of laminate suppliers and fabricators to control copper thickness, make it a variable we can generally ignore.
- In a sensitive, ultra high frequency analog circuit copper thickness variations can have a noticeable effect, but circuits demanding such ultra tight control of copper thickness are rare.
- Copper choice vs resin material is listed on the data sheets or in the specifications for various materials. Material selection will play a role in trace width control and a key role in dielectric thickness control but the fabricator is also a major contributor to proper control of both, especially in high layer count boards. Fabricator selection is an issue that's frequently not given just attention.

All too often the purchasing department of many OEMs and contract assembly houses will make a blind selection of the fabricator based solely on price and delivery. Given the complex nature of quality board fabrication, that's a really bad idea, even in the digital domain. In the high frequency analog domain it's nearly a criminal act. But perhaps that's the subject of another article.

Loss Tangent - tan (δ)

- Loss tangent is a measure of how much of the signal pulse (electromagnetic wave) propagating down the PCB transmission line will be lost in the dielectric region (insulating material between copper layers).
- Loss tangent is a function of the material's resin type and molecular structure (molecular orientation). Lower loss tangent equates to more of the output signal getting to its destination(s).
- The loss factor becomes especially important when working with low level signals like those in many receivers and block down converters (LNB's) or with very high power applications, where a 5% difference in signal loss could mean many watts of lost energy.
- Also of significance in the digital domain are multi-gigabit signals, such as those in ultra high speed Ethernet circuits.

Ideally we want to specify and use materials with very low loss tangent. Unfortunately that can carry a heavy cost penalty, which is why we need to analyze which materials will work and which won't. This gives the freedom to choose a cost effective solution.

- The amount of signal loss in a circuit is not only a function of material type but is also a function of frequency and line length in or on the PCB.

Length will be discussed. Frequency must be viewed differently in digital circuits than in analog circuits. Analog signals consist of sine waves and variations of sine waves and what you see in the time domain is basically what you get in the frequency domain.

- When a sine wave is launched into a transmission line, the frequency of the sine wave propagates unchanged but the amplitude will drop off due to the effects of loss tangent. Since analog signals are sine wave in nature, loss tangent causes a reduction in signal amplitude as the signals propagate. The further a signal travels the greater the reduction in amplitude.
- In contrast digital signals are square waves, which consist of a series of embedded sine waves called harmonics. These harmonics are multiples of the clock frequency and generally have strong amplitude out to a frequency that can be determined by equation:

$$f = 0.35 / Tr \quad [1]$$

where: f – Frequency in GHz

Tr – Signal Rise or Fall time (T_r) in nsec

- This means that digital signals have a bandwidth of frequencies that are affected by Loss Tangent. The bandwidth starts at the clock frequency of the circuit and extends to the frequency determined by equation [1].

As an example, a circuit with 200 psec rise time signals and a clock frequency of 500 MHz will have a bandwidth of concern from 500 MHz to 1.75 GHz. When a digital signal propagates through a transmission line, each of the sine wave harmonics in the rising and falling edge lose amplitude, as the signal propagates, due to loss tangent, with the highest frequency harmonics suffering the highest losses.

- The loss of amplitude of the harmonics is manifested as a degradation of Rise and Fall time of the signal. This can seriously affect timing of level sensitive signals and can affect both timing and circuit performance of edge driven signals (clocks, enables, resets, etc.).
- There is certainly no rule of thumb to decide at what point an analog circuit will be affected by losses. Every analog circuit must be analyzed to determine anticipated loss versus acceptable loss.
- Digital circuits must also be analyzed individually, but in general when losses to the first harmonic exceed approximately 3dB across the total length of the transmission line it can be assumed that circuit performance will be severely affected. That is to say in a 10 inch line, the amount of loss per inch shouldn't be allowed to exceed 0.3 dB. Again, this is a rule of thumb and is not always a safe bet but it's a good estimation of roughly when to be concerned.

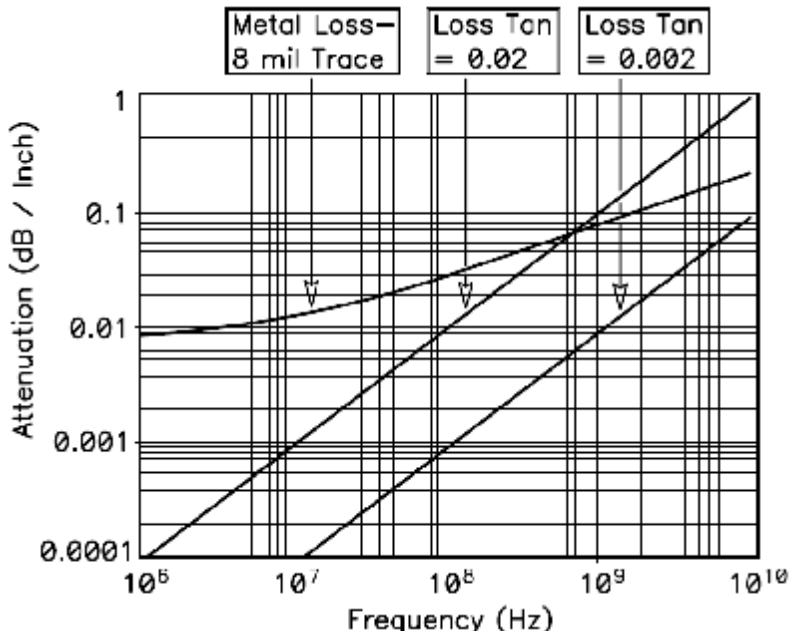


Figure 1 – Graph of Attenuation ($\tan(\delta)$ & Skin Effect) verses Frequency

The graph in Figure 1 can be used to determine the actual amount of loss per inch in materials with a $\tan(\delta)$ of .02 (typical for FR4) and materials with a $\tan(\delta)$ of .002 (typical for several Teflon (PTFE) based materials). Equation [2] was used to build the graphs in Figure 1 and can be used to calculate tan losses for other materials. Notice the graph also shows attenuation for resistive loss in the metal (next section).

$$\alpha = 2.3 f \cdot \tan(\delta) \cdot \epsilon_{eff} \quad [2]$$

where: α – Attenuation in dB / Inch.

f – Frequency in GHz.

$\tan(\delta)$ – Loss Tangent of Material.

ϵ_{eff} – Effective Relative Er of Material.

Resistive Losses and Skin Effect

Voltage drop along a PCB trace, due to resistance in the trace, is a fact of life. From DC through frequencies up to a few MHz, the current in a trace moves through the entire cross sectional area of the trace. At these frequencies resistance is extremely small, hence resistive losses are extremely small. An 8 mil wide trace, at low frequencies, made of 1 ounce copper (1.4 mil) has an approximate resistance of .06 ohms per inch. This was derived from equation [3].

$$R = (\rho L) / A \quad [3]$$

where: R – Trace Resistance in Ohms.

ρ – Bulk Resistivity of Copper (6.787×10^{-7} ohm-in)

L – Trace Length in inches.

A – Cross Sectional Area of the Trace in sq. inches.

When driving a signal into a 50 ohm line with a 50 ohm load, it's easy to see that the resistive drop at these frequencies would be extremely small, in the order of a few milivolts. As frequency increases the energy moving in the trace is forced to the outer perimeter by the large magnetic fields present in higher frequency signals. This is known as skin effect because the majority of the energy is forced to the outer skin of the trace.

Penetration of the signal into the trace is measured in ‘Skin Depths’, with approximately 66% of the energy penetrating to one skin depth and approximately 97% of the energy penetrating to three skins depths. One skin depth at 10 MHz is .0008 inches. At 10 GHz one skin depth is .000028 inches.

Looking at the example of 10 GHz, most of the energy in the trace would be limited to a depth of approximately 84 millionths of an inch. The net result is a decrease in effective cross sectional area of the trace because much of the copper is not used. It’s as if the trace were hollow. Because of skin effect, resistance of an 8 mil trace at 10 GHz will be a little more than 1 ohm per inch. That means the resistive drop from a 3.3 volt signal in a 5 inch, 50 ohm line with a 50 ohm load, at 10 GHz will be greater than 300 mv. In most cases this cannot be ignored. What effect does this have on material choice? In the digital domain, none. Among the materials available for analog boards, as mentioned earlier, some are available with rolled copper. Because of the smooth, dense nature of rolled copper it will suffer less from skin effect losses than its much rougher counterpart, ED copper. According to data gathered by laminate suppliers of high frequency materials, the losses in ED copper are about 12% higher than rolled copper losses, from 3 to 12 GHz. Those needing to calculate skin effect are encouraged to visit Howard Johnson’s web article, “Skin Effect Calculations” (see references). Howard does a great job of walking through the calculation of skin depth and resistance at high frequencies. Howard’s calculations assume ED copper.

When using materials with rolled copper, losses can be adjusted according. At high frequencies, on microstrip traces (referenced to one plane only), almost all the energy will be on the side of the trace nearest the plane. On stripline (referenced to two planes) the energy will balance for centered stripline and will be offset proportionally in off centered stripline. This is called ‘Proximity Effect’. As a result, other than in centered stripline, changes in copper weight (trace thickness) will have little effect on trace resistance at high frequencies. In all cases, changes in width and length will have the greatest effect on resistance at high frequencies.

Combined Effect of Loss Tangent and Skin Effect

In digital circuits resistive drops will have an effect similar to that of loss tangent, meaning rise and fall time of the wave will degrade due to decreased amplitude of the harmonics, with the highest frequency harmonics being affected the most.

In analog circuits the effect is usually a direct loss of signal amplitude.

Looking at the curve for metal loss in Figure 1, we can see that above 1 GHz loss tangent becomes much more severe than skin effect in FR4. To get a true picture of signal loss we need to calculate the combined effects of loss tangent and skin effect. Studies performed by groups such as AMP (Tyco) and NESA (see references) indicate the combined effects of loss tangent and skin effect are often not severe enough, with digital circuits in FR4, to cause circuit malfunction, well into the low GHz operating range. The studies also show that changing material will improve signal quality. But if a circuit will function at a given frequency in a given material, switching to a better grade material at a higher price may offer no benefit. Each circuit should be analyzed based on its particular requirements and available noise and timing budget, especially in the analog domain.

Material Choices –

As mentioned, materials are basically divided into two groups, those designed for digital circuits and those designed for analog circuits. Based on operating parameters, the major differences between the materials are:

- Analog materials generally have a much lower Er that’s more stable over frequency and changing temperature.
- Analog materials generally have tighter tolerance on dielectric thickness.
- Analog materials are often offered with Rolled or ED copper. Digital materials come with ED copper only.
- Only a few analog materials are designed for multilayer applications. All digital materials are designed for multilayer applications.

- Loss tangent varies a great deal across the material choices, but is generally much lower in analog materials, often by a factor of 10 or more.

Some of the materials aimed at the digital arena could be used in an analog circuit and in many cases that might be a good use of resources. In fact many of the materials now considered to be high end digital materials were developed for the commercial end of the high frequency analog arena.

Looking through the specs of these materials it will be apparent which are well suited to analog applications, even at very high frequencies.

Table 1 lists materials for digital boards. Some materials list a broad range for Er.

Within a given material low glass content yields a low Er and high glass content yields a higher Er.

<u>Material</u>	<u>Er (* at 1.0 MHz)</u>	<u>Thickness Tolerance</u>	<u>Copper Style</u>	<u>Multilayer Compatible</u>	<u>Loss Tangent</u>
FR4	3.9 – 4.6*	+/- 1-2 mils	ED Only	Yes	.02 - .03
FR408	3.4 – 4.1*	+/- 1-2 mils	ED Only	Yes	.01 - .015
BT Epoxy	3.9 – 4.6*	+/- 1-2 mils	ED Only	Yes	.015 - .02
Cyanate Ester	3.5 – 3.9*	+/- 1-2 mils	ED Only	Yes	.009
Polyimide	4.0 – 4.5*	+/- 1-2 mils	ED Only	Yes	.01
GETEK	3.5 – 4.2*	+/- 1-2 mils	ED Only	Yes	.012
Nelco 4000-13	3.7 (1GHz)	+/- 1 mil	ED Only	Yes	.01
Nelco 4000-13SI	3.5 (1GHz)	+/- 1 mil	ED Only	Yes	.009
Nelco 6000	3.5 (1GHz)	+/- 1 mil	ED Only	Yes	.008
Nelco 6000SI	3.2 (1GHz)	+/- 1 mil	ED Only	Yes	.005
Speedboard N	3.0 *	+/- 1 mil	Prepreg	Yes	.02
Speedboard C	2.6 – 2.7*	+/- 1 mil	Prepreg	Yes	.004
Arlon 25 / Rogers 4003	3.4 (10GHz)	+/- 1 mil	ED Only	Yes	.0027

Table 1 – Materials intended for Digital Applications.

Of the materials listed above BT Epoxy, Cyanate Ester and Polyimide were developed as replacements for FR4 in applications needing extreme mechanical stability, with Cyanate Ester also offering some improvement in performance. GETEK and FR408 are intended to offer improved electrical performance. The four Nelco materials offer a great deal of improvement in electrical performance and the two Speedboard materials were designed as preps, to use in applications where a low Er material can be mixed with fairly low cost materials to create a board with a lower Er and improved performance. Arlon 25 and Rogers 4003 were originally designed to fit into the analog market as a commercial replacement for some of the high cost, high end military grade laminates. They are listed with the digital materials because many engineers consider them an excellent choice when very high end parameters are required in digital circuits. Table 2 lists materials for analog circuits. The materials listed give an order number for Rogers Corp only. This is not an attempt to push one supplier. The numbers listed are most familiar to the writer. Most of these materials have equivalent choices from other makers of laminates (Arlon, Taconic and 3M – See supplier list at end of article).

<u>Material</u>	<u>Er (10.0 GHz)</u>	<u>Thickness Tolerance</u>	<u>Copper Style</u>	<u>Multilayer Compatible</u>	<u>Loss Tangent</u>
Rogers Ultralam 2000	2.4 – 2.6	+/- .5 mil	ED / Rolled	No	.0019
Rogers 5870	2.3	+/- .5 mil	ED / Rolled	No	.0012
Rogers 5880	2.2	+/- .5 mil	ED / Rolled	No	.0009
Rogers 6002	2.94	+/- .5 mil	ED / Rolled	Yes	.0012
Rogers 3003	3.0	+/- 1 mil	ED / Rolled	Yes	.0013
Rogers 6006	6.15	+/- .5 mil	ED / Rolled	No	.0019
Rogers 6010	10.2	+/- .5 mil	ED / Rolled	No	.0023
Rogers 3006	6.15	+/- 1 mil	ED / Rolled	Yes	.0025
Rogers 3010	10.2	+/- 1 mil	ED / Rolled	Yes	.0035

Table 2 – Materials for Analog Applications.

The Ultralam and the 5000 and 6000 series materials are all approved for military applications. The 3000 series materials are commercial equivalents of the 6000 series materials. Each of these is designed for specific environments and applications, all of which are too lengthy to state in this article. Research of the materials and their equivalents from other suppliers is encouraged. As mentioned, most of these materials have an equivalent from suppliers such as Arlon, Taconic or 3M. Material costs are not listed, as they change frequently. The user is strongly encouraged to talk with their fabricator about cost of the finished board, utilizing one material verses another. Some of the fairly expensive materials are easy to fabricate and might result in a finished board that's less expensive than a cheaper material that creates manufacturing difficulties. Overall costs of the material alone range from \$1.50/sq. ft., for the low end of the FR4 spectrum, to as much as \$100.00/sq. ft, for some of the very high end, analog laminates.

Tg

One material parameter not discussed is Tg.

- All materials exhibit changing temperature coefficients of expansion as temperature increases.
- Tg is the temperature at which materials begin to expand at an uncontrolled rate.
- Boards operating beyond Tg are subject to failure.

This is another parameter the reader is encouraged to understand. A number of articles exist regarding Tg. One excellent article is by Lee Ritchey (Speeding Edge) entitled, A Survey and Tutorial on Dielectric Materials used in the Manufacture of Printed Circuit Boards (see references).

For circuits operating in a broad temperature environment, additional parameters that should be investigated are CTE, CTE and CTE of the base material verses copper.

Conclusion

The reader is encouraged to run through the equations provided for Loss Tangent and check those available on Howard Johnson's website for Skin Effect, then compare the numbers against the available noise and timing budget for the circuit in question. This analysis will show that most digital circuits today (0.2 to 2.0 nsec rise and fall times) can use FR4 as a base material without concern of circuit malfunction. Analog circuits must always be analyzed to compare the operating parameters of the material against the acceptable losses in the circuit, then choose the material most suited to the application, looking at cost as only one of the driving factors. Once a material is chosen, equal care should go into selection of the fabricator for the bare board, keeping in mind that an acceptable level of quality and lowest price may not walk hand in hand. This is especially true for sensitive, high frequency analog boards, requiring fabricators who have the equipment and process controls needed to make boards from the specialized materials discussed. Remember too, fabricators can be a wealth of knowledge about materials.

References

- *Transmission Line Design Handbook*. Brian C. Wadell, 1991. (ISBN #0-89006-436-9)
- *RF & Microwave Design Techniques for PCBs*. Proceedings, PCB Design Conference West, 2000. Lawrence M. Burns.
- *Partitioning for RF Design*. Printed Circuit Design Magazine, April, 2000. Andy Kowalewski - Phillips Corporation.
- *Microstrip Lines and Slotlines*. Gupta, Garg, Bahl and Bhartia, 1996. (ISBN # 0-89006-766-X)
- *Practical Characterization and Analysis of Lossy Transmission Lines* – Eric Bogatin (Giga Test Labs), Mike Resso (Agilent Technologies) and Steve Corey (TDA Systems) – <http://www.agilent.com/cm/rdmfg/appnotes/bogatinfinal.pdf>
- *A Survey and Tutorial of Dielectric Materials Used in the Manufacture of Printed Circuit Boards* – Lee W. Ritchey (SpeedingEdge) <http://www.speedingedge.com/docs/tutorial.doc>
- *PTFE and Low Cost, High Performance Materials for High Speed and High Frequency Applications* – Arturo Aguayo (Rogers Corporation).
- *Skin Effect Calculations* – Howard Johnson – *High Speed Digital Design* (Web article) – <http://www.signalintegrity.com/news/skineffect.htm>.
- *The impact of PWB Construction on High Speed Signals* – Chad Morgan (AMP Circuits and Design (Tyco Electronics)) – <http://www.vita.com/vso/vso20002/amp-pwb.pdf>
- *Limits of FR4 in High Speed Designs* – Edward Sayre, Michael Baxter, Jinhua Chen (NESA) – (http://grouper.ieee.org/groups/802/3/10G_study/public/jan00/sayre_1_0100.pdf)
- *Base Materials for High Speed, High Frequency PC Boards* – Conference Proceedings, PCB West – Rick Hartley (Applied Innovation Inc).

RF System Formulas

Iulian Rosu, YO3DAC / VA3IUL, <http://www.qsl.net/va3iul/>

$$\text{Noise_Floor}_{\text{dBm}} = -174 + 10^{\text{LOG}(\text{BW}_{\text{Hz}})} + \text{Noise_Figure}_{\text{dB}} + \text{Gain}_{\text{dB}}$$

$$\text{Minimum_Detectable_Signal}_{\text{dBm}} = [-174 + 3_{\text{dB}}] + 10^{\text{LOG}(\text{BW}_{\text{Hz}})} + \text{Noise_Figure}_{\text{dB}}$$

$$\text{Spurious_Free_Dynamic_Range}_{\text{dB}} = (1/2) * [174 + \text{IIP2}_{\text{dBm}} - \text{Noise_Figure}_{\text{dB}} - 10^{\text{LOG}(\text{BW}_{\text{Hz}})}]$$

$$\text{Spurious_Free_Dynamic_Range}_{\text{dB}} = (2/3) * [174 + \text{IIP3}_{\text{dBm}} - \text{Noise_Figure}_{\text{dB}} - 10^{\text{LOG}(\text{BW}_{\text{Hz}})}]$$

$$\text{Noise_Figure}_{\text{dB}} = 174 + \text{RX_Sensitivity}_{\text{dBm}} - 10^{\text{LOG}(\text{BW}_{\text{Hz}})} - \text{Signal/Noise}_{\text{dB}}$$

$$\text{RX_Sensitivity}_{\text{dBm}} = -174 + 10^{\text{LOG}(\text{BW}_{\text{Hz}})} + \text{Noise_Figure}_{\text{dB}} + \text{Signal/Noise}_{\text{dB}}$$

$$\text{Signal/Noise}_{\text{dB}} = 174 + \text{RX_Sensitivity}_{\text{dBm}} - 10^{\text{LOG}(\text{BW}_{\text{Hz}})} - \text{Noise_Figure}_{\text{dB}}$$

$$\text{RX_Dynamic_Range}_{\text{dB}} = \text{RX_Sensitivity}_{\text{dBm}} - \text{P1dB}_{\text{dBm}}$$

$$\text{Blocking_Dynamic_Range}_{\text{dB}} = \text{P1dB}_{\text{dBm}} - \text{Noise_Floor}_{\text{dBm}} - \text{Signal/Noise}_{\text{dB}}$$

$$\text{Co-channel_rejection}_{\text{dB}} = \text{Co-channel_interferer}_{\text{dBm}} - \text{RX_Sensitivity}_{\text{dBm}}$$

$$\text{RX_selectivity}_{\text{dB}} = -\text{Co-ch_rejection}_{\text{dB}} - 10^{\text{LOG}[10^{(-\text{IF}_\text{filter_rej}_{\text{dB}})/10}] + 10^{(-\text{LO_spur}_{\text{dBc}})/10}] + \text{IF_BW}_{\text{Hz}} * 10^{(\text{SB_Noise}_{\text{dBc/Hz}})/10}]}$$

$$\text{Image_frequency}_{\text{MHz}} = \text{RF_frequency}_{\text{MHz}} \pm 2^*\text{IF_frequency}_{\text{MHz}}$$

$$\text{Half_IF}_{\text{MHz}} = \text{RF_frequency}_{\text{MHz}} \pm \text{IF_frequency}_{\text{MHz}} / 2$$

$$\text{Half_IF}_{\text{dBm}} = [\text{OIP2}_{\text{dBm}} - \text{RX_Sensitivity}_{\text{dBm}} - \text{Co-channel_rejection}_{\text{dB}}] / 2$$

$$\text{IM_rejection}_{\text{dB}} = [2^*\text{IIP3}_{\text{dBm}} - 2^* \text{RX_Sensitivity}_{\text{dBm}} - \text{Co-Channel_rejection}_{\text{dB}}] / 3$$

$$\text{IIP3}_{\text{dBm}} = \text{Interferer_level}_{\text{dBm}} + [\text{Interferer_level}_{\text{dBm}} - \text{RX_level}_{\text{dBm}} + \text{Signal/Noise}_{\text{dB}}] / 2$$

$$\text{OIP3}_{\text{dBm}} = \text{Pout}_{\text{dBm}} + [\text{IM3}_{\text{dBc}} / 2] = \text{Pout}_{\text{dBm}} + [\text{Pout}_{\text{dBm}} - \text{IM3}_{\text{dBm}}] / 2$$

$$\text{IM3}_{\text{dBm}} = 3^* \text{Pout}_{\text{dBm}} - 2^*\text{OIP3}_{\text{dBm}}$$

$$\text{IM3}_{\text{out unequal_input_levels(left_side)}}_{\text{dBm}} = \text{Pout}_\text{Left}_{\text{dBm}} - 2^*[\text{OIP3}_{\text{dBm}} - \text{Pout}_\text{Right}_{\text{dBm}}]$$

$$\text{OIP2}_{\text{dBm}} = \text{Pout}_{\text{dBm}} + \text{IM2}_{\text{dBc}} = 2^* \text{Pout}_{\text{dBm}} - \text{IM2}_{\text{dBm}}$$

$$\text{IM2}_{\text{dBm}} = 2^* \text{Pout}_{\text{dBm}} - \text{OIP2}_{\text{dBm}}$$

$$\text{IIP2(cascaded_stages)}_{\text{dBm}} = \text{IIP2}_{\text{last stage}}_{\text{dBm}} - \text{Gain}_{\text{total}}_{\text{dB}} + \text{Selectivity @ 1/2 IF}_{\text{dB}}$$

$$\text{IIP2(Direct_Conversion_Receiver)}_{\text{dBm}} \geq 2^*\text{AM_Interferer}_{\text{dBm}} - \text{Noise_Floor}_{\text{dBm}}$$

$$\text{Full_Duplex_Noise@RX_inp}_{\text{dBm}} = -174 - \text{TX_Noise@RX_band}_{\text{dBm/Hz}} - \text{Duplexer_rejection}_{\text{dB}}$$

$$\text{Crest_Factor}_{\text{dB}} = 10^{\text{LOG}[\text{Peak_Power}_{\text{(w)}} / \text{Average_Power}_{\text{w}}]} = \text{Peak_Power}_{\text{dBm}} - \text{Average_Power}_{\text{dBm}}$$

$$\text{MultiCarrier_Peak_to_Average_Ratio}_{\text{dB}} = 10^{\text{LOG}(\text{Number_of_Carriers})}$$

$$\text{MultiCarrier_Total_Power}_{\text{dBm}} = 10^{\text{LOG}(\text{Number_of_Carriers})} + \text{Carrier_Power}_{\text{dBm}}$$

$$\text{Processing_Gain}_{[\text{dB}]} = 10 * \text{LOG}[\text{BW}_{[\text{Hz}]} / \text{Data_Rate}_{[\text{Hz}]}]$$

$$\text{Eb/No}_{[\text{dB}]} = \text{S/N}_{[\text{dB}]} + 10 * \text{LOG}[\text{BW}_{[\text{Hz}]} / \text{Data_Rate}_{[\text{Hz}]}]$$

$$\text{RX_Input_Noise_Power_max}_{[\text{dBm}]} = \text{Sensitivity}_{[\text{dBm}]} + \text{Processing_Gain}_{[\text{dB}]} - \text{Eb/No}_{[\text{dB}]} - \text{Carrier_Noise_Ratio}_{[\text{dB}]} + 10 * \text{LOG}[\text{Bit_Rate}_{[\text{bps}]} / \text{BW}_{[\text{Hz}]}]$$

$$\text{Bandwidth_Efficiency}_{[\text{bps}/\text{Hz}]} = \text{Bit_Rate}_{[\text{bps}]} / \text{BW}_{[\text{Hz}]}$$

$$\text{Integer_PLL_freq_out}_{[\text{MHz}]} = [\text{N}_{(\text{VCO_divider})} / \text{R}_{(\text{Ref_divider})}] * \text{Reference_frequency}_{[\text{MHz}]}$$

$$\text{Required_LO_PhaseNoise}_{[\text{dBc}/\text{Hz}]} = \text{RX_level}_{[\text{dBm}]} - \text{Blocking_level}_{[\text{dBm}]} - \text{Signal/Noise}_{[\text{dB}]} - 10 * \text{LOG}(\text{BW}_{[\text{Hz}]})$$

$$\text{PLL_PhaseNoise}_{[\text{dBc}/\text{Hz}]} = 1\text{Hz}_\text{Normalized_PhaseNoise}_{[\text{dBc}/\text{Hz}]} + 10 * \text{LOG}(\text{Comparison Frequency}_{[\text{Hz}]}) + 20 * \text{LOG}(N)$$

$$\text{PLL_Lock_Time}_{[\text{usec}]} = [400 / \text{Loop_BW}_{[\text{kHz}]}] * [1-10 * \text{LOG}(\text{Frequency_tolerance}_{[\text{Hz}]} / \text{Frequency_jump}_{[\text{Hz}]})]$$

$$\text{PLL_Switching_Time}_{[\text{usec}]} = 50 / F_{\text{comparison}}_{[\text{MHz}]} = 2.5 / \text{Loop_Bandwidth}_{[\text{MHz}]}$$

$$\text{PhaseNoise_on_SpectrumAnalyzer}_{[\text{dBc}/\text{Hz}]} = \text{Carrier_Power}_{[\text{dBm}]} - \text{Noise_Power@Freq_offset}_{[\text{dBm}]} - 10 * \text{LOG}(\text{RBW}_{[\text{Hz}]})$$

$$\text{PLL_Phase_Error}_{\text{RMS } [\circ]} = 107 * 10^{(\text{PhaseNoise}_{[\text{dBc}/\text{Hz}]} / 20)} * \sqrt{\text{Loop_BW}[\text{Hz}]}$$

$$\text{PLL_Jitter}_{[\text{seconds}]} = \text{PLL_Phase_Error}_{\text{RMS } [\circ]} / (360 * \text{Frequency}_{[\text{Hz}]})$$

$$\text{EVM}_{\text{RMS } [\%]} = 1.74 * \text{PLL_Phase_Error}_{\text{RMS } [\circ]}$$

$$\text{TX_PhaseNoise_limit}_{[\text{dBc}/\text{Hz}]} = \text{Power_limit@Offset_from_carrier}_{[\text{dBc}]} + 10 * \text{LOG}(\text{BW}_{[\text{Hz}]})$$

$$\text{ACLR}_{[\text{dBc}]} = 20.75 + 1.6 * \text{Crest_Factor}_{[\text{dB}]} + 2 * [\text{Input_Power}_{[\text{dBm}]} - \text{PA_IIP3}_{[\text{dBm}]} \text{ sine}]$$

$$\text{EVM}_{[\%]} = [10^{(-\text{Signal/Noise}_{[\text{dB}]} / 20)}]^*100 \quad \text{σ} \quad \text{EVM}_{[\text{dB}]} = 20 * \text{LOG}(\text{EVM}_{[\%]} / 100)$$

$$\text{Signal/Noise}_{[\text{dB}]} = 20 * \text{LOG}(\text{EVM}_{[\%]} / 100)$$

$$\text{Corrected_EVM}_{[\%]} = \sqrt{\text{Residual_EVM}_{[\%]} * \text{Measured_EVM}_{[\%]}}$$

$$\text{ADC_SNR}_{[\text{dB}]} = (\text{Nr_of_Bits} * 6.02) + 1.76 + 10 * \text{LOG}(\text{Sampling_Frequency}_{[\text{Hz}]} / 2 * \text{BW}_{[\text{Hz}]})$$

$$\text{ADC_Nyquist_frequency}_{[\text{Hz}]} = \text{Sampling_Frequency}_{[\text{Hz}]} / 2$$

$$\text{ADC_NoiseFigure}_{[\text{dB}]} = \text{Full_Scale_Pin}_{[\text{dBm}]} - \text{SNR}_{[\text{dB}]} - 10 * \text{LOG}(\text{FS_sampling_rate} / 2) - \text{Thermal_Noise}_{[\text{dBm}/\text{Hz}]}$$

$$\text{ADC_NoiseFloor}_{[\text{dBFS}]} = \text{SNR}_{[\text{dB}]} + 10 * \text{LOG}(\text{FS_sampling_rate} / 2)$$

$$\text{ADC_Spurious_Free_Dynamic_Range}_{[\text{dB}]} = \text{Desired_Input_Signal}_{[0\text{dB}]} - \text{Highest_Amplitude_Spurious}_{[\text{dB}]} - \text{Spurious_Level}_{[\text{dB}]} - 10 * \text{LOG}(\text{FS_sampling_rate} / 2)$$

$$\text{ADC_Input_Dynamic_Range}_{[\text{dB}]} = 20 * \text{LOG}(2^{\text{Nr_of_Bits}} - 1)$$

$$\text{VSWR} = (1 + \Gamma) / (1 - \Gamma) = (\text{Vinc} + \text{Vref}) / (\text{Vinc} - \text{Vref}) = (\text{Z}_L - \text{Z}_0) / (\text{Z}_L + \text{Z}_0)$$

$$\text{Reflection_Coefficient } \Gamma = (\text{VSWR} - 1) / (\text{VSWR} + 1) = \text{Vref} / \text{Vinc}$$

$$\text{Return_Loss}_{[\text{dB}]} = -20 * \text{LOG}(\Gamma)$$

$$\text{Mismatch_Loss}_{[\text{dB}]} = -10 * \text{LOG} [1 - \Gamma^2]$$

$$\text{Reflected Power}_{[W]} = \text{Incident Power}_{[W]} * \Gamma^2$$

$$\text{Power Absorbed by the Load}_{[W]} = 4 * \text{Incident Power}_{[W]} * [\text{VSWR}/(1+\text{VSWR}^2)]$$

$$\text{Characteristic Impedance } Z_0 = \sqrt{L/C}$$

$$\text{Resonant Frequency}_{[\text{Hz}]} = 1 / [2*\Pi*\sqrt{L*C}]$$

$$L = X_s / \omega ; C = 1 / (\omega * X_p) ; \omega = 1 / \sqrt{L * C} ; Q_{(\text{series LC})} = X_s / R_s ; Q_{(\text{parallel LC})} = R_p / X_p$$

$$\text{Free Space Path Loss}_{[\text{dB}]} = 27.6 - 20 * \text{LOG}[\text{Frequency}_{[\text{MHz}]}] - 20 * \text{LOG}[\text{Distance}_{[\text{m}]}]$$

$$\text{RX_inp_level}_{[\text{dBm}]} = \text{TX_Power}_{[\text{dBm}]} + \text{TX_Ant_Gain}_{[\text{dB}]} - \text{Free_Space_Path_Loss}_{[\text{dB}]} - \text{Cable_loss}_{[\text{dB}]} + \text{Rx_Ant_Gain}_{[\text{dB}]} + \text{Antenna_Polarization_Mismatch_Loss}_{[\text{dB}]} + \text{Antenna_Factor}_{[\text{dB}]} + \text{EIRP}_{[W]} + \text{NF}_{[\text{dB}]} + \text{Noise_Figure}_{[\text{dB}]} + \text{IP3}_{[\text{dB}]} + \text{IP3}_{[\text{dB}]} + \text{IP3}_{[\text{dB}]} + \dots$$

$$\text{Antenna Polarization Mismatch Loss}_{[\text{dB}]} = 20 * \text{LOG}(\cos \varphi) \quad [\text{for linear polarized antennas}]$$

$$\text{Antenna Factor}_{[\text{dB}]} = 20 * \text{LOG}[(12.56 / \lambda_{[\text{m}]}) * \sqrt{\frac{30}{R_{\text{load}}[\text{ohms}]*10^{(Antenna_Gain[\text{dBi}]/10)}}}]$$

$$\text{EIRP}_{[W]} = \text{Power}_{[W]} * 10^{\text{Antenna_Factor}_{[\text{dB}]} / 10}$$

$$\text{Antenna Near Field}_{[\text{m}]} = 2 * \text{Antenna Dimension}_{[\text{m}]}^2 / \lambda_{[\text{m}]}$$

$$T_e = (\text{Noise Factor}_{[\text{lin}]} - 1) * T_o_{[290K]}$$

$$\text{ENR(Excess Noise Ratio)} = 10 * \text{LOG} [(T_{\text{ENR}} - T_o_{[290K]}) / T_o_{[290K]}]$$

$$\text{Noise Figure Test(Y_Factor_Method)}_{[\text{dB}]} = 10 * \text{LOG}[(10^{(\text{ENR}/10)}) / (10^{(Y/10)})] ; Y = \text{NF}_{\text{out}} - \text{NF}_{\text{inp}}$$

$$\text{RMS Noise Voltage across a Resistor}_{(V)} = \sqrt{[4 * R[\text{ohms}] * k[\text{Boltzmann}] * \text{Temp}[K] * \text{BW}[\text{Hz}]]}$$

<p>IP3 (all linear) – Cascaded Stages</p> $IP3_{INPUT} = 10 \log \left(\frac{1}{\frac{1}{IP_1} + \frac{1}{IP_2} + \dots + \frac{1}{IP_N}} \right)$ <p>$IP3_{INPUT}$: equivalent system input intercept point (dBm)</p> <p>IP_1 : IP3 of first stage transferred to input (mW)</p> <p>IP_N : IP3 of last stage transferred to input (mW)</p> $IP3_{TOTAL} = \frac{1}{\frac{1}{IP3_1} + \frac{G_1}{IP3_2} + \frac{G_1 G_2}{IP3_3} + \frac{G_1 G_2 G_3}{IP3_4} + \dots}$	<p>Noise Factor (all linear) - Cascaded Stages</p> $F_{IN} = F_1 + \frac{F_2 - 1}{G_1} + \frac{F_3 - 1}{G_1 G_2} + \dots$ $\text{Noise Figure}_{[\text{dB}]} = 10 * \text{LOG}(F)$ <p>Noise Factor (all linear) – Identical Cascaded Stages</p> $F_{tot} = 1 + \frac{F - 1}{1 - \frac{1}{G_a}}$ <p>Noise Temperature – Cascaded Stages</p> $T_{eq} = T_1 + \frac{T_2}{G_1} + \frac{T_3}{G_1 G_2} + \dots$ $T_{(1,2,3,\dots,n)} = (\text{Noise Factor}_{[\text{lin}]} - 1) * T_o_{[290K]}$ $NF_{[\text{dB}]} = 10 * \text{LOG} (1 + T_{eq} / T_o_{[290K]})$
---	---

$$\text{AM Modulation Index} = \frac{V_{\max[Vpp]} - V_{\min[Vpp]}}{V_{\max[Vpp]} + V_{\min[Vpp]}} = 2 * \sqrt{\frac{\text{Power}_\text{sideband(usb_lsb)}[W]}{\text{Power}_\text{carrier}[W]}}$$

$$\text{AM Total Power}_{[W]} = \text{Power}_\text{carrier}_{[W]} * [(1 + \text{AM Modulation Index}^2) / 2]$$

$$\text{AM Bandwidth}_{[\text{Hz}]} = 2 * \text{Highest Modulation Frequency}_{[\text{Hz}]} / \text{Max Modulation Frequency}_{[\text{Hz}]}^2$$

$$\text{FM Modulation Index} = \text{Max Frequency Deviation}_{[\text{Hz}]} / \text{Max Modulation Frequency}_{[\text{Hz}]}^2$$

$$\text{FM Bandwidth}_{[\text{Hz}]} = 2 * \text{Max Modulation Frequency}_{[\text{Hz}]} * [1 + \text{FM Modulation Index}]$$